A STUDY ON THE PREDICTABILITY OF THE COMBINED EFFECTS OF MIXTURES OF ANTICANCER DRUGS

PARVINDER SINGH PHUL
BSc. (Hons)

Submitted for the degree of Doctor of Philosophy
The School Of Pharmacy, University of London

January 2006

LIBRARY
THE SCHOOL OF PHARMACY

ProQuest Number: 10104098

All rights reserved

INFORMATION TO ALL USERS
The quality of this reproduction is dependent upon the quality of the copy submitted.

In the unlikely event that the author did not send a complete manuscript
and there are missing pages, these will be noted. Also, if material had to be removed,
a note will indicate the deletion.

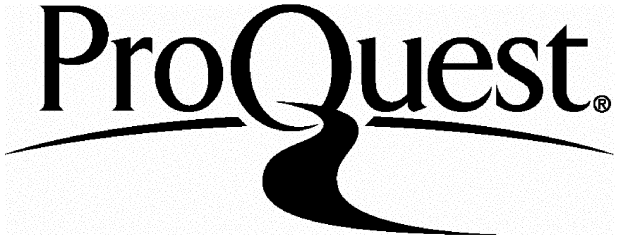

ProQuest 10104098

Published by ProQuest LLC(2016). Copyright of the Dissertation is held by the Author.

All rights reserved.
This work is protected against unauthorized copying under Title 17, United States Code.
Microform Edition © ProQuest LLC.

ProQuest LLC
789 East Eisenhower Parkway
P.O. Box 1346
Ann Arbor, MI 48106-1346

This thesis describes research conducted in the School Of Pharmacy, University of London between October 2001 and September 2005 under the supervision of Dr. Andreas Kortenkamp and Dr. Mark Searcey. I certify that the research described is original and that any parts of the work that have been conducted by collaboration are clearly indicated. I also certify that I have written all text herein and have clearly indicated by suitable citation any part of this dissertation that has already appeared in publication.

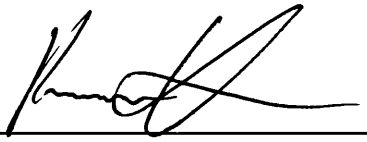

Signature

January 2006

Date

"*Serve your Almighty Lord and Master, and your path in the world hereafter will be easy. Take this easy path, and you shall obtain the fruits of your rewards, and receive honour in the world hereafter.*"

Sri Guru Nanak Dev Ji

ABSTRACT

Advances in the treatment of cancer have lead to increased survival in many tumour patients. Although the use of combination chemotherapy has become an effective means of improving cancer treatment, methods to predict their combined effects systematically are not in widespread use. This study has looked at seven anticancer drugs with a variety of sites of action. These drugs were tested for their cytotoxicity in DU145 and MCF-7 cancer cells, and a mixture prepared of all seven agents combined at a mixture ratio proportional to their potency. Combined effects of this mixture were predicted using dose response curves for each component using the concepts of *independent action* and *concentration addition*. The expectation was that a mixture composed of dissimilarly acting agents should follow the *independent action* prediction. Instead we observed that this prediction model overestimated the combined effect and that the *concentration addition* prediction was found to be more accurate. A possible explanation for this phenomenon may be that although these agents display initial dissimilar sites of action, they may have similarity in their methods of promoting tumour cell death.

Further study was undertaken to search for how these drugs signal for apoptosis. The cells were treated with each agent and mixture, and analysis for induction of apoptosis showed that each single agent and mixture induced increased apoptosis. Expression of the signalling proteins, p53, caspase-3 and caspase-9 were investigated for both cell lines, although expression of one protein or other was found, a common expression was not found for each drug treatment. The aspect of delivering a potentially effective combination of drugs to the tumour site was also explored and a comparison of the toxicity of a free combination of agents with a combination of agents entrapped in a liposome showed no significant difference.

ACKNOWLEDGEMENTS

Firstly I would like to thank my family, both my Mum and Dad and my dear sister Mina for their great support and encouragement over the past four years. I know for a fact that I would never have gotten this far without either one of them. Many thanks must go to my supervisors, both Andreas Kortenkamp and Mark Searcey and to the School of Pharmacy for funding this work. Andreas, thank you for your immense support, through the many ups and downs, I truly appreciate all that you have done.

I would like to thank the many people who have been there when most needed with their knowledge, support and advice. Thanks to my dear colleagues and friends in Toxicology, Ragnor, Jane and Maria-Jose. To Niss, your reassurance in the lab always made the difference to life in Tox, Elisabete for all the guidance with the westerns and to Martin for an in depth insight into the biometrician's mind. Other people I would like to thank include Naash and Kate for previous work with the MTTs, Dave McCarthy for help with imaging and microscopy and to my student Ornella for her assistance and friendship during the western work. I must also mention the group from CDDR and what became my second home during my PhD. To Dr's Vikas Jaitely, Behrooz Nasseri, Gaurang Purohit and Brijesh Patel for all their help with the liposome work. The friendship of so many people such as Amina, Khuloud, Pla and Ao and to the guys from lab 401, Rob, John, Klaus and Sukh for making SOP such a better place to be in.

They say that through difficult and trying situations you learn the best about yourself and others, I have been lucky to of been around so many supporting friends who have helped me through the good times and the bad. To Bal, Kshipra, Suzie, Jazz, Tazz, Ronak, Sits, Yas, Ruz and Dushy, guys you have been immense, thank you so much.

TABLE OF CONTENTS

LIST OF FIGURES

LIST OF TABLES

LIST OF ABBREVIATIONS

5-FU	5-fluorouracil
5-FUdR	5-fluoro-5'-deoxyuridine
AIF	Apoptosis inducing factor
APAF-1	Apoptotic protease activating factor
ATM	Ataxia telengiectasia gene
ATP	Adenosine triphosphate
BSA	Bovine serum albumin
CA	*Concentration addition*
CHOL	Cholesterol
CHOP	Cyclophosphamide, doxorubicin, oncovorin (vincristine) and prednisone
CI	Combination index
DD	Death domain
ddH_2O	Double deionised water
DED	Death effector domain
dH_2O	Deionised water
DHFR	Dihydrofolate reductase
DiSC	Differential staining cytotoxicity
DISC	Death-inducing signalling complex
DLS	Dynamic light scattering
DMF	Dimethylformamide
DMSO	Dimethyl sulphoxide
DNA	Deoxyribonuceic acid
dNTPs	Deoxyribonucleoside triphosphates
DR3/4/5	Death receptor 3/4/5
DSB	Double strand break
dTMP	Deoxythymidine monophosphate
DTT	Dithiothreitol
dUMP	Deoxyuridine monophosphate
ECL	Enhanced chemiluminescence
EDTA	Ethylenediaminetetraacetic acid
FADD	Fas associated death domain
FCS	Foetal calf serum
FH_4	Tetrahydrofolate
FITC	Fluorescein isothiocyanate
g	Acceleration of gravity (9.81 ms^{-2})
GI	Gastrointestinal
GL	Generalised logit model
H_2O_2	Hydrogen peroxide
HCl	Hydrochloric acid
HDC	High dose chemotherapy
HRP	Horse radish peroxidase
IA	*Independent action*
IAP	Inhibitor of apoptosis protein
i.v.	Intravenous
LSB	Laemli sample buffer
LUV	Large unilamellar vesicles
MDR1	Multiple drug resistance gene
MED	Median effect concentration
MEM-α	Minimum essential medium-α

MLV	Multilamellar vesicles
MTD	Maximum tolerated dose
MTT	3,(4,5-dimethylthiazol-2-yl)2,5-diphenyltetrazolium bromide
MTX	Methotrexate
mV	Millivolt
N_2	Nitrogen gas
NADH	Reduced form of nicotinamide adenine dinucleotide
NADPH	Reduced form of nicotinamide adenine dinucleotide phosphate
NF-κB	Nuclear factor of kappa light chain gene enhancer in B-cells
PARP	Poly (ADP-ribose) polymerase
PBS	Phosphate buffered saline
PCS	Photon correlation spectroscopy
PEG	Polyethylene glycol
P-gp	P-glycoprotein
PI	Propidium iodide
PIDD	p53-inducible protein containing a death domain
PMSF	α-toluenesulfonyl fluoride
PS	Phosphatidylserine
psi	Pounds per square inch
PTA	Phosphotungstic acid
RES	Recticuloendothelial system
ROS	Reactive oxygen species
RPM	Revolutions per minute
RNA	Ribonuceic acid
r.t	Room temperature
SDS	Sodium dodecyl sulphate
SDS-PAGE	SDS-polyacrylamide gel electrophoresis
SEM	Standard error of mean
SPC	Soya phosphatidylcholine
SRB	Sulphorhodamine blue
SSB	Single strand break
SUV	Small unilamellar vesicles
T_a	Ambient temperature
TBS	Tris-base solution
TBS-T	TBS-tween
T_c	Transition temperature
TEM	Transmission electron microscopy
TNF	Tumour necrosis factor
TNFR1	TNF receptor type 1
TRADD	TNFR-associated death domain
TRAIL-R1/2	TNF-related apoptosis inducing ligand receptor 1/2
UV	Ultraviolet
VAD	Vincristine, adriamycin (doxorubicin) and dexamethasone
XIAP	IAP protein mapped to the human X chromosome
XTT	2,3-bis(2-methoxy-4-nitro-5-sulfophenyl)-5-[(phenylamino)carbonyl]-2*H*-tetrazolium hydroxide

CHAPTER 1:
INTRODUCTION

For the past two decades the understanding of the basis of cancer biology and the development of cancer has significantly improved. This disease has become an increasingly common problem, with the likelihood that worldwide cancer rates will double by the year 2020 (Eaton, 2003). Improvements in the ways that we can treat cancer have become a vital area of research. A variety of methods have been developed over the years to do this, and these include the use of surgery, radiation and drugs.

One of these forms of treatment includes the use of cytotoxic agents to kill cancerous cells, better known as chemotherapy. Chemotherapy drugs are developed for their potential to cause cell death to tumour cells. Inevitable problems arise, however, due to a lack of selectivity, the acquisition of drug resistance and toxic effects of the drugs used. As such, the treatment with a combination of chemotherapy drugs has become the norm for most tumours. However, efforts to devise effective methods to assess these combinations are often random and vague, with many regimens of combination chemotherapy developed by simple trial and error. This is not an effective or efficient method to continue with into the future. An aim to improve combination therapy would be to devise accurate methods to assess potential drug combinations prior to patient treatment. With advances in the area of mixture effect assessment (Berenbaum, 1985; 1989), these tools are available, and an application to chemotherapy treatment could provide an interesting future.

1.1 THE BASIS OF CANCER CHEMOTHERAPY

Chemotherapy has become the most widely expanding area for cancer research in recent years, although it can trace its origins back to 1946 to when the first drug was administered to patients (Goodman et al., 1984). The object of using chemotherapy drugs is quite simple, to kill the cancerous cells and cause little or no harm to the surrounding healthy cells. To do this, chemotherapy drugs primarily target the rapidly dividing cells commonly associated with many cancers. The treatment of tumours with chemotherapeutic agents results in either direct cell kill or initiation of cell differentiation and apoptosis. Cell death may not occur upon drug exposure, a cell may need to undergo a number of cell divisions before this happens. Due to the fact that not all the cells die after one treatment, further treatments are required until all cancerous cells are eliminated. **Figure 1.1** is a graphical representation of this idea, and follows a number of basic assumptions: a) all tumour cells are equally sensitive to a drug; b) the sensitivity of tumour cells does not change during the course of treatment; and c) there is direct access of the drug to cells independent of the surrounding cells and blood supply. The figure describes how each treatment could result in a three log decrease in tumour cell number followed by 1 log re-growth. This would mean that a course of five treatments of chemotherapy would attain complete tumour cell kill (Skeel, 1999) in an ideal situation. However the usefulness of a particular agent could be severely limited by the emergence of a resistant malignant cell line within the tumour cell population, or the presence of a heterogeneous population. A common observation following chemotherapy treatment is that the first course is successful with the following administrations being gradually less effective until there is little or no effect.

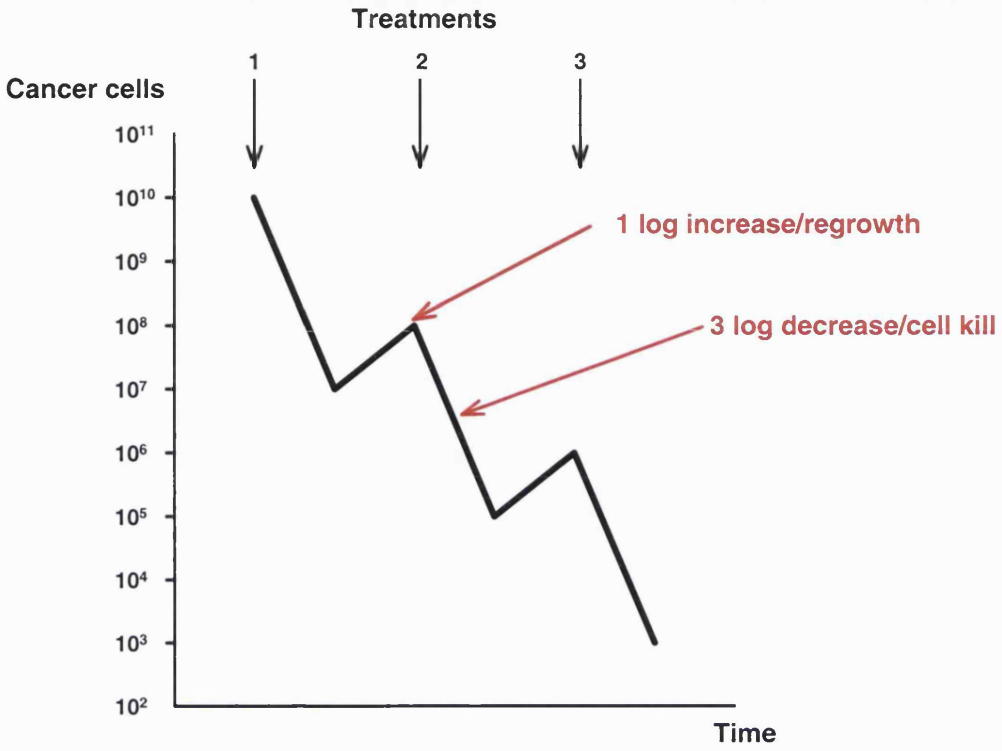

Figure 1.1: Effect of chemotherapy on cancer cell numbers. *This represents an ideal system where chemotherapy kills a constant number of cells after administration of each dose, with constant re-growth between doses. Cell killing is greater than cell growth (Skeel, 1999).*

This phenomenon is commonly known as clinical drug resistance, and for chemotherapy this can either be intrinsic or acquired. Intrinsic resistance comes about if the tumour fails to respond to the first course of chemotherapy (Baird and Kaye, 2003). Acquired resistance is as described above, where there is high response to initial treatment but upon tumour re-growth the cells become resistant to the previously used drug and this may even be the case with new agents as well. There are such a range of anticancer drugs available to clinicians nowadays, and each class of these agents has their distinct site of action upon a cell to cause cytotoxicity.

1.1.1 The cell cycle and the role of chemotherapy drugs

Many cells within the body do not progress through the cell cycle; in fact they are at rest until they are required to divide. The exceptions to this rule include cells in the bone marrow, the gut and follicular cells which are all constantly dividing. For instance, when a cell reaches the end of its life cycle and dies via apoptosis, the neighbouring cells grow and divide to replace it. There are four phases to the cell cycle, the G_1, S, G_2 and the M phases **(figure 1.2)**. DNA is replicated in S phase and the process of mitosis where two copies become separated is called M phase. These two phases are separated by two gap phases. G_1 follows mitosis and G_2 follows S phase. There is also a phase where resting or quiescent cells exit the cell cycle at G_1 phase and enter a phase called G_0 **(figure 1.2)**.

Many chemotherapy agents affect the cell cycle in some manner, dependent upon their initial sites of action in the cell and as such can be classified in this way and the ways in which they can interact with DNA. A classification taken from Pratt (1997) groups these agents in the following way: *i) antimetabolites; ii) covalent DNA-binding drugs (alkylating agents); iii) non-covalent DNA-binding drugs; iv) topoisomerase inhibitors; v) microtubule inhibitors; and vi) drugs affecting endocrine function* and many of these will be discussed further in **chapter 2**.

A few of these agents act at G_1 phase, the phase responsible for protein synthesis. But most chemotherapeutic agents are active during the S phase, when DNA replication is most active, and it is here that these drugs can cause damage much more easily.

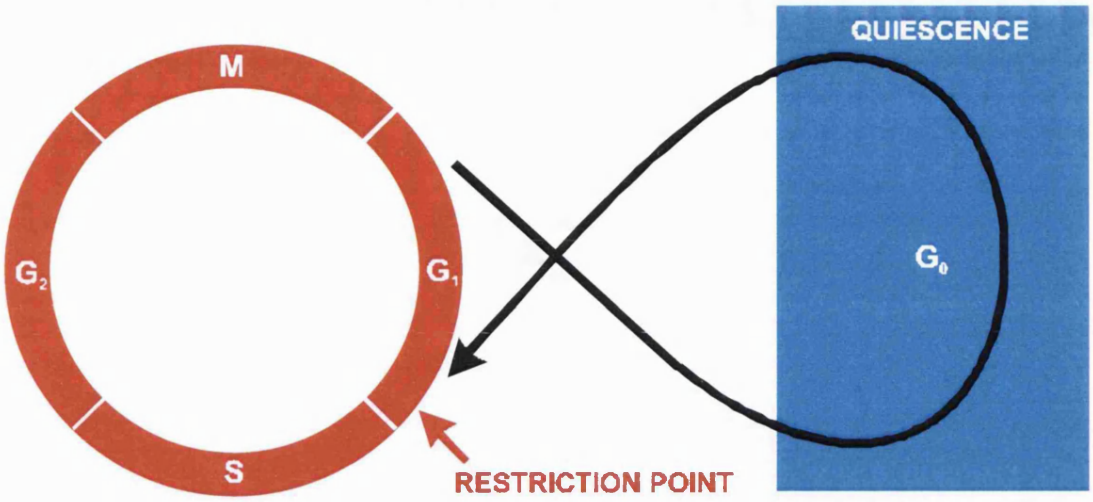

Figure 1.2: The cell cycle. *A cell has four phases: G_1, S, G_2 and M. DNA replication occurs at S phase, mitosis at M phase. Resting or quiescent cells are in G_0.*

Unregulated cell division is a fundamental aspect of understanding tumourigenesis. The cell cycle is highly regulated, as the generation of new cells is only required when needed, and it is in cancer where this control of cell growth can be seen as defective. The basis of the cell cycle and its phases are intact in cancer, but defects to its checkpoint control are thought to lead to the disease (Pardee, 1989; Hartwell and Kastan, 1994). The cell cycle transitions, the entry and exit from S and M phases are the major points of regulation in the cell cycle. The name checkpoint (Hartwell and Kastan, 1994) is given to these regulatory steps, the G_1 restriction point, the G_1/S and G_2/M. These checkpoints are in place to ensure that a phase of the cell cycle does not begin until the preceding phase has been completed. If there is a failure of a checkpoint then apoptosis is activated or the cell becomes genomically unstable and could lead to progression from a normal to a cancerous cell.

The lack of cell cycle regulation, such as at the restriction point and cycle checkpoints result in growth of mutant cells and progression to tumour growth. Mutations are found in many genes in cancer, and many of these change the ability of the cell to regulate the cell cycle, repair DNA, to undergo apoptosis and evade senescence (Hanahan and Weinberg, 2000).

1.1.2 Tumourigenesis

It has become possible over the past few years to understand some of the complex molecular mechanisms that govern a cell's normal operations and therefore be able to determine what causes tumour cells to proliferate abnormally. A number of models have been developed over the past twenty five years to help explain the development and origins of cancer. The first concept regarded cancer as a disease of abnormal cellular differentiation, that there was no change in the overall genetic makeup of the cell but a change in cell phenotype resulting in abnormal cellular development. A second concept suggested that the cause of cancer was related to specific cancer causing viruses that could enter human cells and transform them into malignant cancer cells (Hartwell and Weinert, 1989). Finally, the third model implicated a connection between the development of tumours in humans and animals upon exposure to radiation and certain chemicals. It was the finding by Bruce Ames that a correlation existed between the mutagenic potency of an agent and the tumour incidence in animals (McCann et al., 1975). This implied that these agents damaged genes and in turn the DNA of cells, producing mutant cells with abnormal growth as a direct consequence of mutant genes **(figure 1.3)**. This has now emerged as the dominant way of regarding the origins of cancer.

The discovery of oncogenes described a simple way in which a cancer can develop. A mutation of a proto-oncogene can cause the development of an oncogene that could then initiate malignant cell growth. By 1983 studies showed that instead of just one oncogene being involved with tumourigenesis, it could actually involve two or more genes (Land et al., 1983; Ruley, 1983). The *ras* oncogene, was unable to transform normal embryo cells into tumour cells on its own; in fact the *myc* oncogene was also required (Land et al., 1983).

Figure 1.3 shows a single cell undergoing a single mutation initially on gene A (oncogene). After successful replication the mutation is transferred to the

second generation where it can sustain a second and third mutation upon gene B (tumour suppressor gene). The cell now contains three mutations in at least two different genes and demonstrates characteristics of tumour cell growth (Knudson, Jr., 1971). The idea of the two-hit model of tumourigenesis was suggested by Knudson and colleagues in 1985, a close variation of what **figure 1.3** describes but involves only two events (Knudson, Jr., 1985). At the same time a concept reliant upon successive activation of a series of oncogenes was suggested by Weinberg and Barratt (1983). They suggested that two or more oncogenes must be activated in the right combination, i.e. *ras* has been shown to cooperate with *myc* to form tumours.

A more recent model, based upon colon cancer suggests both the activation of oncogenes and the loss of function of tumour suppressor genes as the cause of cancer (Vogelstein and Kinzler, 1993). This model is based upon several observations of tumour cells. Firstly the cells contain a number of somatic mutations, secondly benign tissue surrounding malignant cells contain similar mutations although they lack at least one of the mutations found in the malignant cells. Finally, certain genes show a tendency to mutate at progressive points of colon cancer.

In addition to oncogenes and tumour suppressor genes, most cancers acquire several other key mutations that enable cancer to progress. Although the exact mutations have yet to be found, researchers have separated them in terms of how they support tumour growth and metastasis. Additional mutations to the genome can help establish new blood supplies to the tumour, evade immune system detection, invasion of the neighbouring tissue, as well as penetrating and reinvading through new blood and tissue layers. Through gradual progression tumour metastasis occurs (Kerrigan et al., 2005).

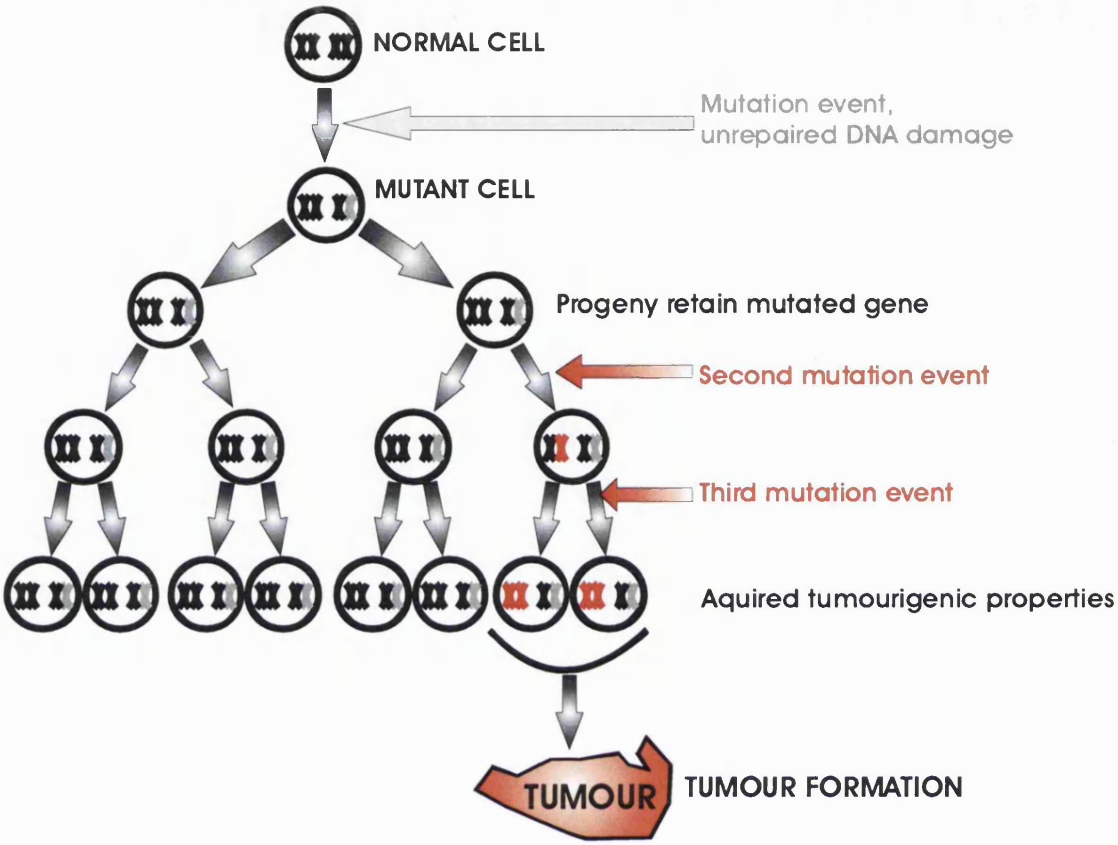

Figure 1.3: Multistep tumourigenesis: *Acquisition of multiple mutations upon two different genes initiates tumour formation.*

1.1.3 Treatment of cancer

What can be defined as the optimal treatment of cancer? There are approximately 10^{13} cells in the human body and during the course of a person's life, cells in a human being undergo 10^{16} cell divisions. As described earlier, this process is complex and prone to errors, thereby resulting in the loss of cellular control and continued expansion. In fact it is not the local growth of tumour cells that can be lethal; it is the spread of these cells, by invasion and by metastases to other parts of the body. There is a vast amount of money and effort being spent on cancer research but there has been little change in overall cure rates over the past thirty years (Price and Sikora, 2002).

At present there are three forms of therapy available to patients and these include:

a) Surgery;
b) Radiotherapy; and
c) Chemotherapy.

The role of chemotherapy has already been described earlier in this chapter, but its role for cancer therapy has always been seen as secondary to either surgery and/or radiotherapy. For the case of solid tumours, clinicians and surgeons consider surgery as the only sure way of ensuring 'complete' tumour removal, with the use of radiotherapy and chemotherapy drugs to kill any remaining tumour cells.

1.1.3.1 Role of surgery in cancer treatment

The role of surgery in cancer treatment has enhanced the survival chances for patients as it directly removes the tumour and reduces the possibility of the spread of the cancer. Surgery remains the most effective form of cancer treatment although can be considered to be the most invasive form as well. Recent advances on this form of therapy have resulted in the retention of the organ and the surrounding tissues, reducing its invasive effects.

1.1.3.2 Role of radiotherapy in cancer treatment

The main aim of radiation therapy is to deliver a dose of ionising radiation to kill tumour cells and yet have little effect on normal tissue. The effect of exposure to ionising radiation results in the generation of free radicals, the most common form of which are known as reactive oxygen species (ROS). These radicals initiate cascade reactions that result in the production of secondary products such as superoxide and hydrogen peroxide which can interfere with repair mechanisms within the cell. The most important target for radiation therapy is DNA, it can cause numerous single strand breaks (SSB), double strand breaks

(DSB) and DNA cross-linking. Much of this DNA damage can be repaired, dependent upon a cell's ability to detect damage with the exception of the unrepairable DSB's (Ward, 1988) as they are large, between 10-20 nucleotides in size (Haber, 2000). The result of this remaining damage results in interference of cell function and ultimately cell death.

1.1.4 Problems associated with cancer chemotherapy

The aim of using chemotherapy drugs is to kill the cancerous cells and cause little or no harm to the surrounding healthy cells. One of the features for some tumour cells is their rapid proliferation, and a variety of chemotherapy drugs can act best upon these types of cells. The evitable downside is that normal cells with high levels of growth can also be affected, such as bone marrow, hair follicles and mucous membranes. This can result in such toxic effects as anaemia, depression of the immune system, bleeding, hair loss as well as gut and GI tract problems. It is these toxic effects and the differences in growth characteristics that limit the effectiveness of this form of cancer therapy. Tumour cells do not necessarily exhibit high levels of proliferation and are therefore no more prone to death from exposure to chemotherapy drugs than normal cells. This has become the main drive for many researchers and pharmaceutical firms to find better selective and therefore more effective drugs.

As described earlier, another common problem for chemotherapy is the acquisition of drug resistance, resulting in diminished effect of drugs upon the tumour. The understanding of how this resistance arises has grown greatly over the years and it has become important to establish new therapeutic methods to overcome it. The causes of drug resistance are described below and fall into two categories. The first cause can be attributed to inadequate drug exposure, and the second to alterations to the cancer cell.

1.1.4.1 Inadequate drug exposure

There are many ways in which the exposure of a drug to tumour cells can be affected. These include:

a) *Insufficient dose:* to achieve maximum cell kill, chemotherapy drugs are given at the maximum tolerated dose (MTD). There has been a recent increase in the use of high dose chemotherapy (HDC) (Lorigan and Vandenberghe, 2002) in order to overcome drug resistance (Odaimi and Ajani, 1987), though use of this strategy inevitably brings about increased risk of toxicity and variation in effectiveness.

b) *Poor drug distribution:* inadequate drug exposure can also be due to poor delivery of the drug to the tumour. If the tumour cells are in a place inaccessible to the drug, then these cells cannot be exposed to the drug and continue to survive. This has been termed the *sanctuary effect* (Haskell, 2001), e.g. the cerebrospinal fluid; the blood-brain barrier makes it difficult for anti-cancer drugs to reach tumour cells. The choice of delivery vehicle can greatly influence the anti-tumour effect of the drug, such as cytotoxic drug encapsulation into liposomes (Lasic and Papahadjopoulos, 1998), microspheres, DNA and the use of monoclonal antibodies (Kohler and Milstein, 1975; Baselga et al., 1996; Foley et al., 1999).

c) *Increased drug metabolism and excretion:* Some drugs are inactive on administration and require transformation before they are active. Many alkylating agents undergo metabolic activation predominately in the liver to form their active, cytotoxic state. The most common route of excretion for anticancer drugs is via the liver and kidneys. Dosing using a variety of agents is dependent on the level of renal function and the condition of the liver.

1.1.4.2 Alterations to the cancer cell during therapy

The second way in which cancer cells can experience drug resistance is by alterations of the cell during therapy. This can result in selection for cells which exhibit certain features that would result in them being able to overcome the drug effect. These cells are already part of the tumour cell population but are

present only in small numbers to begin with. Examples of how this may occur are discussed below and are summarised in **figure 1.4**.

a) *Increased drug elimination from the cell (drug efflux):* The multiple drug resistance gene (MDR1) produces a transmembrane glycoprotein known as P-gp (P-glycoprotein) (Mitchell et al., 1988), which in the presence of intracellular adenosine triphosphate (ATP) pumps drugs out of the cell. These transporters are over expressed in a number of leukaemias and solid tumours such as ovarian cancer (Schneider et al., 1998; Baekelandt et al., 2000) and have been shown to correlate with poor survival.

b) *Decreased drug influx:* Decreased expression of plasma membrane carriers, in turn prevents drugs from entering the cells (Kruh, 2003; Baird and Kaye, 2003).

c) *Alteration of the drug target:* Another contributing factor to acquired drug resistance is the acquisition of genomic mutations as a result of chemotherapy which can result in interference with the binding of the anticancer drug to its target. An example is that of paclitaxel and its reduction of effectiveness after development of tubulin mutations (Poruchynsky et al., 2001). This point can be further complicated by the selection of pre-existing cells in the tumour that already have this feature.

d) *Increased repair of DNA:* The result of exposure to chemotherapy drugs and/or radiotherapy is DNA damage. The cellular response is then to either repair the damage to DNA, tolerate the damage (resistance) or to undergo apoptosis (sensitivity). Resistance would come about if the cells successfully repair the damage or the damage is simply tolerated and DNA replication continues despite damage to the DNA (Zhou and Elledge, 2000).

e) *Evasion of apoptosis:* a number of chemotherapy agents kill cells via apoptosis. The mechanisms involved in this process are numerous and will be discussed later in **chapter 3**, but indications are that there exists a delicate balance between cell cycle arrest (allows the DNA repair and resistance) and apoptosis (mediated cell death). A disruption to any of these mechanisms can determine whether the cell continues to live or to die.

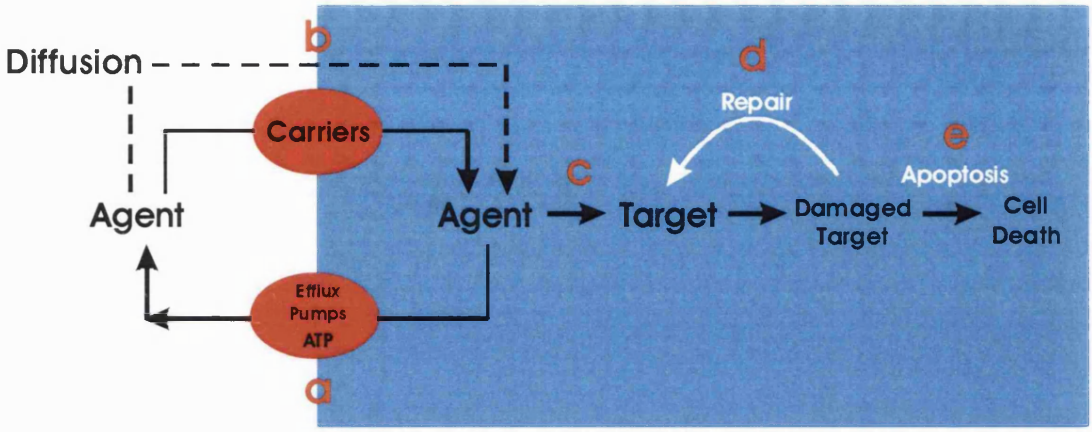

Figure 1.4: A summary of the ways in which selection of cancer cells can result in resistance to cytotoxic anticancer agents. ***a)*** *Increased drug elimination;* ***b)*** *decreased drug influx;* ***c)*** *alteration of the drug target;* ***d)*** *increased repair of DNA; and* ***e)*** *evasion of apoptosis (Kruh, 2003):*

Methods to overcome resistance include the use of HDC, combinations of chemotherapy drugs and alternating combinations of these drugs. The use of HDC can be effective but can lead to toxic effects and low recovery rates whereas the use of combination chemotherapy can allow the use of multiple drugs at less toxic levels. This method of cancer treatment has now been incorporated into most forms of tumour treatment due to its role in reducing high dose effects and drug resistance.

1.2 COMBINATION CHEMOTHERAPY

The more successful approaches to cancer chemotherapy have involved the use of multiple anticancer drugs in combination. This approach is known as combination chemotherapy and is consistently more effective in producing a response in the tumour and in prolonging patient survival when compared to single agent therapy. The two main aims in the use of combination chemotherapy encompass the ideas to minimise toxic effects and to improve efficacy of the drug to the tumour (Berenbaum, 1989). Anticancer drugs are associated with a variety of toxic effects, with varying severity and duration.

Thus a selection of drugs with varying sites of action in the cell and with minimal overlapping toxicity could possibly produce a more effective tumour cell kill. For example, a drug that is nephrotoxic and excreted through the kidneys could be combined with agents that are not nephrotoxic or are excreted in another way. Combination chemotherapy has been discussed as a possible way to combat tumour cell drug resistance. For example, if 1 in 10^5 cells are resistant to drug A, and 1 in 10^5 cells are resistant to drug B, then to treat a tumour consisting of 10^9 cells with either single agent would result in resistant cells surviving. If however both drugs were given together or fairly close after each other, then the likelihood of a resistant clone remaining would be reduced to 1 in 10^{10} (Skeel, 1999).

Many of the more successful combination chemotherapy regimes were developed by trial and error, and all use the following four factors:

a) Only drugs that have an effect on the tumour to be treated can be used, the exception being agents that are inactive to the tumour but can minimise the toxicity to normal tissue. Such an agent is known as a *rescue agent*, e.g. leucovorin administration after high dose methotrexate treatment.

b) Drugs to be used in the combination have different sites of action in a cell, this is to minimise drug resistance.

c) Drugs chosen have different toxic effects or minimal overlapping toxicities, so that they can be given at close to or at MTD levels and reduces the risk of life-threatening cumulative toxicity.

d) Each drug in a combination should be used at its optimal dose and schedule.

A number of treatment regimens involving combination chemotherapy have been established and can be found in **Table 1.1**.

Table 1.1: Commonly used treatment regimens for malignant disease (Markman, 1997)

Malignancy	Anticancer agent
Bladder cancer	M-VAC (cisplatin+doxorubicin+vinblastine+methotrexate)
Breast cancer	Doxorubicin
	Paclitaxel
	Docetaxel
	Tamoxifen
	CMF (cyclophosphamide+5-fluorouracil+methotrexate)
Cervical cancer	Cisplatin
	Cisplatin+ifosfamide
Colorectal cancer	5-fluorouracil+leucovorin
	Irinotecan
Endometrial cancer	Doxorubicin
	Cisplatin+doxorubicin
	Paclitaxel
Esophagael cancer	Cisplatin+5-fluorouracil
Gastric cancer	5-fluorouracil+doxorubicin+mitomycin
Head and neck cancers	Cisplatin+5-fluorouracil
	Methotrexate
Hodgkin's disease	ABVD (doxorubicin+bleomycin+vinblastine+dacarbazine)
	MOPP (nitrogen mustard+vincristine+procarbazine+predisone)
Leukaemia:	
- Acute myeloid	Cytarabine+daunorubicin
- Acute lymphoblastic	Predisone+vincristine+daunorubicin+L-asparaginase+cytarabine+ methotrexate+methotrexate (intrathecal)
- Chronic myeloid	Hydroxyurea or Bulsulphan
- Chronic lymphocytic	Chlorambucil+prednisone
	Fludarabine
Lung cancer	Cisplatin/carboplatin+etoposide
	Cisplatin/carboplatin+paclitaxel
	Cisplatin+vinorelbine
	Paclitaxel
	Docetaxel
Multiple myeloma	Melphalan+prednisone
	VAD (vincristine+doxorubicin+dexamethasone)
Non-Hodgkin's lymphoma	CHOP (cyclophosphamide+doxorubicin+vincristine+prednisone)
	CVP (cyclophosphamide+vincristine+prednisone)
Ovarian cancer	Cisplatin/carboplatin+paclitaxel
	Topotecan
	Etoposide (oral)
	Doxorubicin
Testicular cancer	Cisplatin+etoposide
	Cisplatin+etoposide+bleomycin

1.2.1 The combined effects of agents

The evaluation of a new drug and new combination treatment regimens for oncology follows a defined design. This process is split up into three stages, ranging from toxicity determination to a comparison of existing standard therapy. The first stage is known as a Phase I (pharmacological) study and is used to determine the toxicity associated with the new treatment strategy. The second stage is known as Phase II (developmental) studies and the purpose of these studies is to determine the efficacy of the drug or combination. The final stage is termed Phase III (comparative) clinical studies and is often known as the ultimate test for a treatment regimen.

The idea of optimising possible drug combinations for the treatment of cancer has been a long term goal. If we take an example of a combination of five agents, each with variables such as differing dose levels, number of courses, number of doses per course, intervals between doses and courses, and then this would constitute at least twenty five independent variables. A full scale clinical trial would not hope to cover more than two of these variables, leaving open the question as to whether the tested combinations are really the most effective (Berenbaum, 1989). Yet despite the presence of such a framework for establishing new treatment regimens there is still a lack of structure about how effective regimens of combinations of drugs to treat cancer can be found. As stated earlier, components in a combination are selected based upon their relative toxicities and single agent effectiveness on the tumour of interest. The fact that the selection of a potential anticancer drug combination is still at best 'hit or miss' is worrying indeed. An adequate and effective method to properly test effective combinations of agents prior to treating humans has yet to be established but would be a positive step forward in the progression of cancer treatment.

A common approach to finding an effective combination of agents is to find the optimum level for each variable for each drug and hence combine them for the most effective combined effect. This approach using crude empirical objectives may sound viable, but more often than not this is not the case. For example, in a study of three separate variables, first two variables were optimised and then kept fixed, the third variable was then applied but an optimal combination could not be found (Wampler et al., 1987). Therefore it can be said that the optimal dose of each agent on its own is not necessarily its optimal dose in combination (Berenbaum, 1989).

The increasing expansion of the area of analysing mixture effects may have brought about the potential to predict possible effective anticancer drug combinations for the treatment of cancer. A number of concepts exist based upon pharmacological assumptions about sites and modes of action of the single agents (Drescher and Boedeker, 1995), and provide a possible method to assess the combined effects of agents. These concepts are discussed in greater detail further.

1.3 ASSESSMENT OF MIXTURES

The combined action of chemicals has long been of interest in various fields of science. Possible therapeutic advantages of drug combinations over single agents can be applied to multiple areas of medicine, with particular use in the field of cancer therapy and antibiotic treatment. In the field of toxicology the ability to predict the toxic effects of a mixture is paramount in order to protect humans from possible hazardous effects. Toxicity studies with mixtures have been undertaken for a number of decades, and have evolved from simple binary mixtures to more complex, multiple compound mixture compositions (Könemann and Pieters, 1996).

Recent reviews of the field of assessing the combined effects of agents have drawn up a number of methods to assess mixture effects (Berenbaum, 1985; 1989; Greco et al., 1995). A recurring problem has been in calculating the expected combined effect of a group of agents from their individual effects. With such a wide variety of models seeking to accurately predict these joint effects, it has become critical to validate one model from the next. This issue has also been compounded by the wide range of terminology used to describe the nature of combined action. There has been much discussion as to exactly what the term "non-interaction" or "zero-interaction" mean (Unkelbach, 1992). Many authors have given many different meanings to the term, but the problems stem from the ambiguous definition given to the term "interaction" which has been defined as: "any situation in which there is evidence for one agent influencing response to the other" (Steel, 1979). Interactions can be described as being either synergistic or antagonistic. Synergy in a broad sense is defined as a case of agents "working together", for antagonism the opposite can be said as agents are "working against each other". Each represents a distinct extreme, implying the existence of an intermediate state in which a combination of agents acts in neither way, a case of zero or non-interaction.

The first and most frequently understood meaning for non-interaction is the idea of Loewe additivity originally defined by Loewe and Muischnek (1926), and is known also as *concentration addition*. This idea, by definition, states that an agent cannot interact with itself. This has been described well by the use of a sham experiment of combining an agent with itself. As the same substance cannot interact with itself we can call such a combination non-interactive. Further if two agents share the same shape for their dose-response curves and differ only in potency, then it can be said that they act as a dilution of the other. This model has been further developed and described by Berenbaum (1985; 1989) and has been widely accepted by a number of scientists within the field.

Concentration addition can be expressed mathematically as:

$$\sum_{i=1}^{n} \frac{c_i}{EC_{xi}} = 1 \qquad \textbf{(1.1)}$$

Where n is the number of mixture components, EC_{xi} is the concentration of the ith mixture component that provokes x% effect when applied singly, and c_i is the concentration of the respective component in the mixture. Every fraction (c_i /EC_{xi}) gives the concentration of a compound in the mixture scaled for its relative toxicity. If the sum of each fraction equals 1, then *concentration addition* holds and the joint effect can then be called additive.

The second wide-spread model for non-interaction is based upon the independence property, as was originally developed by Bliss (1939) and is based on the idea of probabilistic independence (Greco et al., 1995). This concept is known as *independent action*. In this case two agents act in a way in which neither interferes with the other but contributes to the overall effect, i.e. substance A acts in the presence of substance B as it would in the absence of substance B. This implies that the action of substance A is not influenced by substance B, a strong reason for why independence is described as non-interactive.

Independent action can be expressed mathematically as:

$$E(c_{mix}) = E(c_1 + \ldots + c_n) = 1 - \prod_{i=1}^{n} [1 - E(c_i)] \qquad \textbf{(1.2)}$$

$E(c_{mix})$ is the overall effect (scaled 0-1) of an n-compound mixture, c_{mix} is the total concentration in the mixture, c_i is the concentration of the ith compound, and $E(c_i)$ is the effect of the ith compound at that concentration if the compound is applied singly.

Berenbaum, in an effort to base these statements quantitatively, proposed three classes of combined action, zero-interaction, synergism and antagonism (Berenbaum, 1985; 1989). These statements were further described in 1992 by Greco and co-workers. **Table 1.2** describes consensus terminology for the combined action of two agents, using the two empirical reference models of Loewe additivity/*concentration addition*, **equation 1.1** (Loewe and Muischnek, 1926) and Bliss independence/*independent action*, **equation 1.2** (Bliss, 1939), designed to establish an agreement on definitions of agent interaction terms.

Table 1.2: Terminology for two-agent combined action concepts (Greco et al., 1992)

	Both agents effective individually; eq. 1.1 as ref model	**Both agents effective individually; eq. 1.2 as ref. model**	**Only one agent effective individually**	**Neither agent effective individually**
Combination effect greater than predicted	Loewe synergism	Bliss synergism	Synergism	Coalism
Combination effect equal to prediction from reference model	Loewe additivity	Bliss independence	Inertism	Inertism
Combination effect less than predicted	Loewe antagonism	Bliss antagonism	Antagonism	

The first two columns are fairly self explanatory, to describe the components of a mixture as being non-interactive the terms such as Loewe additivity and Bliss independence are used. If however the mixture exhibits greater than additivity traits then terms such as synergism, enhancement, potentiation and supra-additivity are used. An effect that shows less than additive effects can be termed as antagonism, inhibition and sub-additivity (Könemann and Pieters, 1996).

When only one agent in a pair is effective own its on then the term "inertism" is used for non-interaction, synergism for an increased effect caused by the second agent, and antagonism if the combined effect is lower. When neither agent is effective on its own, an effective combination can be termed as "coalism", whereas if the combination is ineffective it is another case of inertism.

1.3.1 Assessment of mixtures of anticancer drugs

An improvement in the way to treat cancer, especially with the use of combinations of chemotherapeutic drugs, is seen as an intriguing area for research. The ability to find even more potent and effective combinations of drugs with greater selectivity and efficacy for tumour cells by the use of *in vitro* techniques have been met with various levels of success (Kaufmann et al., 1996) dependent upon drugs used, cell lines, temperature, pH, etc (Drewinko et al., 1976; Katz et al., 1990).

The models derived by Chou and Talalay (1984) have been widely used in the synergy assessment for *in vitro* studies involving anticancer agents (Greco et al., 1996). This is known as the median-effect method and has been an issue of debate over a number of years in regards to how effective it can be for assessing mixture effects (Berenbaum, 1989; Greco et al., 1995). Chou and Talalay divided the agents into two separate classes, mutually exclusive agents and non-mutually exclusive agents. The mutually exclusive agents share a common site of action in terms of binding site, and that a binding site cannot be occupied by more than one mutually exclusive agent, so therefore combinations of these agents would show zero interaction. This is a very similar concept but not the same as *concentration addition*. Non-mutually exclusive agents are subsequently known as having differing binding sites, and that binding to one specific site would have no direct effect on the binding of an agent to another site, and therefore independent drug action. Again this relates closely to the concept of *independent action.*

Much of the derivation of this work has been based upon enzyme kinetics and law of mass action, and many useful equations have been developed from this work. The many assumptions and much of the criteria devised to derive this work have come under much scrutiny, and their application to the assessment of predicting combined effects of anticancer drugs has been questioned by both Berenbaum and Greco. The mutually exclusive model **(equation 1.3, 1.4 & 1.5)** has been compared to the approach devised by Loewe, and shows consistency to this concept for assessing combined effects of agents. The problem has been the derivation for the non-mutually exclusive model which has been argued to be incorrect (Berenbaum, 1989; Greco et al., 1995). **Equation 1.7** incorrectly describes non-interaction between mutually non-exclusive agents as it is derived from an understanding of the mechanisms of action of the agents. In fact this equation describes synergy and not non-interaction (Berenbaum, 1989). The result of this mistake can lead to incorrect calculations of combination index (CI), leading to overestimations of CI and resulting in synergistic combinations being categorised as being non-interactive or antagonistic, and non-interactive combinations shown to be antagonistic.

$$\frac{d_a}{D_a}+\frac{d_b}{D_b}=combination\ \ index=\begin{cases}<1 & \textbf{(synergy)} \quad \textbf{(1.3)}\\ 1 & \textbf{(non-interaction)} \quad \textbf{(1.4)}\\ >1 & \textbf{(antagonism)} \quad \textbf{(1.5)}\end{cases}$$

$$\frac{d_a}{D_a}+\frac{d_b}{D_b}+\frac{d_a\cdot d_b}{D_a\cdot D_b}=combination\ \ index=\begin{cases}<1 & \textbf{(synergy)} \quad \textbf{(1.6)}\\ 1 & \textbf{(non-interaction)} \quad \textbf{(1.7)}\\ >1 & \textbf{(antagonism)} \quad \textbf{(1.8)}\end{cases}$$

Where d_a and d_b are the doses of agents A and B, and D_a and D_b are the isoeffective doses of A and B with the combination. Another of the problems encountered with this method has been in determining whether the agents are mutually exclusive or non-exclusive, i.e. whether two or more agents share a common site of action in terms of binding site or have differing binding sites. In

the context of combinations of anticancer agents this is an important classification, will the effects of a combination of agents with varied sites of action be best predicted using a model for independence or a model for Loewe additivity.

1.4 IS THERE DISSIMILAR ACTION FOR ANTICANCER AGENTS?

There are two general concepts that are widely regarded for the assessment of joint mixture effects; these are known as *independent action* (IA) and *concentration addition* (CA) (Berenbaum, 1985; 1989; Greco et al., 1992; 1995). Each of these concepts is dependent upon prior knowledge of each of the mixture components' primary site of action, whether they act in a dissimilar (IA) or similar (CA) way.

1.4.1 A dissimilar action for a combination of anticancer drugs

The concept of *independent action* or Bliss independence was first developed by Bliss (1939) and has also been referred to as 'joint independent action' (Plackett and Hewlett, 1948), response addition and effect multiplication (Colby, 1967). This concept has often been applied to the assessment of mixtures when the components act with dissimilar modes of action (Backhaus et al., 2000; 2004). The basis of this concept assumes that the mixture components act independent of one another on different sub-systems of a biological organism. This means that if an individual mixture component was present at levels to produce zero effects, then it would not contribute to the overall mixture effect.

The concept of *independent action* has gained some popularity in assessing mutagenic events for multiple drug exposure (Berenbaum, 1985) and has also been applied for mixture toxicity risk assessments. This concept relies upon having accurate single agent effect data in order to predict an overall mixture effect. Work using the marine bacterium, *V. fischeri*, has shown that *independent action* has excellent predictive power when combining fourteen chemicals of differing mechanisms of action in bacteria (Backhaus et al., 2000). Comparison to the alternative concept of *concentration addition* resulted in an overestimation of the mixture toxicity. This has further been supported by algal toxicity of sixteen dissimilarly acting biocides, *independent action* proved to be superior and more accurate in predicting combined toxic effects (Faust et al., 2003).

1.4.2 A similar action for a combination of anticancer drugs

Concentration addition or Loewe additivity was first introduced by Loewe and Muischnek (1926) and this concept is based on the assumption that all components of the mixture act in a similar manner and have a common site of action. Therefore, in concentration addition it is said that each chemical in the mixture behaves like a dilution of another. This means that each agent in the mixture is assumed to contribute to the overall effect in an equieffective manner (Altenburger et al., 2000).

In the field of aquatic toxicology, *concentration addition* has been demonstrated as well suited to predict mixture toxicity of unspecifically acting substances/chemicals (Altenburger et al., 2000). A multi-component mixture of 18 herbicides (Faust et al., 2001) demonstrated highly accurate mixture predictions based upon *concentration addition*, and this was further supported by work of Silva and colleagues (2002) with endocrine disrupting agents. Together they show the potential of using the *concentration addition* concept to

obtain accurate predictions of joint mixture effects, especially in the case of similar-acting compounds.

In the field of anticancer research, much debate has centred on an appropriate model to predict combined drug effects (Berenbaum, 1989; Greco et al., 1995). The median-effect approach developed by Chou and Talalay (1984) has been supported as a possible way to predict mixture effects of anticancer drugs and shows similarity with the method of Loewe additivity (Greco et al., 1996) for the case of mutually exclusive agents. A combination of two taxanes, paclitaxel and cisplatin, has shown close support for Loewe additivity (Levasseur et al., 1997) and supports the case for *concentration addition*, especially for predicting joint effects of similarly acting agents.

1.5 SCOPE OF THIS THESIS

As has been described earlier in this chapter, the role of combination chemotherapy is essential in treating many forms of cancers. Optimisation of effective treatment regimes have till now been developed through trial and error, but the feeling of a general lack of structure in establishing effective combinations of agents remains strong. The ability to find more effective and more potent combinations of drugs using *in vitro* techniques has been explored a number of times with varying levels of success (Drewinko et al., 1976; Katz et al., 1990; Kaufmann et al., 1996). Yet a predictive model to assess mixture effects of a combination of anticancer drugs has still to be resolved.

In order to investigate and to reliably predict the effect of multi-component mixtures, reliable data for single agent effects were required. The study in **chapter 2** assesses whether the multi-component mixture effects of a combination of anticancer drugs with differing sites of action can be accurately predicted from single agent dose-response effects. The mixture effects were

evaluated using the concepts of *independent action* and *concentration addition* which have been used previously to evaluate mixture effects of multi-component mixtures made up of dissimilarly (Backhaus et al., 2000; Backhaus et al., 2004) and similarly (Altenburger et al., 2000; Faust et al., 2001; Silva et al., 2002) acting agents. The model for agents that act in differing ways, i.e. via different sites of action is *independent action* and the concept to predict mixture effects for components that act in a similar way is *concentration addition*. A selection of anticancer agents were chosen each with a differing site of action, a common feature for combination chemotherapy and implying the mixture effect would be best modelled using *independent action*. The results of each single agent's toxic effect and the seven-component mixture was detailed in **chapter 2** and was examined using *in vitro* chemosensitivity assay techniques.

The work in **chapter 3** follows directly from that carried out in **chapter 2**. The seven-component mixture tested in **chapter 2** was found to not follow the prediction based on *independent action* and was closer predicted using *concentration addition* and so a more detailed examination of the single agent's possible mode of action was undertaken. The ability for each of the single agents to initiate apoptosis was first examined. This was to initially understand whether a common mode of cell mediated death was present for each of the treated agents. Both cell lines were treated to the seven-component mixture at their median effect levels and were likewise examined for apoptosis activation to demonstrate a similarity in effect. A more detailed examination of the possible methods in causing cell killing was explored for each of the single agents and for the mixture. Each of the cell lines used had unique characteristics and defects in their cell signalling abilities and these were exploited in order to understand how these drugs were activating this complex signalling pathway.

Finally in **chapter 4** the advantage of packaging this combination of seven agents was explored by entrapping this combination of agents into a liposome formulation. A simple comparison of the toxicity profile for the liposome

entrapped mixture with that of the free, unentrapped mixture showed whether the liposome packaging had any adverse effect to the mixture's toxicity.

CHAPTER 2:

THE ASSESSMENT OF COMBINATION EFFECTS OF ANTICANCER DRUGS

2.1 INTRODUCTION

As described in the previous chapter, the role of combination chemotherapy has become integral to effective cancer treatment. The emphasis has now become to find ways to optimise and improve existing and potentially new drug combinations to treat tumour formation. The two predictive models that have been discussed earlier, *concentration addition* and *independent action*, are well established as predictive models of joint mixture effects. These models were designed with specific applications in mind, in terms of agent modes of action. The model for similarly acting agents, *concentration addition*, and the model for dissimilarly acting agents, *independent action*, can produce very different predictions for combined mixture effects and until now these have not been applied to mixtures of anticancer drugs. The ability to reliably predict the combined effects of a mixture of anticancer drugs will prove useful in determining optimal therapeutic drug combinations. It was the aim of this work to establish whether a mixture of seven dissimilarly acting anticancer agents would be best predicted using *independent action*. Conceptual reasoning as well as knowledge of the single agent's mode of action suggests that *independent action* was the most appropriate model for this composition of mixture. The potential of the concept of *concentration addition* was also assessed to determine whether it could provide an alternative and more accurate predictive model.

2.2 MIXTURE EFFECT PREDICTION MODELS

The presence of both *concentration addition* and *independent action* as models for mixture risk assessment has brought about a great deal of discussion surrounding their appropriate applications. For a case of a combination of agents with a common site of action the concept of *concentration addition* has been accepted as the model to assess their joint toxicity (Calamari and Vighi, 1992). Evidence to support this comes from toxicity studies in aquatic systems (Altenburger et al., 2000; Backhaus et al., 2000; Faust et al., 2001). *Concentration addition* assumes that components of a mixture have similar action, but herein lies the problem, as the term of similar action can be interpreted in differing ways. From a mechanistic point of view, similar action has been defined to apply to agents that competitively and reversibly interact with an identical binding site (Poch, 1993), similar to the mutually exclusive model for median-effect (Chou and Talalay, 1984). Similar action was also taken to mean that agents can cause a similar toxicological response (Berenbaum, 1989). Taking into account endpoints such as cell death or an inhibition of reproduction, then this can encompass a very broad range of chemicals. *Concentration addition* has in fact been suggested to be the 'general solution' to calculate expected effects for any combination of agents without the need to refer to their mechanisms of action (Berenbaum, 1985).

The alternative concept of *independent action* assumes dissimilar action for each component of a mixture. This is based upon each agent interacting at differing sites of action, but often leading to a common toxicological endpoint (Faust et al., 2003). The fractional effects of each individual mixture component are then considered to be independent of each other. Experimental evidence from studies with algae (Faust et al., 2000; Faust et al., 2003) and bacteria (Backhaus et al., 2000), has shown that chemicals with specific and dissimilar modes of action are better described using *independent action*. The fact that this has been studied in two forms of assay, both supporting the predictive power of

independent action for chemicals with strictly dissimilar modes of action, provides a useful tool in the assessment of chemical mixtures. There are however practical limitations that exist for accurate calculation of *independent action*, as the effect $E(c_i)$ elicited by each individual mixture component at the concentration c_i that it is present in the mixture **(equation 1.2)** must be known. This becomes more difficult with decreasing agent concentration and decreasing single agent effects.

The previous studies discussed (Altenburger et al., 2000; Backhaus et al., 2000; Faust et al., 2003) have observed that *concentration addition* consistently predicts a higher toxicity effect than *independent action*, although this difference was quantitatively small and differed by less than a factor of three. The difference between the two predictive models is often not very big and can be dependent on a number of factors. These include the number and concentration ratio of mixture components, the slopes of individual agent concentration-response curves, and the regression models used to model these curves (Drescher and Boedeker, 1995). The fact that *concentration addition* has been shown to overestimate the toxic effects of dissimilarly acting chemicals, may in fact offer a model for worst case estimation of toxicity when low concentration and low effect data are unavailable to construct an *independent action* prediction.

In order to assess the predictive power of *independent action* for a mixture composed of dissimilarly acting anticancer agents, a number of issues were addressed. The first issue dealt with the classification of dissimilar action, and how an agent was defined as being dissimilarly acting, leading onto the selection of a suitable group of agents. The second issue dealt with the composition of the mixture (the number of agents and their overall concentration in the mixture) and how this helped to achieve successful separation of the two predictive models of *independent action* and *concentration addition*. The final issue to be tackled was the choice of toxicity assay and its ability to achieve readily reproducible results.

2.3 SELECTION OF THE MIXTURE COMPONENTS

Individual drugs in use for combination chemotherapy must have unique characteristics in order to be effective in a combination. The drugs must have differing mechanisms that lead to cell death this can make the combination more effective for cancer treatment as these drugs exhibit such varied modes in which to kill tumour cells. How can we decide whether a group of agents acts in a dissimilar way to one another? As discussed before, dissimilar action has been suggested to be based upon each agent interacting with differing molecular target sites, but often leading to a common toxicological endpoint such as cell death (Faust et al., 2003). But much confusion remains on the application of "mechanism", "mode" and "site" of action of a set of agents to apply to *independent action* and *concentration addition* assessments (Borgert et al., 2004).

Mechanism of action: The mechanism of action as described in the field of pharmacology and toxicology, is the molecular sequence of events leading from the absorption of an agent to the biological response in the target organ (Butterworth et al., 1995; Dellarco and Wiltse, 1998; Schlosser and Bogdanffy, 1999; Borgert et al., 2004). Mechanism of action is a stepwise and detailed description of an agent's action at various levels of biological effect. An International Life Sciences Institute (ILSI) panel (Mileson et al., 1998) has recently proposed that chemicals should be considered as having the same mechanism of action if they cause the same critical effect, act on the same molecular targets at the same target tissue and act in the same biochemical mechanism of action by sharing a common toxic intermediate.

Mode of action: The mode of action has been described as the type of response produced in an organism following exposure or can be described as one of the critical steps or features in the mechanism to produce a particular response (Dellarco and Wiltse, 1998; Schlosser and Bogdanffy, 1999; U.S.EPA,

2000; 2001). The mode of action can often be defined for a chemical if the mechanism of action is known, but the reverse cannot be said.

Site of action: The site of action can be defined as the molecular target site of a compound, i.e. for an anticancer drug such as tamoxifen that binds to a specific receptor then the site of action is described as being the estrogen receptor.

Differentiation from common and dissimilar mechanisms, modes and sites of action is a critical area when defining the appropriate prediction model of combination effects. For the context of these studies with such a wide range of anticancer agents available, particular care was taken in the choice of test agents for this particular study. A number of criteria were used to make this choice. Firstly, the drugs had to have been in general clinical use for the treatment of cancer, as this ensured that previous knowledge of the drug in terms of its toxicity and possible mode of action was available. The second and most important criterion for agent selection was the way in which they killed tumour cells. The drugs were chosen dependent on their reported sites of action, and as a basis for combination chemotherapy where the components have multiple sites of action, a selection of drugs with a distinct dissimilarity in the way that they act upon tumour cells were chosen.

2.3.1 The anticancer drugs

Using these criteria, seven anticancer drugs were selected. Two of the drugs, 5-fluoro-5'-deoxyuridine and methotrexate, belong to the antimetabolite class of anticancer drugs. These drugs are structurally similar to naturally occurring compounds such as vitamins, nucleosides, purine and pyrimidine bases and amino acids and can interfere with nucleic acid production by one or both of two mechanisms. They can inhibit the production of deoxyribonucleoside triphosphates (dNTP's) and therefore inhibit DNA synthesis, or they can incorporate themselves into RNA and DNA as they structurally resemble normal

purines and pyrimidines. Most antimetabolites show greatest activity during the S phase of the cell cycle and can be sub-classified dependent on how they inhibit DNA synthesis.

2.3.1.1 Folate antagonists, methotrexate (MTX)

Folic acid functions as a coenzyme in the transfer of CH_3 in the biosynthesis of purines and the conversion of dUMP (deoxyuridine monophosphate) to dTMP (deoxythymidine monophosphate). Folic acid must be reduced by dihydrofolate reductase (DHFR) to tetrahydrofolate (FH_4) **(figure 2.1)**. This provides single carbon units for a variety of metabolic processes.

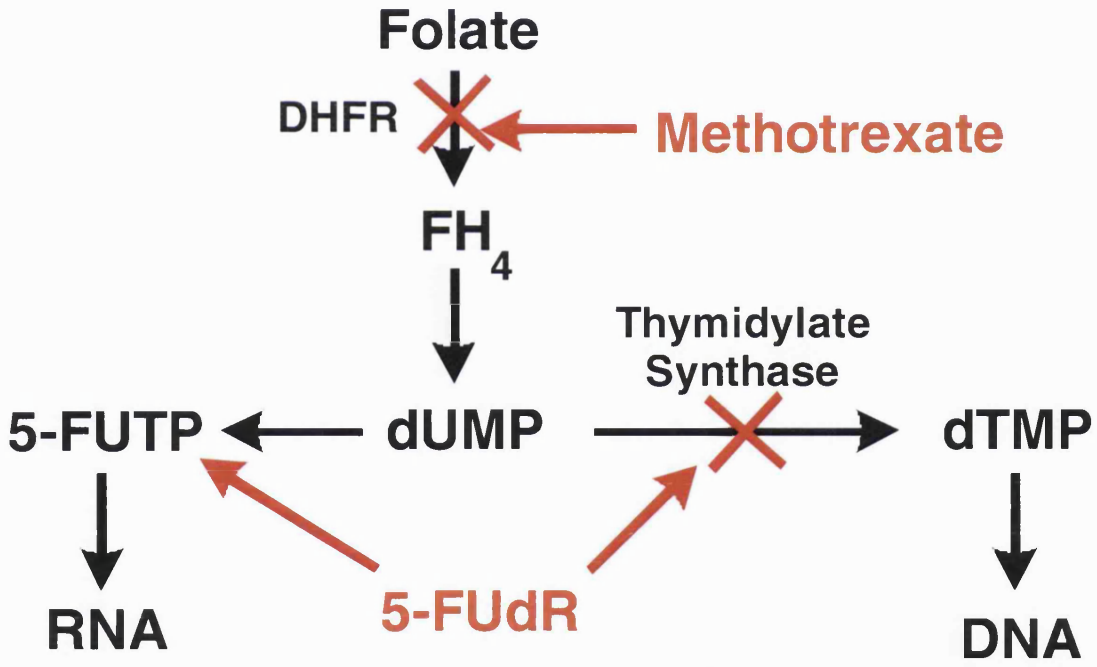

Figure 2.1: Sites of action of antimetabolites on DNA synthetic pathways. *MTX inhibits dihydrofolate reductase (DHFR), resulting in reduced tetrahydrofolate (FH_4) production and DNA synthesis inhibition. 5-FUdR irreversibly binds to thymidylate synthase, resulting in inhibition of dUMP to dTMP conversion and pyrimidine synthesis. There is 5-fluorouridine triphosphate (5-FUTP) incorporation in place of uridine triphosphate (UTP) during the synthesis of RNA.*

MTX **(figure 2.2)** primarily inhibits DHFR activity (Blakeley, 1995) and therefore inhibits newly made (*de-novo* pathway) purine and pyrimidines and causes

interference with both DNA synthesis and repair. MTX has many uses in the treatment of cancer and is routinely used for the treatment of head, neck, breast, lung and gastrointestinal tumours.

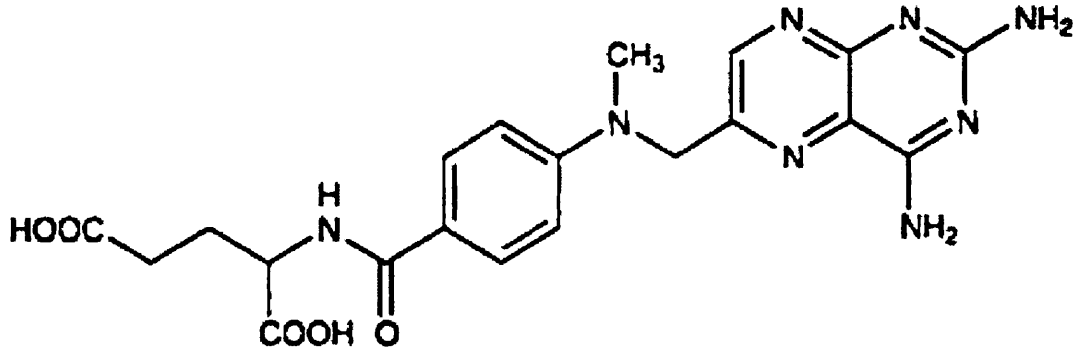

Figure 2.2: Structure of methotrexate (MTX).

2.3.1.2 Pyrimidine antagonists, 5-fluoro-5'-deoxyuridine (5-FUdR)

These drugs are direct inhibitors of thymidylate synthase, an important enzyme in pyrimidine synthesis. The most common of this type of antimetabolite include 5-fluorouracil (5-FU) and 5-fluorodeoxyuridine (5-FUdR) **(figure 2.3)** and closely resemble the pyrimidine bases uracil and thymine. Their best known effect is direct inhibition of thymidylate synthase. As a result, dTMP depletion occurs, and this in turn causes DNA synthesis inhibition, primarily in the S Phase of the cell cycle **(figure 2.1)**.

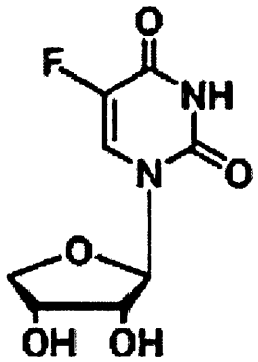

Figure 2.3: Structure of 5-fluoro-5'-deoxyuridine (5-FUdR).

5-FUdR was first synthesised in 1976 (Cook et al.), and has shown clinical activity against different types of solid tumours such as breast and colorectal tumours.

The third choice of agent belongs to the DNA alkylating class of anticancer agent, the nitrogen mustard known as melphalan.

2.3.1.3 Nitrogen mustards, melphalan

These agents form covalent bonds with nucleophilic groups found in proteins and nucleic acid, and therefore cause alkylation of DNA. They are most cytotoxic to rapidly proliferating cells, so they exert their greatest effect during DNA synthesis when there is less time for DNA to undergo repair. Once a nitrogen mustard such as melphalan **(figure 2.4)** is absorbed it is biotransformed to a highly reactive alkylating aziridinium ion that can then interact directly with DNA.

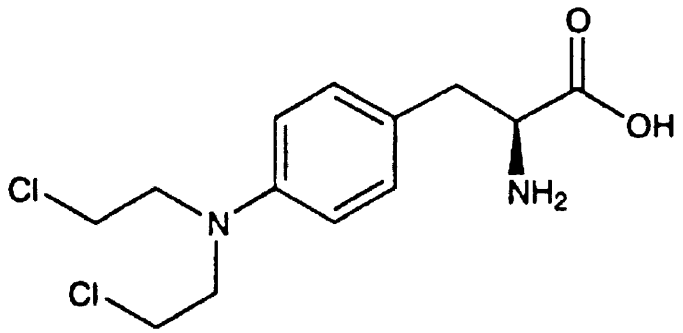

Figure 2.4: Structure of melphalan.

The reactive aziridinium ion can attack nucleophilic groups such as the N-7 of a guanine residue and thereby cause disruption in DNA synthesis by interfering with enzymes such as DNA polymerase (Colvin, 1999) **(figure 2.5)**. Melphalan was developed by Stock and Bergen over fifty years ago and is most commonly used to treat multiple myelomas (George et al., 1972), cancer of the ovary (Howell et al., 1984), and breast cancer (Fisher et al., 1979).

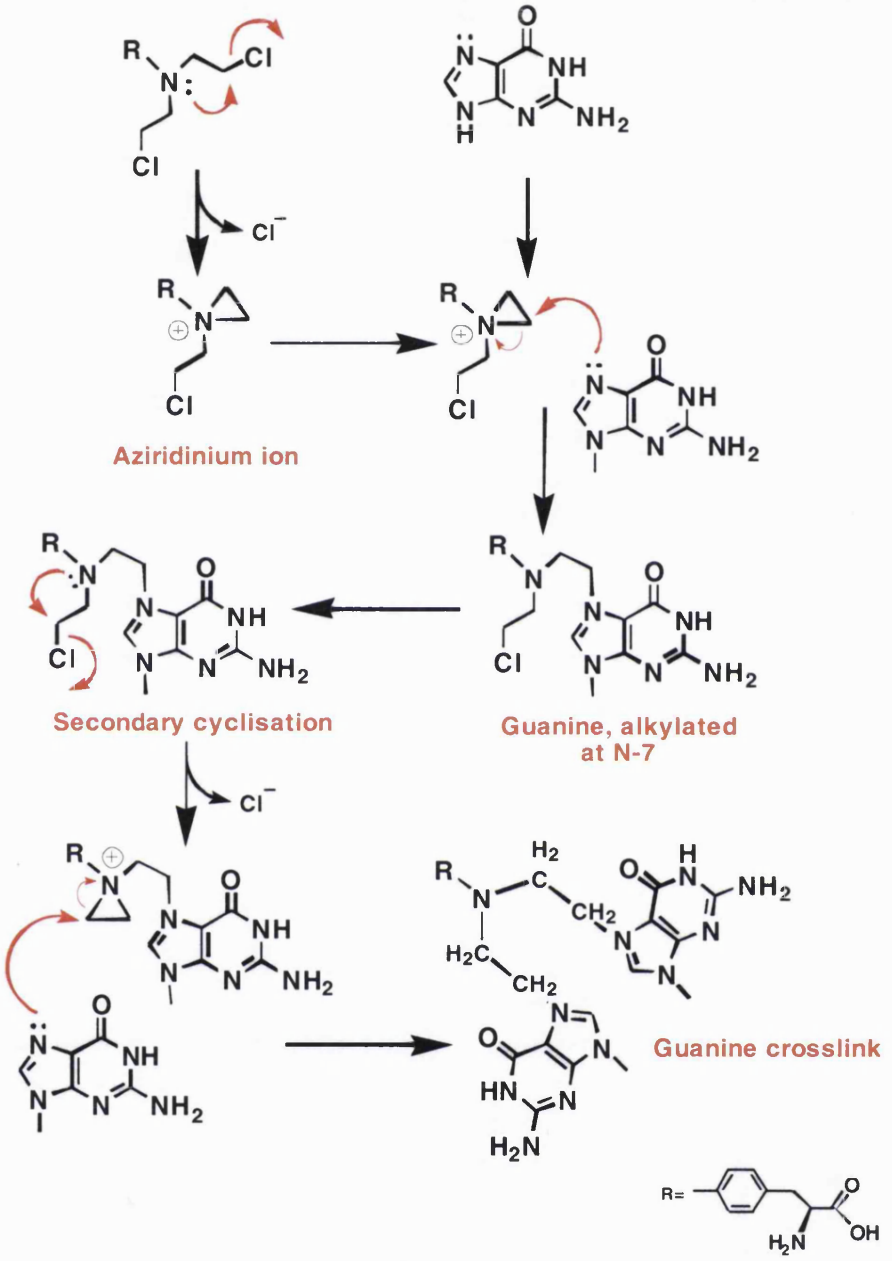

Figure 2.5: Mechanism for the alkylation of DNA with the nitrogen mustard, melphalan. *The loss of a chloride ion results in the formation of a reactive intermediate (aziridinium ion) that reacts with the 7-nitrogen of a guanine residue in DNA. The second chloroethyl arm can then undergo a second cyclisation and lose a second chloride. The second aziridinium ion can react with a second guanine residue in the opposite DNA strand causing cross-linkage of DNA.*

The fourth and fifth choices of anticancer drug both bear close similarity to one another and are members of the class of drugs known as the anthracylines.

Both daunorubicin and doxorubicin hydrochloride are isolated antibiotics from different species of *streptomyces* and bind tightly to double-stranded DNA leading to helix distributions. These intercalating drugs may also cause DNA strand breaks by inhibiting an enzyme known as topoisomerase II. This enzyme is known to assist with the untangling and unpackaging of DNA during replication and transcription.

2.3.1.4 The anthracyclines, daunorubicin and doxorubicin

The anthracyclines were first isolated from *Streptomyces peucetius* during the 1960s. Both daunorubicin **(figure 2.6a)** and doxorubicin **(figure 2.6b)** are structurally similar and only differ at the C14 position of the anthracycline where doxorubicin has an additional hydroxyl group.

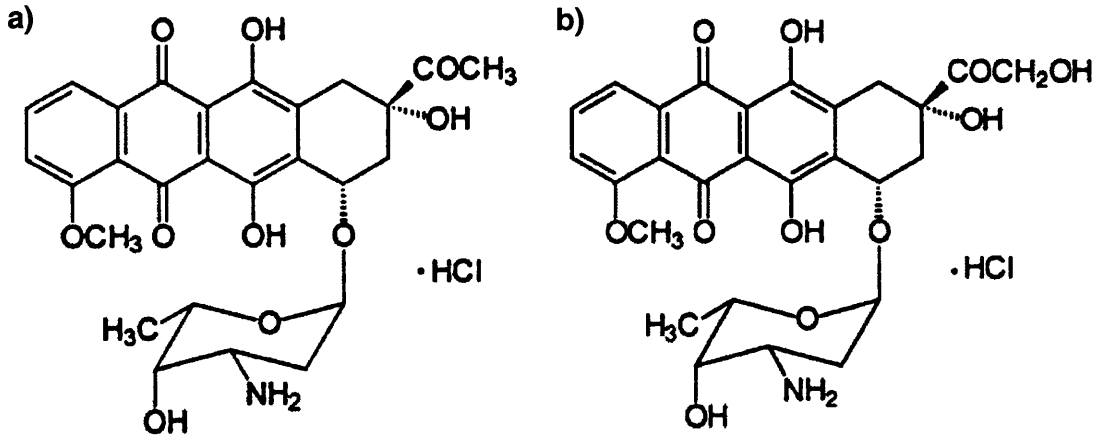

Figure 2.6: Structure of the anthracycline drugs: a) *daunorubicin hydrochloride; and* ***b)*** *doxorubicin hydrochloride. Agents differ in structure at the C14 position, where doxorubicin possesses an additional hydroxyl group.*

They act by intercalating in the minor groove between the base pairs of the DNA helix in a non-covalent way (Waring, 1970). The intercalation could result in local unwinding of the DNA double helix, resulting from separation of the purine and pyrimidine bases **(figure 2.7)**. These agents have also been shown to inhibit topoisomerase I and II but the precise mechanism involved in cell death remains unclear.

These intercalators are used routinely for cancer treatment; daunorubicin is commonly used to treat a number of leukaemias, although doxorubicin is the more commonly used drug and is used to treat tumours of the bladder, breast, liver, lung, prostate and stomach.

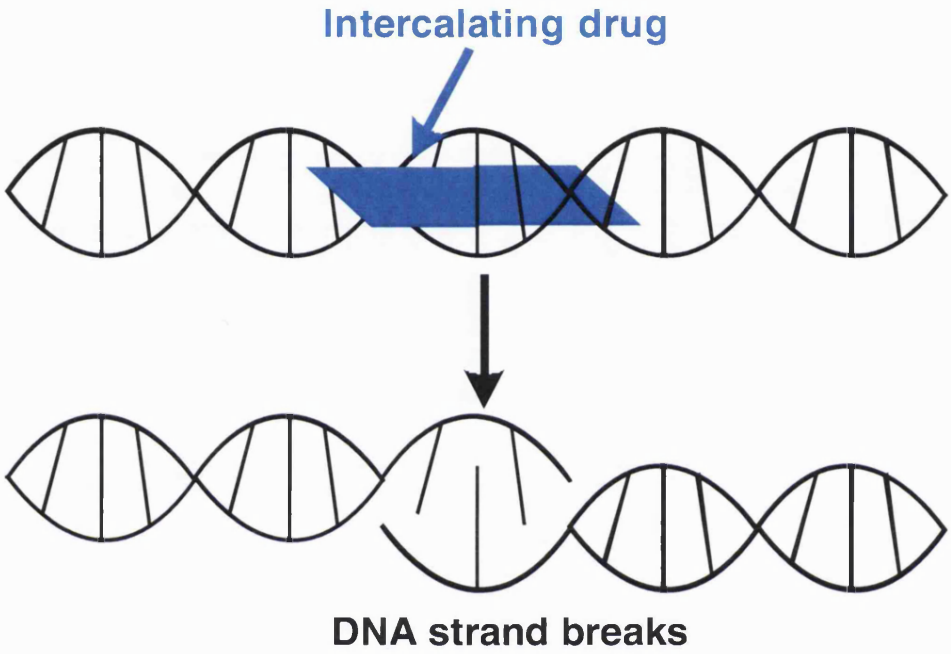

Figure 2.7: Anthracycline/DNA interactions. *The intercalating drugs form tight bonds to DNA and the planar regions of the drugs form a stack between purine and pyrimidine bases*

The sixth agent belongs to the class of agents known to inhibit topoisomerases, etoposide phosphate. Topoisomerases are enzymes that allow regions of DNA to become untangled and unpacked from its usual supercoil (Manuelidis and Chen, 1990) to allow DNA replication and transcription. These enzymes do this by temporarily causing DNA strand breaks, enabling changes to occur until the breaks can be resealed (Schneider et al., 1990). Type I enables a single strand break and type II causes a double strand break. By inhibiting topoisomerase the DNA strand breaks remain and the cells can die **(figure 2.8)**. These agents can be further grouped dependent on their interaction with DNA. The first group include intercalating compounds such as the anthracyclines (daunorubicin and doxorubicin) that can stabilize the cleavable complex. The second group can

stabilize the cleaved complex but do not induce DNA intercalation and include drugs such as etoposide and genistein

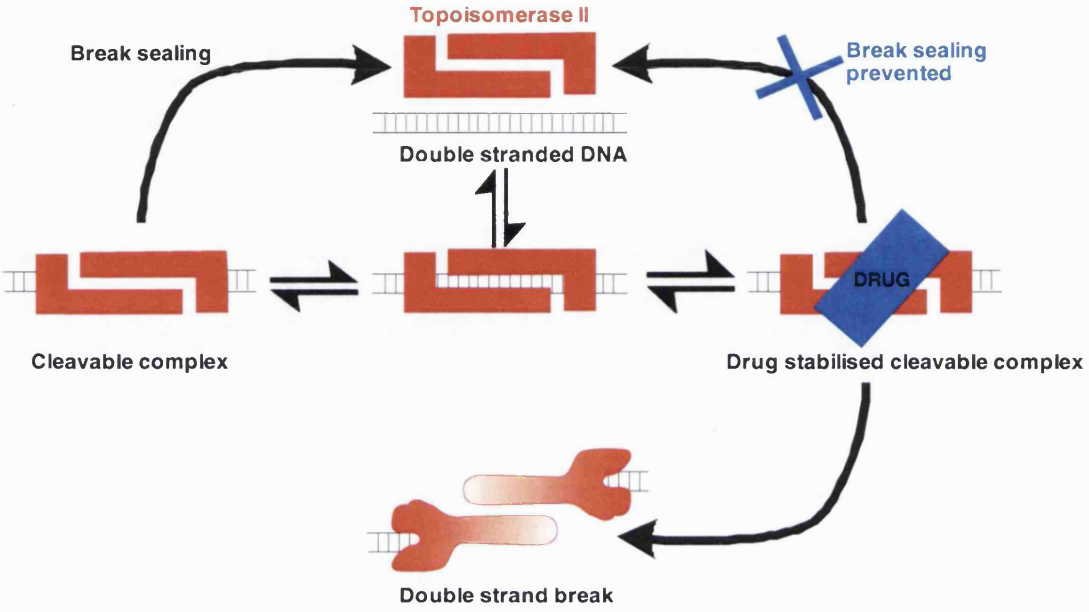

Figure 2.8: DNA damage induced by the inhibition of topoisomerase II. *Topoisomerase II inhibitor binds to the enzyme and stabilises the cleaved complex resulting in the strand break remaining.*

Etoposide **(figure 2.9)** is an active agent for the treatment of various solid tumours, such as ovarian cancer and small cell lung cancer. The drug is a topoisomerase II inhibitor and works by stabilising the cleaved complex, therefore resealing of the nicked DNA strand does not occur **(figure 2.8)** and the strand breaks remain and cells die. Although the exact process of cell killing is not fully understood, etoposide remains an effective drug in the fight against cancer (Koh et al., 2002).

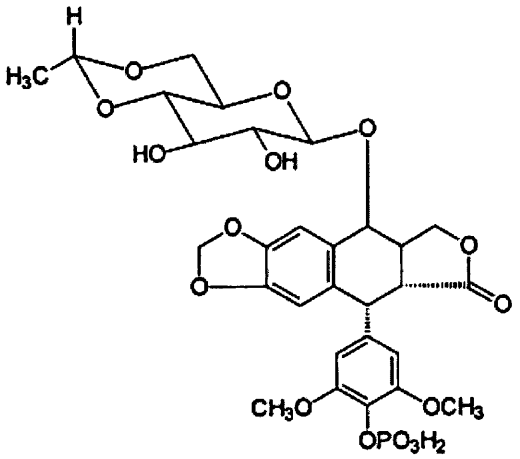

Figure 2.9: Structure of etoposide phosphate.

The final drug, vincristine sulphate, is an inhibitor of microtubule function. Microtubules are responsible for a range of cellular actions and are made up of free tubulin dimers and assembled polymers. These protein polymers oscillate from free tubulin dimers to assembled polymers and this equilibrium is vital in maintaining microtubule function. Microtubule inhibitors such as vincristine sulphate **(figure 2.10)** disrupt the equilibrium between these dimers and polymers as they bind to the tubulin dimers causing less microtubule formation and shifting the equilibrium towards disassembly **(figure 2.11)**.

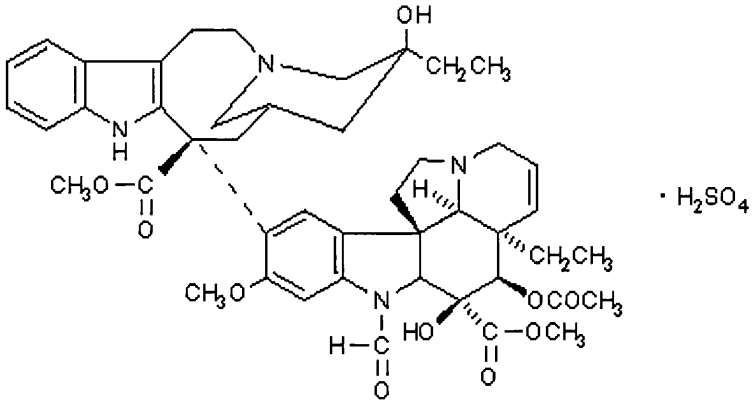

Figure 2.10: Structure of vincristine sulphate.

This results in the destruction of the mitotic spindle and the arrest of cells in the metaphase of mitosis and causes antimicrotubule drug induced cytotoxicity

(Jordan, 1993; Donaldson, 1994). Vincristine and a closely related vinca alkaloid, vinblastine, was first isolated from the plant *catharanthus rosea* (also known as *vinca rosea*) (Rowinsky and Donehower, 1991) and has been used to treat a number of non-solid tumours such as ALL (acute lymphocytic leukaemia) and Hodgkin's/non-Hodgkin's lymphomas in addition to breast cancer.

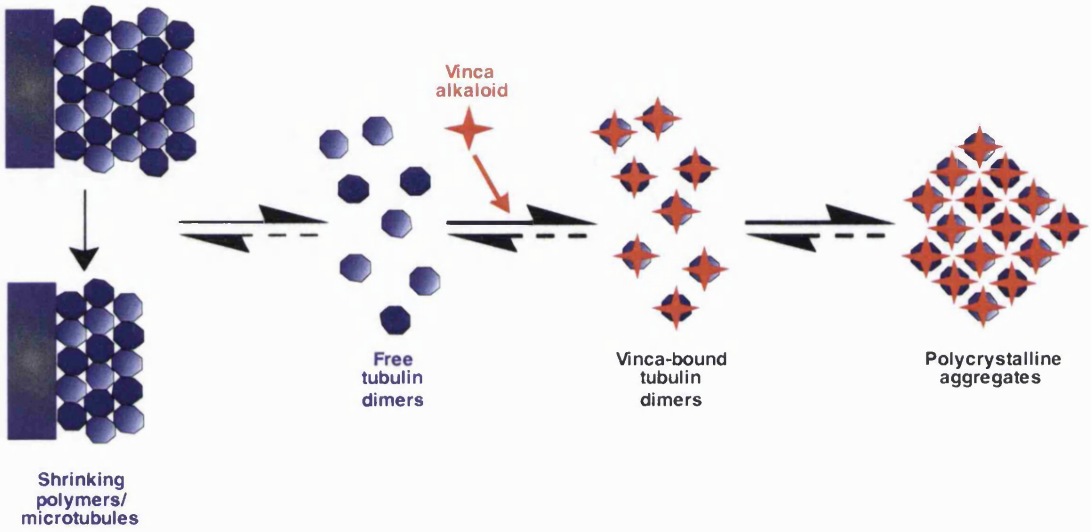

Figure 2.11: Disruption of the tubulin dimer/microtubule equilibrium by vinca alkaloid anticancer agents. *Binding of an agent such as vincristine to free tubulin dimers prevents formation of tubulin aggregates and microtubule assembly. This causes a shift in the equilibrium towards disassembly. Vinca bound tubulin dimers aggregate to form polycrystalline aggregates that further shifts the equilibrium and results in greater disassembly and further microtubule shrinkage.*

2.4 COMPOSITION OF THE MIXTURE

The predictions based upon the concepts of *independent action* and *concentration addition* are very much dependent on a number of factors. These include: the number of mixture components present in the overall mixture; the steepness of each component's dose response relationship; the fraction of each component in the mixture; and the use of non-linear regression model used to model a single agent's concentration and effects. To obtain a clear separation between the two predictions it has been shown that by increasing the number of

individual mixture components increases the separation between the two predictions will occur (Drescher and Boedeker, 1995; Silva et al., 2002). A study of a mixture of eight compounds, each displaying similar sloped dose-response curves to one another, was found to show a very clear separation between *independent action* and *concentration addition* predictions (Silva et al., 2002; Silva, 2003). The idea that all mixture components should display parallel concentration-response curves to formulate a prediction based on *concentration addition* was first discussed by Bliss (1939). This however was dropped as a requisite following revisions made by Hewlett and Plackett (1959). The predictions based upon *independent action* and *concentration addition* have been shown to cope well with response curves of varying slopes and maximal effects (Berenbaum, 1985; Altenburger et al., 2000; Rajapakse et al., 2002).

The careful selection of each component's concentration in the mixture avoids disproportionate contribution of a single agent to the overall mixture effect. The so-called *fixed ratio design* (Altenburger et al., 2000; Backhaus et al., 2000) has been developed and each component of the mixture is mixed at a fixed mixture ratio such as concentrations that produce 50% of the maximum cell kill, the median effect concentrations. An approach such as this ensures that no one component of the mixture contributes more to the total mixture effect and ensures that more potent components are present at lower concentrations in the mixture than less potent agents.

2.5 SELECTION OF ASSAYS FOR CYTOTOXICITY

In order to calculate accurate and complete mixture effect predictions, the entire concentration-response relationships are required to be known for each individual mixture component (Berenbaum, 1989; Backhaus et al., 2000). In order to ensure greater accuracy to base these predictions on, reproducibility in the assay of choice must be achieved. The assay must therefore be able to test a wide variety of treatment concentrations and in many replicates, so as to ensure the reliable calculation of mixture predictions.

2.5.1 Assessing for *in vitro* chemosensitivity

A number of *in vitro* assays have been used to assess a tumour's response to chemotherapy. All of these assays are based on the idea that there exists a relationship between the dose of drug administrated and the response of the tumour cell, i.e. cytotoxicity. It was first reported by Salmon and co-workers (1978), that there was a highly significant correlation between *in vitro* bioassay data from patient tumour stem cells and the clinical response of the patient. Although the clinical applications of *in vitro* assays has advanced little in the following years, the use of *in vitro* chemosensitivity testing on human tumour cells in the assessment of potential new agents, the understanding of mechanisms of drug action and drug resistance has become widespread. The advantages of using assays such as these to evaluate new forms of chemotherapy (including combinations), prior to human testing, are numerous **(table 2.1)** (Bellamy, 1992). Ineffective drugs and treatment regimes can be identified in this manner, therefore eliminating the need for the patients to undergo unsuccessful and toxic courses of chemotherapy. The patient can then be offered alternative therapies much sooner, increasing the chances of successful treatment.

A number of *in vitro* chemosensitivity assays exist, and these can be divided dependent on the way in which they assess a drug's cytotoxic effect. Assays can measure total cell population, such as assays measuring cell viability and metabolic activity, or they can measure the level of cell proliferation, clonogenic assays.

Table 2.1: Advantages to the use of predictive chemosensitivity assays
Initial screening of new agents
In vitro phase II studies of new agents
Tailor chemotherapy to an individual patient
Identify chemosensitivity for patients with unknown primary carcinomas
Establish patterns of cross resistance and sensitivity in relapsing patients

Cell viability assays such as the differential staining cytotoxicity (DiSC) (Weisenthal and Kern, 1991) and sulphorhodamine blue (SRB) assays (Skehan et al., 1990; Keepers et al., 1991), utilise the ability of dead or dying cells to take up a stain via permeable cell membranes. Metabolic assays rely on the measurement of a cell's metabolic activity as a determinant of the cell's viability. Numerous examples exist including the radiometric (BACTEC) assay, the adenosine triphosphate (ATP) bioluminescence assay (Kangas et al., 1984) and the 3,(4,5-dimethylthiazol-2-yl)2,5-diphenyltetrazolium bromide (MTT) assay (Mosmann, 1983; Carmichael et al., 1987). Assays used to measure cell proliferation, the so-called clonogenic assays, such as the human tumour stem cell assay, were developed by Hamburger and Salmon (1977). The assay is somewhat similar to antibiotic testing in bacteria. The tumour cell colonies proliferate on a soft agar surface while normal cells do not, and numbers of cells proliferating in drug treated assays are compared to untreated controls.

The various advantages and disadvantages for many of these assays have been discussed on a number of occasions (Bellamy, 1992; Weyermann et al., 2005). Each individual assay has its own unique advantages and disadvantages, and all of them suffer from an inability to model pharmacokinetic and pharmacodynamic properties that affect drug action *in vivo*. Though the use of such *in vivo* experimentation to explore new drugs and treatment regimens would be ideal, in reality due to ethical and cost implications the only real course of action to understand and test new treatments is via *in vitro* assay testing.

The choice of assay was determined by assessing an assay's ability to produce a high level of data in a rapid and reproducible manner. An assay such as the clonogenic assay was seen as being highly labour intensive, and required the set up of multiple plates to achieve sufficient data for single agents. The MTT assay in comparison provided a simple to use and rapid system to measure the cytotoxic effects of the seven anticancer agents. The data were highly reproducible and the assay worked well for cultured tumour cell lines, as were used for this study.

2.5.2 The MTT assay

The MTT assay was first described as a quantitative colorimetric assay by Mossman (1983), and was designed to measure mammalian cell survival and cell proliferation. The assay exploits the reduction of the yellow tetrazolium salt, MTT, by mitochondrial dehydrogenase of viable cells to a highly colourful blue formazan product. The assay measures cell respiration, and the amount of formazan produced is proportional to the number of functional mitochondria present in the assay. The formazan crystals are insoluble in aqueous media, so they must be solubilised in order to achieve accurate spectrophotometric UV absorbance measurements that directly relate to the number of metabolically active cells that are present.

Over the course of the 1980s differing solubilisation solutions have been developed to help improve the solubilisation of the formazan crystals. Mossman first used an acidic alcohol solution (1983), but this was enhanced three years later, improving the sensitivity of the assay and achieving a greater level of formazan solubilisation (Denizot and Lang, 1986). Optimisation in the amount of MTT used (Tada et al., 1986) and the use of an acidic detergent solubilisation solution (Hansen et al., 1989), further increased the accuracy of the measurements and reduced the level of serum precipitation (a recurring problem with the acidic alcohol solution).

A variation to this assay, the XTT assay, uses another tetrazolium salt, 2,3-bis(2-methoxy-4-nitro-5-sulfophenyl)-5-[(phenylamino)carbonyl]-2*H*-tetrazolium hydroxide. The crystals formed in this case are water-soluble, although metabolism of the XTT dye has been shown to be less efficient than the MTT dye in a variety of cell lines (Scudiero et al., 1988), so the MTT assay remains preferable (Bellamy, 1992).

The mechanism of MTT reduction by cells is not fully understood. Electron donors such as NADH and NADPH readily reduce the MTT salt to its formazan product **(figure 2.12)**. MTT has been found to be membrane impermeable which suggests that MTT is taken up by cells via an endocytic process and the reduced MTT is then transported to the cell surface through exocytosis (Liu et al., 1997). The fact that these processes require ATP production emphasises that the MTT assay acts as a measure of mitochondrial activity, a property that dead cells lack.

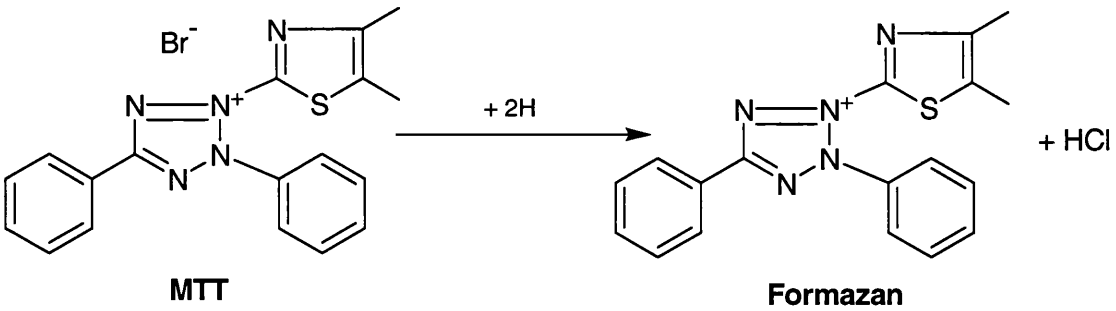

Figure 2.12: Formazan production by MTT. *The conversion of MTT tetrazolium salt to coloured formazan product*

One disadvantage of the MTT assay is its lack of differentiation of healthy cells from those that are in cell cycle arrest. Arrested cells reduce MTT as they are still metabolically active, so in the context of these studies the MTT assay was therefore used only to measure the level of drug induced cell death.

The aim of this study was to explore the accuracy of *independent action* to predict the joint mixture effects of a group of seven dissimilarly acting anticancer drugs. This was studied by measuring single agent cytotoxicity in two tumour

cell lines, the DU145 and MCF-7 cells, using the MTT assay to measure cell killing. As all the chosen test agents acted at dissimilar sites of action, the expectation that the model for *independent action* would provide the most accurate prediction for their mixture effects. This hypothesis was tested experimentally and in addition the model of *concentration addition* was assessed to provide a comparison for additive combination effects.

2.6 EXPERIMENTAL APPROACH

2.6.1 Cell lines and cell culture

The DU145 prostate-tumour-derived cell line (obtained from Professor John Masters, Urology Department, University College London, UK), was cultured in RPMI-1640 (Gibco, Invitrogen Corporation, U.K.) containing 10% $^{v}/_{v}$ Foetal Calf Serum (FCS, Gibco) and supplemented with 1% $^{v}/_{v}$ L-Glutamine (Sigma Chemical Company Ltd., Dorset, UK). The MCF-7 human breast cancer derived cell line (obtained from M. Dufresne, University of Windsor, Ontario, Canada), was cultured in Minimum Essential Medium-α with Glutamax-1 (MEM-α, Gibco), and supplemented with 5% $^{v}/_{v}$ FCS. The cells were incubated in a humidified atmosphere at 37°C in 5% CO_2. Cells were routinely grown in 25 cm^2 canted-neck tissue culture flasks (Greiner Bio-One, UK) split twice weekly using sterile PBS (phosphate buffered saline, Gibco) for washing and trypsin-EDTA (Gibco) for trypsinisation, after formation of a 70% confluent layer. The cells were used for a maximum of ten passages after thawing, so as to minimise the likelihood of genetic alteration. The cells tested negative for mycoplasma contamination.

2.6.2 MTT assay

2.6.2.1 MTT solution/solubilisation solution

MTT (Lancaster, Cat No. 11939) was prepared as a 5 mg/ml stock in sterile PBS, the solution was further sterilised by filtration through a 0.45 µm filter and was stored in 5 ml aliquots at -20°C and protected from the light until use. The solubilisation solution was prepared as 20% $^{w}/_{v}$ of sodium dodecyl sulphate (SDS, BDH, Dorset, UK) dissolved in a solution of 50% dimethylformamide (DMF, Sigma) and 50% deionised water. 2% $^{v}/_{v}$ of 80% glacial acetic acid and 1% $^{v}/_{v}$ 2 M HCl was added to adjust the pH of the solution to 4.7 (Hansen et al., 1989). A second solubilisation solution used by Mosmann and co-workers (1983) was made up for comparison with DMF solution, this contained 0.04 M HCl in isopropanol.

2.6.2.2 MTT assay procedure

The DU145 cells were seeded at a density of 1500 cells/well in flat bottomed 96 well microtitre plates (NUNC) to a volume of 90 µl. Eight wells were left with medium only to act as plate reader blanks and the plates were left to allow the cells to attach and grow by incubating at 37°C in 5% CO_2 for three days. The MCF-7 cells were seeded at a density of 3000 cells/well to a volume of 90 µl. A 10 µl volume of drug solution was then added in a dilution series of ten separate concentrations and left to incubate for another three days at 37°C. The medium and drug solution were removed from each well and replaced by a 120 µl volume of MTT/medium (20 µl of 5 mg/ml MTT added to 100 µl complete medium). After 3½h incubation time at 37°C to allow MTT reduction, a 150 µl volume of solubilisation solution was added to each well and left to incubate at 37°C overnight to allow complete solubilisation of the formazan product. The plate wells were then measured for their optical densities at 570 nm using a Labsystems Multiskan Multisoft plate reader to determine cell viability. For the

HCl/Isopropanol solubilisation solution the plates were read within 1h of addition (Mosmann, 1983).

The cell viability data was represented in a graphical form, plotted as "% cell killing" along the y-axis and "drug concentration" along a logarithmic x-axis. The measurement of "% cell killing" was an estimate of the combined drug induced cell killing, cytostatic effect and cell growth, and was calculated as a percentage of the viability of the untreated control cells.

2.6.3 Cancer drugs and dilution series

2.6.3.1 Drugs

Vincristine sulphate (>95% pure), 5-fluoro-5'-deoxyuridine (5-FUdR, 98% pure) and melphalan (>96% pure) were obtained from Sigma Chemical Company Ltd (Dorset, U.K.). Methotrexate (MTX, >95% pure), doxorubicin hydrochloride (>95% pure), daunorubicin hydrochloride (>95% pure) and etoposide phosphate (>90% pure) were obtained from CN Biosciences (Nottingham, UK). The drugs were used as supplied or made up to 10-1 mg/ml stock solutions in deionised, sterile H_2O and left stored in the dark at -20°C or at 4°C dependent on drug storage conditions.

2.6.3.2 Dilution series

The serial dilutions were made up from the drug stock solutions and were made freshly for each experiment. The ten separate drug concentrations for each individual drug encompassed doses that caused close to zero cell kill to maximal cell kill, these concentrations were decided based upon previous ranging finding studies. Using scatter plots of corrected absorbance values (% cell killing) versus $\log_{10}$ drug concentration, a suitable best-fit nonlinear regression model was selected to analyse the data sets.

2.6.4 Nonlinear regression analysis

2.6.4.1 Use of nonlinear regression models to fit the data

All single agents and mixtures were tested using ten different concentrations, each with at least three replicates run in parallel. The best fitting concentration-response relationship for each agent was determined using a number of nonlinear regression models as described by Scholze and colleagues (2001). Three regression models provided the best fit for the concentration-response relationships for the single agents and the observed mixture effects. These are described in **table 2.2**, in addition to their inverse functions.

Table 2.2: Regression models

Model	***Function***	***Inverse function***
Chapman	$E = \theta_4 (1 - \exp(-\theta_3 . C))^{\theta_2}$	$C = \frac{\ln\left(1 - \left(\frac{E}{\theta_4}\right)^{1/\theta_2}\right)}{-\theta_3}$
Generalised Logit (GL)	$E = \theta_4 \frac{1}{(1 + \exp(-(\theta_1 + \theta_2 \log_{10}(C)))^{\theta_3}}$	$C = \mathrm{POW}\left(\frac{-\ln\left(\left(\frac{1}{(E/\theta_4)}\right)^{1/\theta_3} - 1\right) + \theta_1}{\theta_2}\right)$
Hill	$E = \theta_1 + \left(\frac{\theta_4 - \theta_1}{1 + (C/\theta_2)^{\theta_3}}\right)$	$C = \theta_2 \left(\frac{1}{(\theta_4 - \theta_1)/(E - \theta_1) - 1}\right)^{1/\theta_3}$

POW (*t*) means to raise the value of 10 to the power *t*. E, effect. C, concentration. θ_1, θ_2, θ_3 *and* θ_4, parameters for regression models.

The software program NLREG (Phillip H. Sherrod, USA) was used for the fitting procedure to generate model parameters. The 95% confidence intervals were also calculated for the regression curves using GraphPad Prism 4 software

(GraphPad Software, Inc, USA) and the curve plotting was carried out using SigmaPlot v.8.02 (SPSS Inc, USA).

2.6.5 Calculation of predicted mixture effects

Once dose-response relationships were obtained for each of the single agents and suitable fits established, the predicted responses of the mixture of the seven agents at their median effect levels were calculated. The expected responses were calculated using the two concepts for mixture analysis as described before, *independent action* and *concentration addition.*

The expected mixture effects were tested experimentally using the fixed ratio design as described by Altenburger and colleagues (2000) and Backhaus and colleagues (2000). A master mixture (2 mM for the DU145 cells and 4 mM for the MCF-7 cells) was made up comprising of the seven agents at a fixed mixture ratio and this was serially diluted to cover the range of concentrations generated from the mixture predictions. The mixture ratio chosen was equivalent to the median effect concentration (i.e. each agent was present at concentrations to produce half maximal effect).

The joint effect of the mixture was calculated for both the *concentration addition* and *independent action* concepts using the regression models detailed in **table 2.2**. The equations for these two concepts can be found in **chapter 1** in **section 1.3** and can be expressed in the following manner:

Concentration addition

This concept can be described by the equation:

$$\sum_{i=1}^{n} \frac{c_i}{EC_{xi}} = 1 \qquad \textbf{(1.1)}$$

Where n is the number of mixture components, EC_{xi} is the concentration of the ith mixture component that provokes x% effect when applied on its own, and c_i is the concentration of the respective component in the mixture. The fraction of agent, f_i in the total mixture concentration, EC_{MIX}, can be related to the concentration of a single agent, c_i by the equation:

$$c_i = f_i \times EC_{MIX} \quad \textbf{(2.1)}$$

Substituting this into **equation 1.1** gives:

$$\sum_{i=1}^{n} \frac{f_i \times EC_{MIX}}{EC_{xi}} = 1 \quad \textbf{(2.2)}$$

This equation can be rearranged in terms of EC_{MIX} to:

$$EC_{MIX} = \left[\sum_{i=1}^{n} \frac{f_i}{EC_{xi}} \right]^{-1} \quad \textbf{(2.3)}$$

Knowledge of the fraction of each mixture component in the total mixture (f_i) and of the concentration of each agent i that produces an effect, E enables the calculation of EC_{MIX} that provokes the same effect by using **equation 2.3**. The effect concentrations, EC_{xi} can be calculated using the best fit regression model inverse function as shown in **table 2.2**.

Independent action

The model for *independent action* allows calculation of the overall mix effect, $E(c_{mix})$ by using the following expression

$$E(c_{mix}) = 1 - \prod_{i=1}^{n}[1-E(c_i)] \qquad \textbf{(1.2)}$$

$E(c_i)$ is the fractional possible effect that cannot exceed 1, and when applying this to toxic effects $TE(c_i)$, then a maximal effect E_{MAX} must be defined. In this case it would be 100% cell killing, and this can be represented by:

$$E(c_i) = \frac{TE(c_i)}{E_{MAX}} \qquad \textbf{(2.4)}$$

The effect $TE(c_i)$ can be estimated by using the appropriate regression model, $R_i(c_i)$ for each individual agent **(table 2.2)**, and this modifies **equation 2.4** in the following manner:

$$TE(c_i) = R_i(c_i) \qquad \text{so} \qquad E(c_i) = \frac{R_i(c_i)}{E_{MAX}} \qquad \textbf{(2.5)}$$

The overall fractional effects are given by substituting this back into **equation 1.2** and gives:

$$E(c_{mix}) = 1 - \prod_{i=1}^{n}\left[1 - \frac{R_i(c_i)}{E_{MAX}}\right] \qquad \textbf{(2.6)}$$

By multiplying the fractional effects **(equation 2.6)** by E_{MAX} we can compare the predicted effects with the *concentration addition* predictions,

$$E(c_{mix}) = E_{MAX}\left[1 - \prod_{i=1}^{n}\left[1 - \frac{R_i(c_i)}{E_{MAX}}\right]\right] \qquad \textbf{(2.7)}$$

2.7 RESULTS

2.7.1 Optimisation of MTT assay

During the course of running the MTT assays we looked at the reproducibility of MTT absorption using two different MTT solubilisation protocols. The original and least toxic form was used by Mosmann and co-workers (1983), using an acidic/alcohol (HCl/Isopropanol) solubilisation solution. A more recent development of this assay in 1989 (Hansen et al.) used a DMF based solution (see **section 2.2.2.1** of this chapter). The comparison of the two solutions was conducted by treating the DU145 cells with a concentration range of doxorubicin. At higher drug concentrations there was little difference in the absorption readings for either solution **(figure 2.13)**, however there was greater scatter of the readings at low concentrations of the drug using the HCl/Iso solution compared to the readings from the DMF solution **(figure 2.13)**. There was less variability in the estimation of cell killing for lower concentrations of doxorubicin using the DMF solubilisation solution as it has a greater ability to solubilise the formazan crystals than the HCl/Iso solution. The increased scatter for lower drug concentrations using the HCl/Iso solution meant that accurate estimations for low dose effects were difficult and would make joint effect predictions based on *independent action* very difficult to calculate (Faust et al., 2003). The DMF solution was deemed as the preferred choice of solubilisation solution and was used for each subsequent MTT assay.

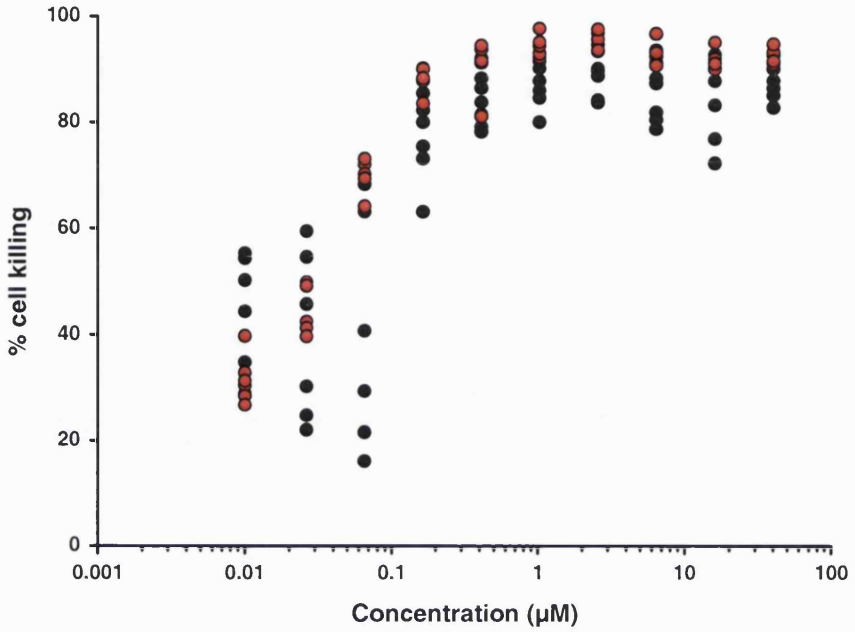

Figure 2.13: Optimisation of MTT solubilisation solution. *Greater variation in data points at low drug concentrations using the HCl/Iso solution (black circles) compared to the DMF solution (red circles). This demonstrates the improved formazan crystal solubilisation of the DMF solution over the acid/alcohol solution. Results are from two independent experiments.*

2.7.2 The variability of the assay

In order to calculate accurate predictions for joint mixture effects, single agent toxicity data must be of reliable and reproducible quality, therefore the variability of the MTT assay was tested with experiments run over a six month period of time. **Figure 2.14** shows the results for the anticancer agent, 5-fluoro-5'-deoxyuridine when tested on DU145 cells. The coloured circles represent each set of single agent data generated from a single assay run for the drug. The variability of the results generated from one MTT assay run to the next was minimal, and demonstrates the ability to 'pool' single agent data from various assay runs to generate a single agent dose-response relationship.

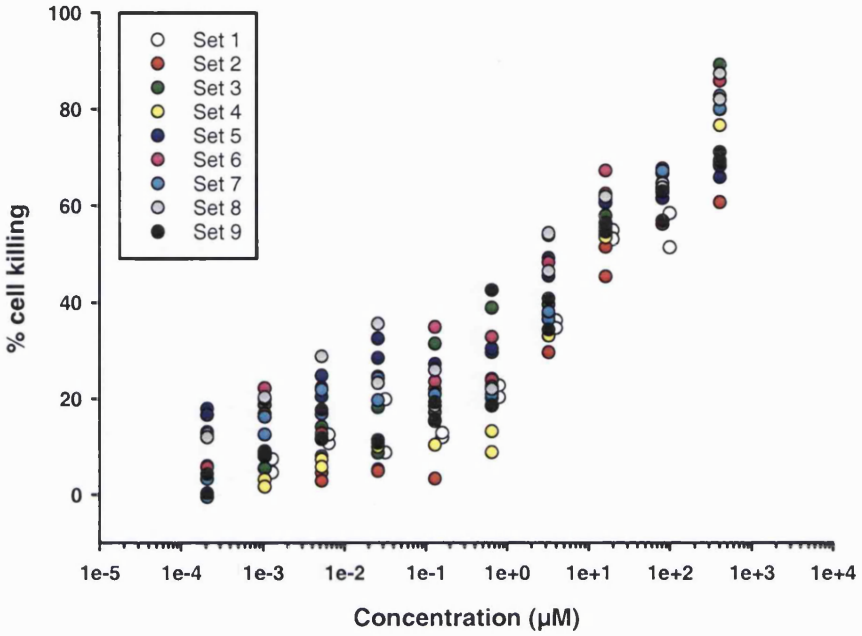

Figure 2.14: Experimental variability of the MTT assay. *Inter-experimental variability of cytotoxicity of 5-fluoro-5'-deoxyuridine on DU145 cells for nine independent experiments (each set of coloured circles). This demonstrated minimal variation between the sets of data, and the 'pool-ability' of multiple data sets.*

Although there was no evidence of variability between different batches of cells, experiments were carried out using cells of similar passage number to ensure greater reproducibility and this also reduced the likelihood of variations between cell batches.

Variations in experimental data were always a potential danger in experiments of this nature, and as reliable single agent data were a prerequisite to generate accurate joint effect predictions the critical nature of assessing single agent data became most important. **Figure 2.15** shows the dose response of vincristine sulphate when administered to DU145 cells. Ten sets of data are represented by coloured circles and triangles, eight of these sets bare close resemblance to one another (coloured circles), and the other two sets (coloured triangles) were distinctly dissimilar and demonstrated a bimodal response.

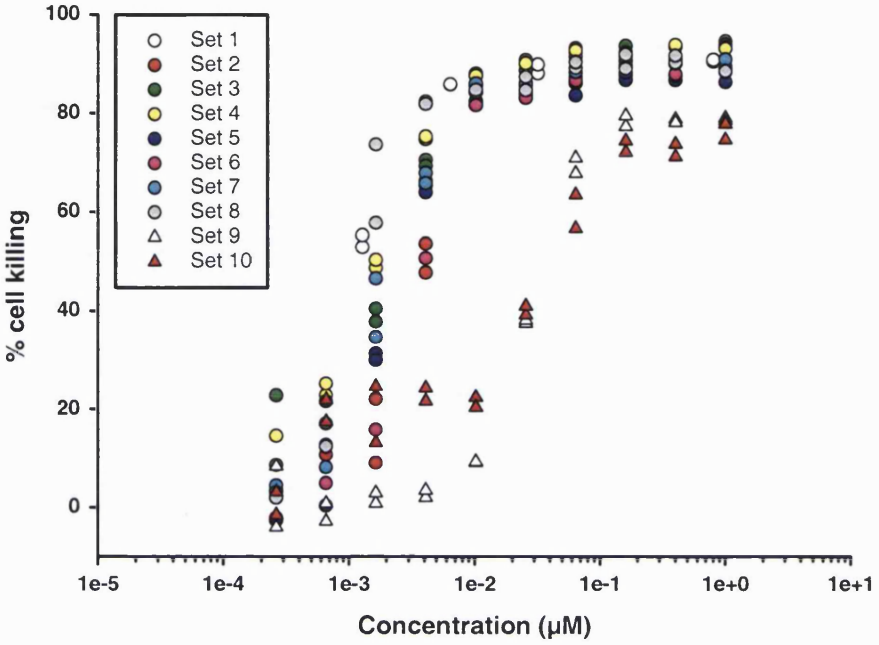

Figure 2.15: Single agent data sets and determination of single agent 'pool'. *DU145 cells treated with vincristine sulphate demonstrated a highly toxic effect for eight sets of experiments (coloured circles). Single agent dose response for vincristine showed evidence of a bimodal response group, two sets of data (coloured triangles). The set of eight experiments was used to generate a regression fit for vincristine sulphate* ***(figure 2.20)****.*

Critical assessment for the single agent response meant that a regression curve including all ten sets of data would not be representative for either sets of data, and that an accurate relationship for vincristine sulphate was best given by using the eight sets of data (circles), as opposed to the other two **(figure 2.20)**.

2.7.3 Concentration-response analysis for the DU145 cells

All the tested anticancer drugs induced a concentration-dependent response in the MTT assay, resulting in decreased cell viability with increasing drug concentration. The cytotoxicity of the seven different agents to the DU145 cells are shown in **figures 2.16-2.20**, and their best-fit regression parameters summarised in **table 2.3**.

2.7.3.1 Single agent responses

2.7.3.1.1 The antimetabolites:

The dose-response curves for both of these agents showed variations in maximal effects, shape and slopes. The curve for 5-FUdR was shallower than any of the other single agents, as is shown in **figure 2.16a**, the range from maximum effect to minimal effect was seven orders of magnitude. In contrast, the slope for the MTX curve was much steeper and the range from minimum to maximum effect was only three orders of magnitude **(figure 2.16b).** MTX displayed the lowest level of maximum cell kill of all seven agents, where the maximum effect was 63.87% of total cells killed.

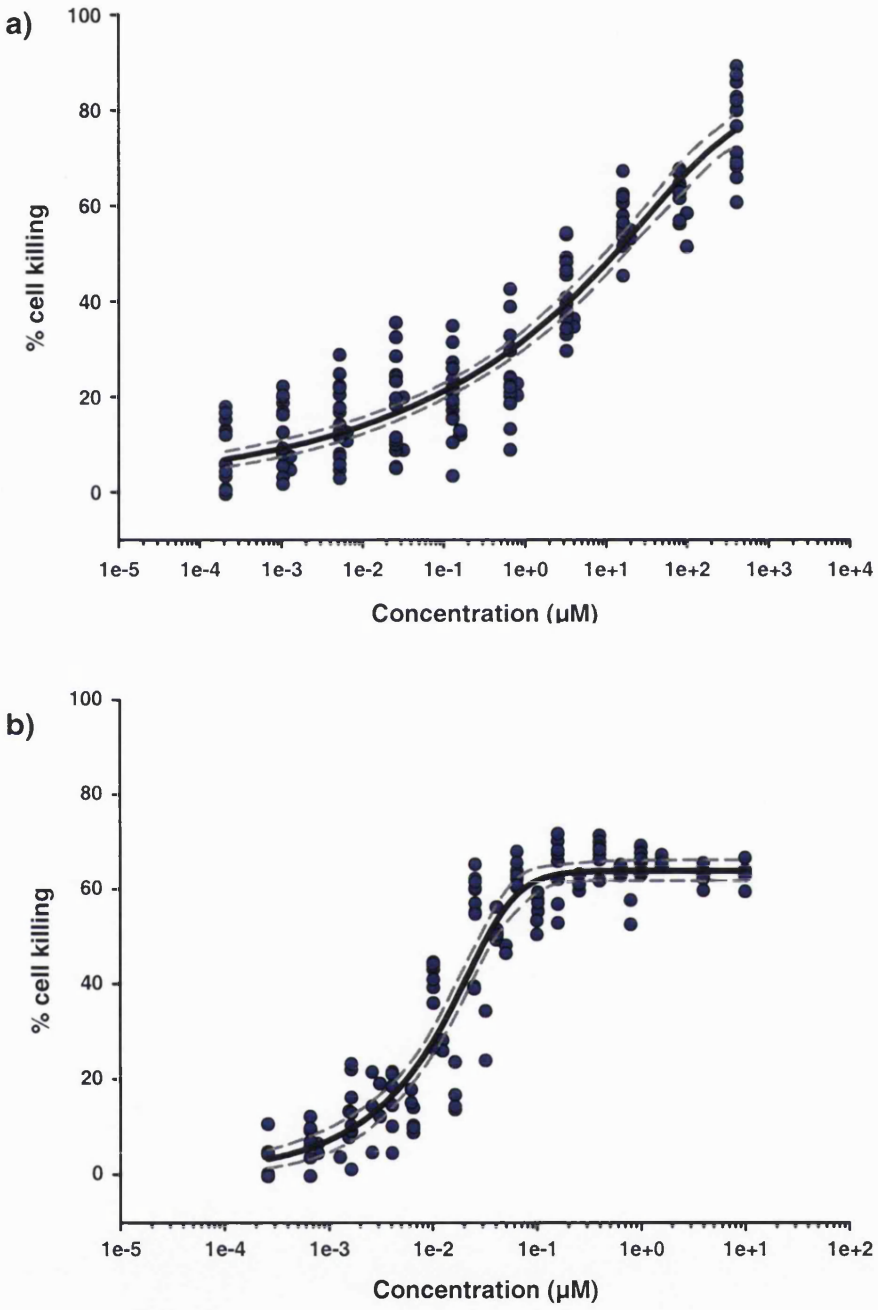

Figure 2.16: Dose response of DU145 cells when treated with 5-fluoro-5'-deoxyuridine and methotrexate. *Individual data points are represented by blue circles (●). The GL model represented by a thick black line was used for both* ***a)*** *5-FUdR and;* ***b)*** *methotrexate. Grey dotted lines represent the upper and lower 95% confidence interval for the regression fit. The data were from a minimum of three independent experiments.*

2.7.3.1.2 Melphalan

A common method for killing tumour cells is to target rapidly dividing cells. DNA alkylators such as melphalan are most effective during DNA synthesis, and bind covalently to nucleophilic groups found on proteins and nucleic acid. **Figure 2.17** shows the effect of treating DU145 cells with a range of concentrations of melphalan and the resulting best-fit curve shows a clear maximal effect. The slope of the curve was much steeper than for 5-FUdR as the range from maximum to minimum effect was only four orders of magnitude. The level of scatter towards the lower melphalan concentrations indicates a heteroskedastic relationship with increased variance at lower concentrations, although the best-fit regression model of general logit copes well in the higher drug concentration range.

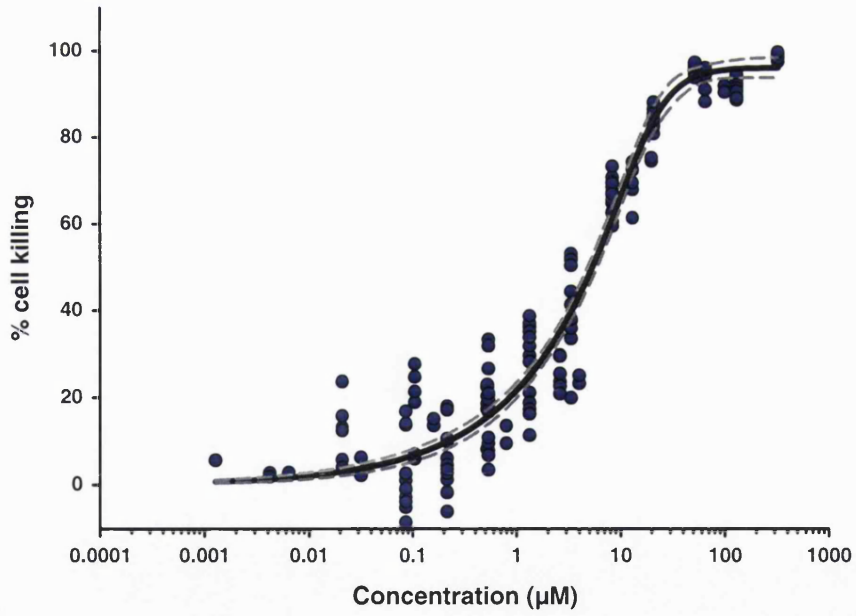

Figure 2.17: Dose response for DU145 cells when treated with melphalan. *The regression model was based upon the GL model shown by the thick black line. Grey dotted lines represent the upper and lower 95% confidence interval for the regression fit. The data were from a minimum of three independent experiments.*

2.7.3.1.3 The anthracyclines

The anthracylines share structural similarity and as shown in **figures 2.18a & b** share similar potency to killing DU145 cells. The slopes for the dose-response relationships for the two agents show great similarity and the range from maximum to minimum cell killing was only four orders of magnitude for both agents. Maximal effects are approximately the same for both drugs, as shown in **table 2.3**, and the median effect concentrations which were 0.0183 μM for daunorubicin and 0.0178 μM for doxorubicin are also very similar.

2.7.3.1.4 Etoposide phosphate

This topoisomerase II inhibitor induces single strand breaks in DNA and is commonly used to treat non-small cell lung carcinomas, lymphomas and stomach tumours. The cytotoxicity of etoposide phosphate when applied to DU145 cells is shown in **figure 2.19**. The slope and maximal effect was similar to that of daunorubicin and doxorubicin, although the etoposide curve was shifted to the right of both of these curves. The slope for the curve representing the etoposide phosphate effect ranged over five orders of magnitude from a maximal to minimal effect. The chapman regression model copes well with the higher range concentrations of etoposide. At lower concentrations of etoposide phosphate we can see a slow and gradual reduction in cell killing with decreasing drug concentration. This results in a fairly shallow dose-response relationship ranging from 0.1 nM to 1 μM etoposide. The median effect concentration for this drug was much higher than those for the anthracyclines **(table 2.3)** and demonstrates that this drug was much less toxic to DU145 cells than the intercalating agents even though they all have been found to inhibit the topoisomerase II.

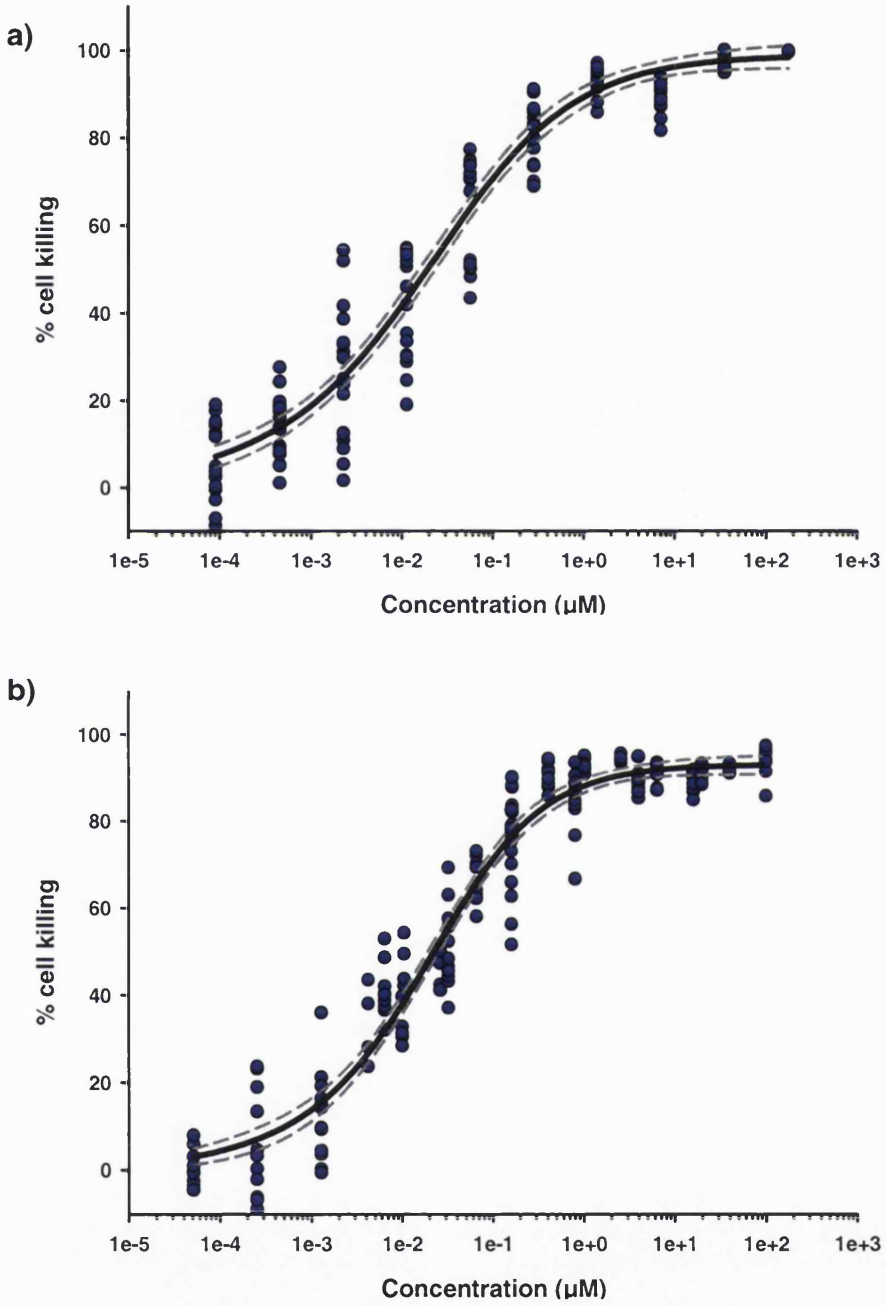

Figure 2.18: Dose response for DU145 cells when treated with daunorubicin and doxorubicin. *The best fit regression model is shown by the thick black lines. The GL model was used for both* ***a)*** *daunorubicin and;* ***b)*** *doxorubicin. Grey dotted lines represent the upper and lower 95% confidence interval for the regression fit and the data shown were from a minimum of three independent experiments.*

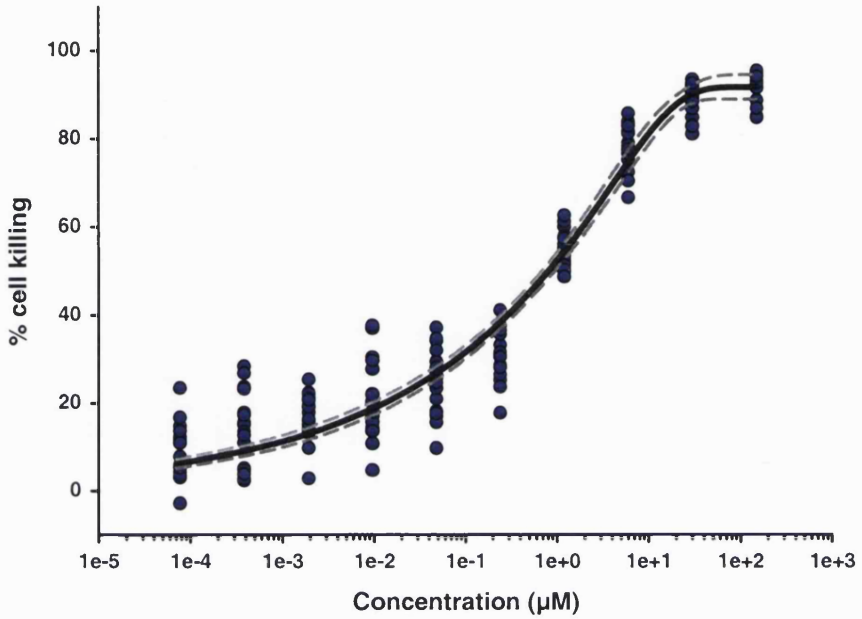

Figure 2.19: Dose response for DU145 cells treated with etoposide phosphate. *The regression model for this agent was based upon the chapman model shown by the thick black line. Grey dotted lines represent the upper and lower 95% confidence interval for the regression fit. The data were from a minimum of three independent experiments.*

2.7.3.1.5 Vincristine sulphate

The most potent of the seven anticancer drugs tested on these cells was vincristine sulphate. The dose-response curve for this drug showed the steepest slope, as the range from minimum to maximum effect was less than two orders of magnitude **(figure 2.20)**. The median effect concentration was also the lowest of all of the agents, as shown in **table 2.3**, meaning that it would be present at the lowest concentration of all agents in the seven-component mixture.

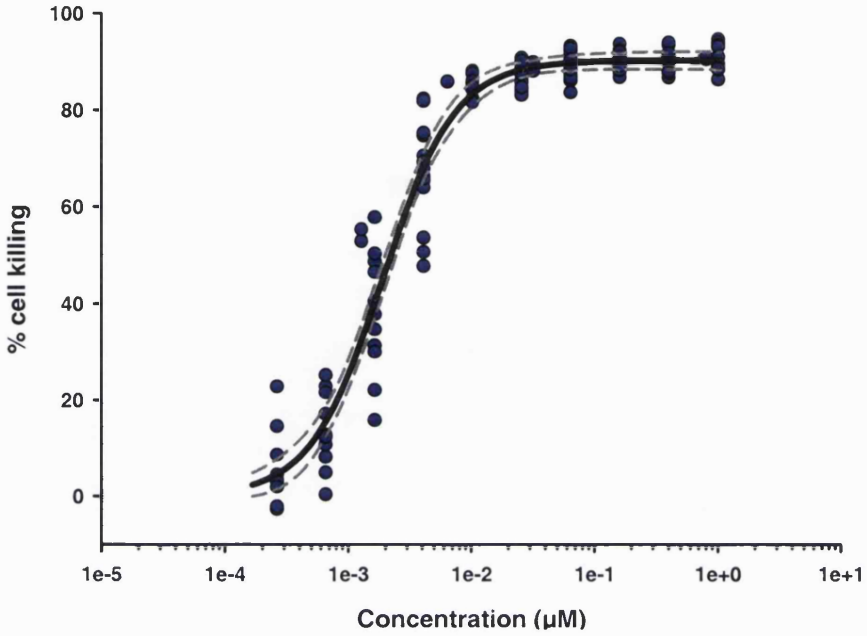

Figure 2.20: Dose response for DU145 cells treated with vincristine sulphate. *The regression model for this agent was based upon the GL model shown by the thick black line. Grey dotted lines represent the upper and lower 95% confidence interval for the regression fit. The data were from a minimum of three independent experiments.*

Table 2.3 shows a summary of the estimated best-fit regression model parameters for each single agent, the mixture ratios of the individual mixture components, and calculated median effect concentrations. This data was used to calculate joint effect predictions based on *independent action* and *concentration addition*.

Table 2.3: Summary of the parameters for the best-fit regression model for each individual agent for DU145 cells

Compound	*Regression model*	*Fraction of drug in mix*[a]	θ_1	θ_2	θ_3	θ_4 *(max)*	*Median effect (μM)*
5-fluoro-5'-deoxyuridine	Gen. Logit	0.3202	-4.1751	1.8182	0.2298	84.2346	4.6246
Daunorubicin	Gen. Logit	0.002028	1.8874	1.3536	0.7275	98.9299	0.0183
Doxorubicin	Gen. Logit	0.002566	2.4716	1.7404	0.6792	93.0738	0.0178
Etoposide phosphate	Chapman	0.2241	-	0.2234	0.08514	91.7303	0.5396
Melphalan	Gen. Logit	0.4497	-6.4646	5.0607	0.2305	96.1042	4.9336
Methotrexate	Gen. Logit	0.001260	7.0842	5.0702	0.2680	63.8708	0.0128
Vincristine sulphate	Gen. Logit	1.172×10^{-4}	9.2294	3.3882	1.0062	90.2313	0.001899

[a] Denotes the ratio of each mixture component and its concentration in the total mixture

θ_1, θ_2, θ_3 and θ_4 are estimated model parameters of the non-linear regression models (summarised in **section 2.5.4, table 2.2**)

2.7.3.2 Predicted and observed mixture effects for DU145 cells

The regression models shown in **section 2.5.4** were used to estimate single agent response curves for the seven individual anticancer drugs. The parameters generated from these fits **(table 2.3)** were used as described in **section 2.5.5** to predict the expected mixture effects of a mixture of seven dissimilarly acting anticancer drugs. The hypothesis for a mixture such as this should result in the prediction based on *independent action* being the most accurate. To explore whether this was the case the models of *independent action* and *concentration addition* were used to calculate the combined effects of a mixture of drugs combined at their respective median effect concentrations. The combined effects were then tested experimentally and compared to the calculated predictions as shown in **figure 2.21**.

The response predicted by *independent action* was surprisingly inaccurate when compared to the regression fit of the observed mixture effects. This was despite the mixture being compiled with a selection of anticancer drugs with dissimilar sites of action. The *independent action* prediction led to a significant overestimation of the observed combined effects, and these were consistently greater than one order of magnitude lower across the entire observed mixture effect range. In contrast the prediction based using *concentration addition* followed close approximation to the observed mixture effects. Comparing the relative concentrations for EC_{50} effects **(figure 2.21)**; for the observed mixture data this was 0.94 μM, for *concentration addition* this was 1.43 μM and for *independent action* this was a much lower value of 0.10 μM.

Both the observed mixture regression model and the *independent action* prediction shared similar maximal responses. The *concentration addition* prediction was however limited in its full effect range, the basis for calculations using this model was reliant upon single agent effect data. As the effect range for methotrexate was limited from zero cell killing to 63.87% **(figure 2.16b)**, the maximal effect predicted using *concentration addition* was limited to this

maximal effect as well, therefore limiting the overall effect range for *concentration addition.*

The slope for each prediction model was similar, both ranging to five orders of magnitude from minimal to maximal cell kill. The observed mixture regression model curve was of a steeper slope than either prediction models, ranging from only four orders of magnitude.

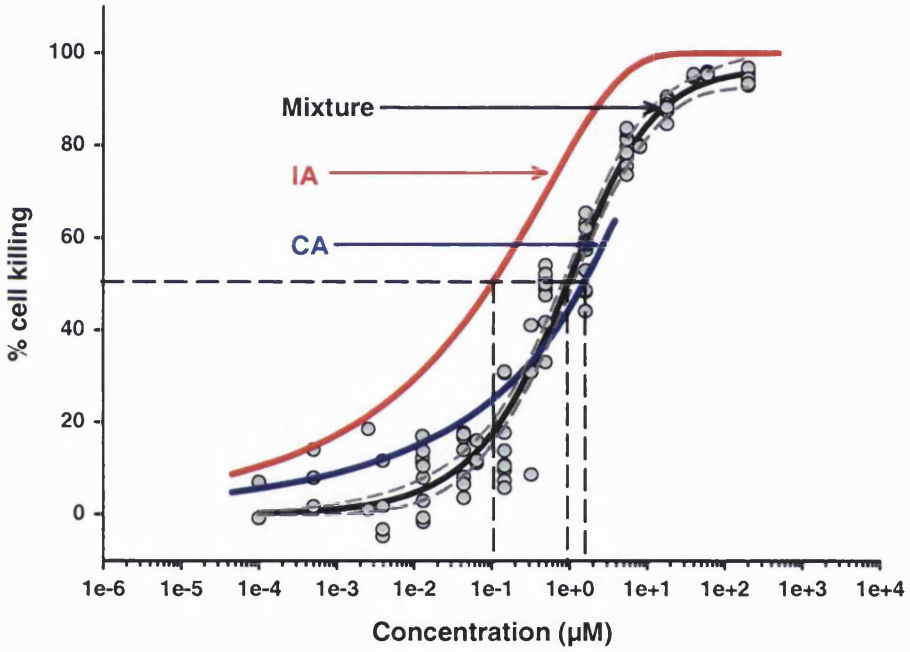

Figure 2.21: Predicted and observed effects of a mixture of the seven tested anticancer drugs for DU145 cells. *Individual data points represented by grey circles (●) from three independent experiments and the best-fit regression model based upon the general logit model shown by the thick black line, labelled mixture. Grey dotted lines represent the upper and lower 95% confidence interval for the regression fit. The solid red line shows the predicted combined effects derived from independent action, labelled IA. The solid blue line labelled CA shows the prediction based upon concentration addition. The black dotted lines represent the EC_{50} concentrations for each response curve. The data was from four independent experiments.*

2.7.3.3 *Contribution of single agents to the overall mixture effects for the DU145 cells*

The initial, shallow portion of the *concentration addition* prediction curve can be described by relative single agent contributions to the overall mixture effect, as shown in **figure 2.22**. The figure describes the elevated contribution that one or two agents have to the overall *concentration addition* prediction model. We can see that both etoposide and 5-FUdR contribute to significant levels at low doses to the overall mixture effect, and that the shallowness of the single agent regression curves for both of these agents influences the low dose *concentration addition* prediction.

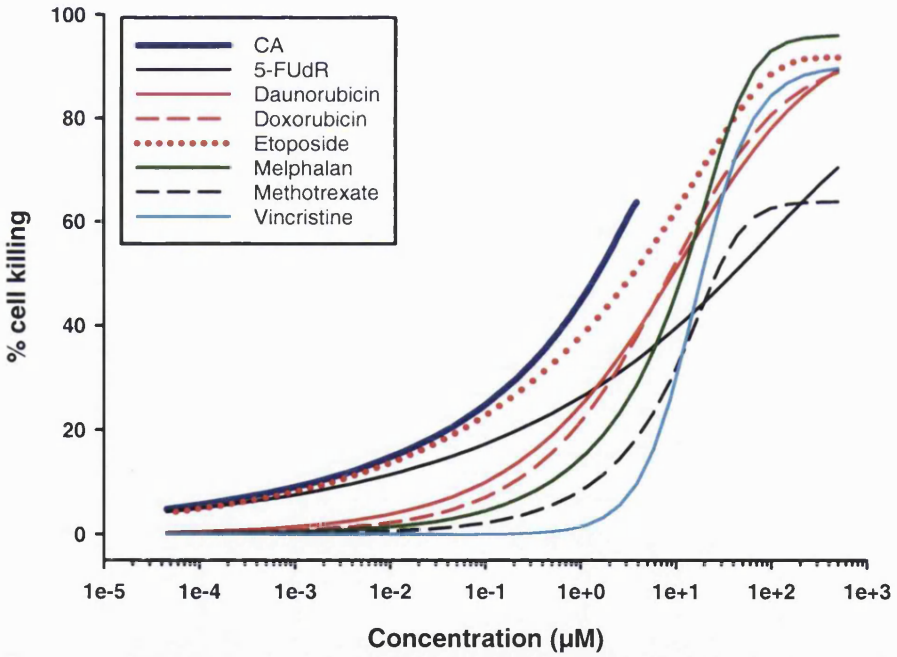

Figure 2.22: Single agent contribution to the overall mixture effect for DU145 cells. *The solid blue line shows the prediction based upon concentration addition. The red lines represent the topoisomerase inhibiting agents, daunorubicin (solid line), doxorubicin (dashed line) and etoposide (dotted line). The black lines represent the antimetabolite agents, 5-fluoro-5'-deoxyuridine and methotrexate. The cyan solid line shows vincristine and the green line melphalan. The shallow nature of the concentration addition curve at low doses was due to the elevated contribution of etoposide and 5-FUdR at these lower concentrations.*

The data shown in **figure 2.21** clearly suggests that the hypothesis that *independent action* best describes the combined mixture effect of seven anticancer drugs with dissimilar sites of action is false. In fact, contrary to this expectation, *concentration addition* clearly describes a more accurate relationship to the data. The observed mixture data sits immediately to the right of the *independent action* prediction curve and in addition to the data showing close resemblance to the *concentration addition* prediction it could also be said that there is some form of antagonism present within the mixture that is causing this shift towards the right.

We wanted to examine whether the accuracy of the concentration addition model to the mixture effects was specific to the DU145 cells or whether it was a more generalised feature. To do this a second comparable tumour cell line derived from breast cancer, the MCF-7 cells was used.

2.7.4 Concentration-response analysis for the MCF-7 cells

The results from the DU145 cells demonstrated a deviation from the *independent action* prediction model for the chosen group anticancer agents. The prediction based using *concentration addition* was much more accurate and suggested that there was a possible similarity in the way in which these agents kill these cells. Exactly why this is cannot be explained without further investigation. A feature of the DU145 cells is the presence of mutation on the *p53* gene (Isaacs et al., 1991) that can adversely affect the way in which these cells signal for cell destruction via apoptosis (this process is described in greater detail in **chapter 3**). Expression of the p53 protein can act as a trigger for further downstream events in the apoptosis pathway and as this protein has impaired activity in these cells it implies that these agents must act beyond this protein and further downstream the pathway. The use of a second cancer cell line, the MCF-7 breast cancer cells, initially was used to determine whether the mixture prediction would agree with the findings of the DU145 cells.

2.7.4.1 Single agent responses

2.7.4.1.1 The antimetabolites:

The dose response relationships on MCF-7 cells for both of these agents share close similarities to the effects to the DU145 cells. The 5-FUdR regression curve was again very shallow, ranging from maximum to minimum over six orders of magnitude **(figure 2.23a).** The maximum effect was also lower in this cell line, 77.58% compared to 84.23% in the DU145 cells. The slope for the MTX curve was very steep and its range was only two orders of magnitude from the maximum effect to minimal effect. The maximal cell killing for the drug was again much lower than for any of the other agents, the maximal effect for MTX was 69.87% cell killing **(figure 2.23b)**.

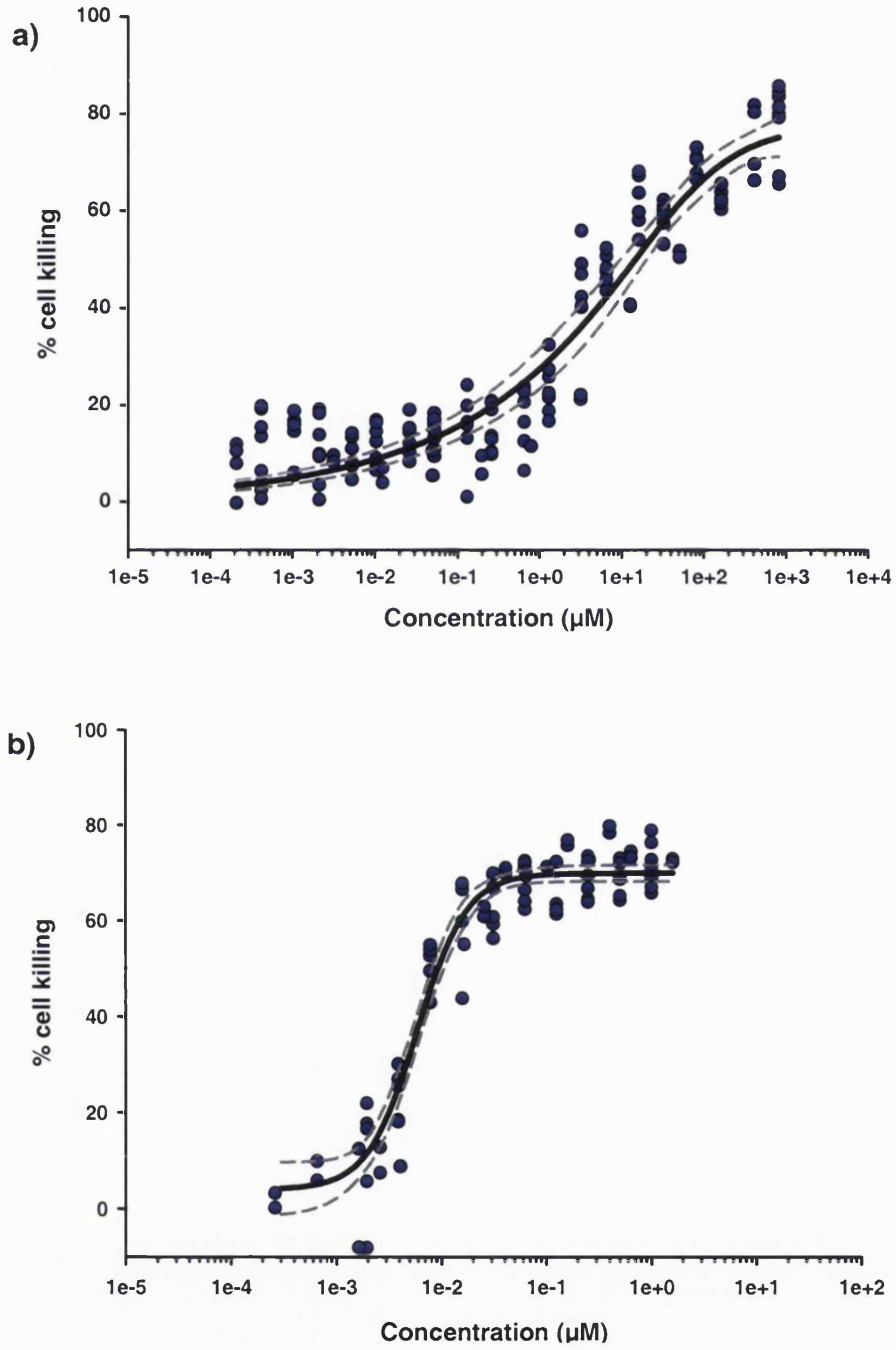

Figure 2.23: Dose response for MCF-7 cells treated with 5-fluoro-5'-deoxyuridine and methotrexate. *Individual data points represented by blue circles (•) and the best fit regression model shown by the thick black line,* ***a)*** *GL model for 5-FUdR;* ***b)*** *Hill asymmetric model for methotrexate. Grey dotted lines represent the upper and lower 95% confidence interval for the regression fit. The data were from a minimum of three independent experiments.*

2.7.4.1.2 Melphalan

The response curve for melphalan was much shallower when compared to the curve for the DU145 cells **(figures 2.17 & 2.24)**, the range from minimum effect to maximum was five orders of magnitude, one more than the DU145 cells. The median effect concentration for MCF-7 cells treated with melphalan was slightly lower (3.58 μM compared to 4.93 μM). Although there was presence of scatter at lower concentrations, the level of heteroskedasticity was less for this cell line.

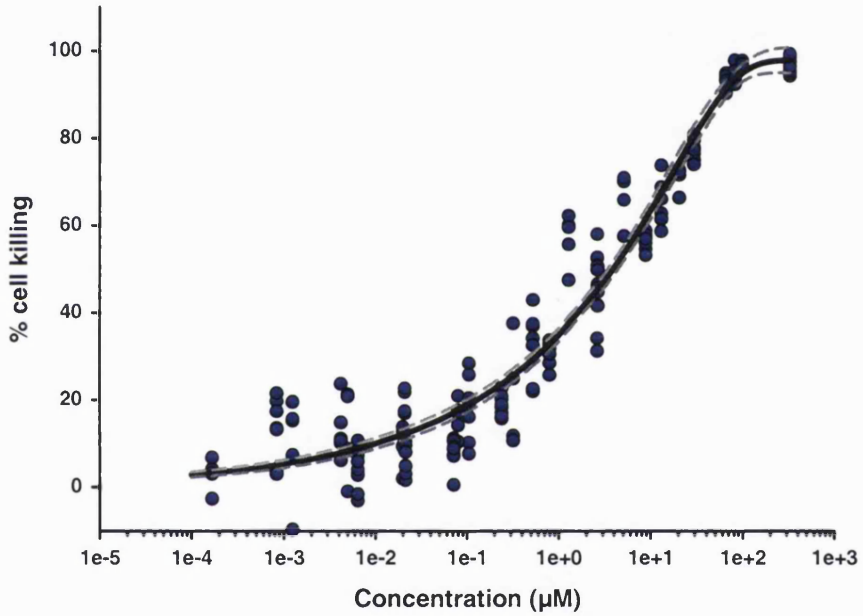

Figure 2.24: Dose response for MCF-7 cells treated with melphalan. *The regression model was based upon the Chapman model shown by the thick black line. Grey dotted lines represent the upper and lower 95% confidence interval for the regression fit. The data were from a minimum of three independent experiments.*

2.7.4.1.3 The anthracyclines

The relationships for both daunorubicin and doxorubicin between the two cell lines once again show close similarity, daunorubicin shares a similar median effect concentration between cell lines (0.018μM for DU145 to 0.023μM for MCF-7), though there was a smaller maximum effect for the MCF-7 cells **(figure 2.25a & table 2.4)**.

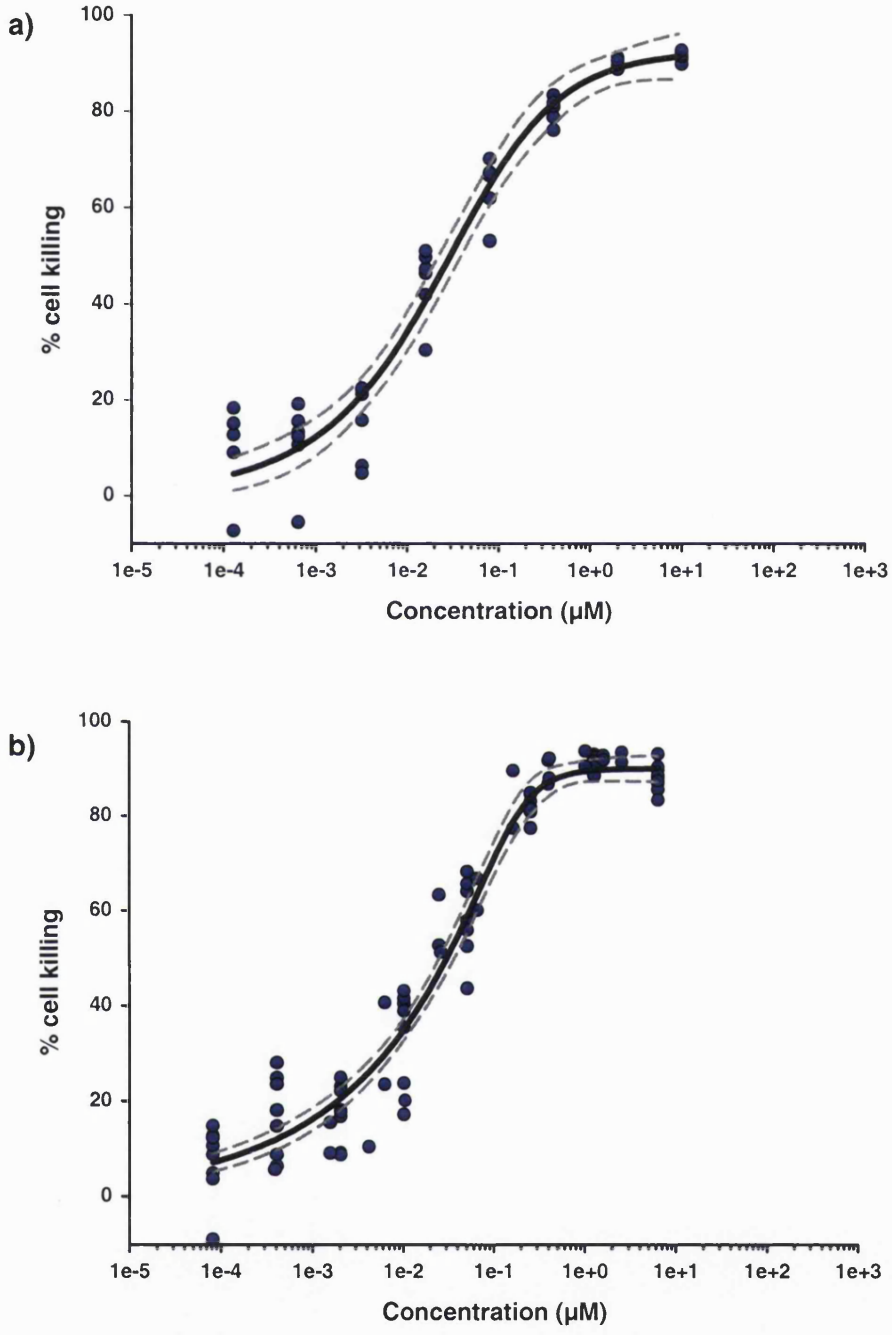

Figure 2.25: Dose response for MCF-7 cells treated with daunorubicin and doxorubicin. *The best fit regression model shown by the thick black lines, the GL model was used for both* ***a)*** *daunorubicin and;* ***b)*** *doxorubicin. Grey dotted lines represent the upper and lower 95% confidence interval for the regression fit. The data was from a minimum of three independent experiments.*

The median effect for MCF-7 cells treated with doxorubicin was slightly higher compared to DU145 cells (0.022 μM to 0.018 μM, **tables 2.3 & 2.4**), though curve maximal effects were similar **(figure 2.25b)**. The slopes of both curves were slightly different as the daunorubicin curve ranged over five orders of magnitude from maximum effect to minimum effect, compared to doxorubicin's four.

2.7.4.1.4 Etoposide phosphate

Etoposide phosphate produced a much shallower best-fit regression curve for the MCF-7 cells compared to the DU145 cells **(figure 2.26)**. The range from maximum effect to the minimum was over seven orders of magnitude, making it the most shallow dose-response curve for any drug in either cell line. The maximum effect was reduced for the MCF-7 cell compared to the DU145s, though the slow gradual reduction in cell killing at lower drug concentrations was very similar in both cell lines.

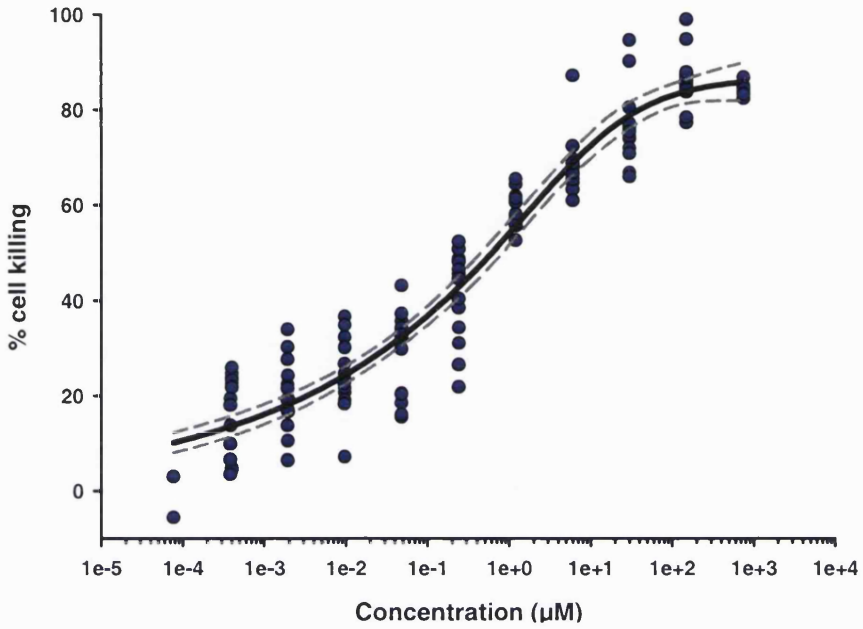

Figure 2.26: Dose response for MCF-7 cells treated with etoposide phosphate. *The regression model was based upon the GL model shown by the thick black line. Grey dotted lines represent the upper and lower 95% confidence interval for the regression fit. The data were from a minimum of three independent experiments.*

2.7.4.1.5 Vincristine sulphate

The slope for the vincristine sulphate curve was less steep for the MCF-7 cells than it was for the DU145 cells, the range from minimum to maximum effect was over five orders of magnitude compared to less than two for the DU145s **(figures 2.20 & 2.27)**. Median effect concentrations **(tables 2.3 & 2.4)** were very low in both cell lines, ranging from 1.899 nM for the DU145 to 0.866 nM for the MCF-7 cells. Vincristine sulphate remained the most potent drug of the seven used in these studies for both cell lines.

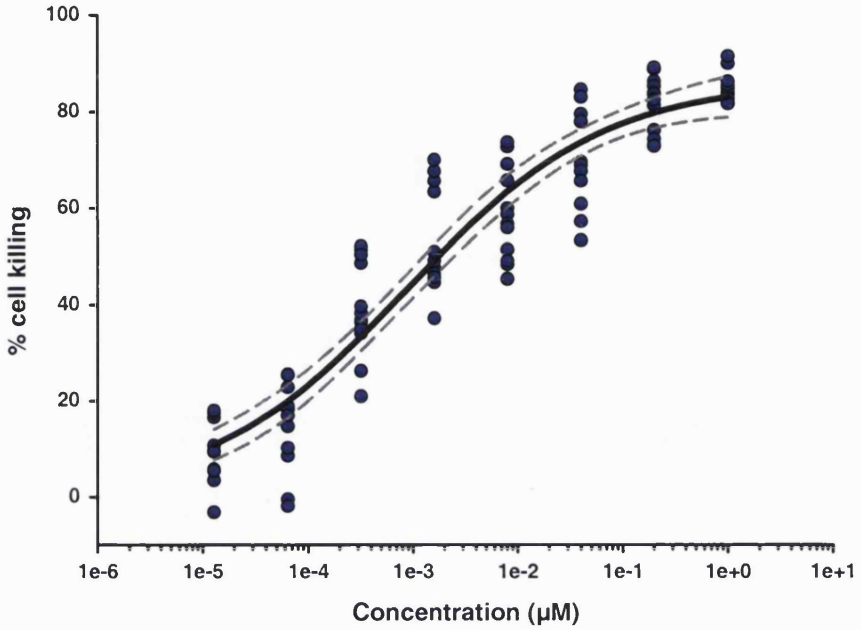

Figure 2.27: Dose response for MCF-7 cells treated with vincristine sulphate. *The regression model was based upon the Hill asymmetric model shown by the thick black line. Grey dotted lines represent the upper and lower 95% confidence interval for the regression fit. The data were from a minimum of three independent experiments.*

A summary of the best-fit regression model parameters and estimated median effect concentrations for each individual agent when treated to the MCF-7 cells is shown in **table 2.4**. The fraction of each agent present in the seven component mixture are shown and were used to calculate mixture effect predictions for both *concentration addition* and *independent action*, and as established for work on the DU145 cells.

Table 2.4: Summary of the parameters for the best-fit regression model for each individual agent for MCF-7 cells

Compound	*Regression model*	*Fraction of drug in mix*[a]	θ_1	θ_2	θ_3	θ_4 *(max)*	*Median effect (μM)*
5-fluoro-5'-deoxyuridine	Gen. Logit	0.4988	-3.5248	1.9570	0.2922	77.5766	4.3562
Daunorubicin	Gen. Logit	0.001568	2.2519	1.7788	0.6437	92.4549	0.02306
Doxorubicin	Gen. Logit	0.001478	3.2929	4.3395	0.1761	89.9728	0.02180
Etoposide phosphate	Gen. Logit	0.04739	-1.7526	1.6849	0.2466	86.8117	0.2562
Melphalan	Chapman	0.4494	-	0.2720	0.02272	97.8350	3.5828
Methotrexate	Hill	9.102×10^{-4}	3.9737	0.005855	1.8646	69.8707	0.005488
Vincristine sulphate	Hill	4.646×10^{-4}	0	0.0008656	0.4601	86.2499	0.0008656

[a] Denotes the ratio of each mixture component and its concentration in the total mixture

θ_1, θ_2, θ_3 and θ_4 are estimated model parameters of the non-linear regression models (summarised in **section 2.5.4, table 2.2**)

2.7.4.2 Predicted and observed mixture effects

In the same manner as for the DU145 cells, the combined mixture effects were tested experimentally with the MCF-7 cells. These were directly compared to the *independent action* and *concentration addition* predictions calculated from the single agent best-fit parameters shown in **table 2.4**.

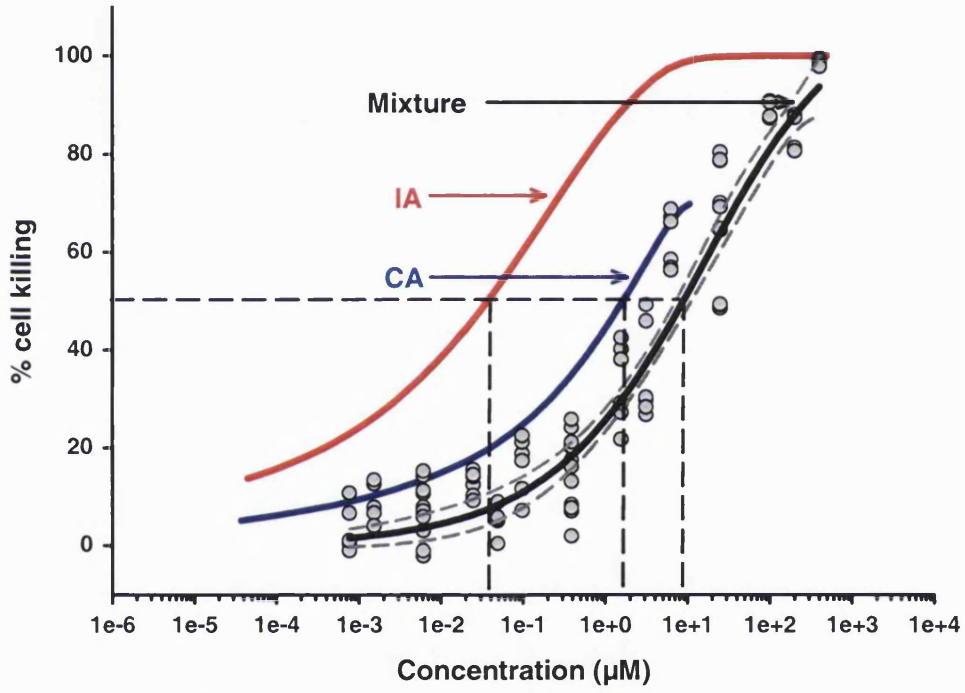

Figure 2.28: Predicted and observed effects of a mixture of the seven tested anticancer drugs for MCF-7 cells. *Individual data points represented by grey circles (•) from three independent experiments and the best-fit regression model based upon the general logit model shown by the thick black line, labelled mixture. Grey dotted lines represent the upper and lower 95% confidence interval for the regression fit. The solid red line shows the predicted combined effects derived from independent action, labelled IA. The solid blue line labelled CA shows the prediction based upon concentration addition. The black dotted lines represent the EC_{50} concentrations for each response curve. The data were from four independent experiments.*

The prediction based upon *independent action* was again inaccurate compared to the observed mixture effects **(figure 2.23)**. The overestimation of the independent action prediction to the observed mixture effects seen for the

DU145 cells was more pronounced for the MCF-7 cells, this time they were consistently over two orders of magnitude apart. The *concentration addition* prediction was again the more accurate predictive model for a mixture of these agents. A comparison at EC_{50} concentrations **(figure 2.28)** for each curves shows that the value for the observed mixture (8.84 μM) was more comparable to the *concentration addition* prediction (1.44 μM) than for the *independent action* prediction (0.038 μM).

The maximal observed mixture effects were to the same level as the *independent action* prediction curve. The full effect range could not be calculated for the *concentration addition* predictions much like for the DU145 cells. The single agent effects for methotrexate followed the trend for the MCF-7 cells as for the DU145s and so the maximum cell kill was 69.87% **(figure 2.23b)**, leading to the *concentration addition* prediction curve being reduced in effect range. The slopes for each curve were similar for both prediction models and for the mixture regression model, ranging to around five orders of magnitude.

The findings from the MCF-7 cells further supports those from the DU145 cells, that the prediction based upon *independent action* is inaccurate for this group of drugs with known dissimilar sites of action. This confirms that this effect is not cell line specific and can be classed as a generalised situation. The concentration addition prediction was better in this case as well, though possible antagonism in the mixture effect cannot be ruled at without further investigation.

2.7.4.3 Contribution of single agents to the overall mixture effects for the MCF-7 cells

Exploring the contribution of the single agents to the overall mixture effect shows that as for the DU145 cells, the drug etoposide phosphate contributes significantly to the low dose portion of the *concentration addition* prediction curve **(figure 2.29)**. At mixture concentrations higher than 0.1 μM, the drug

vincristine sulphate contributes significantly and this was not seen in the other cell line and was entirely due to the shallowness of this drugs dose-response curve when treated to the MCF-7 cells **(figure 2.27)**. Contrary to the DU145 cells, 5-FUdR has a smaller influence on the mixture prediction models as even though the regression curve was shallow in the MCF-7 cells, as it was for the DU145s, its effects are shifted far to the right of the prediction curve.

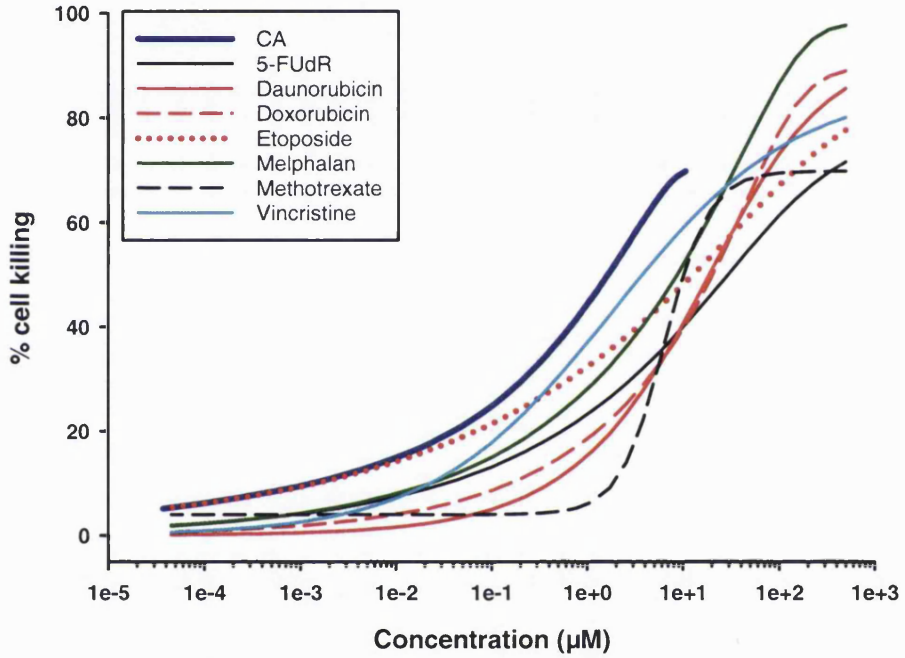

Figure 2.29: Single agent contribution to the overall mixture effect for MCF-7 cells. *The solid blue line shows the prediction based upon concentration addition. The red lines represent the topoisomerase inhibiting agents, daunorubicin (solid line), doxorubicin (dashed line) and etoposide (dotted line). The black lines represent the antimetabolite agents, 5-fluoro-5'-deoxyuridine and methotrexate. The cyan solid line shows vincristine and the green line melphalan. The shallow nature of the concentration addition (CA) curve at low doses was due to the elevated contribution of etoposide and 5-FUdR at these lower concentrations.*

2.8 DISCUSSION

The work of both Backhaus and Altenburger in 2000, and Faust in 2001 and 2003 has helped to elucidate the effectiveness of both *independent action* and *concentration addition* predictive models when predicting mixture effects for dissimilarly and similarly acting agents. The seven anticancer agents used for this study was chosen specifically to be of a dissimilar nature in the way in which they kill cells and it was the aim to assess whether the model for dissimilar action, *independent action*, was the more accurate in predicting its mixture effects.

2.8.1 Single agent toxicities

The individual toxicities of the seven anticancer agents to both cell lines showed great variation. **Tables 2.3 & 2.4** show that the median effect concentrations for each agent covers over four orders of magnitude (0.87 nM for MCF-7 cells treated with vincristine sulphate to 4.93 μM for DU145 cells treated with melphalan). The microtubule inhibitor, vincristine sulphate, was the most potent of all seven drugs in both cell lines, although the steepness of its dose-response curve in the MCF-7 cells was much less than for DU145 cells **(figures 2.20 & 2.27)**. The concentration-response curve for the pyrimidine antagonist methotrexate showed lower maximal effects than for the other six agents. For DU145 cells the maximum cell killing was 63.87% of total cell kill, for MCF-7 cells this was 69.87%.

All of the dose-response curves were fitted using three non-linear regression fits, the Hill asymmetric, the Chapman and the generalised logit models **(table 2.2)** and all agents displayed sigmoidal concentration-response curves, each with varying shape and steepness. Given the fact that the shapes and slopes for each agent's dose-response curve was dissimilar to one another was not a

surprise. Each agent had a specific site of action and was likely to have differing methods for initiating and causing cell death. An adequate predictive model for the combination effects for this particular mixture again suggests *independent action* over *concentration addition*.

2.8.2 The prediction based on concentration addition

The predictive power of *concentration addition* proved to be much more accurate than that for *independent action*, proving wrong the hypothesis that *independent action* would accurately predict the mixture effects for a seven component mixture of dissimilarly acting anticancer drugs. **Figures 2.21 & 2.28** demonstrate the relative accuracy of the *concentration addition* prediction curves over the *independent action* prediction curves. For the DU145 cells the relative EC_{50}s for each curve shows the closeness of *concentration addition* to the observed mixture effects (1.43 μM for *concentration addition* compared to 0.94 μM for the mixture). In contrast the EC_{50} for the *independent action* prediction was much lower at 0.10 μM and overestimates the overall mixture effect. For the MCF-7 cells the *concentration addition* prediction was closer to the observed mixture effects than the *independent action* prediction **(figure 2.28)**, relative EC_{50}s for each curve demonstrates how inaccurate the prediction for dissimilarly acting agents was. The EC_{50} for IA was 0.038 μM, for *concentration addition* it was 1.44 μM and for the observed mixture effects it was 8.84 μM.

The shapes and slopes of single agent regression curves have a great influence upon the outcomes of the *independent action* and *concentration addition* predictions (Drescher and Boedeker, 1995). Considering the differing shapes and slopes of the single agent dose-response curves for both cell lines in this study, the prediction based on *concentration addition* was surprisingly close to the observed effects. This problem had been encountered before in a study of 18 herbicides (Faust et al., 2001) when a number of single agents displayed

varying shapes and slopes for their dose-responses, but it was found that the predictive value of *concentration addition* was not affected. The presence of single agents with shallow curves like those for etoposide and 5-FUdR can result in elevated low effect predictions for both *independent action* and *concentration addition*, as can be seen in **figures 2.22 & 2.29**. The *concentration addition* prediction concept however has been shown to cope well with response curves of varying slopes (Berenbaum, 1985; Altenburger et al., 2000; Rajapakse et al., 2002).

2.8.3 The inaccuracy of independent action

Independent action has been shown to overestimate mixture toxicity of this selection of seven anticancer drugs. There was a larger difference between the EC_{50} values from the observed to the *independent action* prediction than from the observed to the *concentration addition* prediction. It was also seen that the separation of the *independent action* curve to the observed regression curve was much smaller for the DU145 cells than for the MCF-7 cells. In view of the consistent overestimation of mixture effects by the more appropriate mixture model of *independent action*, it may be argued that these agents are not acting as dissimilarly as first thought. Although great consideration was taken into the choice of agent, and these agents do all act at dissimilar sites of action, could it be that these varying sites of action are in fact causing a common similar mechanism of cell killing. Classification of anticancer drugs according to their mode and site of action at first appears straight-forward as it is simply by how they initially act on cells. These agents can also then act in other ways, as many have very direct mechanisms to kill cells, while others involve a multitude of factors to cause cell death. This is precisely why these agents are used to treat carcinogenic tissue, due to their broad-spectrum cell killing. It does however make it very difficult to assume that for chemicals that appear mechanistically dissimilar it is best to model with *independent action*, and for mechanistically similar chemicals to model with *concentration addition* (Borgert et al., 2004).

In conclusion, we have shown that detailed knowledge of the individual mixture components are required in order to accurately predict their combined mixture effects. Our study demonstrates that the multi-component mixture of anticancer drugs cannot be accurately predicted by the concept of *independent action*. In fact we found that *concentration addition* provided an all round more accurate model to predict mixture effects. Exactly why this is must be further examined, these agents were chosen to be a dissimilar as possible, but could it be that they are actually acting in a similar manner? Detailed knowledge for each agent's mechanism of action was required to establish the merits and limitations for each predictive model. This question was addressed in **chapter 3** by examining the possibility that these agents had a commonality in their mechanism of cell killing.

CHAPTER 3:

COMMON SIGNALLING PATHWAY ACTIVATION

3.1 INTRODUCTION

A common feature of many of the anticancer drugs available for cancer treatment nowadays is that they exhibit a great variety of modes of cell death. In many cases these drugs have known sites of action, but an exact understanding of the mechanism of action is often lacking. Following on from the results and findings from the previous chapter, we have seen how predictions based upon *concentration addition* gave consistently better reflections of the observed mixture effects for a seven-component combination of anticancer drugs with varying sites of action. In contrast, *independent action* yielded overestimations of joint effects. Thus, we are facing a paradoxical situation: on the one hand, knowledge about the sites of action leads to the expectation that *independent action* should produce accurate predictions of combination effects. On the other hand, the empirical observations could suggest that the anticancer drugs acted in a similar fashion.

The criteria used to define similar or dissimilar action of mixture components are not well defined (Berenbaum, 1989; Greco et al., 1995). At one extreme of the spectrum of opinions, interactions with the same molecular target, by identical toxic intermediates is required for the agents to be defined as being similar. In this case, in a narrow sense we could say similar mechanisms. If this definition were adopted in our case, the mixture of seven anticancer drugs would have to be seen as composed of dissimilarly acting drugs, because interactions are with a variety of molecular targets, and the intermediates involved are varied. According to this view, *independent action* should apply. The opposite position is described by the view that "similar action" should be taken to mean the induction

of phenomenologically similar effects, i.e. cell killing. In this case there would be similarity in the mode of action of drugs, and *concentration addition* should apply to the mixtures of seven anticancer drugs (Berenbaum, 1989; Borgert et al., 2004).

It is therefore conceivable that the criteria used to distinguish dissimilar acting agents may require further clarification. An exploration of the modes of action for each of the agents chosen for this study was required to solve this particular issue, and it could quite simply be that these agents, while having differing sites of action, in fact have a commonality in their mechanisms of causing cell death. This approach was developed in two stages. The first was to explore in the simplest context whether there was a common activation by all single agents in the process of inducing apoptosis (Kerr et al., 1972). The process of apoptosis is a complex mechanism in the mediation of cell death in the homeostasis of multi-cellular organisms, and can be seen as a major target for a number of cytotoxic anticancer drugs. Thus, are all seven anticancer drugs able to induce apoptosis, and, if so, would this fulfil the similarity criterion required for *concentration addition*? The second stage was to move towards the more restrictive definition of "similar action" and to probe whether all drugs exhibited the same specific mechanisms of action in initiating apoptosis in greater detail. This was done by examining the activation of a number of important signalling proteins within the apoptotic pathway after treatment with each of these anticancer drugs.

3.2 CELL KILLING AND POSSIBLE MECHANISMS OF ACTION

Apoptosis is a normal process in cellular development and tissue maintenance. There are two main forms of cell death that occur naturally in the body, these are known as necrosis and apoptosis (Kerr et al., 1972). There are many

morphological changes that occur to a cell undergoing apoptosis and these include loss of membrane integrity, condensation of cytoplasm and nucleus, and DNA cleavage. These dying cells become fragmented, apoptotic bodies, and are eliminated by phagocytic cells causing no surrounding tissue damage or inflammation, unlike in necrosis. Such an important physiological process must be strictly regulated and controlled. To this end a number of diseases and conditions have been attributed to abnormal induction of apoptosis. Examples include Alzheimer's, Hodgkin's (Lorenzen et al., 1997), cancer (Thompson, 1995) and AIDS (Wang et al., 1998). This has become a wide-ranging field at present, indeed induction of apoptosis by anticancer agents has been regarded as the chief mechanism leading to tumour cell death. Many tumour cells' ability to undergo apoptosis is muted and this is largely due to the presence of mutated or dysfunctional genes related to apoptotic regulation being found in human cancers (McGill, 1997). The challenge of anticancer drug therapy is to overcome the cancer cells' compromised ability for apoptosis. Two possible processes have been suggested (Brown and Wouters, 1999; Tannock and Lee, 2001) that may lead to apoptosis following cancer treatment: i) induction of apoptosis by radiation or drugs due to stimulation of apoptotic signal mechanisms; ii) treatment causes lethal damage to cells, triggering an apoptotic response to kill cells **(figure 3.1)**. In the case of the former there is room to look at a drug's effectiveness at directly activating apoptotic events and therefore this represents potential to take advantage of this feature for optimisation and manipulation to increase drug treatment effectiveness. If it is the latter case, where cell (DNA) damage is caused by anticancer drug treatment, then cell death is primarily due to apoptosis, and those cells that do not die are resistant to this process (Brown and Wouters, 1999).

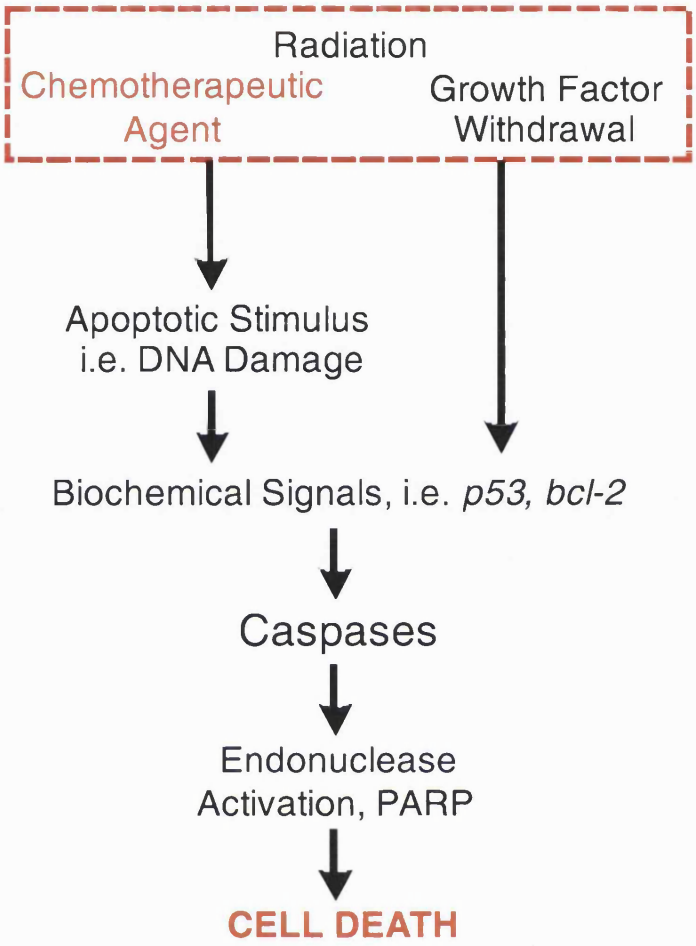

Figure 3.1: Processes of cell death following cancer treatment. *Following cancer treatment there are a number of processes that can lead to the activation of apoptosis signalling and induced cell death.*

The genes thought to be most important for the regulation of apoptosis are the ones for the tumour suppressor gene, p53 and members of the Bcl-2 gene family (Reed et al., 1996; Brown and Wouters, 1999). It is assumed that apoptosis plays a major role in cell killing by DNA-damaging anticancer drugs and that those cells with mutations in these genes should be resistant to their induction of apoptosis (Reed et al., 1996; Rudin and Thompson, 1997). The aspect of drug resistance is a major problem for the treatment of a number of tumours and so the need to understand exactly how anticancer drugs activate pathways leading to cell death has become most important. The variety of drugs available can target DNA, RNA, topoisomerases I and II, dNTP's or

microtubules, as have been used and described in **chapter 2**, but their precise mechanisms of action leading to cell death are far from clear.

Apoptosis has been found to be mediated by a variety of pathways, ranging from activation of death receptors and ligands to mediation of the p53 protein. A brief explanation of some of these processes is summarised below.

3.2.1 Death receptors & ligands

A cell can receive a variety of conflicting signals in order to mediate self destruction. Commonly the first step in the activation of signal pathways resulting in apoptosis is via a number of cellular receptors. Signal molecules bind to the intracellular domains of these receptors, and these are released or activated upon receptor activation. Death receptors belong to the TNF (tumour necrosis factor) receptor gene superfamily that share cysteine rich extracellular domains (Gruss and Dower, 1995), and an intracellular cytoplasmic sequence known as the 'death domain' (Tartaglia et al., 1993; Nagata, 1997). These domains interact with a cell's apoptotic machinery, mediating the activation or inactivation of apoptosis. The main types of death receptors are known as: i) CD95 (or Fas); ii) TNFR type 1; iii) DR3 (death receptor 3); iv) DR4 (or TNF-related apoptosis inducing ligand receptor 1, TRAIL-R1); and v) DR5 (or TRAIL-R2). The ligands that activate these receptors are structurally related to these receptors and also belong to the TNF gene superfamily (Gruss and Dower, 1995). CD95 ligand, CD95L (or Fas ligand, FasL) binds to CD95 (Fas); TNF binds to TNFR1; Apo3 ligand, Apo3L (TWEAK) binds to DR3; and Apo2L or TRAIL binds to DR4 and to DR5 (Ashkenazi and Dixit, 1998).

3.2.1.1 Fas (or CD95) and Fas ligand (FasL)

These components act together to induce three types of apoptotic response: i) deletion of activated mature T cells at the end of an immune response (Nagata,

1997); ii) killing of virus-infected cells by cytotoxic T cells and natural killer cells; and iii) killing of inflammatory cells at 'immuno-privileged sites' such as the eye. Binding of FasL to Fas receptors leads to aggregation of death receptor domains **(figure 3.2a)**. The adapter protein Fas associated death domain (FADD) then binds its own death domain to other aggregated death domains and can then activate the caspase-8 protease (Boldin et al., 1996) that in turn can activate the caspase cascade and an apoptotic response.

3.2.1.2 TNF and TNFR1

TNF binds to TNFR1 and activates the transcription factors NF-κB and AP-1. The binding of TNF causes trimerisation of TNFR1 and leads to its adapter protein TRADD (TNFR-associated death domain) (Hsu et al., 1995) to cluster to other death domains. TRADD can recruit a number of signalling molecules that can stimulate and inhibit number of signalling pathways (Ashkenazi and Dixit, 1998), one of which is via FADD which can mediate apoptosis activation (Hsu et al., 1996; Chinnaiyan et al., 1996; Varfolomeev et al., 1996) **(figure 3.2b)**.

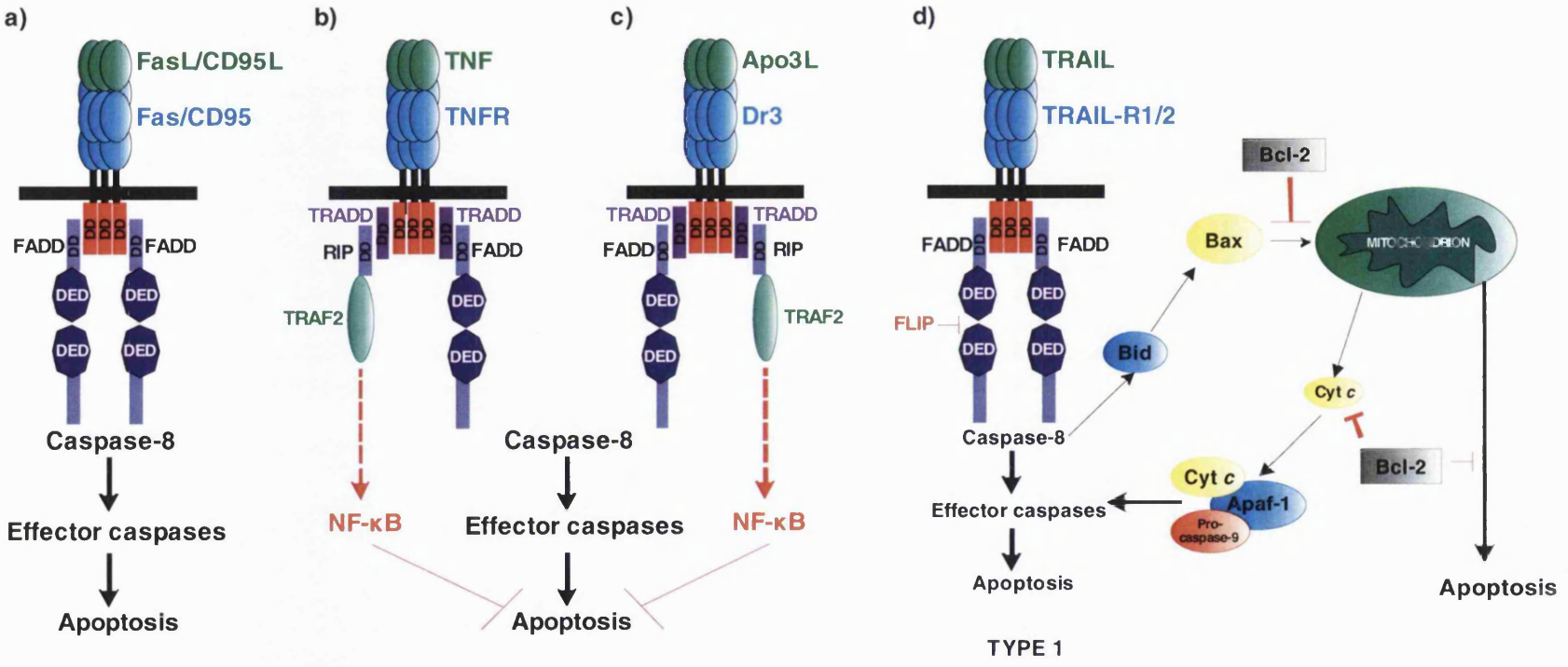

Figure 3.2: Apoptosis signalling by death receptors. a) *CD95/Fas receptor binds to CD95L/FasL. Clustering of Fas associated death domain, FADD leads to caspase-8 activation and caspase cascade signalling. Both* ***b)*** *TNF and* ***c)*** *Apo3 share similarity in activating TRADD to activate apoptosis and the NF-κB pathway.* ***d)*** *Binding of TRAIL to TRAIL receptors leads to FADD recruitment and in turn activates caspase-8 and apoptosis. DD, death domain; DED, death effector domain (Ashkenazi and Dixit, 1998; Dlamini et al., 2004).*

3.2.1.3 Apo3L and DR3

This death receptor shows close similarity to TNFR1 (Chinnaiyan et al., 1996; Varfolomeev et al., 1996) and triggers responses similar to TNFR1 i.e. apoptosis and NF-κB activation. DR3 binds to Apo3L and activates NF-κB through TRADD and apoptosis activation is mediated through TRADD and FADD **(figure 3.2c)**.

3.2.1.4 TRAIL

TRAIL has been shown to induce apoptosis through binding to its receptors DR4 and DR5. Binding of TRAIL leads to receptor trimerisation and clustering of intracellular death domains, leading to the formation of the death-inducing signalling complex (DISC). This receptor trimerisation results in binding to FADD and subsequent activation of caspase-8 and caspase-10 and caspase cascade activation (Wang and El-Deiry, 2003) **(figure 3.2d)**.

3.2.2 The mitochondria and the Bcl-2 family

The role of the mitochondria is very important in the regulation of cell death as they modulate the release of apoptotic signalling factors following the activation of apoptosis. It has been shown that the mitochondrial membrane undergoes a level of transient permeability that can lead to the release of these factors (Dlamini et al., 2004). Two of these factors are known as cytochrome *c* (Green and Reed, 1998) and apoptosis inducing factor (AIF) and begin a proteolytic cascade eventually leading to nuclear damage and cell death. A mitochondrial protein known as second mitochondria-derived activator of caspases (Smac and also know as DIABLO) can also be released from mitochondria and act to inhibit IAP (inhibitor of apoptosis proteins) from interacting with caspase-9 and caspase-3 and therefore increasing apoptosis **(figure 3.3)**.

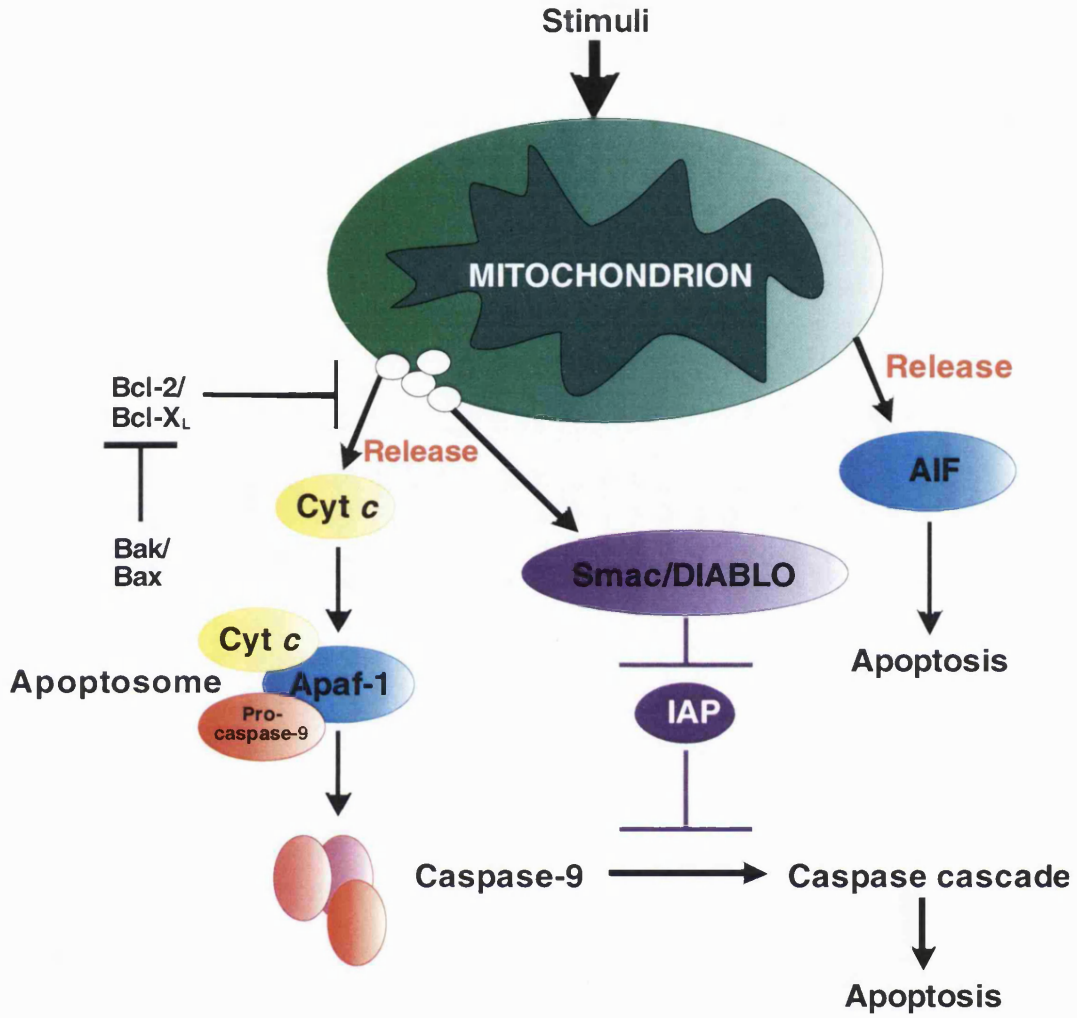

Figure 3.3: The role of mitochondria in apoptosis. *Cytochrome c (cyt c) and Smac are released from the intermembrane space of mitochondria as a result of stimuli causing conformational change and/or activity of Bak/Bax proapoptotic molecules. Apoptosome formation occurs following Apaf-1 and cyt c binding together that in turn bind to procaspase-9. This can then activate effector caspases such as caspase-3 and -7. IAP (inhibitor of apoptosis) can prevent caspase-9 from activating the caspase cascade, but can be inhibited by release of Smac/DIABLO released from mitochondria. AIF (apoptosis inducing factor) can also cause apoptosis but its precise mechanism is still unknown (Kroemer et al., 1997; Dlamini et al., 2004).*

3.2.2.1 Cytochrome c

The role of cytochrome *c* in apoptosis was first described in 1996 (Liu et al.). Cytochrome *c* is an important protein in the electron transport chain. Research into its role in modulating mitochondrial activation of apoptosis has shown that cytochrome *c* was prevented from release by the anti-apoptotic protein Bcl-2

and therefore blocked apoptosis (Yang et al., 1997; Kluck et al., 1997). The protein cytochrome *c* is normally found within the inter-membrane space of the mitochondria and is associated with the anionic phospholipid cardolipin. It is the disassociation of cytochrome *c* to cardolipin that leads to the release of cytochrome *c* into the cytosol (Orrenius, 2004) following stimuli for apoptosis (Liu et al., 1996). Another protein is then released from the mitochondria at the same time as cytochrome *c* and is called APAF-1 (apoptotic protease activating factor). This binds to caspase-9 (Li et al., 1997) to form a complex known as the apoptosome **(figure 3.3)**, which then leads to further activation of the caspase cascade (Orrenius, 2004; Green and Kroemer, 2004).

3.2.2.2 Bcl-2 protein family

At least fifteen members have been identified in mammalian cells (Dlamini et al., 2004), and all members contain at least one of four conserved homology domains known as BH1 to BH4 (Adams and Cory, 1998). These members play an important role in apoptosis, the Bcl-2 proto-oncogene is anti-apoptotic and acts to block apoptosis occurring. In most non-apoptotic cells, Bcl-2 sits on the outer mitochondrial membrane, where it prevents cytochrome *c* release from mitochondria (Orrenius, 2004; Green and Kroemer, 2004). Other members of the Bcl-2 family also act to block apoptosis and are known as Bcl-X_L, Mcl-1 and A1. However other members can actively promote cell death and these include Bax, Bad, Bak, Bid and Bcl-xs. These move from other cellular organelles to the mitochondria in response to apoptotic stimuli, where they encourage the release of cytochrome *c* from the mitochondria. It is possible that protein-protein interactions between Bcl-2 family members are important functionally to either promote cell death or to block it.

3.2.3 Caspases

The caspases are a series of cytosolic cysteine proteases (Alnemri et al., 1996; Thornberry and Lazebnik, 1998) that are important for the process of apoptosis and have been detected in all cells undergoing apoptosis regardless of the apoptotic stimuli or origin (Strasser et al., 2000). All known caspases cleave their protein substrates immediately after Asp residues and of the twelve known human caspases, six are thought to be definitely involved in apoptosis. These can be sub-divided into two groups based upon their pro-domains and roles in cell death. The first group is known as effector (or 'downstream') caspases and are responsible for most of the cleavages that disassemble a cell following apoptosis, and include caspase-3, -6, and -7 **(figure 3.4)**. The second group is known as the initiator (or 'upstream') caspases and can initiate the cascade of proteases (Kaufmann et al., 2000), and are known as caspase-8, -9, and -10. Caspase-8 and -9 are the major initiator caspases and when activated can cleave and activate the effector caspases (Nicholson and Thornberry, 1997; Kaufmann et al., 2000). As described earlier, activation of death receptors can result in activation of the initiator caspase-8 and caspase-10. Caspase-9 is the initiator caspase in mitochondrial dependent apoptosis (Chen and Wang, 2002). Some of these caspases, especially the effector caspases, can cleave and inactivate a number of vital proteins within the cell. These can include repair enzymes, PARP (poly (ADP-ribose) polymerase), MDM2 (an inhibitor of p53) and protein kinase Cδ (Thornberry and Lazebnik, 1998). IAPs can also play a role in inhibiting proteolytic cascades (Deveraux and Reed, 1999) **(figure 3.4)**. XIAP (an IAP protein that has been mapped to the human X chromosome) has been shown to inhibit the effector caspases of caspase-3 and caspase-7.

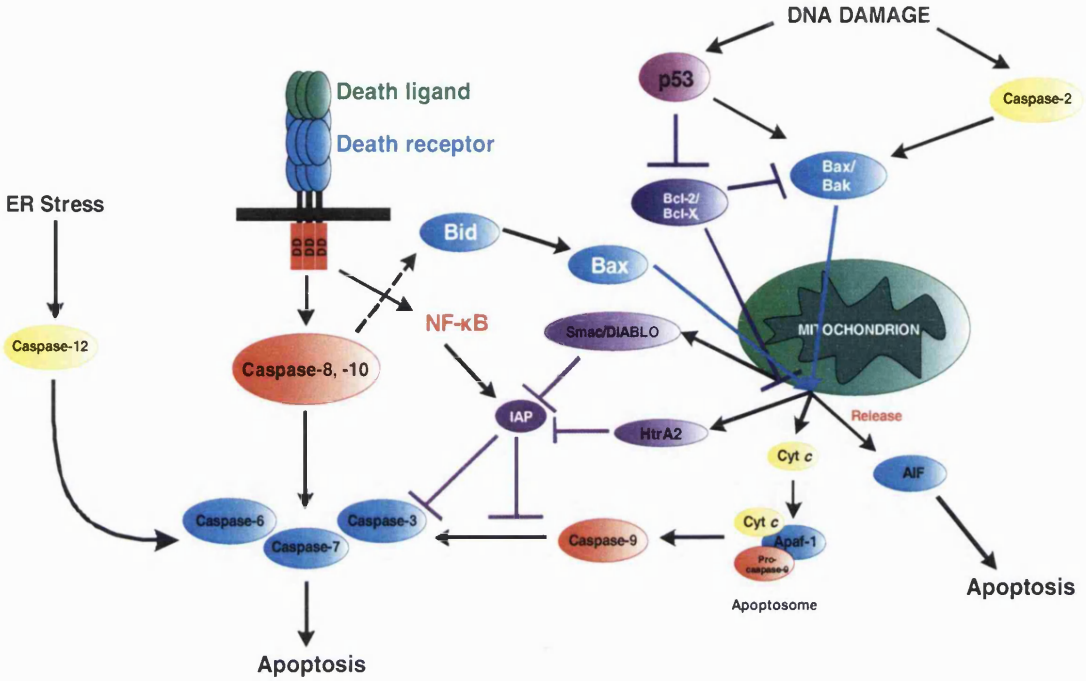

Figure 3.4: The caspase cascade. *Caspase mediated apoptosis can occur via death receptor and mitochondria-dependent apoptosis. Binding of ligands to death receptors results in activation of the initiator caspase-8 and -10. Exposure of cells to agents that can cause DNA damage or inhibit DNA repair results in the release of cytochrome c from the mitochondria into the cytosol. Activation of caspase-9 occurs via formation of the apoptosome with Apaf-1/procaspase-9/cytochrome c. Active initiator caspase-8,-9 & -10 cause the activation of the effector (downstream) caspase-3, -6 & -7. AIF released from mitochondria causes caspase-independent apoptosis (Guo et al., 2002; Chen and Wang, 2002).*

3.2.4 The tumour suppressor gene, p53

The tumour suppressor genes normally act to regulate and suppress cell proliferation and many of these genes are components of signalling pathways involved in receiving and regulating growth inhibitory signals. Tumour formation and uncontrolled cell proliferation can therefore occur if there is a loss of function of a tumour suppressor gene.

p53 is a tumour suppressor gene important for regulation of cell growth, and has been found to be mutated in over 50% of cancers. This gene acts in response to a number of forms of cellular stress, causing mediation of cell proliferation.

Activation occurs by DNA damage, hypoxia, DNA repair, cellular senescence, apoptosis and unusual oncogene expression (Fridman and Lowe, 2003). Mutation and therefore inactivation of this gene may result in tumour cell growth as it is known to have a role in transcriptional regulation, i.e. p53 suppresses a number of promoters by binding to them.

The role of p53 in promoting apoptosis is important in its tumour suppressing abilities and p53 has been shown to induce expression of proteins that target both the death receptor mediated and mitochondrial induced apoptotic pathways (Vousden, 2000). p53 can induce the expression of death receptors such as Fas and Killer/DR5 (TRAIL-R2) (Burns and El-Deiry, 2003; Tanikawa et al., 2003), it can also activate cytoplasmic proteins such as p53-inducible protein containing a death domain (PIDD) (Lin et al., 2000) and Bid (Sax and El-Deiry, 2003). Proteins that act on the mitochondria such as Bax (Miyashita and Reed, 1995), Bak, NOXA (Oda et al., 2000) and p53 up-regulated modulator of apoptosis (PUMA) (Nakano and Vousden, 2001; Yu et al., 2001) are also mediated by p53 and trigger cytochrome *c* release and the activation of the Apaf-1/caspase-9 apoptosome (Dlamini et al., 2004).

Greater understanding of the control of p53 has come from the discovery of regulators such as MDM2, ARF and Parc (El-Deiry, 2003). MDM2 mediates the half-life of p53 as it targets p53 for ubiquitin-dependent proteolysis (Kubbutat et al., 1997), but interestingly MDM2 also serves as a transcriptional target for p53 (Perry et al., 1993), so p53 directly activates expression of its own negative regulator in a negative feedback loop. The degradation caused by MDM2 has been shown to be overcome by phosphorylation of p53. The ataxia telangiectasia gene (ATM) is capable of phosphorylating p53 *in vitro* (Banin et al., 1998; Canman et al., 1998; Khanna et al., 1998). ATM is activated in response to ionising radiation and may recognise DNA damage caused by the radiation, resulting in p53 stabilisation and activation (Kastan et al., 1992; Maya et al., 2001). **Figure 3.5** summarises the pathways involved with the activation and inactivation of p53.

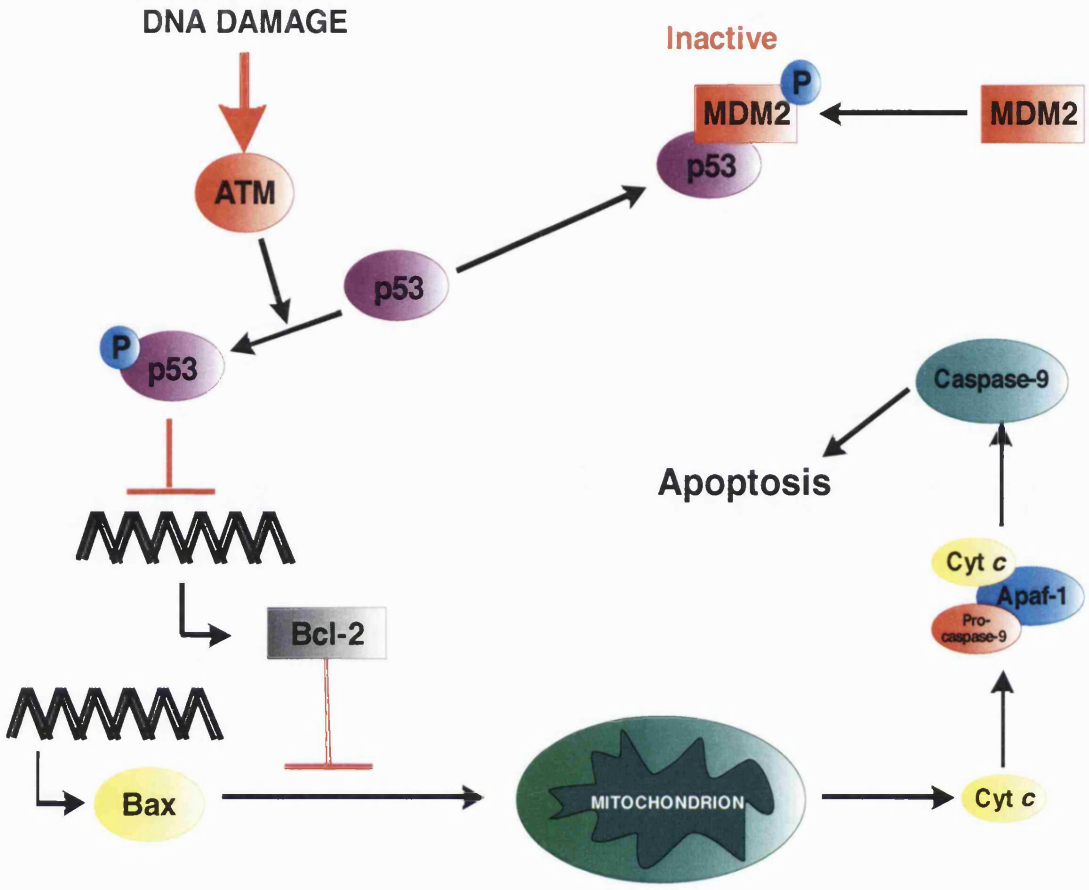

Figure 3.5: ATM/p53 signalling pathway. *ATM activation by damage to DNA causes DNA repair and blockage of cell cycle progression. This can occur by ATM-dependent phosphorylation of p53 that causes growth arrest to enable a cell to undergo repair or if sufficiently damaged, apoptosis. Phosphorylated p53 can also inhibit Bcl-2 and results in increased mitochondrial cytochrome c release and therefore increased caspase mediated apoptosis. p53 degradation occurs by the oncoprotein MDM2 which binds to p53.*

3.3 FEATURES OF CELL LINES USED

The two tumour cell lines used through the course of this study include the prostate cancer DU145 cells and the breast cancer MCF-7 cells. Each cell line showed some variation in their toxicity to each of the seven anticancer drugs and to a *fixed ratio* mixture (shown in **sections 2.6.3 & 2.6.4**). Detailed below are some of the features of each of these cell lines and how they could be

utilised in order to determine possible mechanisms of action for the cytotoxic effects for each of the agents used.

3.3.1 Features of the DU145 cell line

The DU145 cell line was originally derived from a 69 year old man with prostate adenocarcinoma (Stone et al., 1978) and is one of a number of prostate cancer cell lines used to model the *in vitro* characteristics of prostate cancer. The DU145 cells exhibit one of the prime features of prostate adenocarcinoma (Carter et al., 1990), the cells possess a mutation in the p53 gene (Isaacs et al., 1991). As described earlier, the p53 gene plays an important role in the mediation of apoptosis and is often mutated in human cancers. There are many different pathways associated in the process of apoptosis and although the DU145 cells display impaired p53 dependent activity, there is recent evidence to suggest that these cells also have a p53-independent activity to initiate apoptosis (Zhang et al., 2003). This study has suggested that MDM2, a signalling protein associated with the expression of p53, shows activity dependent and independent to p53. This study helps to illustrate that a defect at one regulatory site of apoptosis does not diminish a cell's ability to undergo the process of cell-mediated apoptosis by some other mechanism.

DU145 cells have also been shown to have activated multiple caspases (caspase-3, -7, -8 and -9) following treatment with methylseleninic acid (Jiang et al., 2001), a precursor to a selenium metabolite. The feature of mutated expression of p53 was utilised during the course of this study to explore other possible mechanisms of induced cell killing that may be activated in common by each of the agents used in **chapter 2** to treat these cells.

3.3.2 Features of the MCF-7 cell line

The MCF-7 breast cancer cell line was originally derived from a pleural effusion taken from a woman with metastatic breast carcinoma (Soule et al., 1973) and has been commonly used to model oestrogen-positive breast cancer. To determine possible mechanisms of action for drug-induced cell killing, a couple of features of the MCF-7 cell line were used. In contrast to the DU145 cells, the MCF-7 cells possesses no mutation to its p53 gene (Gudas et al., 1996) and can express the wild-type p53 protein normally. This feature of the cells provided an interesting comparison between the two cell lines, one with a functional tumour suppressor gene and one with a mutated and inactive form. For the agents treated to the MCF-7 cells this opened up the whole signalling pathway associated with expression of p53 that was unavailable for the DU145 cells.

Another feature of the MCF-7 cells in the process of cell killing via apoptosis was through the coordinated activation of a group of proteases known as caspases (Alnemri et al., 1996; Thornberry and Lazebnik, 1998) and has been discussed previously in this chapter. One of the effector caspases, caspase-3, is a key caspase in the signalling process of the caspase cascade (Zheng et al., 1998; Woo et al., 1998) and is believed to play an important role in apoptotic execution. The MCF-7 breast cancer cells have been shown to be deficient in caspase-3 due to a deletion mutation in exon 3 of the gene that encodes it (Janicke et al., 1998). The deficiency of caspase-3 in this cell line has been used as a possible reason for chemotherapeutic resistance and a study that reconstituted this protease into the MCF-7 cell line demonstrated an increase in sensitivity of MCF-7 cells to doxorubicin and etoposide-induced apoptosis (Yang et al., 2001).

During the course of this work we built upon the findings from **chapter 2**, that a mixture prediction based on agents with dissimilar sites of action was less

accurate than the prediction for agents with similar sites of action. We attempted to establish a more detailed idea of possible mechanisms of action for each drug when treated to each of the cell lines, to search for the possibility that they each shared a common mechanism of action. We tested each of the seven agents and the mixture to each of the cell lines, and evaluated the ability of these agents to activate apoptosis. A more detailed exploration of possible mechanisms of action was then undertaken by utilising the defects described for each cell line, namely the lack of the functional protease caspase-3 for the MCF-7 cells or a functional p53 gene for the DU145 cells.

3.4 EXPERIMENTAL APPROACH

3.4.1 Test agents used

The test agents consisting of 5-fluoro-5'-deoxyuridine, daunorubicin, doxorubicin, etoposide phosphate, melphalan, methotrexate and vincristine sulphate were prepared as described in **section 2.5.3.1**. Drug solutions were prepared fresh for each experiment from stored stocks.

3.4.2 Cell lines and cell treatment

The DU145 and MCF-7 cells were grown and maintained in conditions described in **section 2.5.1**.

3.4.2.1 Treatment for Annexin V staining:

For cell treatment to determine level of cell apoptosis the cells were seeded at a density of $1x10^5$ cells in 25 cm^2 canted-neck culture flasks and grown for 72h to

approximately 60% confluency in 5 ml RPMI (DU145 cells) and MEM-α (MCF-7 cells). Media solutions of 5 ml were prepared containing drug solutions at concentrations equivalent to their median effect **(table 3.1)**. Culture media was removed from each flask and the cells were washed with 5 ml sterile PBS solution, media containing the drug was then added to the cells and left for 24h. An untreated control was also prepared for each experiment to similar conditions, in addition to a positive control treated with serum-deprived media.

Table 3.1: Summary of drug concentrations used to treat DU145 and MCF-7 cells

Compound	***DU145 cells, median effect level (μM)***	***MCF-7 cells, median effect level (μM)***
5-fluoro-5'-deoxyuridine	4.6246	4.3562
Daunorubicin	0.0183	0.02306
Doxorubicin	0.0178	0.0218
Etoposide phosphate	0.5396	0.2562
Melphalan	4.9336	3.5828
Methotrexate	0.0128	0.005488
Vincristine sulphate	0.001899	0.0008656
Mixture	2.2433	13.0190

3.4.2.2 Treatment for protein expression:

For cell treatment to determine protein expression for apoptotic signalling, the cells were seeded at a density of $3x10^5$ cells in 75 cm^2 canted culture flasks (Greiner Bio-One) and were grown in 15 ml of supplemented medium (as above)

to 60% confluency. The culture media was then removed from each flask and cells washed with 10 ml sterile PBS. The each cell line was then treated with six differing treatment conditions. They were exposed for 2, 4, 6 and 24h to each single drug and to a seven-component mixture at final concentrations equal to 1x, 5x and 10x median effect. Negative and positive controls were treated for the same periods with complete media and serum deprived media, respectively.

3.4.3 Cell viability staining using Trypan Blue & Annexin V

3.4.3.1 Test for viability, use of trypan blue

One of the features associated with cell death is the loss of cell membrane integrity and this can be assessed with the use of dyes such as Trypan Blue. Cells with permeable membranes take up this water soluble dye, whereas the charge of this dye prevents penetration into viable cells. Trypan Blue exclusion is a useful tool to estimate cell death but gives no indication of mode of cell death, as both necrotic cells and apoptotic cells take up the dye. It has also been seen that cells in primary stages of apoptosis may retain membrane integrity for several hours and therefore exclude this dye and may be classified as being viable. Trypan Blue was prepared as a 0.4% $^{w}/_{v}$ stock solution in sterile PBS and stored at room temperature (r.t). After drug treatment the drug solution media was removed and cells were trypsinised. Following trypsinisation, the cells were resuspended in 5 ml complete medium and centrifuged for 5 min at 1000 rpm at r.t. The supernatant was discarded to remove all traces of serum and the resultant pellet was resuspended in 5 ml serum free medium. A 1:1 dilution of cell suspension with Trypan Blue was thoroughly mixed and cell viability determined by counting the number of cells using a Neubauer haemocytometer under a light microscope. Cell viability was estimated as a percentage of viable cells by:

$$\%\ \text{of viable cells} = \frac{\text{number of viable cells}}{\text{total cell number (dyed + viable)}} x100 \qquad \textbf{(3.1)}$$

3.4.3.2 Test for apoptosis & necrosis, Annexin V & Propidium Iodide stain

The cell-surfaces, of apoptotic cells have been known to undergo modification, and evidence suggests that phosphatidylserine (PS), which is normally found internally of the plasma membrane, is externalized during apoptosis for many cell types (Fadok et al., 1992a; 1992b; 1993; Koopman et al., 1994; Martin et al., 1995; Homburg et al., 1995). This event has been found to occur very early in apoptosis, possibly before any nuclear changes have occurred. A specific probe for PS, Annexin V coupled to a fluorophore, fluorescein isothiocyanate (FITC) (Reutelingsperger et al., 1985), has been used to demonstrate changes in PS distribution during apoptosis (Koopman et al., 1994; Homburg et al., 1995; Martin et al., 1995) and has been shown to be an effective and sensitive method to detect cells undergoing apoptosis.

Preparation of staining solution: A staining solution containing Annexin V-FITC and propidium iodide was prepared immediately before cell staining. 10 µl of annexin V-FITC stain was combined with 10 µl propidium iodide (PI) and made up with 1 ml HEPES buffer solution (Annexin-V-Fluos, Staining Kit, Roche Diagnostics GmbH, Mannheim, Germany). The solution was kept in the dark until added to resuspended cell pellets.

Cell staining: Following Trypan Blue exclusion testing, a sample of the cells containing $2x10^5$ cells was washed twice with sterile PBS. All supernatant was discarded and to each resuspended pellet of cells was added 100 µl of the staining solution. The cells were kept in the dark and incubated for 20 min at r.t and then viewed on a Neubauer haemocytometer using a fluorescence microscope.

3.4.4 Fluorescence microscopy & apoptotic quantification

The stained cells were viewed and captured using a Nikon Microphot-FXA, fluorescence microscope immediately after staining. The dual-stained cells were

excited at 488 nm, and cells stained with fluorescein-coupled Annexin V emitted at 517 nm (green, **figure 3.6a**), and cells stained with PI emitted at 617 nm (red/orange, **figure 3.6b**). Cells undergoing secondary necrosis stained dually with both annexin V and PI (red/orange nuclear staining and green PS cell membrane staining, **figure 3.6c**).

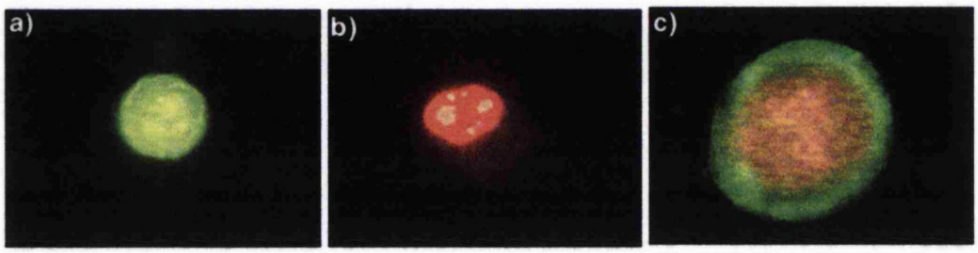

Figure 3.6: Dual stained MCF-7 cells with Annexin V-Fluos and propidium iodide. *Cell populations were scored according to stain taken up by cell,* ***a)*** *apoptotic cell fluorescing green,* ***b)*** *necrotic cell red/orange in colour, and* ***c)*** *secondary necrotic cell with dual red/orange nuclear staining (PI) and green membrane staining.*

The stained cell solution was mounted onto a haemocytometer to count the number of total cells in addition to the number of apoptotic, secondary necrotic and necrotic cells that were present **(figure 3.7)**. The level of apoptosis was quantified as the percentage of apoptotic, secondary necrotic and necrotic cells from the total number of staining cells.

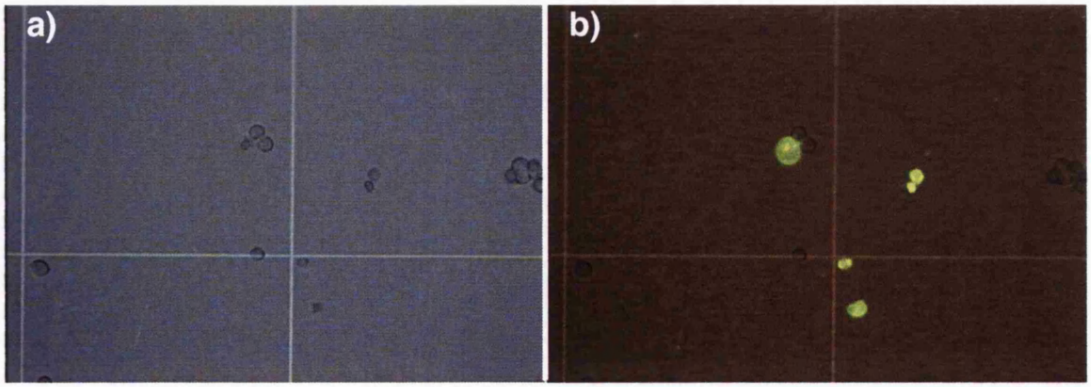

Figure 3.7: Counting of Annexin V/PI stained cells. ***a)*** *Cells were counted under visible light to determine total cell number,* ***b)*** *the number of stained cells; apoptotic, secondary necrotic and necrotic cells were counted under fluorescence when excited at 488 nm.*

3.4.5 Protein expression using SDS-PAGE

The basis of SDS-polyacrylamide gel electrophoresis (SDS-PAGE) is to provide a rapid and inexpensive technique to separate proteins according to their molecular mass. Cell protein extracts are prepared containing the strongly anionic detergent SDS, a reducing agent such as 2-mercaptoethanol or DTT (dithiothreitol) and heat to denature and dissociate the proteins before loading onto a resolving polyacrylamide gel. The denatured proteins bind to SDS and become negatively charged and these complexes migrate through the polyacrylamide gel towards the anode according to protein size. Small molecular weight proteins migrate faster through the gel than larger proteins, and the use of standard molecular weight protein markers makes it possible to estimate the molecular weight of the sample protein.

The most common form of SDS-PAGE uses the discontinuous buffer system first developed in the 1960s (Orstein, 1964; Davis, 1964), and uses the differences in the pH and ionic strength between the buffer used to cast the gel and the buffer used in the gel tank reservoirs to improve gel resolution. Protein samples are loaded onto a stacking gel of high porosity (approx 5% acrylamide), and migrate quickly to the surface of a lower porosity resolving gel (ranging from 5% to 15% acrylamide). The degree of protein separation through an acrylamide gel is dependent on the absolute concentrations of acrylamide and bisacrylamide used to cast the gel and the level of cross-linking. Cross-linking is dependent on the level of bisacrylamide present and adds rigidity and strength to the gel. Low percentage acrylamide gels are used for high molecular weight proteins, with high percentage gels used for smaller proteins.

3.4.5.1 Preparation of cell lysates

Following completion of treatment regimens, the cells were washed twice with 10 ml sterile PBS and kept at 4°C. The cells were lysed with 300 µl of laemli sample buffer (LSB, 62 mM Tri-base pH 6.8, 10% glycerol, 2% SDS and 5% 2-

mercaptoethanol) with the addition of protease inhibitors aprotinin (Sigma, final concentration of 1 µg/ml), leupeptin (Sigma, final concentration of 1 µg/ml) and α-toluenesulfonyl fluoride (PMSF, final concentration of 100 µg/ml, Acros Organics, Leicestershire, UK). The cells were scraped off the flask surface using a cell scraper and DNA was sheared by repeatedly passing the lysate solution through a 25 gauge hypodermic needle (Becton Dickinson, UK) to reduce sample viscosity. The lysates were then denatured by boiling at 100°C for 5 min and stored at -20°C.

3.4.5.2 Bradford assay

Measurement of the total protein concentration present in the cell lysates was undertaken using the Bradford assay. Protein standard solutions were prepared by adding total protein concentrations of a BSA protein standard (bovine serum albumin, Sigma) ranging from 0-10 µg to 0.5 ml dH_2O. In parallel, 2 µl of each lysate sample was added and mixed to 500 µl dH_2O. A volume of 500 µl Bradford reagent (Bio-Rad, Hertfordshire, UK) was added to all samples, lysates samples and protein standards and mixed thoroughly. 250 µl of each standard and lysates sample was pipetted into a 96 well multi-titre plate (Nunc) in duplicate wells and optical density measured at 570 nm on a Labsystem Multiskan Multisoft plate reader. The concentration of total protein for each lysate sample was then calculated from the resulting BSA standard curve.

3.4.5.3 Electrophoresis and immunoblotting

Electrophoresis: Polyacrylamide gels were cast using Mini Protean gel casting apparatus (Bio-Rad), and stacking (5% acrylamide) and resolving (12% acrylamide) gels were prepared according to Sambrook and colleagues (1989). Cell lysate samples were prepared before loading onto the gel with the addition of 1x SDS gel-loading buffer (80 mM Tris-HCl (pH 6.8), 2% SDS, 10% glycerol, 0.1% bromophenol blue and 0.5% 2-mercaptoethanol). A biotinylated protein ladder (New England Biolabs, NEB, Hitchin, UK) was also loaded onto the gel to

enable estimation of protein band molecular weight. The samples were resolved at 80 V for 2h using a Tris-glycine electrophoresis buffer (25 mM Tris-base, 190 mM glycine, 0.1% SDS, pH 8.3) in the top and bottom reservoirs of the gel tank.

Immunoblotting: Following electrophoresis, the proteins were transferred onto 0.45 µm pore nitrocellulose membranes (Amersham, Buckinghamshire, UK) at 40 V for 1h at r.t using a Tris-glycine transfer buffer (25 mM Tris-base, 190 mM glycine, 0.1% SDS, 20% methanol and pH 6.8). After protein transfer, each nitrocellulose membrane was incubated for 1h in 25 ml TBS solution (20 mM Tris-base, 0.14 M NaCl and pH 7.6) containing 0.1% Tween-20 (TBS-T, Sigma) and 5% $^{w}/_{v}$ skimmed milk (blocking buffer) with gentle agitation at r.t. Each membrane was then washed three times with 15 ml TBS-T for 5 min at a time. The membranes were then incubated overnight at 4°C with gentle agitation with a primary antibody diluted 1:1000 or 1:2000 in 10 ml blocking buffer. For detection of expression of the tumour suppressor protein, p53, a murine monoclonal antibody was used at a dilution of 1:2000 (NEB). For detection of caspase-3 activation a rabbit polyclonal anti-caspase-3 antibody (NEB, 1:1000 dilution) and its cleaved activated form (NEB, 1:1000) was used. The detection of caspase-9 expression and cleavage of its activated form was detected using a rabbit polyclonal anti-caspase-9 antibody (NEB, 1:1000) and anti-cleaved caspase-9 antibody (NEB, 1:1000). Following primary antibody incubation overnight, each membrane was washed three times with 15 ml TBS-T for 5min. The membranes were then incubated for 1h with a HRP-linked (horse-radish peroxidase) secondary antibody diluted 1:1000 in 10 ml blocking buffer. The membranes probed with the p53 antibody were incubated with anti-mouse IgG HRP-linked antibody (NEB), and membranes probed with caspase antibodies were incubated with anti-rabbit IgG HRP-linked antibody (NEB). To detect the presence of the biotinylated protein ladder, an anti-biotin HRP-linked antibody was also added to the secondary dilution buffer at a dilution of 1:1000. The membranes were then washed for a further three times with TBS-T as described earlier.

3.4.5.4 Detection using Enhanced Chemi-Luminescence (ECL)

Detection of probed proteins transferred to the nitrocellulose membranes was carried out using the enhanced chemiluminescence detection system. 4 µl of 30% $^{w}/_{v}$ hydrogen peroxide (H_2O_2, Sigma) was added to 10 ml of an ECL buffer solution containing 100 mM Tris-HCl (pH 8.5, 4°C), 90 mM p-coumaric acid in DMSO (dimethyl sulphoxide) and 250 mM luminol in DMSO. The HRP linked to the secondary antibodies hydrolyse the H_2O_2 to H_2O and O_2, and it is this O_2 that oxidises luminol to produces luminescence that can be captured by using ECL hyperfilms (Amersham).

3.4.5.5 Stripping and re-probing of membranes

The membranes were incubated with stripping buffer (100 mM 2-mercaptoethanol, 2% SDS and 62.5 mM Tris-Cl, pH 6.7) at 50°C, for 30 min with gentle agitation. TBS-T was then used to rinse the blots, which could then be re-blocked and re-probed as described in **section 3.4.5.3**.

3.5 RESULTS

3.5.1 Assessment of cell viability following treatment with single agents and mixture

Cell viability was estimated for each cell treatment using the Trypan Blue exclusion method as described. The cells were exposed to single anticancer agents and to a mixture of the seven agents for a period of 24h. The cells were treated at median effect concentrations for each single agent and mixture for each cell line **(table 3.1)**. There was no evidence of cell toxicity for either cell line at this treatment concentration. Overall cell viability ranged from 96 to 99% for the DU145 cells **(figure 3.8)** for all single agents and the mixture. For the

MCF-7 cells the cell viability ranged from 96% to 98.5% with the exception of melphalan which was slightly lower at 91.5%.

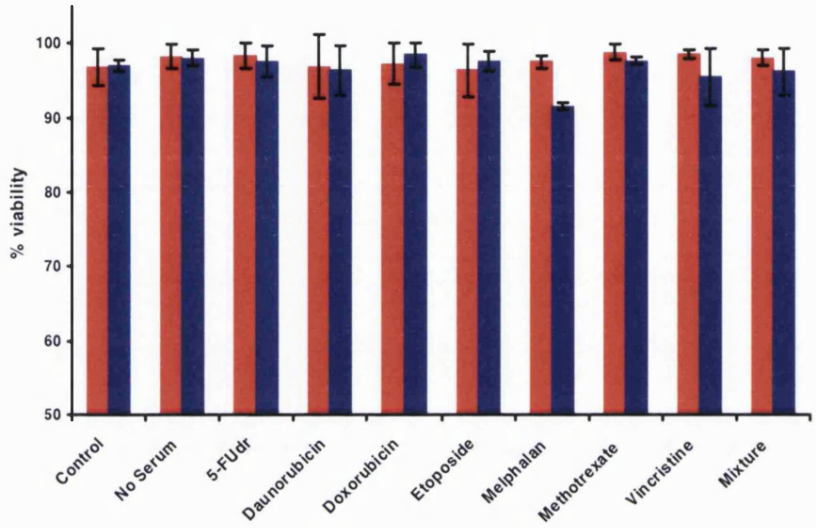

Figure 3.8: Estimation of cell viability after treatment of cells with single agents and mixtures. *The red columns represent the DU145 cells and show high viability for all drug treatments including the mixture (96-99% viability). The blue columns represent the MCF-7 cells and display a similar pattern of high cell viability (96-98.5%), with the exception of melphalan which had a slightly lower percentage viability of 91.5%. Data was taken from a minimum of three independent experiments and ± 1 s.d.*

3.5.2 Induction of apoptosis after treatment with single agents and mixture

The treated cells were dually stained with the fluorescein-linked PS binding protein, Annexin V, and with the fluorescent nuclear stain, propidium iodide. The level of a cell's ability to take up the Annexin V stain was attributed to the level of cells undergoing apoptosis **(figure 3.6a)**, any increase from control samples was considered to have increased the induction of apoptosis in the cells. Cells staining highly for PI were considered necrotic **(figure 3.6b)** as the increased nuclear membrane permeability allowed PI entry to stain nucleic acid, a distinct feature of necrotic cells. A third population of cells had undergone early stage

apoptosis but had reached a stage of nuclear membrane permeability, a state termed, secondary necrosis **(figure 3.6c)**.

3.5.2.1 DU145 cells

The DU145 cells were treated with each individual anticancer drug at median effect concentrations for cytotoxicity in the MTT assay (see **chapter 2**). A mixture composed in the same manner as **chapter 2** was also administered to these cells at its median effect concentration. The numbers of apoptotic, secondary necrotic and necrotic cells were counted and were presented as a percentage of the total number of stained cells **(figure 3.9)**. When studying the proportion of staining cells only, we could see that the cells dead or dying were predominately apoptotic. All of the drug treatments caused an increase in apoptotic cells except for daunorubicin, which had an increased level of necrotic cells, 17.9% of cell membrane permeable staining cells **(figure 3.9)**.

In summary, we can show that there was an increase in the level of apoptosis for the DU145 cells following treatment with each single anticancer agent and with a seven-component mixture. Establishing this effect with the DU145 cells clarified that these cells were most likely dying as a result of activation of apoptotic signalling pathways. Before examining this further, these experiments were repeated in the MCF-7 cells to establish whether this was the case for these cells as well.

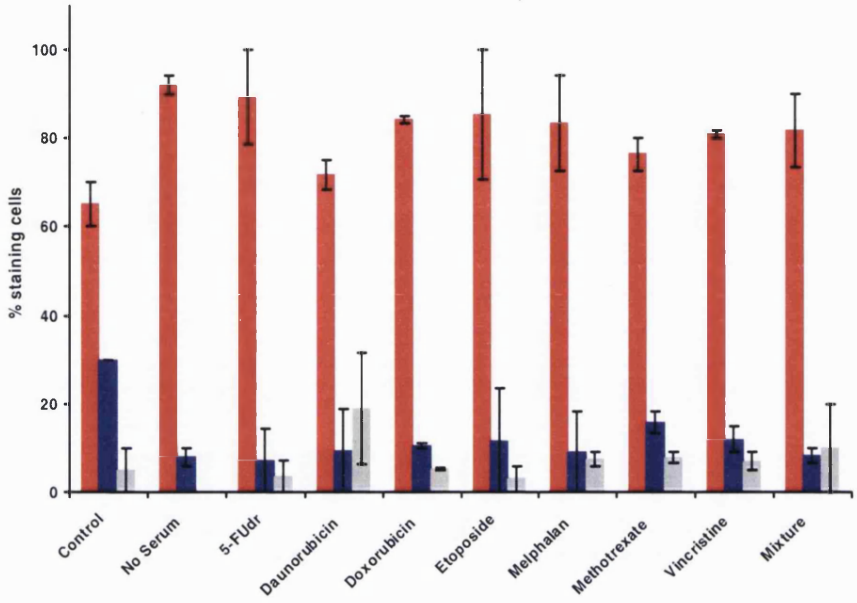

Figure 3.9: Level of apoptosis in the total number of staining DU145 cells following treatment with single drugs and the mixture. *The percentage of cells undergoing apoptosis (red columns) was noticeably increased in comparison to the secondary necrotic cells (blue columns) and necrotic cells (grey columns). Data taken from mean of two independent experiments ± 1 SEM.*

3.5.2.2 MCF-7 cells

The MCF-7 cells were treated in a similar manner to the DU145 cells, each agent and mixture was treated at its median effect concentration (depicted in **table 3.1**). There was increased apoptosis compared to the untreated controls for all single agents and the mixture **(figure 3.10)**. Looking at the number of staining cells, there was a significant increase in the proportion of apoptotic positive cells for all single drug and mixture treated cells compared to the untreated controls. The number of secondary necrotic and necrotic cells was of a small number once again for each of the treated cells, the highest being less than 14% of total staining cells being necrotic following vincristine sulphate.

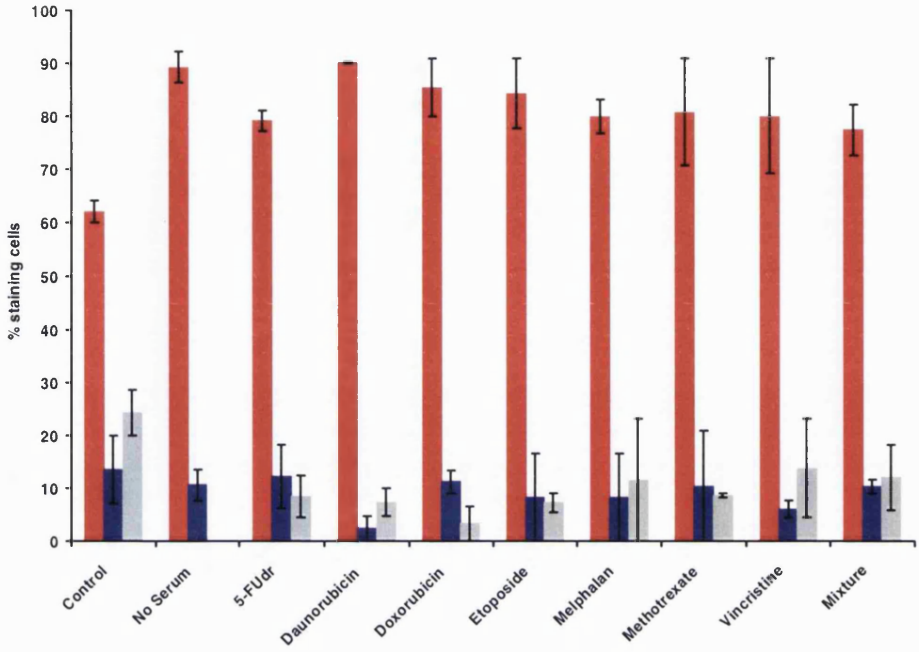

Figure 3.10: Level of apoptosis in the total number of staining MCF-7 cells following treatment with single drugs and the mixture. *The percentage of cells undergoing apoptosis (red columns) when treated with single agents and the mixture was significantly increased in comparison to the untreated controls. The secondary necrotic cells (blue columns) and necrotic cells (grey columns) were much smaller in proportion. Data taken from mean of two independent experiments ± 1 SEM.*

Overall, both cell lines displayed an increased level of cells undergoing apoptosis following treatment with median effect concentrations of each single anticancer drug and a seven-component mixture. This increase compared to untreated controls was very much apparent in the DU145 cells as the percentage of apoptotic cells was increased compared to the total number of staining cells. There was an increase in apoptotic cells for the MCF-7 cells, although this was not as high for all treatment conditions. We can now see that there was a common activation of apoptosis for all anticancer drugs and with the mixture in both cell lines. This confirms a similarity in effect to this level, but elucidation of the exact mechanism of apoptosis activation was required to establish whether these agents were initiating the process of apoptosis in a similar way. The next section describes an attempt to find this commonality.

3.5.3 Expression of the tumour suppressor gene, p53

3.5.3.1 Expression in the DU145 cells

The inactivation of the p53 gene in many tumours has shown that this gene is mutated in many human cancers. As has been discussed earlier, several prostate cancer cell lines were shown to contain mutations of their p53 gene. A mutation at this gene has been shown for the DU145 cell line (Isaacs et al., 1991) and these cells express this protein at sufficient levels in order to be detectable by immunoblotting. This suggests that the p53 expressed by DU145 cells has an extended half-life, a common feature of a mutated p53 gene (Finlay et al., 1988). **Figure 3.11** shows that untreated control DU145 cells synthesize the p53 protein and this accumulates in sufficient amounts to be detected by immunoblotting. Although the western blotting detection method can detect increased expression of this protein, it cannot distinguish between functioning wild type p53 and the non-functional mutant p53. The cells were treated with median effect level concentrations for 24h.

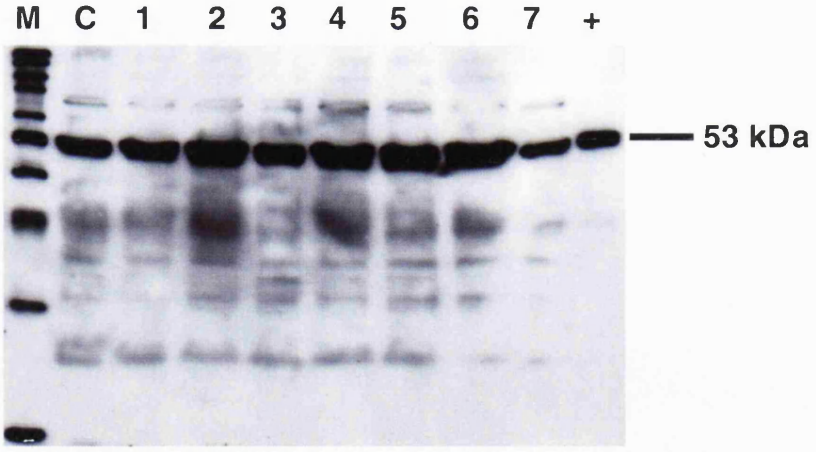

Figure 3.11: Expression and accumulation of p53 protein in the DU145 cells. *Lane M, protein size marker; C, control; 1, 5-FUdR treated; 2, daunorubicin treated; 3, doxorubicin treated; 4, etoposide treated; 5, melphalan treated; 6, methotrexate treated; 7, vincristine treated; +, UV treated cos cells (positive control). All DU145 cell lysates, even untreated cells, expressed a form of p53 protein (Isaacs et al., 1991).*

3.5.3.2 Expression in the MCF-7 cells

Unlike the DU145 cells, the MCF-7 cells express an unmutated p53 gene (Gudas et al., 1996) and expression of the p53 protein can be detected post treatment for each single agent and the seven-component mixture. **Figure 3.12** summarises the expression of p53 in the MCF-7 cells following treatment with each of the seven anticancer drugs and a mixture. The MCF-7 cells were treated as described in **section 3.4.2.2** using six different treatment schedules, shown as lanes 1-6 in **figure 3.12**.

The western blot showing the expression of p53 in cells treated with 5-FUdR **(figure 3.12a)** showed that after 24h exposure to the median effect concentration of this drug, there was increased expression of p53. A recent study has shown that there was no increase in p53 levels following 24h 5-FU treatment to MCF-7 cells (Zoli et al., 2005), although these cells were treated with 5-FU, the precursor of 5-FUdR, so may bear minimal similarity, with my results. Following treatment with both daunorubicin **(figure 3.12b)** and doxorubicin **(figure 3.12c)** there was increased p53 expression with increasing exposure time of the cells to the drugs. There was zero to low levels of p53 after 2h exposure (lane 4), increasing after 4h (lane 5) and 6h (lane 6) until a saturation point after 24h at increasing median effect concentrations (lanes 1, 2 & 3). p53 expression has been shown to be increased following daunorubicin treatment in MCF-7 cells (Moller et al., 2002) as well as for doxorubicin treatment (Gupta et al., 2001). After treatment with etoposide, the MCF-7 cells exposed for 24h at median effect concentrations of the drug expressed low levels of p53 **(figure 3.12d)**. Exposure to this drug generally shows increased levels of apoptosis activation as it inhibits the synthesis of the oncoprotein MDM2 and results in increased expression of p53. Exposure to melphalan resulted in increased expression of p53 in relation to untreated control after 24h treatment at the highest concentration of the drug, at 10x MED **(figure 3.12e)**. Following exposure to methotrexate at varying concentrations and treatment times, there was no increase in p53 protein synthesis **(figure 3.12f)**. The lack of p53 expression could be a result of a level of resistance of these cells to methotrexate as has been shown previously when combined with oestrogen

exposure (Thibodeau et al., 1998), although this was not explored any further in this study.

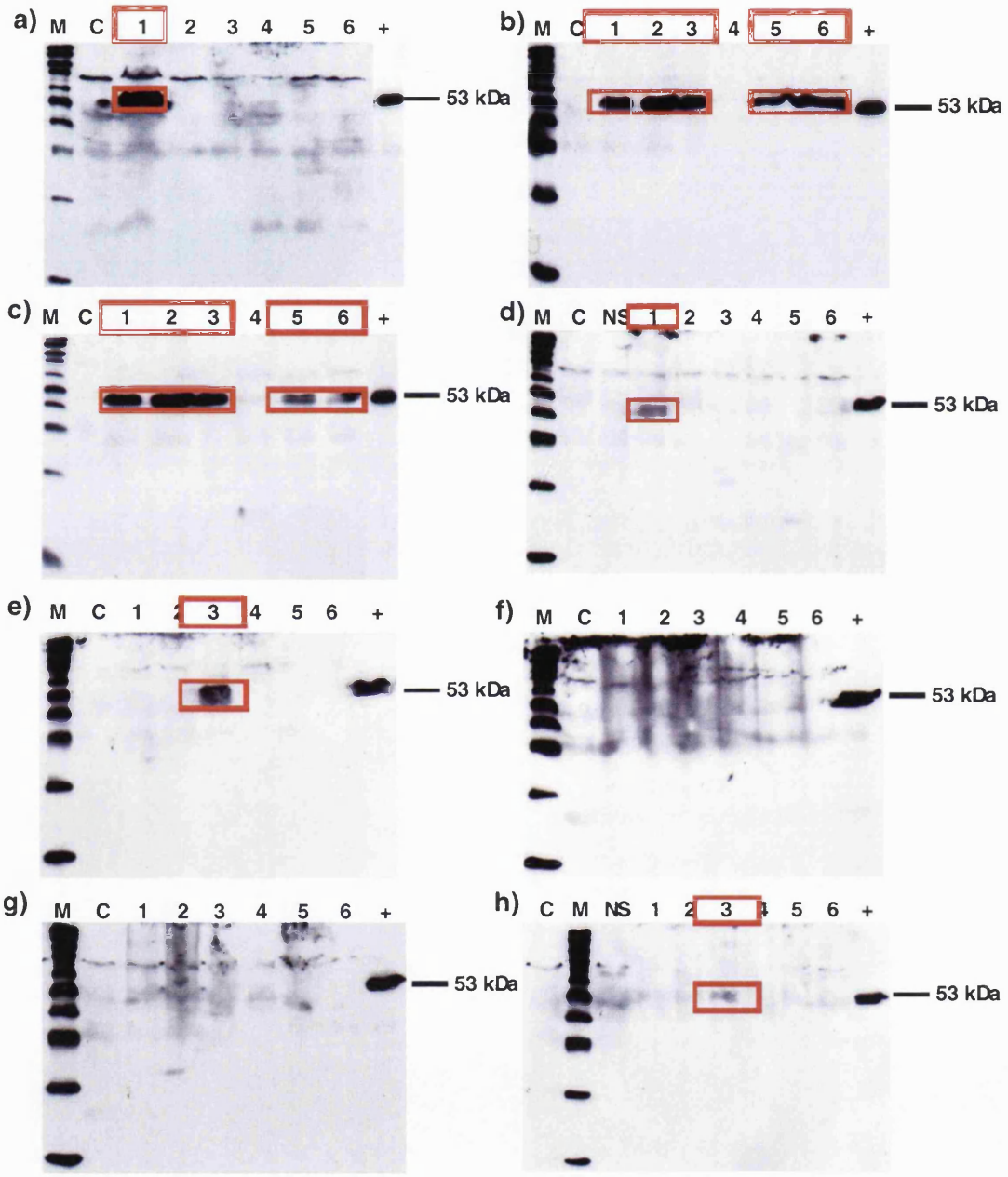

Figure 3.12: Expression of p53 in single agent and mixture treated MCF-7 cells. *Lane M, protein size marker; C, control; NS, no-serum treated; 1, treated 24h at 1x median effect level (MED); 2, treated 24h at 5x MED; 3, treated 24h at 10x MED; 4, treated 2h at 1x MED; 5, treated 4h at 1x MED; 6, treated 6h at 1x MED; +, cos cells UV-treated (positive control).* ***a)*** *5-FUdR treated;* ***b)*** *daunorubicin treated;* ***c)*** *doxorubicin treated;* ***d)*** *etoposide treated;* ***e)*** *melphalan treated;* ***f)*** *methotrexate treated;* ***g)*** *vincristine treated;* ***h)*** *seven-component mixture treated cells.*

Vincristine treated MCF-7 cells showed very little sensitivity in increasing p53 protein levels. There was a faint band seen at the 2h treated cell sample **(figure 3.12g, lane 4)**, and this was somewhat of a surprise as vincristine treated MCF-7 cells have previously been shown to markedly increase p53 expression (Vayssade et al., 2002). **Figure 3.12h** shows the effect of treating MCF-7 cells with the seven-component mixture on the synthesis of p53. We can see that there was only a slight increase in expression and that only after 24h exposure at 10x MED. Overall six of the seven agents led to increased levels of p53 expression following exposure to the MCF-7 cells. The exception was the methotrexate treated cells that may somehow show some level of drug resistance and the vincristine treated cells although there was a faint band following 2h drug exposure. All cell treatments showing evidence of increased p53 expression demonstrated this following 24h drug exposure **(figures 3.12a, b, c, d, e & h)**.

3.5.4 Activation of the caspase cascade

The caspase cascade was summarised earlier in this chapter and two caspases were chosen to probe for changes in their expression levels following exposure to each single agent and to the seven-component mixture. The procaspase-3 and the procaspase-9 proteases were probed and cascade activation measured by cleavage to their activated, smaller protein forms cleaved caspase-3 and cleaved caspase-9, respectively.

3.5.4.1 Expression of procaspase-9 and activated cleaved complex

The protease caspase-9 is one of the initiator caspases along with caspase-8 and -10. Uncleaved procaspase-9 (47 kDa) forms a complex known as the apoptosome when complexed to Apaf-1. Release of mitochondrial cytochrome c causes the cleavage of the apoptosome to the activated form of caspase-9 (37

kDa) that can in turn cleave procascase-3 to its active state and initiate the caspase cascade.

3.5.4.1.1 DU145 cells

The cells were treated for 24h with median effect concentrations of each single agent and the whole cell lysates were probed with antibodies for procaspase-9 and its cleaved activated form. **Figure 3.13** shows that cleavage of the apoptosome occurred in four of the seven treatment conditions, for doxorubicin, etoposide phosphate, melphalan and methotrexate treated DU145 cells. There was low level expression of the cleaved product for vincristine treated cells, but no bands were present for both 5-FUdR and daunorubicin treated cells.

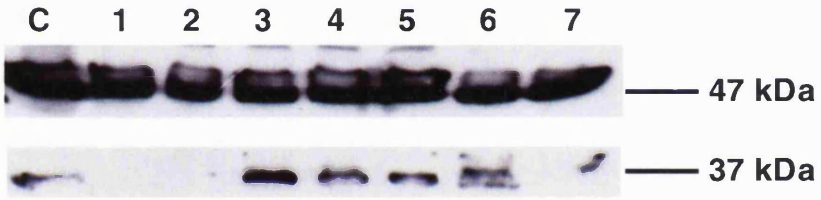

Figure 3.13: Expression of procaspase-9 and cleaved caspase-9 in single agent treated DU145 cells. *Lane C, control; 1, 5-FUdR treated; 2, daunorubicin treated; 3, doxorubicin treated; 4, etoposide treated; 5, melphalan treated; 6, methotrexate treated; 7, vincristine treated. Procaspase-9 was expressed in all treatment conditions (47 kDa band), cleaved activated caspase-9 shown with 37 kDa band was expressed for doxorubicin, etoposide, melphalan and methotrexate treated cells. There were low levels for the control cells and for the vincristine treated cells. No bands were present for the cleaved caspase for 5-FUdR and daunorubicin treated cells.*

3.5.4.1.2 MCF-7 cells

The MCF-7 cells were treated in the same manner as the DU145 cells and **figure 3.14** shows that not all of the treated cells expressed procaspase-9. The methotrexate treated cells expressed none of the uncleaved product, and little levels were seen for both doxorubicin and etoposide treated cells. Bands for the cleaved protein could be seen for the following drugs: 5-FUdR (low levels),

daunorubicin (very low), etoposide, melphalan and methotrexate. There was no band at 37 kDa for either the doxorubicin or vincristine treated cells.

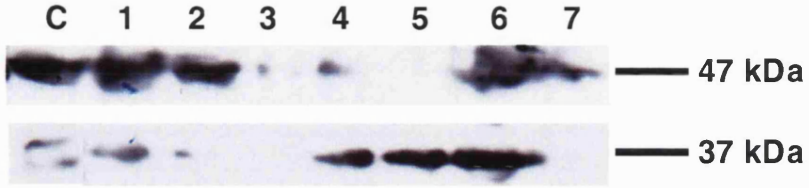

Figure 3.14: Expression of procaspase-9 and cleaved caspase-9 in single agent treated MCF-7 cells. *Lane C, control; 1, 5-FUdR treated; 2, daunorubicin treated; 3, doxorubicin treated; 4, etoposide treated; 5, melphalan treated; 6, methotrexate treated; 7, vincristine treated. Procaspase-9 was expressed in all treatment conditions (47 kDa band) except for low levels in the doxorubicin and etoposide treated cells. There was no band for procaspase-9 for melphalan treated cells. The cleaved activated caspase-9 shown with 37 kDa band was expressed for etoposide, melphalan and methotrexate treated cells. There were low levels for the control cells and for the 5-FUdR and daunorubicin treated cells. No bands were present for the cleaved caspase for doxorubicin and vincristine treated cells.*

For both cell lines we could see activation of caspase-9 in the etoposide, melphalan and methotrexate treated cells. Conversely, cleavage product as a result of 5-FUdR, daunorubicin and vincristine were of very low or zero levels implying differing mechanisms of apoptosis activation for these drugs.

3.5.4.2 Expression of caspase-3 and activated cleaved complex

3.5.4.2.1 DU145 cells

The DU145 cells express the protein procaspase-3 normally, unlike the MCF-7 cells. Each whole cell lysate sample for each drug treatment was probed for the expression of procaspase-3 protein (35 kDa) and for the active cleaved protein, cleaved caspase-3 (17 kDa).

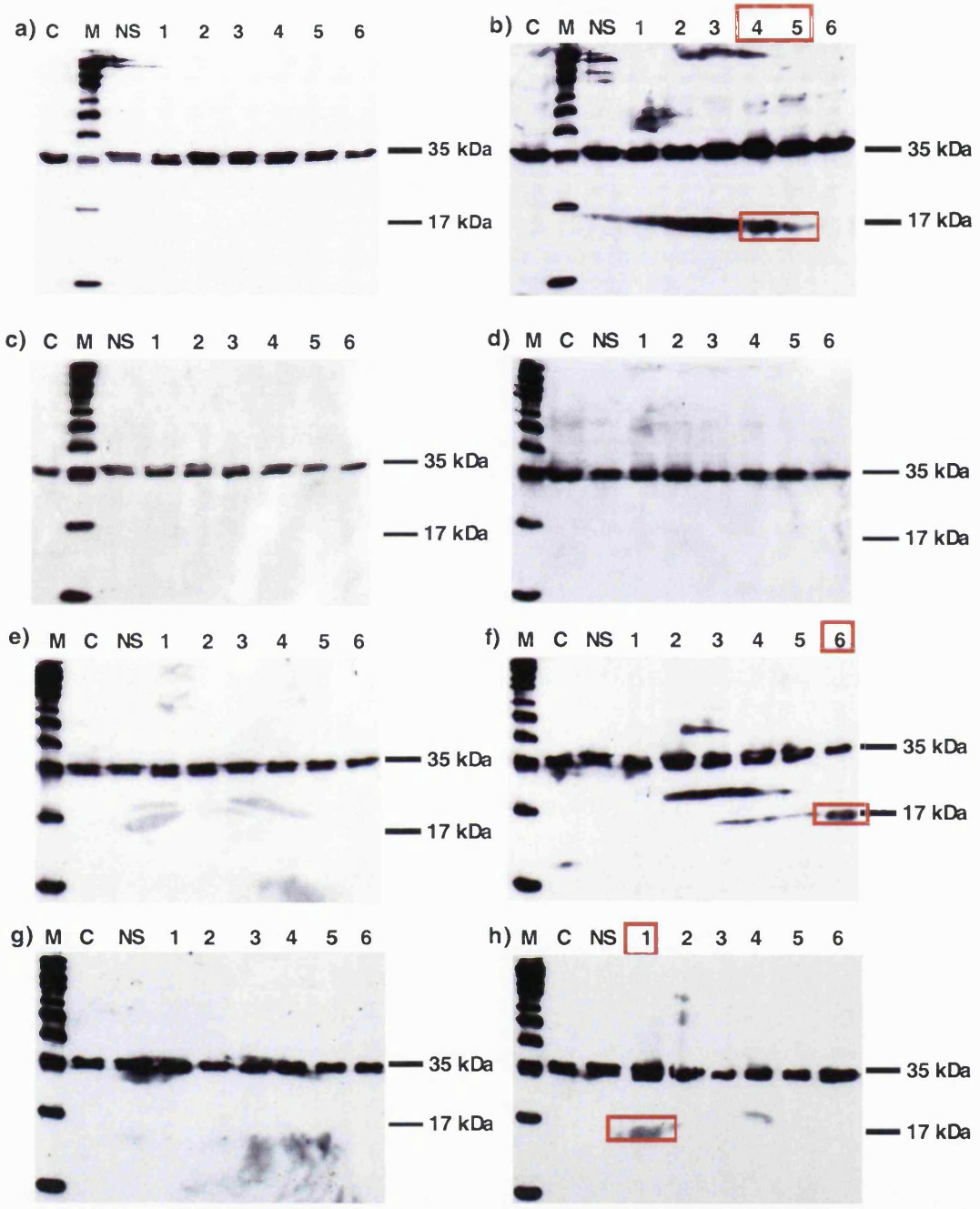

Figure 3.15: Expression of procaspase-3 and cleaved caspase-3 in single agent and mixture treated DU145 cells. *Lane M, protein size marker; C, control; NS, no-serum treated; 1, treated 24h at 1x median effect level (MED); 2, treated 24h at 5x MED; 3, treated 24h at 10x MED; 4, treated 2h at 1x MED; 5, treated 4h at 1x MED; 6, treated 6h at 1x MED; +, cos cells UV-treated (positive control).* ***a)*** *5-FUdR treated;* ***b)*** *daunorubicin treated;* ***c)*** *doxorubicin treated;* ***d)*** *etoposide treated;* ***e)*** *melphalan treated;* ***f)*** *methotrexate treated;* ***g)*** *vincristine treated;* ***h)*** *mixture treated cells. Inactivate caspase-3 was expressed in all treatment conditions (35 kDa band), cleaved activated caspase-3 shown with 17 kDa band. The red boxes illustrate exposure conditions that resulted in cleavage of the procaspase-3 protease.*

Of the eight different drug treatments, only three led to the cleavage of procaspase-3 and a subsequent activation of caspase-3. These three treatments are shown in **figure 3.15** and are daunorubicin, methotrexate and the seven-component mixture. Following daunorubicin treatment at 1x MED for 2h and 4h there was cleavage of caspase-3 and this shows that this event occurs very early after first time of drug exposure as expression after 4h was lower than at 2h **(figure 3.15b)**. Treatment of the DU145 cells with methotrexate for 6h at 1x MED showed that there was an increase in levels of the cleaved caspase-3 protein **(figure 3.15f)**. DU145 cells treated for 24h at 1x MED with the seven-component mixture also showed an increase in caspase-3 cleavage product **(figure 3.15h)**. The other five agents show no activation of the caspase-3 protein at any of the treatment conditions tested for the DU145 cell line.

3.5.4.2.2 MCF-7 cells

The MCF-7 cells are deficient in caspase-3 (Janicke et al., 1998) and so could not be probed for this effector caspase and its cleaved form. Confirmation of negative expression of caspase-3 in the MCF-7 cell lysates treated with each drug and mixture was undertaken and the cells did not produce any of this protein (data not shown).

3.5.5 Mixed model predictions

The relationship between the observed mixture effects and the predictions for both cells lines never brought about exact fits between observed effects and predictions. This prompted a revisit to the assumptions made when formulating these mixture predictions. From the group of seven tested agents with dissimilar sites of action, there were five agents (a group of three agents and a group of two) that could possibly be deemed as being similarly acting to one another.
Three of the drugs could be grouped together. Two of these were daunorubicin and doxorubicin that share structural similarity and act as intercalating agents.

These drugs are also known to inhibit the enzyme topoisomerase II, which a third drug, etoposide phosphate, can also inhibit. In addition, two more drugs, 5-fluoro-5'-deoxyuridine and methotrexate, both belong to the antimetabolite class of drug, and although they both act at differing stages of DNA synthesis, they both interfere with this process. This broader sub-classification meant that we could calculate a mixed model prediction for *independent action* for both cell lines. This was done by calculating the *concentration addition* mixture effect predictions for the topoisomerase inhibitors (daunorubicin, doxorubicin and etoposide), and for the antimetabolites (5-FUdR and methotrexate). A seven component mixture had now become a four component mixture (composed of topoisomerase inhibitors, antimetabolites, vincristine sulphate and melphalan). A new four-component *independent action* prediction (IA_{MIXED}) was then calculated for both cell lines as shown in **figures 3.16 & 3.17**.

We can see a clear change in the characteristics of the IA_{MIXED} curve compared to the standard *independent action* prediction **(figure 3.16)**. The IA_{MIXED} curve bears close resemblance to the *concentration addition* prediction. The EC_{50} concentration for the IA_{MIXED} curve was 0.71 μM, and for *concentration addition* this was 1.43 μM. This might have been expected as five of the original seven components were now predicted using *concentration addition*, the seven component mixture switching to a four component mixture. The lower number of mixture components has previously resulted in the predictive models of independent action and concentration addition to become closer (Drescher and Boedeker, 1995) as can be seen in **figures 3.16 & 3.17**. The close similarity between the predictions based on *concentration addition* and the IA_{MIXED} models suggests a possible enhancement of the existing *independent action* predictive model, and in the case for DU145 cells good agreement of the IA_{MIXED} prediction with the observed mixture effects. The EC_{50} values for IA_{MIXED} was 0.71 μM and very close to that for the observed mixture 0.94 μM. The idea of possible antagonism in the mixture can be eliminated as with the use of the modified prediction IA_{MIXED} there is no deviation from observed mixture data and the

mixture prediction models and therefore the antagonism has been replaced by an additive effect (Berenbaum, 1989).

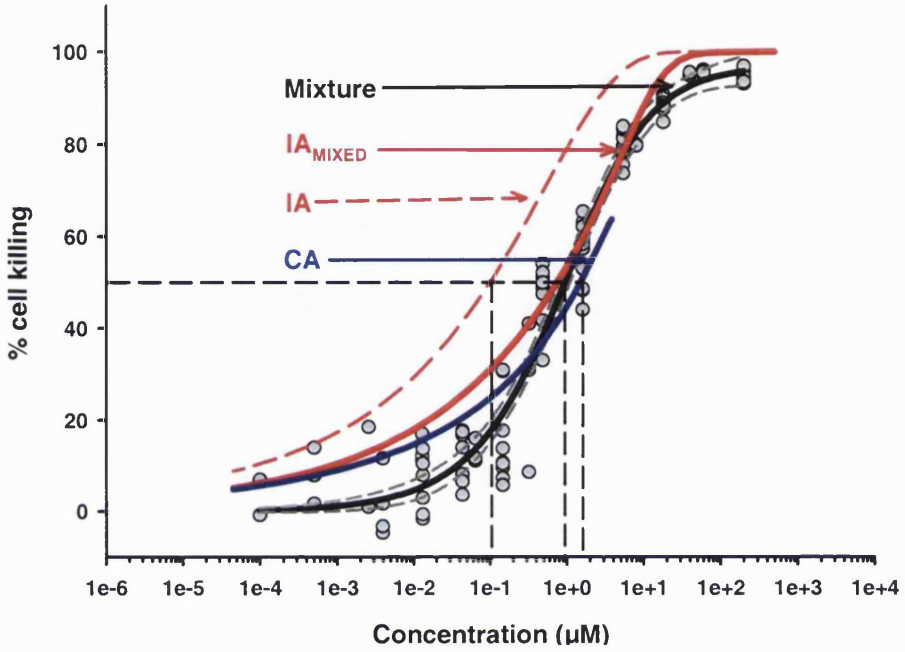

Figure 3.16: Mixed model observed and predicted effects for DU145 cells. *The two antimetabolite drugs were treated as a single mixture component, and the anthracyclines and etoposide combined as a second component, in addition to melphalan and vincristine sulphate. The solid red line represents the mixed model IA prediction shifted to the right of the initial IA prediction (red dotted line, found in* ***figure 2.21****). The black dotted lines represent the* EC_{50} *concentrations for each response curve.*

The modification to the *independent action* predictive model was repeated in a similar manner for the MCF-7 cells, as shown in **figure 3.17**. The IA_{MIXED} curve had again shifted towards the right, the EC_{50} value increases from 0.038 µM for the *independent action* curve to 0.17 µM, moving closer to the *concentration addition* prediction curve. The agreement for the IA_{MIXED} prediction model was not as good for this particular cell line, the separation between the IA_{MIXED} model and the observed effects regression model was still of two orders of magnitude. The *concentration addition* prediction has consistently shown closer agreement to the observed mixture effects for both cell lines, confirming the inaccuracy of the *independent action* predictions for this group of anticancer drugs.

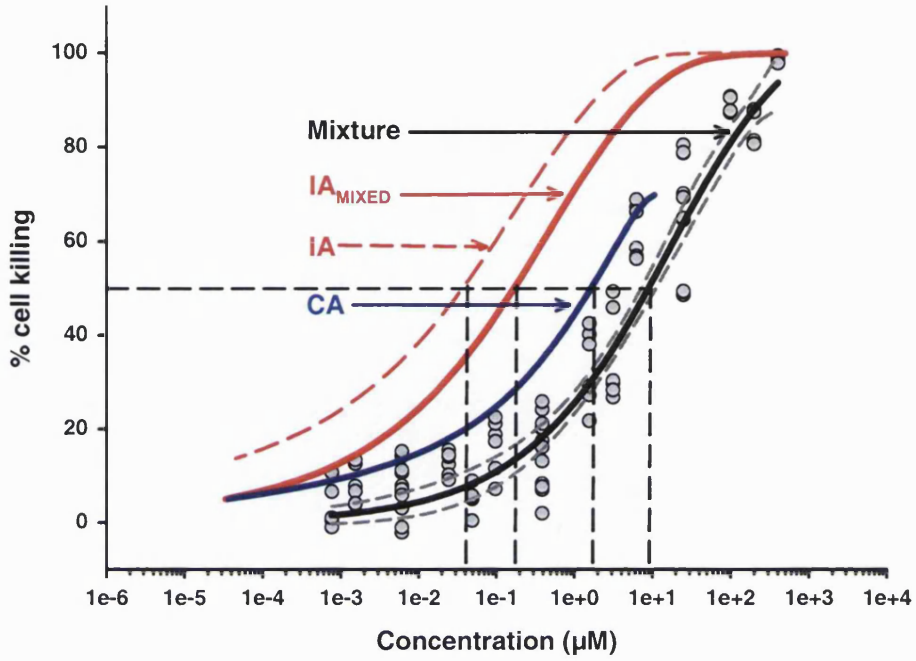

Figure 3.17: Mixed model observed and predicted effects for MCF-7 cells. *The two antimetabolite drugs were treated as a single mixture component, and the anthracyclines and etoposide combined as a second component, in addition to melphalan and vincristine sulphate. The solid red line represents the mixed model IA prediction shifted to the right of the initial IA prediction (red dotted line, found in* ***figure 2.28****). The* IA_{MIXED} *prediction was much closer to the CA prediction giving a more accurate predictive model for these agents than the original IA model. The black dotted lines represent the* EC_{50} *concentrations for each response curve.*

This approach was further employed by integrating the findings from p53 expression for the MCF-7 cells, procaspase-3 cleavage for the DU145 cells and procaspase-9 cleavage of both cell lines. Basing similarity assumptions on the activation of either one of these signalling proteins new IA_{MIXED} predictions could be calculated.

3.5.5.1 DU145 cells, procaspase-9 and procaspase-3 cleavage

The result from **figure 3.13** suggests a common activation of the initiator caspase, procaspase-9, for four of the seven drugs; doxorubicin, etoposide phosphate, melphalan and methotrexate. A *concentration addition* prediction

model was calculated for the combined effects for these four drugs and then a new $IA_{MIXED,Caspase-9}$ prediction modelled. **Figure 3.18** shows that the modification to the original *independent action* prediction has brought it closer to the observed mixture effects, the EC_{50} was 0.26 μM for the $IA_{MIXED,Caspase-9}$ prediction curve, compared to 0.71 μM for IA_{MIXED} and for the observed mixture 0.94 μM.

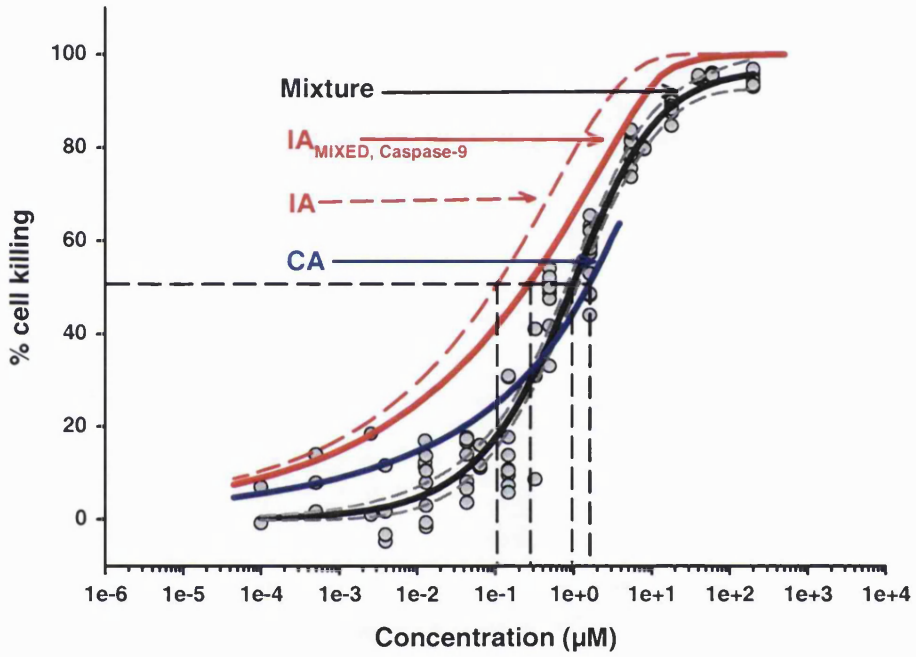

Figure 3.18: Mixed model based on procaspase-9 cleavage for DU145 cells. *The drugs doxorubicin, etoposide phosphate, melphalan and methotrexate were treated as a single mixture component, and the modified IA model calculated with three more mixture components, 5-FUdR, daunorubicin and vincristine sulphate. The solid red line represents the mixed model IA prediction shifted to the right of the initial IA prediction (red dotted line, found in* ***figure 2.21****). The $IA_{MIXED,Caspase-9}$ prediction was much closer to the CA prediction giving a more accurate predictive model for these agents than the original IA model. The black dotted lines represent the EC_{50} concentrations for each response curve.*

In a similar manner, **figure 3.19** shows the result of the modification of the *independent action* model as a result of the findings from **figure 3.15**, drug induced cleavage of procaspase-3 for DU145 cells. There was a shift towards the right for the $IA_{MIXED,Caspase-3}$ curve but it was not as pronounced as for the IA_{MIXED} curve **(figure 3.16)** and $IA_{MIXED,Caspase-9}$ curve **(figure 3.18)**. EC_{50} for the

$IA_{MIXED,Caspase-3}$ curve was 0.185 μM, much lower than for either of the other *independent action* modified models.

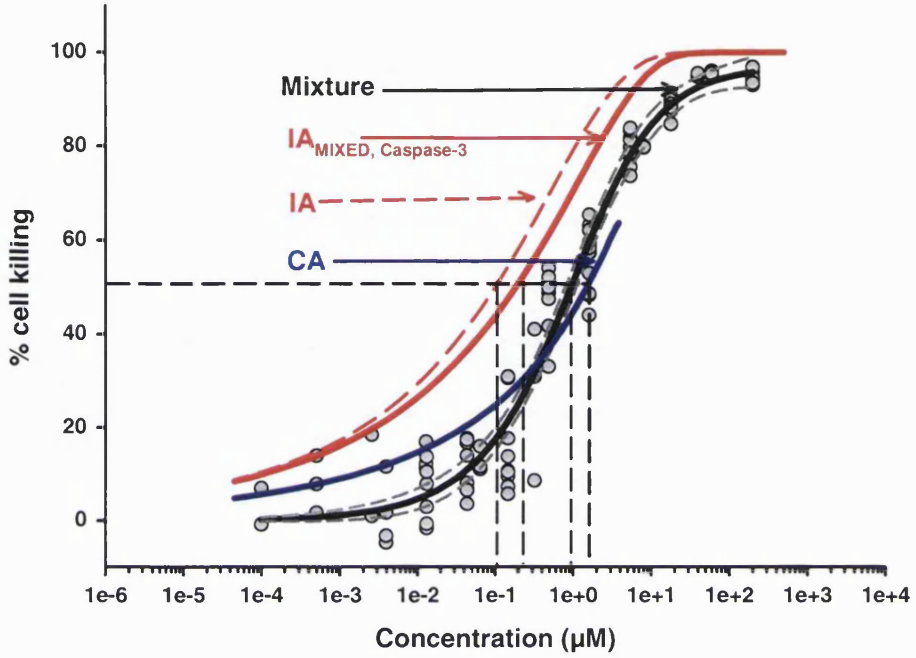

Figure 3.19: Mixed model based on procaspase-3 cleavage for DU145 cells. *The drugs daunorubicin and methotrexate were treated as a single mixture component, and the modified IA model calculated with five more mixture components, 5-FUdR, doxorubicin, etoposide phosphate, melphalan and vincristine sulphate. The solid red line represents the mixed model IA prediction shifted to the right of the initial IA prediction (red dotted line). The $IA_{MIXED,Caspase-3}$ prediction was slightly closer to the CA prediction. The black dotted lines represent the EC_{50} concentrations for each response curve.*

These two modifications of the *independent action* predictive model have improved the accuracy to predict the combined effects of these seven agents, but the best model remained *concentration addition*, although the modification shown in **figure 3.16** showed good agreement between the IA_{MIXED} curve and the observed mixture effects especially at higher concentrations of the mixture.

3.5.5.2 MCF-7 cells, p53 and procaspase-9 cleavage

Following treatment with five of the seven anticancer drugs, there was increased expression of p53 in the MCF-7 cells **(figure 3.12)**. These single agents were 5-

FUdR, daunorubicin, doxorubicin, etoposide phosphate and melphalan. The single agent effects for these five agents were then combined together to create a new five-component *concentration addition* prediction model that was then used to modify the *independent action* predictive model. In addition to these five agents that activate p53, the $IA_{MIXED,p53}$ model was calculated using two more mixture components, methotrexate and vincristine sulphate, which did not express significant levels of p53 **(figure 3.12)**. The new modified prediction model was shown in **figure 3.20** and demonstrates a significant right shift of the original *independent action* model.

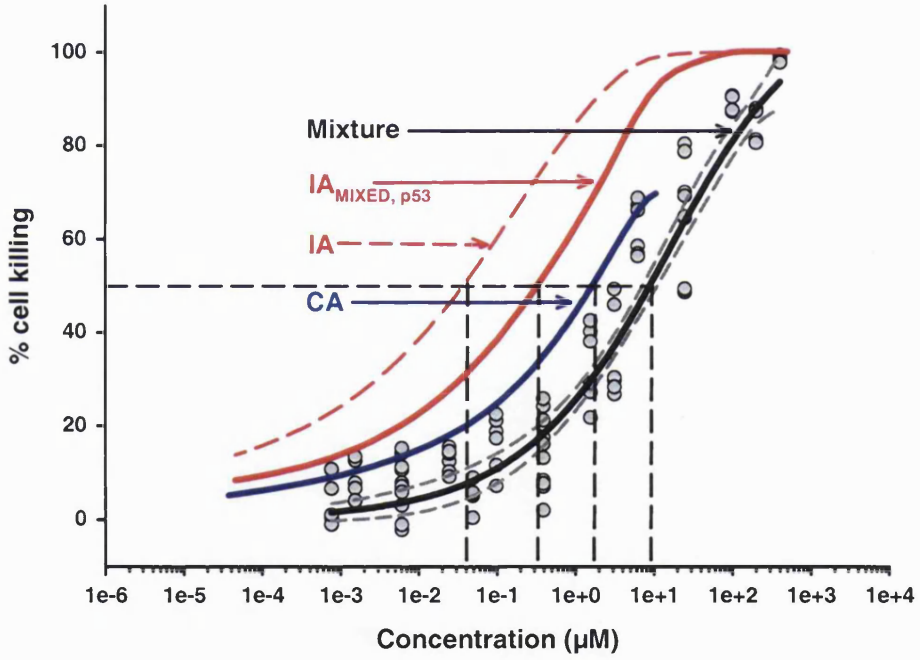

Figure 3.20: Mixed model based on p53 expression for MCF-7 cells. *The drugs 5-FUdR, daunorubicin, doxorubicin, etoposide phosphate and melphalan were treated as a single mixture component, and the modified IA model calculated with two more mixture components, methotrexate and vincristine sulphate. The solid red line represents the mixed model IA prediction shifted to the right of the initial IA prediction (red dotted line, found in* ***figure 2.28****). The* $IA_{MIXED,p53}$ *prediction was much closer to the CA prediction giving a more accurate predictive model for these agents than the original IA model. The black dotted lines represent the* EC_{50} *concentrations for each response curve.*

The EC_{50} for the $IA_{MIXED,p53}$ curve was 0.33 μM compared to 0.038 μM for the original *independent action* curve and leads to a decrease in separation between the *concentration addition* and *independent action* curves.

Cleavage of the initiator caspase, procapase-9 was also used to modify the independent action predictive model. In this case for MCF-7 cells, three agents showed activation of caspase-9, etoposide phosphate, melphalan and methotrexate. These were combined in much a similar way to **figures 3.16 to 3.20** and resulted in an $IA_{MIXED,Caspase-9}$ curve that was slightly shifted to the right of the existing *independent action* curve **(figure 3.21)**.

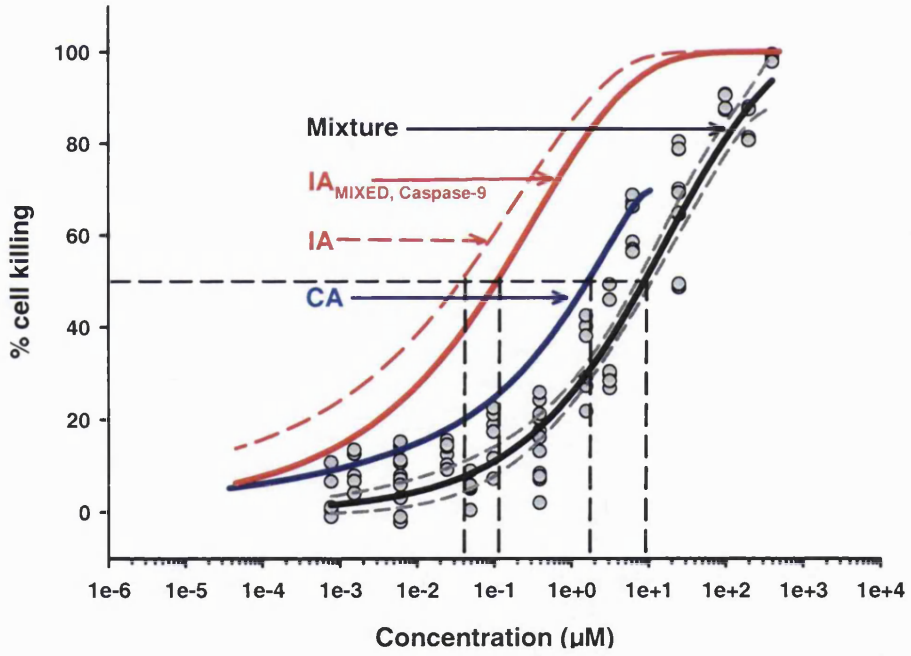

Figure 3.21: Mixed model based on procaspase-9 cleavage for MCF-7 cells. *The drugs etoposide phosphate, melphalan and methotrexate were treated as a single mixture component, and the modified IA model calculated with four more mixture components, 5-FUdR, daunorubicin, doxorubicin and vincristine sulphate. The solid red line represents the mixed model IA prediction shifted to the right of the initial IA prediction (red dotted line). The $IA_{MIXED,Caspase-9}$ prediction was slightly closer to the CA prediction. The black dotted lines represent the EC_{50} concentrations for each response curve.*

The shift towards the right was less extreme than for either of the previous *independent action* modifications for MCF-7 cells. The EC_{50} was 0.11 μM for the $IA_{MIXED,Caspase\text{-}9}$ curve, much lower than for the $IA_{MIXED,\ p53}$ curve and for the IA_{MIXED} curve, showing that although this modification was more accurate than the original *independent action* model **(figure 2.28)**, the most accurate model was using the $IA_{MIXED,p53}$ curve. In any case whether with modification or not, the model for *independent action* was still inaccurate in comparison to the *concentration addition* model.

3.6 DISCUSSION

The findings from the previous chapter demonstrated the relative inaccuracy of one of the predictive models used to assess joint effects for drugs. The model used to predict the effects of agents with dissimilar modes of action, *independent action*, was found to consistently overestimate the joint effects for a group of seven anticancer drugs. The results from **chapter 2** have led us to reassess how we can classify similar and dissimilar acting drugs, with the view to improve the overall prediction.

In this chapter we have examined the idea that a common mechanism in cell killing was possible for each of the seven tested anticancer agents, and may be the cause for the relative accuracy of the prediction based on *concentration addition* to the observed mixture effects. This was explored in two ways. First, induction of apoptosis by these drugs was assessed to establish whether there was a broad range commonality at this level. The second stage explored the activation of a number of important signalling proteins in the apoptosis pathway following treatment with each of these drugs.

3.6.1 A common level in the induction of apoptosis

The assessment for measuring the level of cell undergoing apoptosis used the feature of fluorescently staining levels of PS externalised during the initial stages of apoptosis (Fadok et al., 1992a; 1992b; 1993; Koopman et al., 1994; Homburg et al., 1995). Treatment with each individual agent and the seven-component mixture did not result in increases in cell toxicity at the levels of concentration the cells were treated at. The effect was similar with both cell lines used and cell viability did not drop below 96% **(figure 3.8)**, except for the MCF-7 cells treated to melphalan, where 91.5% of viable cells were present. For the DU145 cells treated with these drugs, we saw that there were increased levels of apoptotic cells for each treated drug in the stained cell population **(figure 3.9)**. In support, the MCF-7 cells acted in much of a similar way as all drugs treatments including the seven component mixture, showed increased levels of cells undergoing apoptosis compared to untreated control cells **(figures 3.10)**. We could see now that the first stage of development for our hypothesis was true, indeed the cells were undergoing increased apoptosis as a result of exposure to these drugs, including the seven-component mixture. A more detailed explanation of how these drugs were killing these cells was now required.

3.6.2 Signalling by the suppressor gene, p53

As discussed earlier in this chapter **(section 3.3)**, the two cell lines chosen had different abilities to express the tumour suppressor gene, p53. The DU145 cells possess a mutation at this gene and therefore express a mutated form of p53 (Isaacs et al., 1991) that impairs its ability to undergo p53 mediated apoptosis **(figure 3.11)**. The MCF-7 cells, however, can express this protein as a normal cell would and could demonstrate the expression levels of this protein following exposure to each of these drugs. **Figure 3.12** summarises the findings in the MCF-7 cell line. There were increased levels of expression of p53 for six of the

eight drug treatments. Only methotrexate and vincristine sulphate (low levels) failed to exhibit any increase in p53 expression **(figure 3.12f & g)** and it has been shown that when exposed to oestrogens, the MCF-7 cells develop a resistance to methotrexate (Thibodeau et al., 1998). Whether this was the particular case was open to question, as no oestrogenic chemicals were present at any stage of cell treatment or the media and solutions. As can be seen later, it appears that methotrexate induces activation of apoptosis via a p53-independent manner.

3.6.3 Signalling by the initiator caspase-9

The expression of the initiator caspase, procaspase-9, was examined for both cell lines. For the DU145 cells we show increased levels of the activated cleaved caspase-9 in four of the seven drugs treated **(figure 3.13)**. There was low level expression for vincristine, but it was more prominent in doxorubicin, etoposide phosphate, melphalan and methotrexate treated DU145 cells. Activation of the apoptosome can occur after activation of the p53 tumour suppressor gene **(figure 3.5)**, so the levels found for doxorubicin, etoposide, melphalan and methotrexate could be a downstream effect of this; that is, if the DU145 cells had a fully functional p53 gene, which it doesn't. This could mean that DU145 cells exposed to these four drugs may be undergoing some form of mitochondrial-mediated apoptosis, but further examination by looking at Bax/Bak/Bcl-2/Bcl-X_L expression is required to fully understand if this was the case.

Unlike the DU145 cells, the expression levels of the activated form of caspase-9 could be related to the amount of p53 expressed in the MCF-7 cells. Of the seven drugs treated, three drugs showed increased levels of cleaved caspase-9 product **(figure 3.14)**. The MCF-7 cells treated with etoposide, melphalan and methotrexate showed the presence of a band at 37 kDa. Both etoposide and melphalan levels can be explained by increased p53 expression, but for

methotrexate there was no increase in levels of p53 whatsoever. Methotrexate is a folate antagonist and acts by inhibiting DHFR and therefore inhibits DNA synthesis (Blakeley, 1995). Its mechanism of action in killing cells is unlikely to involve p53, and is more likely to be initiated by death receptor or mitochondrial mediated apoptosis.

3.6.4 Signalling by the effector caspase-3

The effector caspase-3 can be found the furthest downstream of all the signalling molecules we have looked at. This protein is absent from the MCF-7 cell line (Janicke et al., 1998) but is present at normal levels for the DU145 cells. **Figure 3.15** summarises the results for the DU145 cells after treatment with each of the drugs and the seven component mixture. Of the eight different drug treatments, three showed activation of this effector caspase, daunorubicin, methotrexate and the mixture treated cells. Following on from the findings from caspase-9, **figure 3.4** shows that procaspase-3 can be activated following activation of caspase-9. For the three drugs in the DU145 cells that activated caspase-9, only methotrexate could also express caspase-3. We can say that the picture for methotrexate treatment to DU145 cells is much clearer as it does not activate p53, activates the initiator caspase-9 and the effector caspase-3. This implies a death receptor or mitochondrial mediated activation of apoptosis that may be further explored by examining activation of FADD, TRADD and caspase-8 expression for death receptors, and levels of the pro-apoptotic Bcl-2 family members present in the whole cell lysate sample.

3.6.5 The IA_{MIXED} modification models

The *independent action* prediction was modified by implementing a further categorisation of the individual mixture components. The first modifications **(figures 3.16 & 3.17)** were carried out in the following way, the drugs

daunorubicin, doxorubicin and etoposide phosphate were grouped together as all inhibit the enzyme topoisomerase II and an appropriate *concentration addition* prediction was made for their mixture effects. Two further drugs were grouped, 5-FUdR and methotrexate as both belong to the antimetabolite class of anticancer drugs. The resultant modified *independent action* prediction (IA_{MIXED}) demonstrated a shift to the right from the unmodified *independent action* prediction **(figure 3.16 & 3.17)**. For the DU145 cells the modification brought the IA_{MIXED} model much closer to the *concentration addition* prediction and may well be due to the reduced number of components in the overall mixture causing a reduction in predictive model separation (Payne et al., 2000). The closeness of both the IA_{MIXED} model to the *concentration addition* model in **figure 3.16** could also be explained by the relative influence of two of the components to the predictions. In the DU145 cells the drugs vincristine sulphate and melphalan demonstrated lower overall contribution to the mixture effects **(figure 2.22)**. This meant that the other five agents contributed significantly to the *concentration addition* prediction model in the initial seven component mixture **(figure 2.21)**. The resultant four component mixture model IA_{MIXED} was greatly influenced by *concentration addition*, leading to its curve bearing close resemblance to the *concentration addition* model. This was not the case for the MCF-7 cells as the IA_{MIXED} model shifts less significantly towards the right towards the *concentration addition* prediction **(figure 3.17)**. The two drugs of vincristine sulphate and melphalan have more contribution to the overall mixture effect as shown in **figure 2.29** and therefore the five agents modelled by *concentration addition* to construct the modified IA_{MIXED} model were not as influential and the curve was less *concentration addition*-like.

Further modification of the *independent action* model (IA_{MIXED}) using the findings from single agent common expression of p53 **(figure 3.12)**, procaspase-9 cleavage **(figure 3.13 & 3.14)**, and procaspase-3 cleavage **(figure 3.15)**, did not further improve the accuracy of the predictive power of *independent action* compared to the *concentration addition* model **(figures 3.18 to 3.21)**.

The attempt was made to assess possible mechanisms of action for each of these agents in both of these cell lines. A common mechanism of action in the strict pharmacological sense, for all of the single agents used, was not found from the signalling proteins looked at. Exploration of the wide variety of signalling pathways that could be involved in the activation of apoptosis by these chemicals can be highly varied, as there are so many determinants to activate this process, and all could not be explored during the course of these studies.

However, our results do lend support to the notion that a phenomenological similarity criterion is fulfilled with the anticancer drugs incorporated into the mixtures. All agents, singly and in combination, induced apoptosis, and therefore showed a similar mode of action. It appears that this is sufficient to fulfil the similarity requirements of *concentration addition*.

CHAPTER 4:

DRUG COMBINATIONS & LIPOSOMES

4.1 INTRODUCTION

The practice of using carrier vehicles to deliver drugs to parts of the body as a means of therapy has grown considerably in the past few decades. The ability to transport a potentially beneficial anticancer agent, to a specific tumour site, without the drug being degraded or siphoned off to other parts of the body would be advantageous to successful drug therapy. Combination chemotherapy has become the norm for cancer treatment and a number of approaches have been considered when using liposomes as a vehicle for entrapping anticancer agents for use in combination therapy. Firstly, the liposomal drug can be treated alongside other agents in their free form, i.e. liposomal doxorubicin and free cyclophosphamide. A second approach is simply to administer one liposomal drug in combination with another liposomal drug. This leads on to a third approach in which more than one entrapped drug could be administered in a liposomal formulation. To overcome the changes in the pharmacokinetics and pharmacology that is prone to happen to free drug administration, the final approach to entrap a combination of agents into a single liposome was explored. This approach can help to deliver an effective combination of agents to a tumour without risk of one or two agents being differentially distributed around the body and therefore improve treatment success rate.

It is the aim of this work to establish whether the previously discussed anticancer drug combination in **chapters 2** and **3** can be entrapped in this manner, and whether there are any changes in the toxic effects of this

combination. In order to establish this, first the applications and therapeutic uses of liposomes were discussed, including their method of synthesis, determining their size and charge, and their resultant anticancer drug toxic effects.

4.1.1 Liposomes

Liposomes or phospholipid vesicles are small particles that enclose an aqueous volume within a lipid membrane. They can form spontaneously when phospholipids are dispersed in aqueous solution, to produce vesicles of varying size from nanometres to tens of microns in diameter. The liposome membrane forms a bilayer structure that is in principle identical to the lipid portion of natural cell membranes. It is this similarity in membrane structure that has lead to increased research into the area of drug targeting. As these particles have the ability to mimic the behaviour of natural membranes, it therefore makes them a safe and efficient method for delivering drugs for a variety of medical applications.

Liposomes were first shown to have a scientific use by A.D. Bangham and co-workers (1965) and have been used since the 1970s (Gregoriadis and Ryman, 1972) as a means to deliver a variety of agents to specific sites around the body. Use of these vesicles as a method for delivery has helped to minimise many of the potential problems associated with direct drug use, i.e. increased toxicity, premature drug inactivation and inability of the drug to reach the target. A wide variety of molecules can be incorporated in the aqueous volume of liposomes, or at the lipidic bilayer interface **(figure 4.1)**.

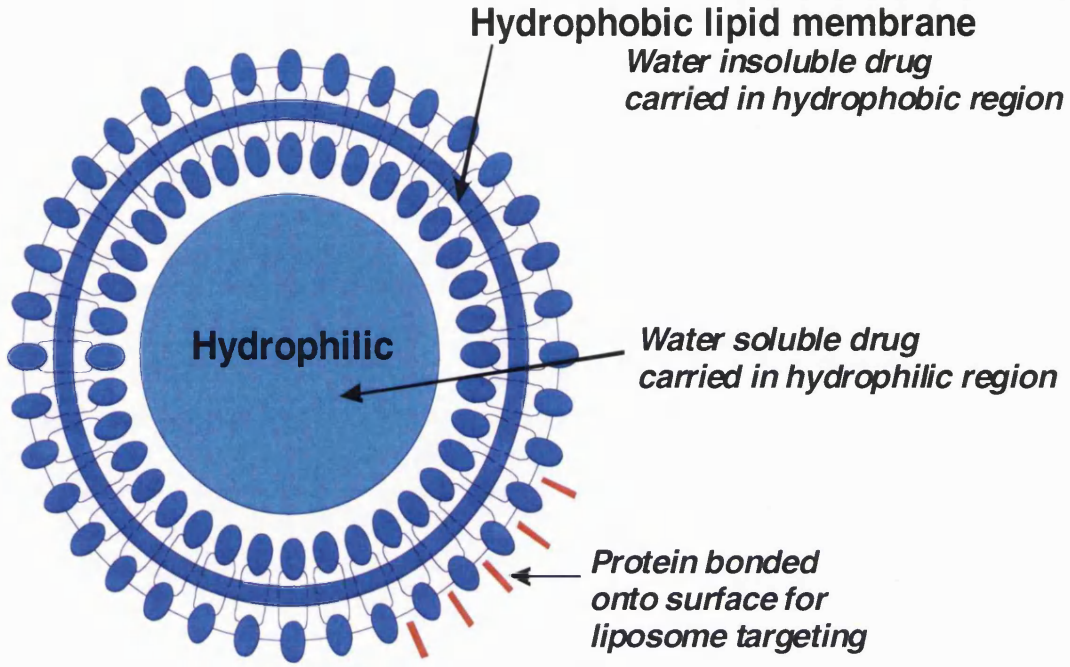

Figure 4.1: Liposome structure. *Incorporation of a variety of molecules into the hydrophobic lipid bilayer of the liposome or the hydrophilic aqueous volume*

There are a range of different liposomes that can be formed and these can be categorised dependent upon the size of the liposomes **(figure 4.2)**. They can vary from very small sized vesicles (0.015 μm) to very large (5 μm) and can be composed of single or multiple bilayer membranes. Multilamellar vesicles (MLV) have multiple bilayer membranes and range in size from 0.1-1 μm. Small unilamellar vesicles (SUV) are the smallest possible sized liposomes and range in size from 0.015 μm to 0.1 μm. Large unilamellar vesicles (LUV) are the largest sized liposomes and have a diameter size of around 1 μm or above.

Much of the recent work with drug-containing liposomes has tried to control and optimise the behaviour of these particles to improve their pharmacological action, ensuring that they can carry the drug to the intended target (Gregoriadis et al., 1998). The early drug delivery work in the 1970s using liposomes was initially disappointing as the liposomes were easily destabilised, causing premature release of drug molecules. Liposomes in current use have improved physical properties to overcome these problems and enhance their therapeutic

effects over the corresponding conventional therapies. The incorporation of cholesterol into the bilayer structure (Gregoriadis and Davis, 1979) and the use of phospholipids with higher transition temperature (T_c, temperature that fatty acids melt) than ambient temperature (T_a, temperature the bilayers are in a fluid or rigid state) has led to more stable liposomes. To counter possible increased removal of liposomes from the circulation via spleen and liver macrophages, vesicle size (Gabizon et al., 1990) and surface charge (Gregoriadis, 1994) have been varied. Although these approaches have demonstrated improved therapeutic effects, there are still further advances that can be made to ensure greater selectivity and targeting for liposomal drug delivery. These include incorporation of ligands and site-directing complexes into the liposome surface (Gregoriadis, 1988).

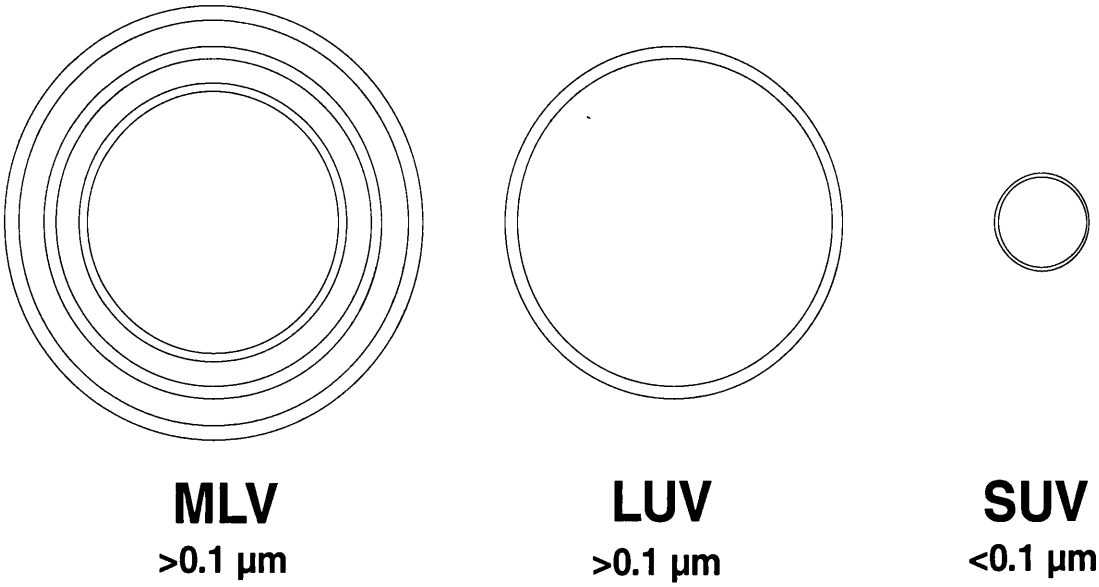

Figure 4.2: Types of liposome characterised by their size and number of lamellae. *Multilamellar vesicles (MLV) range in size from 0.1-1 µm, large unilamellar vesicles (LUV) have a diameter size of around 1 µm or above and small unilamellar vesicles (SUV) that range in size from 0.015 µm to 0.1 µm.*

4.1.2 The role of liposomes in cancer therapy

A major problem for cancer chemotherapy is the toxic side effects of anticancer agents. Less than 1% of the free drug administered reaches target cells, with the rest damaging non-target cells (Lasic and Papahadjopoulos, 1998). Effective delivery of the drug has become one of the main barriers to effective treatment of solid tumours. Many small molecule chemotherapeutic agents have a large volume of distribution when administered by i.v. injection (Speth et al., 1988; Drummond et al., 1999), which results in a very narrow therapeutic index with high toxicity to normal healthy tissue. Encapsulation of the drug into a suitable carrier such as a liposome has been seen as a possible way to reduce this volume of distribution and therefore increase the level of drug penetrating the tumour (Papahadjopoulos et al., 1991; Martin, 1998). The liposome can also protect the drug from premature metabolism and inactivation in the plasma of the body and give an overall increase in the therapeutic effect when compared to conventional chemotherapy (Papahadjopoulos et al., 1991; Gabizon, 1994; Martin, 1998).

The aqueous space enclosed within a liposome provides an ideal compartment in which to entrap a variety of chemotherapy agents and possibly provide an innovative vehicle to deliver a potentially effective combination of agents. The choice of drugs is most important in this respect, as they must first have a proven effect against the tumour of interest and secondly be efficiently entrapped within a liposome. The liposome can also be varied in properties such as surface charge and size, to ensure improved pharmacokinetics and distribution of the drug in the body (New, 1989).

Liposome size can be varied with the preparation of lipid suspensions by extrusion through filters of specific pore size (Olson et al., 1979), although the eventual size of these liposomes can be slightly larger (20-50%) than the membrane pore size. In general, liposomes of increasing size are more rapidly

taken up by the RES (reticuloendothelial system) and therefore lead to decreased liposome circulation times and increased clearance (Senior et al., 1985). The RES has long been identified as the major site of liposome accumulation in the body. It is associated with the liver, spleen and the lung, and it is the phagocytic cells that reside in the RES that remove liposomes from the blood, mainly by associating proteins to the liposome surface (Chonn et al., 1992; Woodle et al., 1994). Liposomes are very rapidly taken up by phagocytic cells and are then degraded in lysosomes, the entrapped material is then released into the lysosome and in turn into the cell cytoplasm.

The size of a liposome may also be an important parameter in determining liposome accumulation in tumours. Liposomes are able to enter tumours due to a discontinuous tumour vasculature that varies in pore size from 100 to 780 nm in size (Yuan et al., 1995; Hobbs et al., 1998). A comparison of relative rate of tumour accumulation between 50 nm sized daunorubicin entrapped liposomes (Forssen et al., 1992) and 100 nm sized doxorubicin entrapped vesicles (Mayer et al., 1997) has shown more rapid drug tumour accumulation for the smaller vesicles.

In addition to the size of the liposomes, the surface charge can greatly alter a liposome's pharmacokinetics. Early studies have shown the use of negatively charged lipids in the composition of liposomes results in increased RES uptake (Senior et al., 1985; 1987). However this has been found to be a much more complex event and cannot be modelled this simply. The reality is that different liposomes, even if they are composed of different phospholipid headgroups of similar charge, may have very different methods for their *in vivo* uptake and distribution (Daemen et al., 1997).

Other methods to increase the circulation time of liposomes have included the attachment of a polymer coating such as PEG (polyethylene glycol) to the surface of the liposome to reduce the rate of RES uptake (Allen et al., 1991; Lasic et al., 1991) and provide steric stabilisation (Drummond et al., 1999).

4.1.3 Combination therapy involving liposomes

The use of a combination of drugs has become standard for cancer chemotherapy due to their improved therapeutic results. It has been well documented that this method with the use of multiple agents provides a more effective form of tumour treatment. This is very much evident when faced with the heterogeneity of tumour cells with variations in cell sensitivity to various anticancer drugs.

Liposome encapsulation of doxorubicin has been shown to have reduced toxicity on drug sensitive normal tissue when compared to conventional free doxorubicin treatment (Gabizon et al., 1982; Olson et al., 1982; Rahman et al., 1985). The success of liposomal formulations of doxorubicin (Ranson et al., 1997; Muggia et al., 1997), daunorubicin (Gill et al., 1995; Tulpule et al., 1998) and vincristine (Gelmon et al., 1999) has led to their use in combination with other anticancer drugs. Liposomal doxorubicin has been tested in combination with cyclophosphamide for therapeutic activity to breast cancer (Batist et al., 2001). Vincristine is a drug that is often used in combination with other anticancer drugs, such as the VAD (vincristine, doxorubicin and dexamethasone) regimen and CHOP (cyclophosphamide, doxorubicin, oncovin *(vincristine)* and prednisone) regimens (Saxon et al., 1999), so in order to achieve maximum cell kill, liposomal vincristine will more than likely need to be given in combination with other anticancer agents. This brings us back to the three approaches to liposomal combination chemotherapy discussed earlier. A liposomal drug can be treated in combination with single or a group of free agents. It can also be treated alongside another entrapped drug, or alternatively a combination could be entrapped into a single liposome formulation. For each of these approaches there lies the potential for interactions between the various drugs as well as the liposomal drugs, causing a change in the pharmacology of the drugs and their pharmacokinetics.

In this chapter we considered the third approach and examined the possible applications of entrapping a combination of seven anticancer drugs into a single liposomal formulation. Once this was done, the toxicity of these liposomes were compared to those obtained for these drugs in the free form to establish whether liposomal encapsulation had any effect in overall drug toxicity.

4.2 EXPERIMENTAL APPROACH

4.2.1 Preparation of liposomes

Liposomes are composed of lipid bilayers and can be constructed in a stage by stage process dependent upon what application they are to be used for. The group of hydrophilic agents used in **chapters 2** and **3** were entrapped into liposomes using the dehydration-rehydration vesicle (DRV) method (Gregoriadis, 1998), which has been shown to be best applied in this case. Briefly, these test agents consisted of 5-fluoro-5'-deoxyuridine, daunorubicin, doxorubicin, etoposide phosphate, melphalan, methotrexate and vincristine sulphate. These drugs were prepared as described in **section 2.5.3.1** and were prepared fresh for each experiment from stored stocks.

To prepare liposomes, first a lipid film was formed and upon hydration, MLVs are formed of varying sizes. To obtain a homogenous and uniform liposome population, one of two methods can be employed, these are sonication and membrane extrusion (see below). The resultant SUVs were then added to a drug solution to be entrapped and then freeze dried to obtain drug entrapped DRVs.

The lipid used for the preparation of the liposomes was obtained from Lipoid GmbH, Germany. The lipids used **(figure 4.3)** were soya phosphatidylcholine (SPC) and cholesterol (CHOL) (Sigma) and liposomes were prepared in a

composition containing SPC/CHOL (ratio 1:1, where 1=32 µmol) and were prepared according to the DRV method.

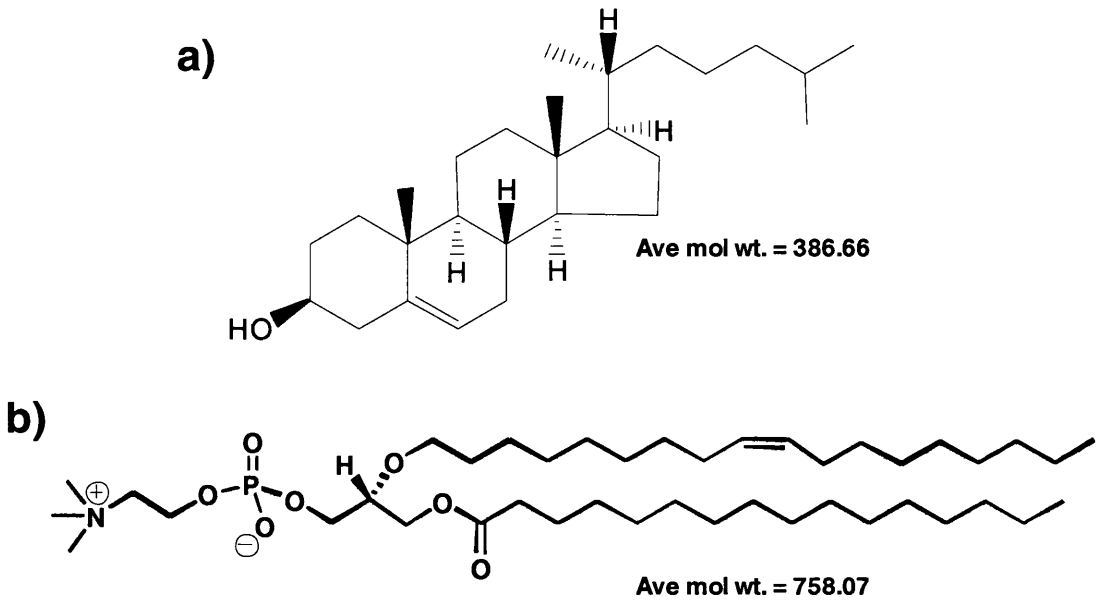

Figure 4.3: Structure of the lipids. a) *Cholesterol (CHOL);* ***b)*** *phosphatidylcholine (PC)*

The lipid composition was dissolved in 99% chloroform (BDH) to produce neutral liposomes, and the chloroform solution was evaporated using a rotary evaporator at 30-37°C (Buchi Rotavapor-R) on vacuum with a steady rotation speed of 60 rpm. The lipid film formed on the inside of the flask was flushed with oxygen free N_2 to remove all traces of solvent from the flask and lipid film. The lipid was then hydrated with 10 ml sterile double deionised H_2O (ddH_2O), and the flask shaken over a vortexer to obtain a milky suspension of MLVs. The suspension was left standing at 25°C for 2h, during which time multilamellar liposomes of various sizes were formed.

To obtain a liposome suspension of reduced and homogeneous size, two general techniques were used. These were probe sonication and membrane extrusion.

4.2.1.1 Sonication:

The first method involves the process of sonication to transfer a high level of energy to the lipid suspension. The exposure of high intensity sound waves ensures rapid homogenisation of the solution and transfer from a heterogeneous solution of large sized liposomes to smaller sized particles. This method was first employed in 1969 (Huang) and produced small vesicles after exposure of MLVs to ultrasonic irradiation and is still the most widely used method. There are two methods of sonication, using either a probe **(figure 4.4)** or a bath, the choice of which is dependent on the volume of lipid suspension. The probe is employed for small volumes (high concentration lipid) and the bath for large volumes of dilute lipids. For the context of this work we used small volumes of concentrated lipid in suspension, so probe sonication was used to produce smaller sized vesicles.

After hydration of the lipid film and formation of MLVs, the suspension was sonicated using a titanium probe (Sanyo Soniprep 150 Sonicator) to produce an opaque to clear suspension of SUVs. This was obtained using twenty sonication cycles, each lasting 30s with a 60s rest interval between each cycle.

The SUV suspension was left to stand at 25°C for 2h and then centrifuged at 3800 rpm (2500 *g*) for 10 min (Denley, BR401, UK) to remove any large foreign matter (titanium probe particles and undispersed lipid).

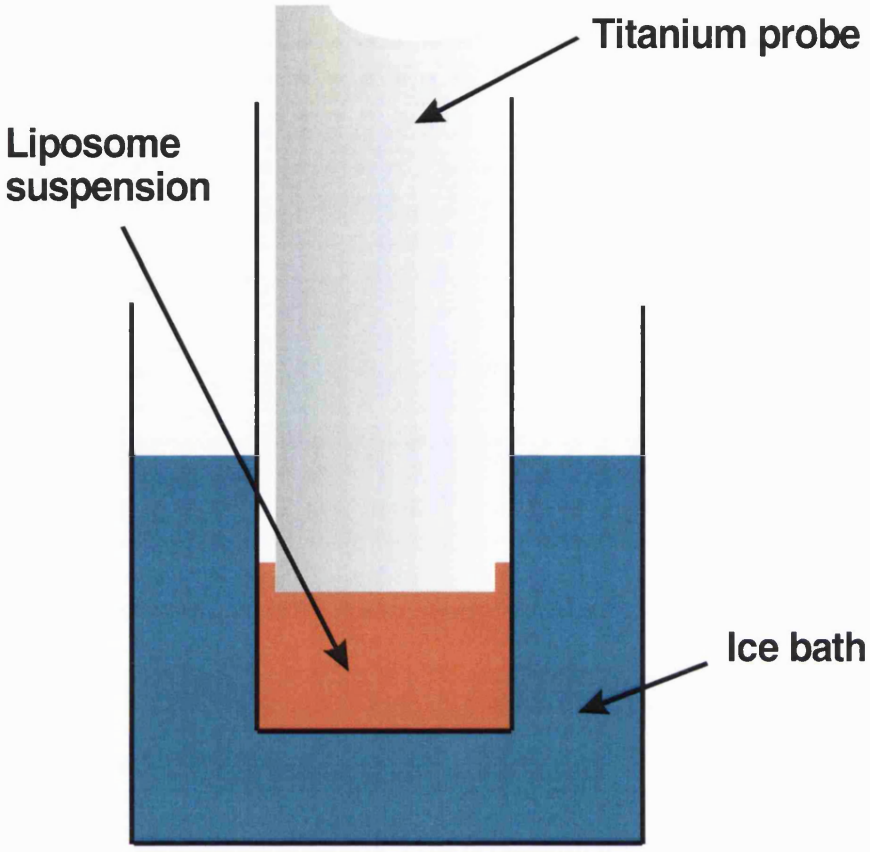

Figure 4.4: Preparation of liposomes by titanium probe sonication of liposome suspension. *High intensity sound waves transferred to liposome suspension.*

4.2.1.2 Membrane extrusion:

Liposome extrusion is a process in which MLVs are gently reduced in size by passing them through a membrane filter of defined pore size (Olson et al., 1979). The vesicles are physically extruded under pressure through a polycarbonate membrane containing pores of a pre-determined size. The pores go straight through from one side of the membrane to the other **(figure 4.5)** and under pressure the phospholipid vesicles of similar size to the pores can squeeze through. Liposomes of much larger size, however, are broken up and emerge from the membrane pore much smaller than before. After several passes through the membrane the liposomes will be reduced in size to that similar to the membrane pore diameter.

After formation of MLVs, 10 ml sterile ddH_2O was added to the milky suspension, and was extruded through two stacked 100 nm pore size polycarbonate membranes (Isopore VCTP, Millipore GmbH, Germany) under 100 psi nitrogen **(figure 4.5)**. The suspension was dispersed through these membranes ten times at room temperature to produce a clear to opaque solution with vesicles of size of around 100 nm in diameter.

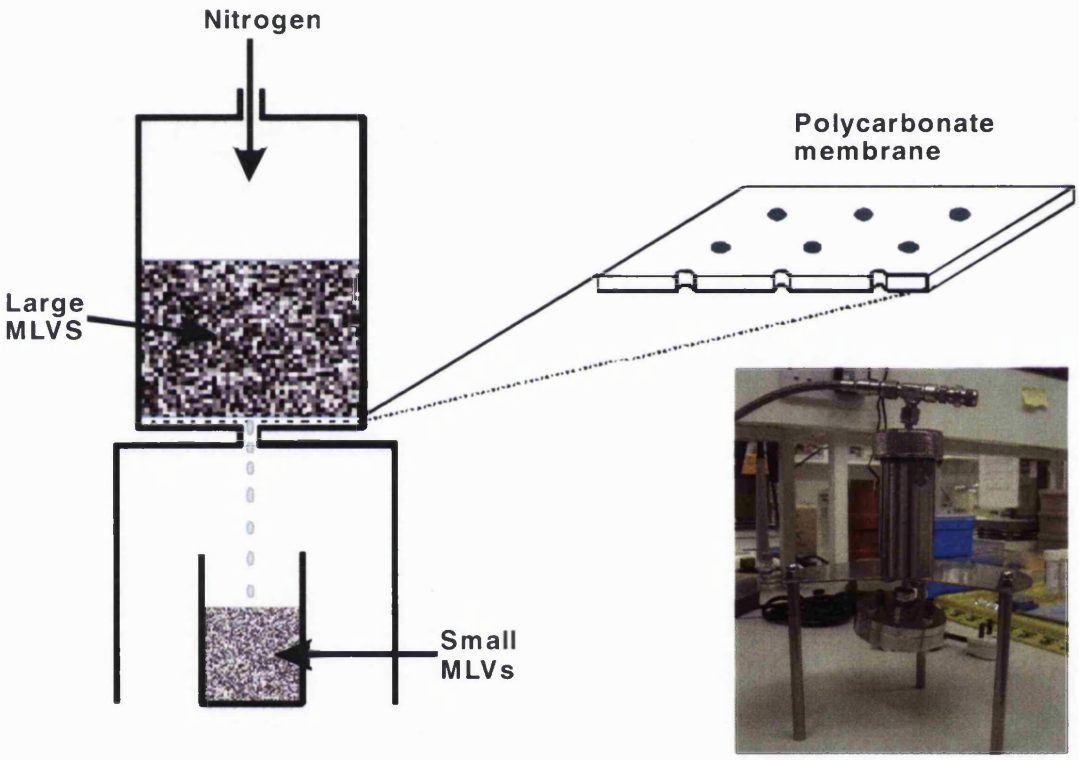

Figure 4.5: Extrusion of the liposome suspension. *Polycarbonate membrane pores and extruder assembly and membrane extrusion dispersion process.*

4.2.1.3 Drug entrapment

Each aqueous drug solution was prepared as in **chapter 2** and seven-component mixture composed for the DU145 and MCF-7 cells using the fractions found in **tables 2.3 & 2.4** respectively. The drug solutions were then added to the extruded liposome suspension in a 1:1 ratio (drug solution:lipid solution) and control liposomes prepared using sterile ddH_2O. This mixture was rapidly frozen with liquid nitrogen with steady rotation and freeze-dried (Edwards

Freeze, Modulyo Pirani 10 Freeze Dryer) overnight to yield an amorphous powder.

Following the freeze-drying process, the powder was rehydrated with 2 ml sterile ddH_2O and swirled vigorously to ensure complete dissolution of the powder and left to stand at 25°C for 60 min; to allow formation of DRVs. The DRV suspension was centrifuged at 20,000 rpm for 60 min at 4°C, (Beckman J2-21M/E, Beckman, UK). The supernatant was removed and retained for drug encapsulation study and the pellet (drug containing DRVs) was resuspended in 2 ml sterile ddH_2O and centrifuged again to remove all traces of unentrapped material. The supernatant was again retained for drug encapsulation estimation (see **section 4.2.2**) and the pellet resuspended in 1 ml sterile PBS ready for use immediately in MTT assay.

4.2.2 Measurement of fluorescence to assess the concentration of fluorescent compounds

The level of drug encapsulation was measured fluorometrically using a Perkin Elmer LS-50-B spectrofluorometer (excitation: 480 nm; emission 590 nm) (Amselem et al., 1990). The level of drug entrapment was determined by using standard curves constructed from standard concentration solutions for doxorubicin and the seven-component mixtures. 3 ml of each drug solution was transferred to a quartz fluorescence cuvette and then the fluorescence of the solution measured. Calculations of drug concentration from the fluorescence intensities of the unentrapped drug solutions (supernatant obtained after ultracentrifugation), were then subtracted from the concentration of the drug solution added to the liposome suspension. An estimate of the entrapped drug concentration could then be calculated.

4.2.3 Cytotoxicity assay

4.2.3.1 MTT Assay procedure

The cytotoxic effect of a free seven-component mixture of drugs or a liposome encapsulated seven-component mixture of drugs on the DU145 and MCF-7 cells was assayed using the MTT assay (Mosmann, 1983) as described previously **(chapter 2)**. The cells were treated with a 10 µl volume of free drug or liposome encapsulated drug solution, followed by three days growth. The cells were treated using a dilution series of ten separate concentrations and then left to incubate for another three days at 37°C. The addition of MTT to the treated wells was followed by an addition of a solubilisation solution, and this enabled spectrophotometric measurement of the level of formazan product and therefore a measure of viability for each treatment.

4.2.3.2 Dilution Series

The serial drug dilutions for the free drugs were made up from the drug stock solutions fresh for each experiment. The liposome encapsulated drug solutions were prepared at the time of treatment to prevent liposome degradation, and diluted by half sequentially to give ten concentrations of the encapsulated drug liposome solution.

4.2.4 Measurement of vesicle size and zeta potential

4.2.4.1 Sizing

The vesicle size of the SUVs was measured in two ways, the first was by using a Zetasizer 3000 (Malvern Instruments, Malvern, UK). Particle size is measured using photon correlation spectroscopy (PCS, also known as dynamic light scattering, DLS). This technique measures the fluctuations in intensity of scattered light as particles in a sample undergo Brownian movement. For sizing,

the samples were made up to 10 ml with ddH_2O and transferred to a cuvette and placed in the Zetasizer cell. Three repeat measurements were carried out at 25ºC to obtain size distributions within samples.

The second method to measure the size and composition of the liposomes used cryo-transmission electron microscopy (TEM) using a Philips/FEI CM120 Bio Twin Transmission Electron Microscope (Philips AG, The Netherlands). Due to the lower wavelength of electrons when compared to light, TEM imaging allows higher magnification and resolution imaging compared to conventional light microscopy and a magnification of 350,000 times can be generally achieved for most materials.

Imaging using TEM involved a number of steps; first the sample was frozen and negatively stained with a 1% PTA (phosphotungstic acid) solution. The sample was then placed on a metal grid and clamped into a stage in the column of the microscopė. A high energy electron beam of varying intensity dependent on resolution required travelled down this column and passed through the liposome sample onto photographic film. As the electron beam passes through the sample, features from different levels within the object become superimposed on the film (Bonetta, 2005).

4.2.4.2 Zeta potential

The zeta potential of a particle is the overall charge that a particle acquires in a particular environment. Knowledge of a liposome's zeta potential can help to predict its *in vivo* character and can be measured using laser Doppler velocimetry. This technique applies a voltage over a pair of electrodes at either side of a cell containing the suspension of particles. Charged particles are attracted to the oppositely charged electrodes and their velocity and charge is measured. To measure zeta potential the samples were injected and analysed immediately on the Zetasizer 3000 with He-Ne laser; the angle of measurement was 90 degrees. Three repeat measurements were carried out at 30s intervals

and both size and zeta data was analysed using PCS v1.52 for Windows (Malvern Instruments, Malvern, UK).

4.2.5 Data analysis

All single agents and mixtures were tested by preparing serial dilutions of the free drug and liposomal entrapped drug preparations and using ten different concentrations. The curve plotting was carried out using SigmaPlot v.8.02.

4.3 RESULTS

4.3.1 Optimisation of liposome preparation technique

The most common method for producing liposomes involves the use of sonication with the transference of high energy to the lipid suspension resulting in the formation of smaller and more uniform vesicles **(figure 4.4)**. An important consideration for the preparation of these liposomes concerned sterility of the produced liposomes for later treatment to cultured cells. Probe sonication can increase the susceptibility for sample microbial contamination. The cells appeared in very bad condition prior to MTT addition with the presence of microbial organisms in the wells of the higher concentrated liposome solution. This resulted in active formation of formazan by the actively respiring organisms in the contaminated wells, giving a false positive measurement of cell viability **(figure 4.6)**. The membrane-extruded liposomes proved to be sterile and showed there was no variation in cell toxicity for a range of liposome concentrations (right side plate in **figure 4.6**).

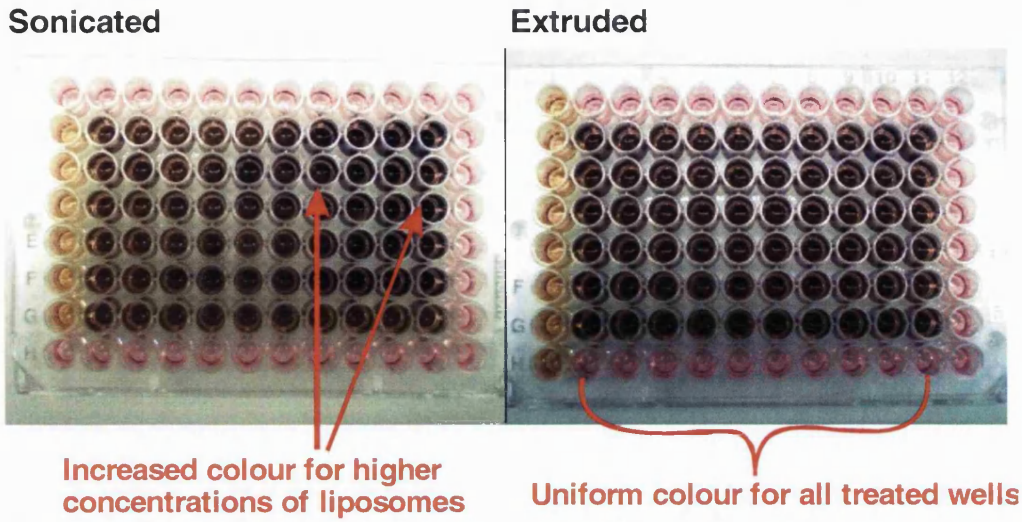

Figure 4.6: Increased formazan production of sonicated liposomes. *High concentrations of sonicated liposomes treated to the MCF-7 cells were found to increase formazan production as a result of microbial contamination. Cells treated with extruded liposomes showed consistency of colour over a range of lipid concentrations.*

Figure 4.7 demonstrates the consistency in cell viability for a range of lipid concentrations of control membrane extruded liposomes. The higher concentrated sonicated liposomes demonstrated increased formazan production as a result of actively respiring microbials in the wells and therefore increased estimation of cell viability. The extruded liposomes showed a more consistent level of toxicity and little variation from high concentrations of lipid to low concentrations.

Due to the use of a probe sonicator, sterility of the sample liposomes could not be guaranteed, even with use of aseptic techniques at all stages. Liposomes cannot be sterilized by exposure to high temperatures and are sensitive to irradiation, so the only option left was filtration. The process of extrusion incorporates membrane filtration to reduce liposome size which at 100 nm pore diameter size can also sterilize the lipid suspension, so the process of extrusion was employed to prepare drug entrapped liposomes for MTT assay treatment.

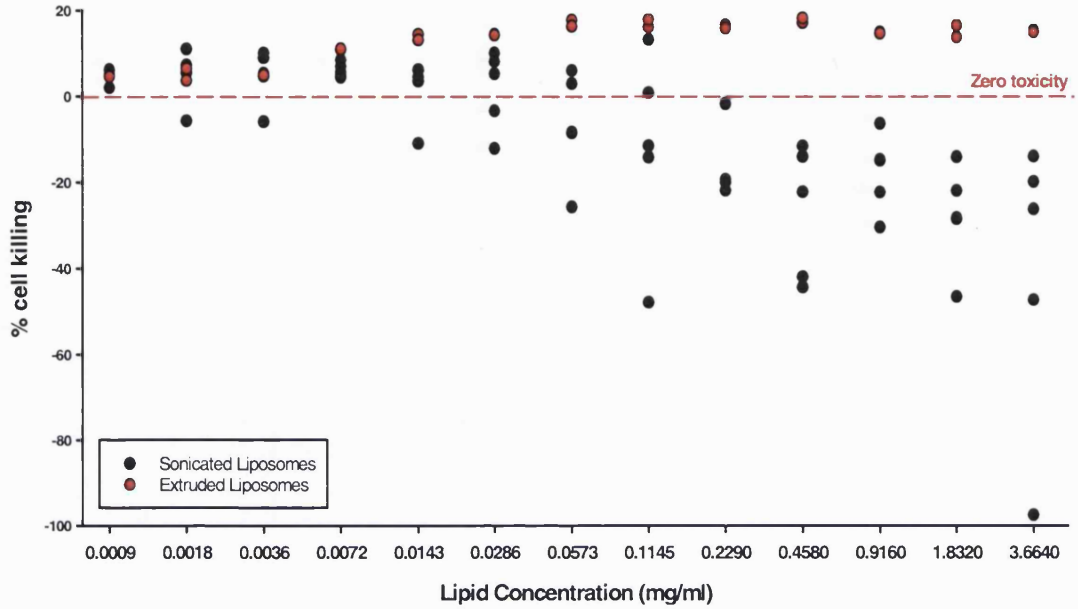

Figure 4.7: Variable viability of sonicated liposomes and consistency of extruded liposomes. *The higher concentrated sonicated liposomes displayed increased levels of microbial contamination resulting in increased formazan production and inaccurate estimation of cell viability. The extruded liposomes however displayed low to minimal variation in cell viability. Experiments run using MCF-7 cells.*

4.3.2 Drug entrapment during the DRV method and *in vitro* cytotoxicity of liposome encapsulated drugs

4.3.2.1 Doxorubicin entrapped liposomes

The entrapment efficiency was determined by the measurement of the doxorubicin fluorescence intensity for a set of standard solutions of free doxorubicin, **figure 4.8a** shows the emission maxima for standard doxorubicin solutions from 0.1 µM to 6.25 µM. A standard curve was then generated **(figure 4.8b)** and was used to calculate the level of doxorubicin entrapped in the liposomes. The solutions was excited at 480 nm and emission recorded at 590 nm (Amselem et al., 1990).

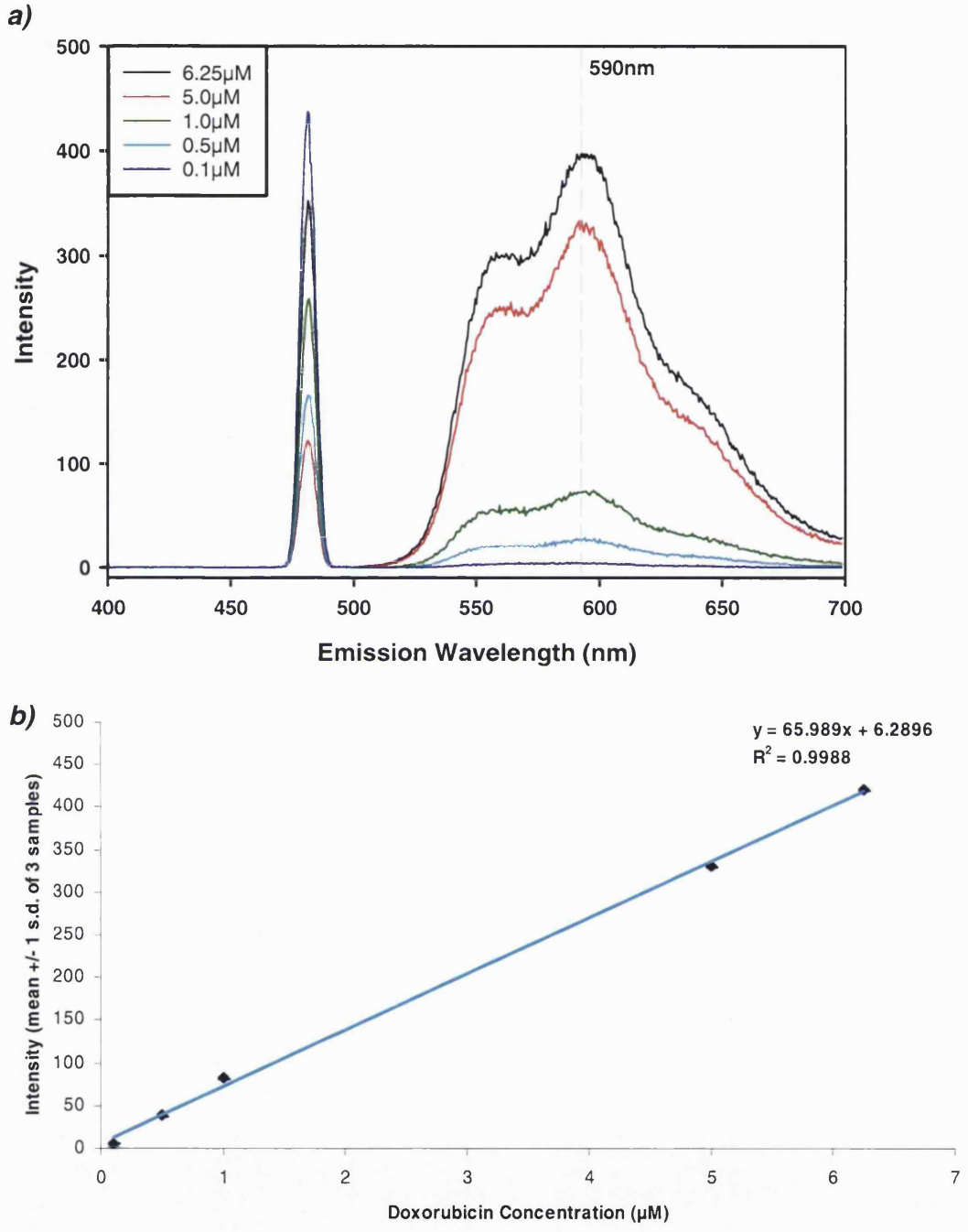

Figure 4.8: Measurement of doxorubicin entrapment. a) *The emission spectra of standard solutions of doxorubicin, 0.1 µM to 6.25 µM (excitation: 480 nm; emission 590 nm). Mean values, n=3.* ***b)*** *Doxorubicin standard curve constructed from emission spectra. Mean of three readings ± 1 s.d.*

Entrapment efficiency was calculated in the following manner. The standard curve for doxorubicin **(figure 4.8b)** and the resultant regression line **(equation 4.1)** was used to determine the unentrapped doxorubicin concentration by measurement of the fluorescence of the centrifuged supernatant **(section 4.2.1.3)**.

$$\text{Doxorubicin concentration} = \frac{\text{fluorescence intensity} - 6.286}{65.989} \qquad \textbf{(4.1)}$$

A subtraction of this value from the initial added doxorubicin concentration (free doxorubicin) gave an estimation of entrapped drug concentration and a measure of entrapment efficiency.

A solution of 17.2 μM doxorubicin was entrapped by 39.37% into PC:CHOL liposomes, while the second concentration of 1.72 μM was entrapped by 26.18% **(table 4.1)**.

Table 4.1: Liposome drug entrapment of doxorubicin

Doxorubicin concentration (μM)			***Drug entrapment (%)***
Free drug	***Supernatant, unentrapped drug (mean value ± s.d., n=3)***	***Entrapped drug***	
17.2	10.428 ± 0.285	6.772	39.37
1.72	1.270 ± 0.452	0.450	26.18

Determination of the entrapment efficiency was an important step to calculate the concentration of liposomal doxorubicin applied to the cultured cells. This was achieved by preparing serial dilutions of liposomal entrapped doxorubicin preparations (using both 17.2 μM and 1.72 μM doxorubicin). Using the respective measured drug entrapment percentages, the concentration axes of concentration-response plots could be scaled to reveal the effective concentrations of doxorubicin. Concentration-response curves for liposomal entrapped doxorubicin were recorded in DU145 and MCF-7 cells and compared with the effects obtained in experiments with the free, unentrapped drug. If the entrapment efficiency was measured correctly in each case, then the resulting concentration-response curves should be similar with those of the free drug. When this comparison was made, the cytotoxic effects of the liposomal entrapped doxorubicin preparations showed close agreement with the effect of the free drug, both in DU145 **(figure 4.9a)** and MCF-7 cells **(figure 4.9b)**.

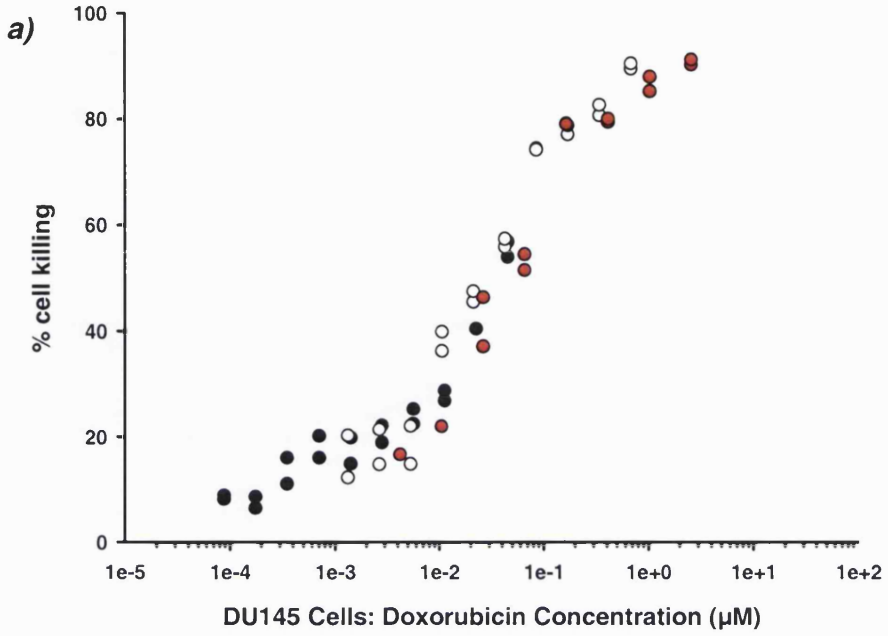

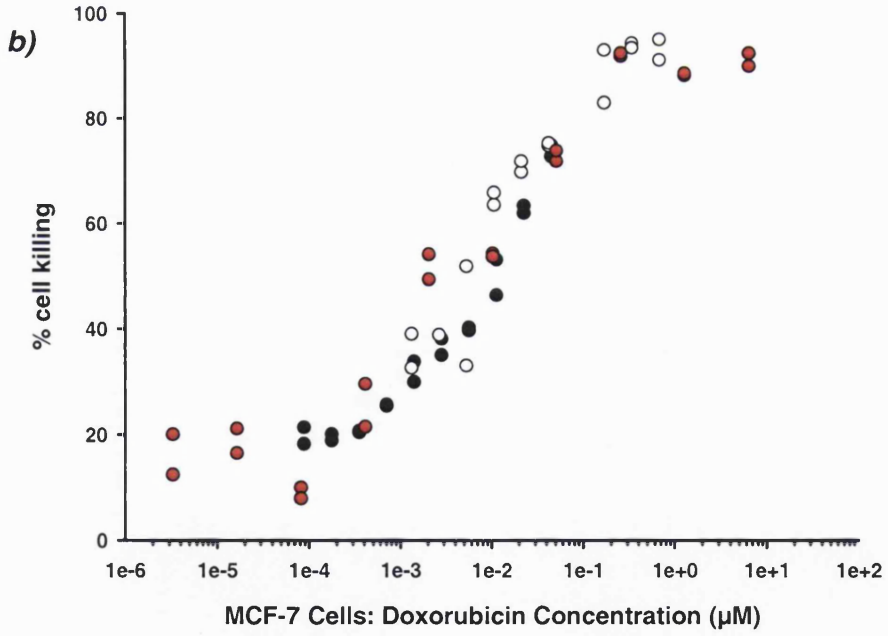

Figure 4.9: The cytotoxic effect of encapsulated doxorubicin. *The cells were treated with serial dilutions of initial entrapped concentrations of 17.2 μM (white circles) and 1.72 μM (black circles) doxorubicin and a direct comparison to the cytotoxicity of free doxorubicin (red circles) demonstrates good agreement between the effects of liposomal doxorubicin and the free drug. Graph* ***a)*** *results for DU145 cells; and* ***b)*** *results for MCF-7 cells.*

4.3.2.2 Seven-component mixture entrapped liposomes

To calculate the entrapment of the seven-component mixture, each mixture component was examined for its fluorescence intensity and its possible contribution to the overall fluorescence of the mixture solution. **Figure 4.10** shows the emission spectra for each single agent when excited at 480 nm, with emission at 590 nm, the wavelengths used for the fluorimetric determinations of doxorubicin. Each single agent concentration was made up to the concentration found in a 200 μM seven-component mixture solution for the DU145 cells (shown in **chapters 2** and **3**, and in **table 4.2**).

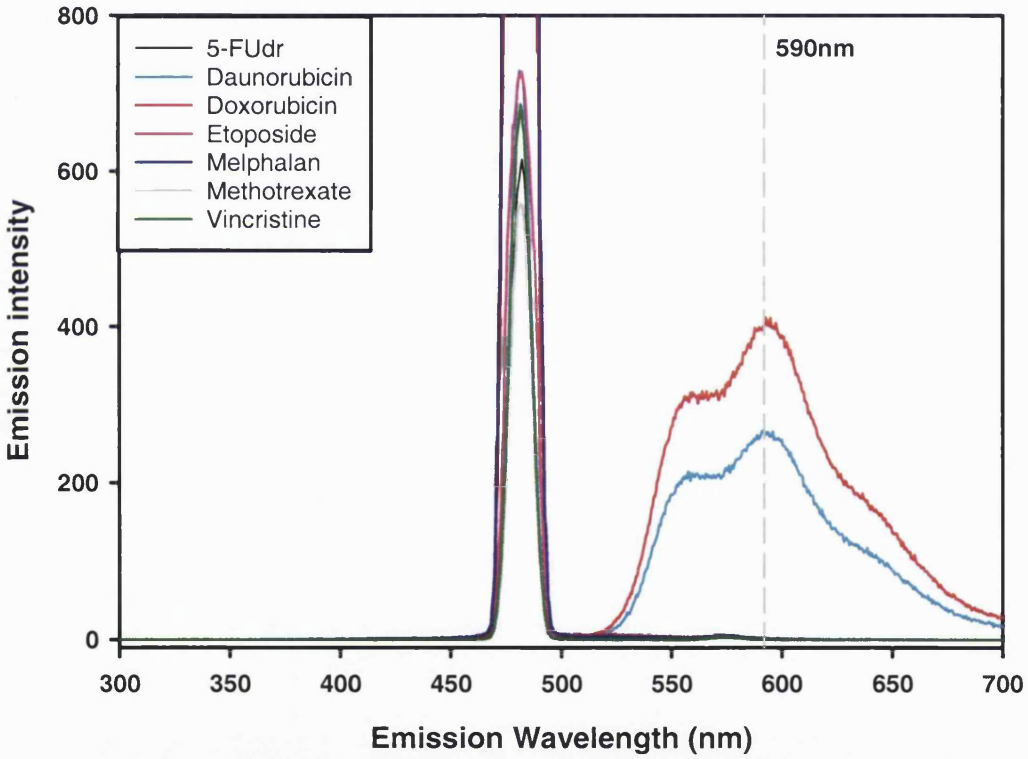

Figure 4.10: Emission spectra for each single agent solution at concentrations present in the DU145 seven-component mixture. *Both daunorubicin and doxorubicin show fluorescence, the other five agents show no fluorescence. Mixture entrapment was then calculated relative to the daunorubicin and doxorubicin fluorescence in the mixture. Excitation: 480 nm; emission 590 nm. Mean values, n=3.*

Table 4.2: Fraction of single agent present in the seven-component mixture for DU145 cells

Drug component	*Fraction of drug in mixture*	*Single agent concentration in 200 μM mixture solution (μM)*
5-fluoro-5'-deoxyuridine	0.3202	64.0465
Daunorubicin	0.002028	0.4056
Doxorubicin	0.002566	0.5132
Etoposide phosphate	0.2241	44.8269
Melphalan	0.4497	89.9323
Methotrexate	0.00126	0.2520
Vincristine sulphate	1.1721×10^{-4}	0.02324

Of the seven agents, only daunorubicin and doxorubicin were found to fluoresce significantly at this wavelength, and this was further supported when viewing fluorescence of single agent solutions when exposed to UV-light.

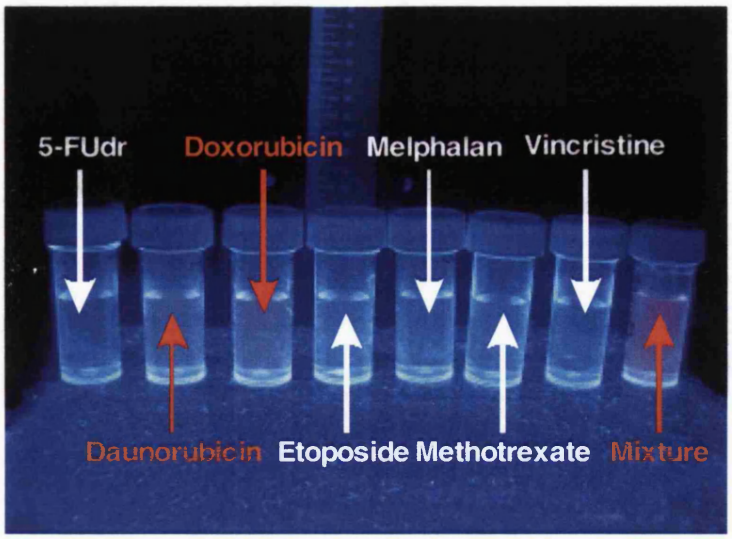

Figure 4.11: Individual drug solution fluorescence when exposed to UV-light. *Daunorubicin and doxorubicin were the only single agents to fluoresce. The seven-component mixture fluoresced when exposed to UV-light due to the presence of these two agents.*

Figure 4.11 showed that there was increased fluorescence for both anthracyclines drugs when present at concentrations found in the seven-component mixture for DU145 cells during exposure to UV radiation. A solution made up of the seven individual agents also demonstrated fluorescence after UV exposure.

Calibration curves were prepared from a set of standard solutions ranging from 400 μM to 2 μM (composition of solution can be found in **table 4.2**) for the mixture for DU145 cells **(figure 4.12a)**, and from 1000 μM to 4 μM (composition of solution can be found in **table 4.3**) for the mixture for MCF-7 cells **(figure 4.12b)**.

Table 4.3: Fraction of single agent present in the seven-component mixture for MCF-7 cells

Drug component	*Fraction of drug in mixture*	*Single agent concentration in 1000 μM mixture solution (μM)*
5-fluoro-5'-deoxyuridine	0.4988	498.8366
Daunorubicin	0.001568	1.5683
Doxorubicin	0.001478	1.4779
Etoposide phosphate	0.04739	47.3927
Melphalan	0.4494	449.3498
Methotrexate	9.102×10^{-4}	0.9102
Vincristine sulphate	4.646×10^{-4}	0.4646

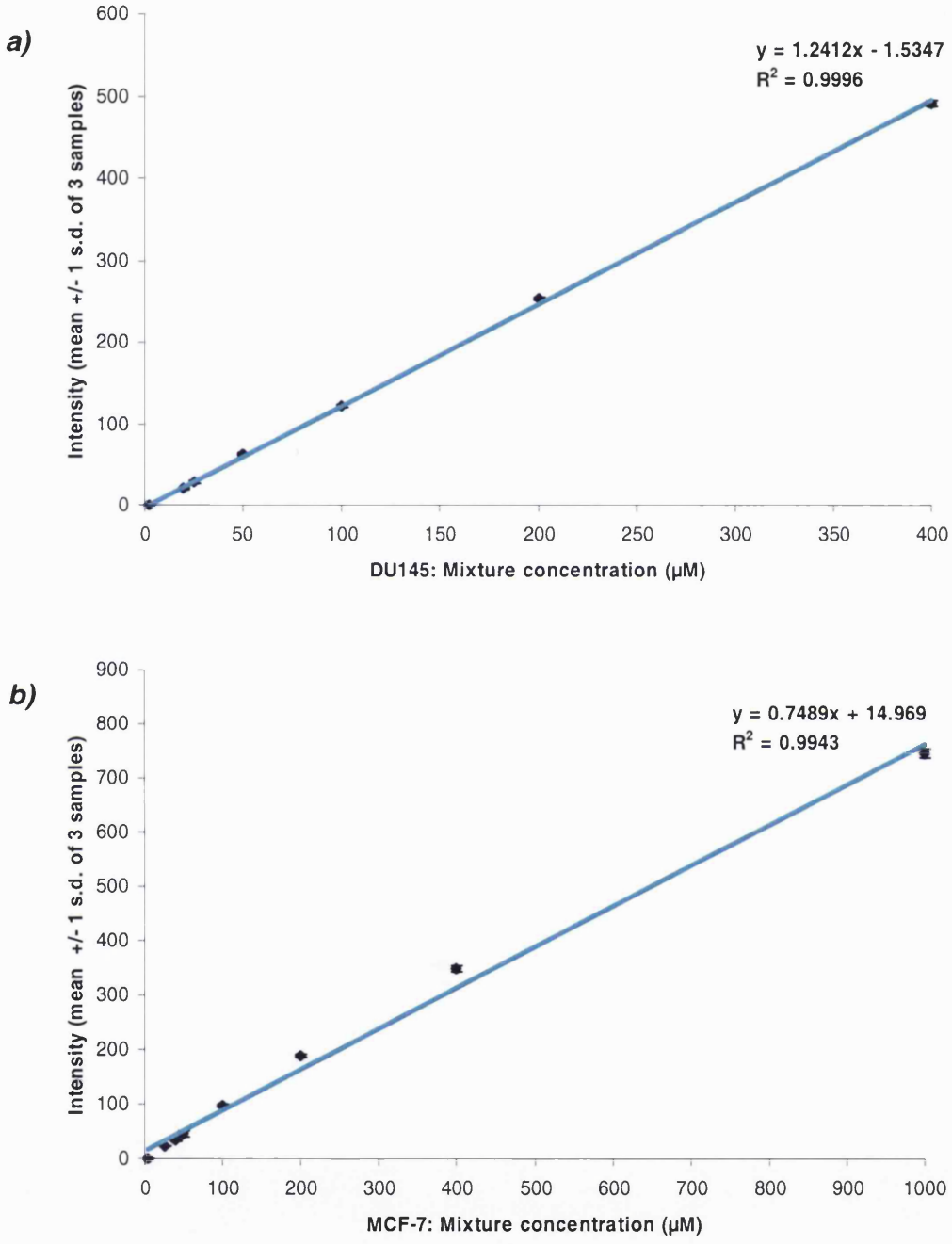

Figure 4.12: Standard calibration curves for seven-component mixtures. *Each drug was present at concentrations equivalent to the mixture ratios for* ***a)*** *DU145 cells* ***(table 4.3)****; and* ***b)*** *MCF-7 cells* ***(table 4.4)****. Excitation: 480 nm; emission: 590 nm. Mean of three readings ± 1 s.d.*

The entrapment efficiency for the MCF-7 seven-component mixture liposomes ranged from 53% to 65.5%, the higher concentration liposomes showing a higher level of drug entrapment (65.5%, 2 mM), compared to 53.78% for the 500 μM liposomes. For the DU145 seven-component mixture liposomes, the entrapment efficiency was lower for the higher concentration liposomes (1 mM) with entrapment efficiency 24.44% **(table 4.4)**.

Table 4.4: Liposome drug entrapment of seven-component mixtures

		Mixture concentration (μM)		
	Free mixture concentration	***Supernatant, unentrapped drug (mean value, ± s.d., n=3)***	***Entrapped drug concentration***	***Drug entrapment (%)***
DU145:	**1000**	755.571 ± 14.110	244.429	24.44
MCF-7:	**2000**	690.048 ± 9.599	1309.952	65.50
	500[a]	231.103 ± 3.909	268.897	53.78

[a] liposomes were prepared but not used for MTT assay

The entrapment efficiencies for these liposomes demonstrated that the higher concentration drug solutions were much more efficiently encapsulated and would be the more effective set of liposomes to use for MTT experiments.

Cytotoxicity of the free seven-component mixture was discussed in **chapter 2** and demonstrated the predictive powers of models such as *concentration addition* and *independent action*. We have demonstrated that a prediction based upon *concentration addition* predicts better for the combined toxic effect of a seven component mixture of differing initial sites of action **(figures 2.21 & 2.28)**. A direct comparison of the effects of the free drug combinations with liposome encapsulated formulations was carried out. To scale the effective concentrations

of the entrapped drugs, the procedure described above for doxorubicin administered singly was utilised **(figure 4.9)**. Since the concentrations, and therefore the entrapment efficiencies, for the other drugs could not be measured, the additional assumption had to be made that the entrapment efficiencies measured for the fluorescing drugs doxorubicin and daunorubicin were a good reflection of the efficiencies of the remaining anticancer agents in the mixture. Again, if this assumption is correct, then the appropriately scaled concentration-axes of the effect plots of the liposomal preparations should yield curves matching with those of the free mixtures. For both the DU145 and the MCF-7 cells there were minimal differences in toxicity between the free drug treated cells and the encapsulated drug combination **(figures 4.13 and 4.14)**.

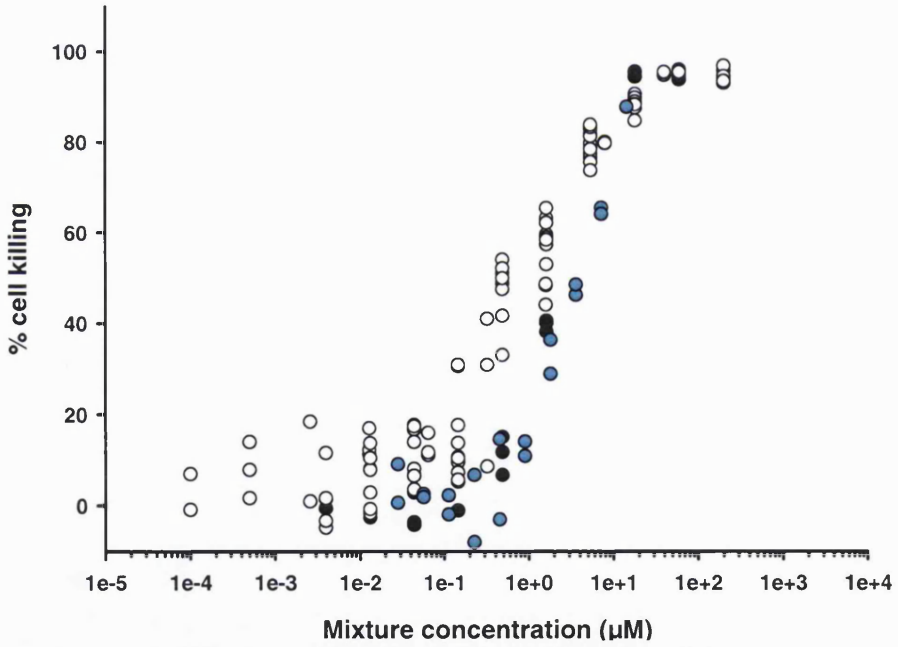

Figure 4.13: The cytotoxic effect on DU145 cells treated with liposomes encapsulated with a seven-component mixture of anticancer drugs. *The DU145 cells were grown for 72h in 96 well microtitre plates and treated with sequential concentrations of the free mixture and the encapsulated mixture for a further 72h. Cytotoxicity to the cells was assessed by the MTT assay as described in the materials and methods section of this chapter. A direct comparison of the cytotoxicity of the free mixture previously tested (white circles,* ***figure 2.21****), a free seven-component mixture run in parallel (black circles) and the liposomal mixture (cyan circles). The toxicity of the liposomal mixture demonstrated little variability to the toxicity of the free mixture.*

These results demonstrate that there was little difference in toxicity between the free treated agents to the liposomal encapsulated agents, and that the pharmacological effect of these agents on these cells remained even when delivered within a lipid vehicle.

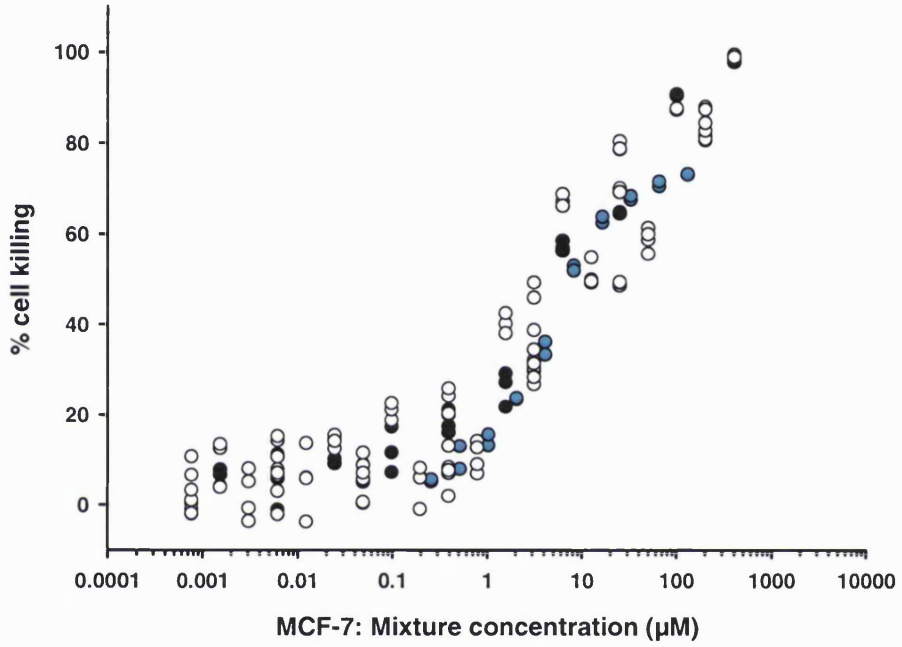

Figure 4.14: The cytotoxic effect on MCF-7 cells treated with liposomes encapsulated with a seven-component mixture of anticancer drugs. *A comparison of the cytotoxicity of the free seven-component mixture (white circles) as previously tested in* ***chapter 2 (figure 2.28)****, a free mixture run in parallel (black circles), and a liposomal mixture (cyan circles). The toxicity between the liposomal drug mixture and the free drugs demonstrated little variability.*

4.3.3 Size of drug entrapped liposomes

4.3.3.1 Uniformity of particle size

The sizes of the liposomes as described earlier were determined by the extrusion process and by passing the liposome solution through double stacked polycarbonate membranes of 100 nm pore size. The presence of fluorescent drugs such as daunorubicin and doxorubicin meant that sizing using PCS was

not possible due to an adverse level of light scattering due to these drugs. Particle size measurements were as a result, difficult to estimate from PCS measurements. Liposome size was therefore confirmed by the use of cryo-TEM, as shown in **figure 4.15** below. The micrographs show that the size of the blank liposomes and the drug encapsulated liposomes fall around the 100 nm range.

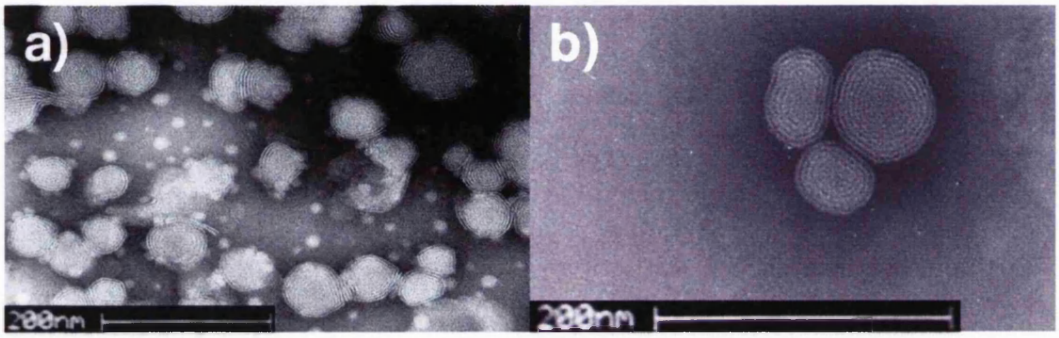

Figure 4.15: Cryo-TEM micrographs of SPC:CHOL liposomes. *The formation of lipid bilayers for liposomes and the range of size was approximately 100 nm.* ***a)*** *Formation of blank control liposomes; and* ***b)*** *formation of seven-component mixture entrapped liposomes. Samples were negatively stained with 1% PTA.*

4.3.3.2 Effect of charge on the mixture entrapped liposomes

Measurements of the surface charge of these liposomes can be used to help determine the type of interaction between the drug and the carrier; i.e. whether the drug is encapsulated within the body of the liposome or simply adsorbed on the surface. This is an important area used to determine whether an encapsulated drug is protected from enzymatic degradation, or whether it may be released very rapidly after administration.

Liposomes composed from lipid such as SPC and CHOL form a neutrally charged particle with a zeta potential near zero. **Table 4.5** summarises the surface charge of the blank and the entrapped liposomes. The charge for the control liposomes was near to a neutral value, -6.7 mV. The mixture entrapped liposomes demonstrated a higher negative zeta potential in comparison to the control liposomes. This property could mean that there is incorporation of one or

more drugs to the liposome surface resulting in an overall negative surface charge to the liposome.

Table 4.5: Zeta potential of entrapped liposomes

Liposome sample		*Entrapped drug, mV (mean value ± s.d., n=3)*
Water		-6.7 ± 1.131
DU145: mixture	**0.1 µM**	-42. 433 ± 1.801
	10 µM	-40.667 ± 3.262
	1000 µM	-34.833 ± 3.179
MCF-7: mixture	**0.2 µM**	-45.920 ± 5.118
	20 µM	-43.275 ± 5.435
	2000 µM	-42.160 ± 2.940

4.4 DISCUSSION

The use of liposomes as an effective carrier for a variety of agents has long been established (Lasic and Papahadjopoulos, 1998), and the application to cancer chemotherapy with the possibility to be able to delivery high levels of the drug to a specific site sounds promising. Liposomes encapsulated with doxorubicin, daunorubicin and vincristine have been used to great effect (Ranson et al., 1997; Tulpule et al., 1998; Gelmon et al., 1999), yet the area of combination chemotherapy has seen little progress up until now.

The results of these studies have shown that there is little to no variation in the overall toxicity of the free mixture when compared to liposome encapsulated mixture, for both the DU145 and the MCF-7 cell lines. This demonstrates that

there is no significant change in toxicity as a result of encapsulating a seven-component anticancer drug mixture into liposomes. The model for toxicity has been based upon the MTT assay, so although it can give good accurate data for *in vitro* toxicity, the *in vivo* effect is much more difficult to predict. Any deviation from the free drug effect to the liposomal effect can be attributed to differential entrapment of the mixture. An overall variation in the mixture ratio of the encapsulated drug mixture can be the result of some drugs being preferentially entrapped compared to some of the others. A variation in the overall mixture ratio would cause a shift in the liposomal seven mixture effect dependent on the drug preferentially entrapped, allowing either one or two drugs to contribute more significantly to the overall mixture effect.

The encapsulation efficiency and determination of the amount of drug present within the liposomes was an important step to establish the final cell treatment concentration. Inaccurate calculation of encapsulation would result in another possible shift in the concentration-response curve for the liposomal drug effect. The method used for measuring the amount of mixture encapsulated into liposomes was dependent on the fluorimetric intensity of daunorubicin and doxorubicin present in the mixture **(figure 4.11)**. In this way the whole mixture entrapment concentration could be calculated, and then an appropriate treatment concentration determined. This is one of the major issues to overcome for this range of work and correct measurement of the encapsulation efficiency, as well as ensuring complete mixture encapsulation, are important steps to formulate effective combinations of liposomal drug.

Knowledge of the liposomes' size and zeta potential can provide some information as to their probable pharmacokinetics and their likely circulation time. It has previously been seen that the presence of negatively charged liposomes may lead to increased uptake by the RES and therefore reduced circulation (Senior et al., 1985; Senior, 1987). Although the liposomes produced for this study were of a neutral nature, incorporation of anticancer drugs produced negatively charged liposomes **(table 4.5)**. Effective removal of free,

unentrapped drugs from the liposome solution **(section 4.2.1.3)** prior to treatment and zeta potential measurement ensured that all unentrapped drug was removed. The highly negative zeta potential measurements from entrapped liposomes could only be due to one or more drugs becoming incorporated to the liposome membrane surface.

Whether these particles can be protected with the use of PEG (Woodle et al., 1994) to avoid phagocytosis has yet to be tried out but would seem to be a possible further step. The prime aim for much of the carrier delivery systems at present has been site directed targeting and liposome delivery is no different. An integration of ligands and site-directing complexes to the liposome surface (Gregoriadis, 1988) and other forms of liposome surface engineering are further steps to the road of improved liposomal chemotherapy treatment.

Although this work has only looked at the effect of toxicity from the free to encapsulated mixture, it provides an adequate start point for looking into viable combinations for cancer chemotherapy, with an application for the use of a carrier mechanism to deliver the combination to the site of the tumour. The advantage of avoiding potential degradation and sequestration of drug to other parts of the body, coupled with the ability for surface targeting, ensures that although producing liposomal drugs is a more expensive procedure, the possibility to improve present chemotherapy remains high.

CHAPTER 5:

GENERAL DISCUSSION AND CONCLUSIONS

Recent advances in the treatment of cancer have lead to increased survival in many tumour patients through the use of drug combinations. Although the use of combination chemotherapy has become an effective means of improving cancer treatment, methods to predict their combined effects systematically are not in widespread use. A number of concepts can be used to predict mixture effects, and these are reliant upon knowledge of the type of agents the mixture is composed from. The first is known as *concentration addition*, and assumes that all agents act in a similar manner via a similar site of action; and the second, known as *independent action* assumes that these agents act dissimilarly using different sites of action. In this study we have looked at a group of seven anticancer drugs with a number of sites of action and compared their observed combined effects to their predicted combined effects using the *independent action* and *concentration addition* models. The aim was to establish a suitable *in vitro* assay model combined with an accurate predictive model for joint effects, which could accurately assess potentially therapeutic combinations of anticancer drugs.

5.1 EVALUATING THE COMBINATION EFFECTS FOR ANTICANCER DRUGS

Although there is a constant need to improve present therapy for cancer, the techniques used to evaluate potentially advantageous combinations of

anticancer drugs is still somewhat random. As has been discussed in **chapter 1**, the models for predicting combination effects are often reliant upon prior knowledge of a drug's site of action and on the accuracy of basing predictions on knowledge of single agent effects (Berenbaum, 1985; 1989). The widespread use of the median-effect method for assessing the synergistic effects for *in vitro* studies involving anticancer drugs has been an issue for debate for a number of years (Berenbaum, 1989; Greco et al., 1995). This method, developed by Chou and Talalay (1984) bears some resemblance to those initially developed by Loewe (1926) (mutually exclusive) and Bliss (1939) (non-mutually exclusive). However inaccuracies in the non-mutually exclusive model have shown that calculations for combination effects can be mistaken as being antagonistic (Berenbaum, 1989; Greco et al., 1995).

There is still no accurate and established model to predict combination effects for a mixture of anticancer drugs. Two models have shown promise in predicting the combined effects of similarly acting (Altenburger et al., 2000; Faust et al., 2001) and dissimilarly acting agents (Backhaus et al., 2000; 2004; Faust et al., 2003) and were used to evaluate the mixtures tested in this study. The two models used here were *independent action* and *concentration addition*. Until now no valid comparison of these two models has been undertaken for anticancer drugs, although the use of Loewe additivity has been suggested as a viable model (Greco et al., 1996). For the course of this study we have assessed the accuracy of the *independent action* model using a selection of seven anticancer drugs with dissimilar sites of action. A model such as this should be an accurate predictive model for this group of drugs. Surprisingly this was not the case, and as shown in **chapter 2** and **figures 2.21 & 2.28**, the *independent action* prediction consistently overestimated the mixture effect. The model for *concentration addition* gave a more accurate prediction for the combined effects for this mixture, suggesting that these agents perhaps did not act as dissimilarly as was first assumed. A case could be made that these drugs are dissimilar in their initial sites of action, but it was also possible that they have very similar mechanisms in which to kill cells. Therefore in **chapter 3** we set out to test this

hypothesis, to provide further insight as to the mode of action for each of these drugs in each cell line and to provide further information as to whether they should be classified as being similar or dissimilar acting.

5.2 EXPLORING THE MECHANISMS OF ACTION FOR THESE DRUGS

The findings from the experiments evaluating the combined effects of a mixture of anticancer drugs have shown that a prediction based on *independent action* was more inaccurate compared with *concentration addition.* The hypothesis that these drugs with dissimilar sites of action may have a similar mode of action was tested in **chapter 3**. Initially the drugs were tested to see if they all induced a form of mediated cell killing known as, apoptosis. All seven agents increased the level of apoptosis in the two cell lines tested **(figures 3.9 & 3.10)**, without increasing overall cell toxicity **(figure 3.8)**. A common and similar increase in apoptosis was confirmed, so further analysis of activation of the apoptotic pathway was carried out.

We assessed the potential of the DU145 cells to undergo apoptosis by expression of the initiator caspase procaspase-9 and the effector caspase procaspase-3. Expression of these proteins are the direct result of increased death receptor and/or mitochondrial-dependent apoptosis. Of the seven anticancer drugs tested, four drugs (doxorubicin, etoposide, melphalan and methotrexate) showed increased activation of the initiator caspase, caspase-9. The possible downstream target for caspase-9 was procaspase-3 and only daunorubicin and methotrexate showed increased levels of cleaved caspase-3 expression. There was no commonly activated signalling protein for all seven agents to suggest a similar mechanism of action, although a mechanism for methotrexate induced cell killing was made much clearer.

The MCF-7 cells were assessed for expression of the tumour suppressor gene, p53, and also for the initiator caspase, procaspase-9. Levels of p53 were increased after treatment with five of the seven agents and the seven-component mixture. All five of the agents showed increased levels of p53 expression after 24h exposure to the drug, including the seven-component mixture treated. The effect of vincristine on p53 activation was very slight and very rapid, **figure 3.12g** shows that after 2h exposure there was a slight increase in p53, but this disappeared after 4h. The single agent that did not increase levels of p53 was methotrexate. Following on from the findings from the DU145 cells which had impaired p53 expression (Isaacs et al., 1991), this confirmed that methotrexate may indeed cause apoptosis activation via a p53-independent manner, which has been demonstrated for other agents (Corazzari et al., 2005). Three drugs showed an increase in caspase-9 activation, etoposide, melphalan and methotrexate **(figure 3.14)**. These were three of the four drugs seen to activate caspase-9 in the DU145 cells **(figure 3.13)** and confirmed this as a possible mechanism of action for these three drugs. There again was no common activation of signalling protein for apoptosis, but the pathway for apoptosis activation remains extensively large and we have but looked at only a small piece of the jigsaw.

5.3 MODES OF DRUG DELIVERY

The use of predictive models to enhance therapeutic regimens for combinations of drugs has been seen as one step, a second is in the delivery of this improved combination to the tumour. Liposomes have recently been established as an effective method to deliver a number of anticancer drugs to tumour sites (Lasic and Papahadjopoulos, 1998). These drugs include the anthracyclines; doxorubicin and daunorubicin, as well as the microtubule inhibitor, vincristine. The ability to enclose a single agent or a collection of agents into a single particle poses an interesting and possibly exciting prospect to enhance

chemotherapy (Lasic and Papahadjopoulos, 1998; Saxon et al., 1999). Recent work has also shown the effectiveness of combining more than one agent within a nanoparticle. An anti-angiogenic drug, combretastatin, in addition to doxorubicin, has been incorporated into phospholipid envelopes and has been shown to reduce systemic toxicity as well as increased tumour cell kill. Comparison of single drug containing particles to particles containing both drugs showed improved survival in mice treated with the combined drugs (Sengupta et al., 2005; Bangham, 2005).

In a differing manner the work conducted in **chapter 4** studied the comparison in the toxic effect between free administered drugs to liposome encapsulated drugs. The combination of seven anticancer agents used for the studies in **chapters 2 & 3** were encapsulated into neutral liposomes and their toxic effect examined. The results have shown that there was little to no variation in the overall toxicity between the two preparations, so there was no impairment in toxic effect attributed to the entrapment process.

The strong issue of this work was the ability to encapsulate each individual drug efficiently into liposomes. A case of differential entrapment of one or more components in the mixture would drastically shift the liposome mixture effect as the overall mixture ratio would alter. Evidence of this was not seen and the dose-response profiles for the encapsulated drugs were similar to those of the free drug. The ability to accurately calculate the amount of drug entrapped into liposomes was crucial to construct these dose-response curves. Determination of the entrapment efficiency was dependent on the fluorescent ability of two of the seven drugs and **figure 4.10** confirmed that only the anthracyclines (daunorubicin and doxorubicin) were fluorescent at the emission wavelength used to measure the fluorescence intensity of the mixture.

There was no decrease in drug toxicity as a result of liposome encapsulation and this offers a possible advantage over conventional combination chemotherapy. With surface engineering and integration of ligands and site directing complexes (Gregoriadis, 1988), liposomes have the ability to target specific sites in the body and deliver a potentially effective combination of drugs

to this site. The delivery system can also help reduce drug degradation and sequestration to other parts of the body.

5.4 FUTURE WORK

The possibilities of future work entail a number of different options. Further work to establish the findings for our mixture work would clarify the importance of using both predictive models to assess joint effects of these agents. With greater elucidation of each drug's mode and mechanism of action we can further improve the classification of the drugs in a similar and dissimilar context and consequently establish an appropriate model to accurately predict its combined mixture effects. Once this can be reliably done, many possible therapeutic combinations can be assessed with the view for potentially useful synergistic combinations to be found.

The use of *in vitro* chemosensitivity assays to enhance therapeutic regimens for cancer has been the object of intense research over the years (Kaufmann et al., 1996) but the problem of interpreting cancer cell line sensitivity to anticancer drugs and humans is a difficult one. An approach to test effective anticancer drugs using patient tumour derived tumour cells has been employed using an assay known as the Adenosine Triphosphate Tumour Chemosensitivity Assay (ATP-TCA), measuring the production of ATP {Andreotti, 1995 480 /id;Kurbacher, 2005 470 /id}. Testing of potentially effective single agents and combinations on tumour derived tissue and relating to clinical treatment may provide an effective answer to increasing response rates in treated patients. This approach has been shown to increase clinical response and survival in primary ovarian cancers (Kurbacher and Cree, 2005) and colorectal adenocarcinoma (Whitehouse et al., 2003) and may be a possible method to effectively assess potentially useful drug combinations in an *in vitro* manner (Cree and Kurbacher, 1999). Combination of this approach with a potentially

effective method of predicting the combined effects of a mixture of anticancer drugs could provide a potentially useful technique to improving cancer therapy for the future.

Finally, work to improve the delivery mechanisms for a potentially useful combination of anticancer drugs has great prospect. Assuming methods to ensure complete integration of the combination into the delivery vehicle can be established, coupled with effective surface targeting, then an enhancement of existing cancer therapy will be found.

APPENDIX 1:

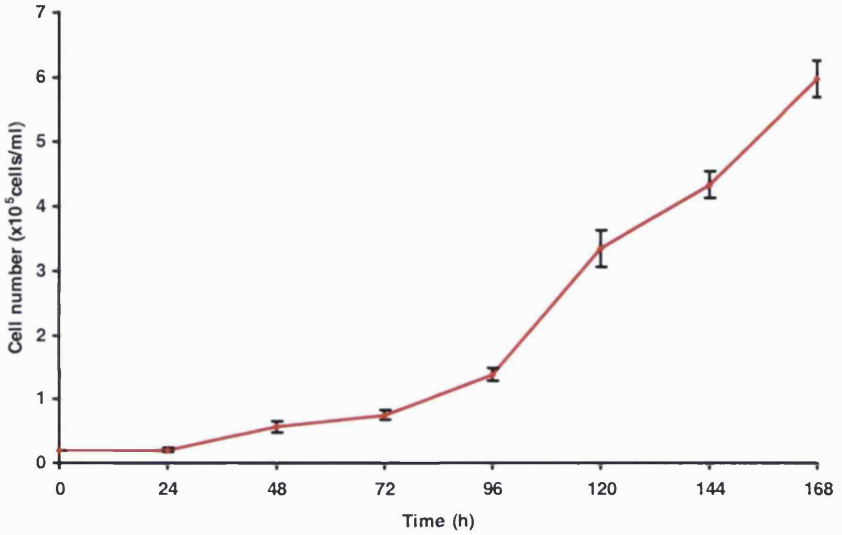

Figure A1.1: Growth curve for DU145 cells. *0.2x10^5 cells/ml were seeded in 75 cm^2 flasks in 15 ml RPMI medium supplemented with 10% FCS. Cells were harvested at each 24h time point by trypsinisation and counted. Data taken from mean three independent experiments ± 1 s.d.*

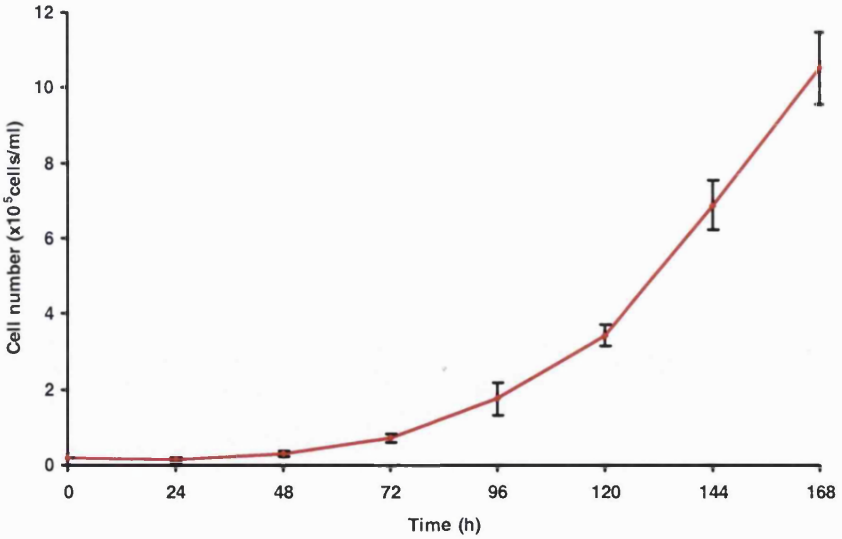

Figure A1.2: Growth curve for MCF-7 cells. *0.2x10^5 cells/ml were seeded in 75 cm^2 flasks in 15 ml MEM-α medium supplemented with 5% FCS. Cells were harvested at each 24h time point by trypsinisation and counted. Data taken from mean three independent experiments ± 1 s.d.*

APPENDIX 2:

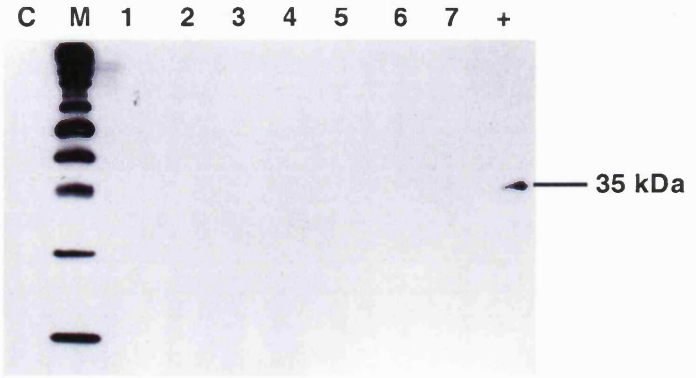

Figure A2.1: Expression of procaspase-3 in single agent treated MCF-7 cells. *Lane C, control; 1, 5-FUdR treated; 2, daunorubicin treated; 3, doxorubicin treated; 4, etoposide treated; 5, melphalan treated; 6, methotrexate treated; 7, vincristine treated; +, UV treated cos cells (positive control). All MCF-7 cell lysates, even untreated controls do not express the effector caspase, procaspase-3 (35 kDa band) as had been shown previously (Janicke et al., 1998). The cells were treated at MED for 24h*

REFERENCES

Adams,J.M. and Cory,S. (1998). The Bcl-2 protein family: arbiters of cell survival. Science *281*, 1322-1326.

Allen,T.M., Hansen,C., Martin,F., Redemann,C., and Yau-Young,A. (1991). Liposomes containing synthetic lipid derivatives of poly(ethylene glycol) show prolonged circulation half-lives in vivo. Biochim. Biophys. Acta *1066*, 29-36.

Alnemri,E.S., Livingston,D.J., Nicholson,D.W., Salvesen,G., Thornberry,N.A., Wong,W.W., and Yuan,J. (1996). Human ICE/CED-3 protease nomenclature. Cell *87*, 171.

Altenburger,R., Backhaus,T., Boedeker,W., Faust,M., Scholze,M., and Grimme,L.H. (2000). Predictability of the toxicity of multiple chemical mixtures to *Viberio Fischeri*: Mixtures composed of similarly acting chemicals. Environ. Toxicol. Chem *19*, 2341-2347.

Amselem,S., Gabizon,A., and Barenholz,Y. (1990). Optimization and upscaling of doxorubicin-containing liposomes for clinical use. J. Pharm. Sci. *79*, 1045-1052.

Andreotti,P.E., Cree,I.A., Kurbacher,C.M., Hartmann,D.M., Linder,D., Harel,G., Gleiberman,I., Caruso,P.A., Ricks,S.H., and Untch,M. (1995). Chemosensitivity testing of human tumors using a microplate adenosine triphosphate luminescence assay: clinical correlation for cisplatin resistance of ovarian carcinoma. Cancer Res. *55*, 5276-5282.

Ashkenazi,A. and Dixit,V.M. (1998). Death receptors: signaling and modulation. Science *281*, 1305-1308.

Backhaus,T., Altenburger,R., Boedeker,W., Faust,M., Scholze,M., and Grimme,L.H. (2000). Predictability of the toxicity of a multiple mixture of dissimilarly acting chemicals to *Viberio Fischeri*. Environ. Toxicol. Chem *19*, 2348-2356.

Backhaus,T., Arrhenius,A., and Blanck,H. (2004). Toxicity of a mixture of dissimilarly acting substances to natural algal communities: predictive power and limitations of independent action and concentration addition. Environ. Sci. Technol. *38*, 6363-6370.

Baekelandt,M.M., Holm,R., Nesland,J.M., Trope,C.G., and Kristensen,G.B. (2000). P-glycoprotein expression is a marker for chemotherapy resistance and prognosis in advanced ovarian cancer. Anticancer Res. *20*, 1061-1067.

Baird,R.D. and Kaye,S.B. (2003). Drug resistance reversal--are we getting closer? Eur. J. Cancer *39*, 2450-2461.

Bangham,A.D., Standish,M.M., and Watkins,J.C. (1965). Diffusion of univalent ions across the lamellae of swollen phospholipids. J. Mol. Biol. *13*, 238-252.

Bangham,J. (2005). A tiny timely vehicle. Nat Rev Cancer *5*, 670.

Banin,S., Moyal,L., Shieh,S., Taya,Y., Anderson,C.W., Chessa,L., Smorodinsky,N.I., Prives,C., Reiss,Y., Shiloh,Y., and Ziv,Y. (1998). Enhanced phosphorylation of p53 by ATM in response to DNA damage. Science *281*, 1674-1677.

Baselga,J., Tripathy,D., Mendelsohn,J., Baughman,S., Benz,C.C., Dantis,L., Sklarin,N.T., Seidman,A.D., Hudis,C.A., Moore,J., Rosen,P.P., Twaddell,T., Henderson,I.C., and Norton,L. (1996). Phase II study of weekly intravenous recombinant humanized anti-p185HER2 monoclonal antibody in patients with HER2/neu-overexpressing metastatic breast cancer. J. Clin. Oncol. *14*, 737-744.

Batist,G., Ramakrishnan,G., Rao,C.S., Chandrasekharan,A., Gutheil,J., Guthrie,T., Shah,P., Khojasteh,A., Nair,M.K., Hoelzer,K., Tkaczuk,K., Park,Y.C., and Lee,L.W. (2001). Reduced cardiotoxicity and preserved antitumor efficacy of liposome-encapsulated doxorubicin and cyclophosphamide compared with conventional doxorubicin and cyclophosphamide in a randomized, multicenter trial of metastatic breast cancer. J. Clin. Oncol. *19*, 1444-1454.

Bellamy,W.T. (1992). Prediction of response to drug therapy of cancer. A review of in vitro assays. Drugs *44*, 690-708.

Berenbaum,M.C. (1985). The expected effect of a combination of agents: the general solution. J. Theor. Biol. *114*, 413-431.

Berenbaum,M.C. (1989). What is synergy? Pharmacol. Rev. *41*, 93-141.

Blakeley,R.L. (1995). Eukaryotic dihydrofolate reductase. Adv. Enzymol. Relat. Areas Mol. Biol. *70*, 23-102.

Bliss,C.I. (1939). The toxicity of poisons applied jointly. Annals of Applied Biology *26*, 585-615.

Boldin,M.P., Goncharov,T.M., Goltsev,Y.V., and Wallach,D. (1996). Involvement of MACH, a novel MORT1/FADD-interacting protease, in Fas/APO-1- and TNF receptor-induced cell death. Cell *85*, 803-815.

Bonetta,L. (2005). Zooming in on electron tomography. Nat Meth *2*, 139-145.

Borgert,C.J., Quill,T.F., McCarty,L.S., and Mason,A.M. (2004). Can mode of action predict mixture toxicity for risk assessment? Toxicol. Appl. Pharmacol. *201*, 85-96.

Brown,J.M. and Wouters,B.G. (1999). Apoptosis, p53, and tumor cell sensitivity to anticancer agents. Cancer Res. *59*, 1391-1399.

Burns,T.F. and El-Deiry,W.S. (2003). Cell death signaling in maligancy. Cancer Treat. Res. *115*, 319-343.

Butterworth,B.E., Conolly,R.B., and Morgan,K.T. (1995). A strategy for establishing mode of action of chemical carcinogens as a guide for approaches to risk assessments. Cancer Lett. *93*, 129-146.

Calamari,D. and Vighi,M. (1992). A proposal to define quality objectives for aquatic life for mixtures of chemical substances. Chemosphere *25*, 531-542.

Canman,C.E., Lim,D.S., Cimprich,K.A., Taya,Y., Tamai,K., Sakaguchi,K., Appella,E., Kastan,M.B., and Siliciano,J.D. (1998). Activation of the ATM kinase by ionizing radiation and phosphorylation of p53. Science *281*, 1677-1679.

Carmichael,J., DeGraff,W.G., Gazdar,A.F., Minna,J.D., and Mitchell,J.B. (1987). Evaluation of a tetrazolium-based semiautomated colorimetric assay: assessment of chemosensitivity testing. Cancer Res. *47*, 936-942.

Carter,B.S., Ewing,C.M., Ward,W.S., Treiger,B.F., Aalders,T.W., Schalken,J.A., Epstein,J.I., and Isaacs,W.B. (1990). Allelic loss of chromosomes 16q and 10q in human prostate cancer. Proc. Natl. Acad. Sci. U. S. A *87*, 8751-8755.

Chen,M. and Wang,J. (2002). Initiator caspases in apoptosis signaling pathways. Apoptosis. *7*, 313-319.

Chinnaiyan,A.M., Tepper,C.G., Seldin,M.F., O'Rourke,K., Kischkel,F.C., Hellbardt,S., Krammer,P.H., Peter,M.E., and Dixit,V.M. (1996). FADD/MORT1 is a common mediator of CD95 (Fas/APO-1) and tumor necrosis factor receptor-induced apoptosis. J. Biol. Chem *271*, 4961-4965.

Chonn,A., Semple,S.C., and Cullis,P.R. (1992). Association of blood proteins with large unilamellar liposomes in vivo. Relation to circulation lifetimes. J. Biol. Chem. *267*, 18759-18765.

Chou,T.C. and Talalay,P. (1984). Quantitative analysis of dose-effect relationships: the combined effects of multiple drugs or enzyme inhibitors. Adv. Enzyme Regul. *22*, 27-55.

Colby,S.R. (1967). Calculating Synergistic and Antagonistic Responses of Herbicide Combinations. Weeds *15*, 20-22.

Colvin,M.E. (1999). Chemical factors in the action of phosphoramidic mustard alkylating anticancer drugs: roles for computational chemistry. Current Pharmaceutical Design *5*, 645-663.

Cook,A.F., Holman,M.J., Kramer,M.J., and Trown,P.W. (1979). Fluorinated pyrimidine nucleosides. 3. Synthesis and antitumor activity of a series of 5'-deoxy-5-fluoropyrimidine nucleosides. J. Med. Chem *22*, 1330-1335.

Corazzari,M., Lovat,P.E., Oliverio,S., Di,S.F., Donnorso,R.P., Redfern,C.P., and Piacentini,M. (2005). Fenretinide: a p53-independent way to kill cancer cells. Biochem. Biophys. Res. Commun. *331*, 810-815.

Cree,I.A. and Kurbacher,C.M. (1999). ATP-based tumor chemosensitivity testing: assisting new agent development. Anticancer Drugs *10*, 431-435.

Daemen,T., Velinova,M., Regts,J., de,J.M., Kalicharan,R., Donga,J., van der Want,J.J., and Scherphof,G.L. (1997). Different intrahepatic distribution of phosphatidylglycerol and phosphatidylserine liposomes in the rat. Hepatology *26*, 416-423.

Davis,B. (1964). Disc Electrophoresis. II. Method and application to human serum proteins. Ann. N. Y. Acad. Sci. *121*, 404-427.

Dellarco,V.L. and Wiltse,J.A. (1998). US Environmental Protection Agency's revised guidelines for Carcinogen Risk Assessment: incorporating mode of action data. Mutat. Res. *405*, 273-277.

Denizot,F. and Lang,R. (1986). Rapid colorimetric assay for cell growth and survival. Modifications to the tetrazolium dye procedure giving improved sensitivity and reliability. J. Immunol. Methods *89*, 271-277.

Deveraux,Q.L. and Reed,J.C. (1999). IAP family proteins--suppressors of apoptosis. Genes Dev. *13*, 239-252.

Dlamini,Z., Mbita,Z., and Zungu,M. (2004). Genealogy, expression, and molecular mechanisms in apoptosis. Pharmacol. Ther. *101*, 1-15.

Donaldson,K.L. (1994). Activation of p34cdc coincident with taxol-induced apoptosis. Cell Growth and Differentiation *5*, 1041-1050.

Drescher,K. and Boedeker,W. (1995). Assessment of the combined effects of substances: The relationship between concentration addition and independent action. Biometrics *51*, 716-730.

Drewinko,B., Green,C., and Loo,T.L. (1976). Combination chemotherapy in vitro with *cis*-dichlorodiammineplatinum(II). Cancer Treat. Rep. *60*, 1619-1625.

Drummond,D.C., Meyer,O., Hong,K., Kirpotin,D.B., and Papahadjopoulos,D. (1999). Optimizing liposomes for delivery of chemotherapeutic agents to solid tumors. Pharmacol. Rev. *51*, 691-743.

Eaton,L. (2003). World cancer rates set to double by 2020. BMJ *326*, 728a.

El-Deiry,W.S. (2003). The role of p53 in chemosensitivity and radiosensitivity. Oncogene *22*, 7486-7495.

Fadok,V.A., Laszlo,D.J., Noble,P.W., Weinstein,L., Riches,D.W., and Henson,P.M. (1993). Particle digestibility is required for induction of the phosphatidylserine recognition mechanism used by murine macrophages to phagocytose apoptotic cells. J. Immunol. *151*, 4274-4285.

Fadok,V.A., Savill,J.S., Haslett,C., Bratton,D.L., Doherty,D.E., Campbell,P.A., and Henson,P.M. (1992a). Different populations of macrophages use either the vitronectin receptor or the phosphatidylserine receptor to recognize and remove apoptotic cells. J. Immunol. *149*, 4029-4035.

Fadok,V.A., Voelker,D.R., Campbell,P.A., Cohen,J.J., Bratton,D.L., and Henson,P.M. (1992b). Exposure of phosphatidylserine on the surface of apoptotic lymphocytes triggers specific recognition and removal by macrophages. J. Immunol. *148*, 2207-2216.

Faust,M., Altenburger,R., Backhaus,T., Blanck,H., Boedeker,W., Gramatica,P., Hamer,V., Scholze,M., Vighi,M., and Grimme,L.H. (2001). Predicting the joint algal toxicity of multi-component s-triazine mixtures at low-effect concentrations of individual toxicants. Aquat. Toxicol. *56*, 13-32.

Faust,M., Altenburger,R., Backhaus,T., Blanck,H., Boedeker,W., Gramatica,P., Hamer,V., Scholze,M., Vighi,M., and Grimme,L.H. (2003). Joint algal toxicity of 16 dissimilarly acting chemicals is predictable by the concept of independent action. Aquat. Toxicol. *63*, 43-63.

Faust,M., Altenburger,R., Backhaus,T., Boedeker,W., Scholze,M., and Grimme,L.H. (2000). Predictive assessment of aquatic toxicity of multiple chemical mixtures. J. Environ. Qual *29*, 1063-1068.

Finlay,C.A., Hinds,P.W., Tan,T.H., Eliyahu,D., Oren,M., and Levine,A.J. (1988). Activating mutations for transformation by p53 produce a gene product that forms an hsc70-p53 complex with an altered half-life. Mol. Cell Biol. *8*, 531-539.

Fisher,B., Sherman,B., Rockette,H., Redmond,C., Margolese,R., and Fisher,E.R. (1979). 1-phenylalanine mustard (L-PAM) in the management of premenopausal patients with primary breast cancer: lack of association of disease-free survival with depression of ovarian function. National Surgical Adjuvant Project for Breast and Bowel Cancers. Cancer *44*, 847-857.

Foley,J.F., Vose,J.M., and Armitage,J.O. (1999). Current Therapy in Cancer. (Philadelphia: W.B. Saunders Company).

Forssen,E.A., Coulter,D.M., and Proffitt,R.T. (1992). Selective in vivo localization of daunorubicin small unilamellar vesicles in solid tumors. Cancer Res. *52*, 3255-3261.

Fridman,J.S. and Lowe,S.W. (2003). Control of apoptosis by p53. Oncogene *22*, 9030-9040.

Gabizon,A., Dagan,A., Goren,D., Barenholz,Y., and Fuks,Z. (1982). Liposomes as in vivo carriers of adriamycin: reduced cardiac uptake and preserved antitumor activity in mice. Cancer Res. *42*, 4734-4739.

Gabizon,A., Price,D.C., Huberty,J., Bresalier,R.S., and Papahadjopoulos,D. (1990). Effect of liposome composition and other factors on the targeting of liposomes to experimental tumors: biodistribution and imaging studies. Cancer Res. *50*, 6371-6378.

Gabizon,A.A. (1994). Liposomal anthracyclines. Hematol. Oncol. Clin. North Am. *8*, 431-450.

Gelmon,K.A., Tolcher,A., Diab,A.R., Bally,M.B., Embree,L., Hudon,N., Dedhar,C., Ayers,D., Eisen,A., Melosky,B., Burge,C., Logan,P., and Mayer,L.D. (1999). Phase I study of liposomal vincristine. J. Clin. Oncol. *17*, 697-705.

George,R.P., Poth,J.L., Gordon,D., and Schrier,S.L. (1972). Multiple myeloma--intermittent combination chemotherapy compared to continuous therapy. Cancer *29*, 1665-1670.

Gill,P.S., Espina,B.M., Muggia,F., Cabriales,S., Tulpule,A., Esplin,J.A., Liebman,H.A., Forssen,E., Ross,M.E., and Levine,A.M. (1995). Phase I/II clinical and pharmacokinetic evaluation of liposomal daunorubicin. J. Clin. Oncol. *13*, 996-1003.

Goodman,L.S., Wintrobe,M.M., Dameshek,W., Goodman,M.J., Gilman,A., and McLennan,M.T. (1984). Landmark article Sept. 21, 1946: Nitrogen mustard therapy. Use of methyl-bis(beta-chloroethyl)amine hydrochloride and tris(beta-chloroethyl)amine hydrochloride for Hodgkin's disease, lymphosarcoma, leukemia and certain allied and miscellaneous disorders. By Louis S. Goodman, Maxwell M. Wintrobe, William Dameshek, Morton J. Goodman, Alfred Gilman and Margaret T. McLennan. JAMA *251*, 2255-2261.

Greco,W.R., Bravo,G., and Parsons,J.C. (1995). The search for synergy: a critical review from a response surface perspective. Pharmacol. Rev. *47*, 331-385.

Greco,W.R., Faessel,H., and Levasseur,L. (1996). The search for cytotoxic synergy between anticancer agents: a case of Dorothy and the ruby slippers? J. Natl. Cancer Inst. *88*, 699-700.

Greco,W.R., Unkelbach,H.D., Poch,G., Suhnel,J., Kundi,M., and Bodeker,W. (1992). Consensus on concepts and terminology for combined-action assessment: The Saariselkä Agreement. Arch. Complex Environment. Studies *4*, 65-69.

Green,D.R. and Kroemer,G. (2004). The pathophysiology of mitochondrial cell death. Science *305*, 626-629.

Green,D.R. and Reed,J.C. (1998). Mitochondria and apoptosis. Science *281*, 1309-1312.

Gregoriadis,G. (1998). Genetic vaccines: strategies for optimization. Pharm. Res. *15*, 661-670.

Gregoriadis,G. (1988). Liposomes as a drug delivery system: optimization studies. Adv. Exp. Med. Biol. *238*, 151-159.

Gregoriadis,G. (1994). The immunological adjuvant and vaccine carrier properties of liposomes. J. Drug Target *2*, 351-356.

Gregoriadis,G. and Davis,C. (1979). Stability of liposomes in vivo and in vitro is promoted by their cholesterol content and the presence of blood cells. Biochem. Biophys. Res. Commun. *89*, 1287-1293.

Gregoriadis,G., McCormack,B., Morrison,Y., Saffie,R., and Zadi,B. (1998). Liposomes in Drug Targeting. In Cell Biology: A Laboratory Handbook, J.E. Cellis, ed. (New York: Academic Press), pp. 131-140.

Gregoriadis,G. and Ryman,B.E. (1972). Fate of protein-containing liposomes injected into rats. An approach to the treatment of storage diseases. Eur. J. Biochem. *24*, 485-491.

Gruss,H.J. and Dower,S.K. (1995). Tumor necrosis factor ligand superfamily: involvement in the pathology of malignant lymphomas. Blood *85*, 3378-3404.

Gudas,J.M., Nguyen,H., Li,T., Sadzewicz,L., Robey,R., Wosikowski,K., and Cowan,K.H. (1996). Drug-resistant breast cancer cells frequently retain expression of a functional wild-type p53 protein. Carcinogenesis *17*, 1417-1427.

Guo,Y., Srinivasula,S.M., Druilhe,A., Fernandes-Alnemri,T., and Alnemri,E.S. (2002). Caspase-2 induces apoptosis by releasing proapoptotic proteins from mitochondria. J. Biol. Chem *277*, 13430-13437.

Gupta,S., Radha,V., Furukawa,Y., and Swarup,G. (2001). Direct transcriptional activation of human caspase-1 by tumor suppressor p53. J. Biol. Chem *276*, 10585-10588.

Haber,J.E. (2000). Partners and pathwaysrepairing a double-strand break. Trends Genet. *16*, 259-264.

Hamburger,A.W. and Salmon,S.E. (1977). Primary bioassay of human tumor stem cells. Science *197*, 461-463.

Hanahan,D. and Weinberg,R.A. (2000). The hallmarks of cancer. Cell *100*, 57-70.

Hansen,M.B., Nielsen,S.E., and Berg,K. (1989). Re-examination and further development of a precise and rapid dye method for measuring cell growth/cell kill. J. Immunol. Methods *119*, 203-210.

Hartwell,L.H. and Kastan,M.B. (1994). Cell cycle control and cancer. Science *266*, 1821-1828.

Hartwell,L.H. and Weinert,T.A. (1989). Checkpoints: controls that ensure the order of cell cycle events. Science *246*, 629-634.

Haskell,C.M. (2001). Cancer Treatment. (Philadelphia: W.B. Saunders and Company).

Hewlett,P.S. and Plackett,R.L. (1959). A unified approach for quantal responses to mixtures of drugs: non-interactive action. Biometrics *15*, 591-610.

Hobbs,S.K., Monsky,W.L., Yuan,F., Roberts,W.G., Griffith,L., Torchilin,V.P., and Jain,R.K. (1998). Regulation of transport pathways in tumor vessels: role of tumor type and microenvironment. Proc. Natl. Acad. Sci. U. S. A *95*, 4607-4612.

Homburg,C.H., de,H.M., von dem Borne,A.E., Verhoeven,A.J., Reutelingsperger,C.P., and Roos,D. (1995). Human neutrophils lose their surface Fc gamma RIII and acquire Annexin V binding sites during apoptosis in vitro. Blood *85*, 532-540.

Howell,S.B., Pfeifle,C.E., and Olshen,R.A. (1984). Intraperitoneal chemotherapy with melphalan. Ann. Intern. Med. *101*, 14-18.

Hsu,H., Shu,H.B., Pan,M.G., and Goeddel,D.V. (1996). TRADD-TRAF2 and TRADD-FADD interactions define two distinct TNF receptor 1 signal transduction pathways. Cell *84*, 299-308.

Hsu,H., Xiong,J., and Goeddel,D.V. (1995). The TNF receptor 1-associated protein TRADD signals cell death and NF-kappa B activation. Cell *81*, 495-504.

Huang,C. (1969). Studies on phosphatidylcholine vesicles. Formation and physical characteristics. Biochemistry *8*, 344-352.

Isaacs,W.B., Carter,B.S., and Ewing,C.M. (1991). Wild-type p53 suppresses growth of human prostate cancer cells containing mutant p53 alleles. Cancer Res. *51*, 4716-4720.

Janicke,R.U., Sprengart,M.L., Wati,M.R., and Porter,A.G. (1998). Caspase-3 is required for DNA fragmentation and morphological changes associated with apoptosis. J. Biol. Chem *273*, 9357-9360.

Jiang,C., Wang,Z., Ganther,H., and Lu,J. (2001). Caspases as key executors of methyl selenium-induced apoptosis (anoikis) of DU-145 prostate cancer cells. Cancer Res. *61*, 3062-3070.

Jordan,M.A. (1993). Mechanisms of mitotic block and inhibition of cell proliferation by taxol at low concentrations. Proc. Natl. Acad. Sci. U. S. A *90*, 9552-9556.

Kangas,L., Gronroos,M., and Nieminen,A.L. (1984). Bioluminescence of cellular ATP: a new method for evaluating cytotoxic agents in vitro. Med. Biol. *62*, 338-343.

Kastan,M.B., Zhan,Q., El-Deiry,W.S., Carrier,F., Jacks,T., Walsh,W.V., Plunkett,B.S., Vogelstein,B., and Fornace,A.J., Jr. (1992). A mammalian cell cycle checkpoint pathway utilizing p53 and GADD45 is defective in ataxia-telangiectasia. Cell *71*, 587-597.

Katz,E.J., Vick,J.S., Kling,K.M., Andrews,P.A., and Howell,S.B. (1990). Effect of topoisomerase modulators on cisplatin cytotoxicity in human ovarian carcinoma cells. Eur. J. Cancer *26*, 724-727.

Kaufmann,S.H., Mesner,P.W., Jr., Samejima,K., Tone,S., and Earnshaw,W.C. (2000). Detection of DNA cleavage in apoptotic cells. Methods Enzymol. *322*, 3-15.

Kaufmann,S.H., Peereboon,D., Buckwalter,C.A., Svingen,P.A., Growchow,L.B., Donehower,R.C., and Rowinsky,E.K. (1996). Cytotoxic effects of topotecan combined with various anticancer agents in human cancer cell lines. J. Natl. Cancer Inst. *88*, 734-741.

Keepers,Y.P., Pizao,P.E., Peters,G.J., van Ark-Otte,J., Winograd,B., and Pinedo,H.M. (1991). Comparison of the sulforhodamine B protein and tetrazolium (MTT) assays for in vitro chemosensitivity testing. Eur. J. Cancer *27*, 897-900.

Kerr,J.F., Wyllie,A.H., and Currie,A.R. (1972). Apoptosis: a basic biological phenomenon with wide-ranging implications in tissue kinetics. Br. J. Cancer *26*, 239-257.

Kerrigan, D., Kelly, J., and Hollen, B. Understanding Cancer and Related Topics: Understanding Cancer Genomics. Natl.Cancer Inst. 28-1-2005. Electronic Citation

Khanna,K.K., Keating,K.E., Kozlov,S., Scott,S., Gatei,M., Hobson,K., Taya,Y., Gabrielli,B., Chan,D., Lees-Miller,S.P., and Lavin,M.F. (1998). ATM associates with and phosphorylates p53: mapping the region of interaction. Nat. Genet. *20*, 398-400.

Kluck,R.M., Bossy-Wetzel,E., Green,D.R., and Newmeyer,D.D. (1997). The release of cytochrome c from mitochondria: a primary site for Bcl-2 regulation of apoptosis. Science *275*, 1132-1136.

Knudson,A.G., Jr. (1985). Hereditary cancer, oncogenes, and antioncogenes. Cancer Res. *45*, 1437-1443.

Knudson,A.G., Jr. (1971). Mutation and cancer: statistical study of retinoblastoma. Proc. Natl. Acad. Sci. U. S. A *68*, 820-823.

Koh,Y., Nishio,K., and Saijo,N. (2002). Mechanisms of Action of Cancer Chemotherapeutic Agents: Topoisomerase Inhibitors. In The Cancer Handbook, M.R.Alison, ed. (USA: John Wiley and Sons Ltd), pp. 1313-1322.

Kohler,G. and Milstein,C. (1975). Continuous cultures of fused cells secreting antibody of predefined specificity. Nature *256*, 495-497.

Könemann,W.H. and Pieters,M.N. (1996). Confusion of concepts in mixture toxicology. Food Chem. Toxicol. *34*, 1025-1031.

Koopman,G., Reutelingsperger,C.P., Kuijten,G.A., Keehnen,R.M., Pals,S.T., and van Oers,M.H. (1994). Annexin V for flow cytometric detection of phosphatidylserine expression on B cells undergoing apoptosis. Blood *84*, 1415-1420.

Kroemer,G., Zamzami,N., and Susin,S.A. (1997). Mitochondrial control of apoptosis. Immunol. Today *18*, 44-51.

Kruh,G.D. (2003). Introduction to resistance to anticancer agents. Oncogene *22*, 7262-7264.

Kubbutat,M.H., Jones,S.N., and Vousden,K.H. (1997). Regulation of p53 stability by Mdm2. Nature *387*, 299-303.

Kurbacher,C.M. and Cree,I.A. (2005). Chemosensitivity testing using microplate adenosine triphosphate-based luminescence measurements. Methods Mol. Med. *110*, 101-120.

Land,H., Parada,L.F., and Weinberg,R.A. (1983). Tumorigenic conversion of primary embryo fibroblasts requires at least two cooperating oncogenes. Nature *304*, 596-602.

Lasic,D. and Papahadjopoulos,D. (1998). Medical Applications of Liposomes. (Amsterdam: Elsevier Science B.V.).

Lasic,D.D., Martin,F.J., Gabizon,A., Huang,S.K., and Papahadjopoulos,D. (1991). Sterically stabilized liposomes: a hypothesis on the molecular origin of the extended circulation times. Biochim. Biophys. Acta *1070*, 187-192.

Levasseur,L.M., Greco,W.R., Rustum,Y.M., and Slocum,H.K. (1997). Combined action of paclitaxel and cisplatin against wildtype and resistant human ovarian carcinoma cells. Cancer Chemother. Pharmacol. *40*, 495-505.

Li,P., Nijhawan,D., Budihardjo,I., Srinivasula,S.M., Ahmad,M., Alnemri,E.S., and Wang,X. (1997). Cytochrome c and dATP-dependent formation of Apaf-1/caspase-9 complex initiates an apoptotic protease cascade. Cell *91*, 479-489.

Lin,Y., Ma,W., and Benchimol,S. (2000). Pidd, a new death-domain-containing protein, is induced by p53 and promotes apoptosis. Nat. Genet. *26*, 122-127.

Liu,X., Kim,C.N., Yang,J., Jemmerson,R., and Wang,X. (1996). Induction of apoptotic program in cell-free extracts: requirement for dATP and cytochrome c. Cell *86*, 147-157.

Liu,Y., Peterson,D.A., Kimura,H., and Schubert,D. (1997). Mechanism of cellular 3-(4,5-dimethylthiazol-2-yl)-2,5-diphenyltetrazolium bromide (MTT) reduction. J. Neurochem. *69*, 581-593.

Loewe,S. and Muischnek,H. (1926). Uber Kombinationswirkungen. 1. Mitteilung: Hilfsmittel der Fragestellung. Arch. Exp. Pathol. Pharmakol. *114*, 313-326.

Lorenzen,J., Thiele,J., and Fischer,R. (1997). The mummified Hodgkin cell: cell death in Hodgkin's disease. J. Pathol. *182*, 288-298.

Lorigan,P. and Vandenberghe,E. (2002). High Dose Chemotherapy, Principle and Practice. (London: Martin Dunitz Ltd).

Manuelidis,L. and Chen,T.L. (1990). A unified model of eukaryotic chromosomes. Cytometry *11*, 8-25.

Markman,M. (1997). Basic Cancer Medicine. (Philadelphia: W.B. Saunders Company).

Martin,F.J. (1998). Clinical pharmacology and antitumour efficiency of DOXIL (pegylated liposomal doxorubicin). D.Lasic and D.Papahadjopoulos, eds. (New York: Elsevier Science BV), pp. 635-688.

Martin,S.J., Reutelingsperger,C.P., McGahon,A.J., Rader,J.A., van Schie,R.C., LaFace,D.M., and Green,D.R. (1995). Early redistribution of plasma membrane phosphatidylserine is a general feature of apoptosis regardless of the initiating stimulus: inhibition by overexpression of Bcl-2 and Abl. J. Exp. Med. *182*, 1545-1556.

Maya,R., Balass,M., Kim,S.T., Shkedy,D., Leal,J.F., Shifman,O., Moas,M., Buschmann,T., Ronai,Z., Shiloh,Y., Kastan,M.B., Katzir,E., and Oren,M. (2001). ATM-dependent phosphorylation of Mdm2 on serine 395: role in p53 activation by DNA damage. Genes Dev. *15*, 1067-1077.

Mayer,L.D., Dougherty,G., Harasym,T.O., and Bally,M.B. (1997). The role of tumor-associated macrophages in the delivery of liposomal doxorubicin to solid murine fibrosarcoma tumors. J. Pharmacol. Exp. Ther. *280*, 1406-1414.

McCann,J., Choi,E., Yamasaki,E., and Ames,B.N. (1975). Detection of carcinogens as mutagens in the Salmonella/microsome test: assay of 300 chemicals. Proc. Natl. Acad. Sci. U. S. A *72*, 5135-5139.

McGill,G. (1997). Apoptosis In Tumorigenesis And Cancer Therapy. Front Biosci. *2*, d353-d379.

Mileson,B.E., Chambers,J.E., Chen,W.L., Dettbarn,W., Ehrich,M., Eldefrawi,A.T., Gaylor,D.W., Hamernik,K., Hodgson,E., Karczmar,A.G., Padilla,S., Pope,C.N., Richardson,R.J., Saunders,D.R., Sheets,L.P., Sultatos,L.G., and Wallace,K.B. (1998). Common mechanism of toxicity: a case study of organophosphorus pesticides. Toxicol. Sci. *41*, 8-20.

Mitchell,M.S., Kempf,R.A., Harel,W., Shau,H., Boswell,W.D., Lind,S., and Bradley,E.C. (1988). Effectiveness and tolerability of low-dose cyclophosphamide and low-dose intravenous interleukin-2 in disseminated melanoma [corrected]. J. Clin. Oncol. *6*, 409-424.

Miyashita,T. and Reed,J.C. (1995). Tumor suppressor p53 is a direct transcriptional activator of the human bax gene. Cell *80*, 293-299.

Moller,A., Malerczyk,C., Volker,U., Stoppler,H., and Maser,E. (2002). Monitoring daunorubicin-induced alterations in protein expression in pancreas carcinoma cells by two-dimensional gel electrophoresis. Proteomics. *2*, 697-705.

Mosmann,T. (1983). Rapid colorimetric assay for cellular growth and survival: application to proliferation and cytotoxicity assays. J. Immunol. Methods *65*, 55-63.

Muggia,F.M., Hainsworth,J.D., Jeffers,S., Miller,P., Groshen,S., Tan,M., Roman,L., Uziely,B., Muderspach,L., Garcia,A., Burnett,A., Greco,F.A., Morrow,C.P., Paradiso,L.J., and Liang,L.J. (1997). Phase II study of liposomal doxorubicin in refractory ovarian cancer: antitumor activity and toxicity modification by liposomal encapsulation. J. Clin. Oncol. *15*, 987-993.

Nagata,S. (1997). Apoptosis by death factor. Cell *88*, 355-365.

Nakano,K. and Vousden,K.H. (2001). PUMA, a novel proapoptotic gene, is induced by p53. Mol. Cell *7*, 683-694.

New,R.R.C. (1989). Liposomes-A practical approach. (Oxford: IRL Press).

Nicholson,D.W. and Thornberry,N.A. (1997). Caspases: killer proteases. Trends Biochem. Sci. *22*, 299-306.

Oda,E., Ohki,R., Murasawa,H., Nemoto,J., Shibue,T., Yamashita,T., Tokino,T., Taniguchi,T., and Tanaka,N. (2000). Noxa, a BH3-only member of the Bcl-2 family and candidate mediator of p53-induced apoptosis. Science *288*, 1053-1058.

Odaimi,M. and Ajani,J. (1987). High-dose chemotherapy. Concepts and strategies. Am. J. Clin. Oncol. *10*, 123-132.

Olson,F., Hunt,C.A., Szoka,F.C., Vail,W.J., and Papahadjopoulos,D. (1979). Preparation of liposomes of defined size distribution by extrusion through polycarbonate membranes. Biochim. Biophys. Acta *557*, 9-23.

Olson,F., Mayhew,E., Maslow,D., Rustum,Y., and Szoka,F. (1982). Characterization, toxicity and therapeutic efficacy of adriamycin encapsulated in liposomes. Eur. J. Cancer Clin. Oncol. *18*, 167-176.

Orrenius,S. (2004). Mitochondrial regulation of apoptotic cell death. Toxicol. Lett. *149*, 19-23.

Orstein,L. (1964). Disc Electrophoresis. I. Background and Theory. Ann. N. Y. Acad. Sci. *121*, 321-349.

Papahadjopoulos,D., Allen,T.M., Gabizon,A., Mayhew,E., Matthay,K., Huang,S.K., Lee,K.D., Woodle,M.C., Lasic,D.D., Redemann,C., and . (1991). Sterically stabilized liposomes: improvements in pharmacokinetics and antitumor therapeutic efficacy. Proc. Natl. Acad. Sci. U. S. A *88*, 11460-11464.

Pardee,A.B. (1989). G1 events and regulation of cell proliferation. Science *246*, 603-608.

Payne,J., Rajapakse,N., Wilkins,M., and Kortenkamp,A. (2000). Prediction and assessment of the effects of mixtures of four xenoestrogens. Environ. Health Perspect. *108*, 983-987.

Perry,M.E., Piette,J., Zawadzki,J.A., Harvey,D., and Levine,A.J. (1993). The mdm-2 gene is induced in response to UV light in a p53-dependent manner. Proc. Natl. Acad. Sci. U. S. A *90*, 11623-11627.

Plackett,R.L. and Hewlett,P.S. (1948). Statistical aspects of the independent joint action of poisons, particularly insecticides. I. The toxicity of a mixture of poisons. Ann. Appl. Biol. *35*, 347-358.

Poch,G. (1993). Combined effects of drugs and toxic agents. In Modern Evaluation in Theory and Practice, (Wien: Springer).

Poruchynsky,M.S., Giannakakou,P., Ward,Y., Bulinski,J.C., Telford,W.G., Robey,R.W., and Fojo,T. (2001). Accompanying protein alterations in malignant cells with a microtubule-polymerizing drug-resistance phenotype and a primary resistance mechanism. Biochem. Pharmacol. *62*, 1469-1480.

Pratt,W.B., Ruddon,R.W., Ensminger,W.D., and Maybaum,J. (1997). The Anticancer Drugs. (New York: Oxford University Press).

Price,P. and Sikora,K. (2002). Treatment of Cancer. (London: Arnold).

Rahman,A., White,G., More,N., and Schein,P.S. (1985). Pharmacological, toxicological, and therapeutic evaluation in mice of doxorubicin entrapped in cardiolipin liposomes. Cancer Res. *45*, 796-803.

Rajapakse,N., Silva,E., and Kortenkamp,A. (2002). Combining xenoestrogens at levels below individual no-observed-effect concentrations dramatically enhances steroid hormone action. Environ. Health Perspect. *110*, 917-921.

Ranson,M.R., Carmichael,J., O'Byrne,K., Stewart,S., Smith,D., and Howell,A. (1997). Treatment of advanced breast cancer with sterically stabilized liposomal doxorubicin: results of a multicenter phase II trial. J. Clin. Oncol. *15*, 3185-3191.

Reed,J.C., Miyashita,T., Takayama,S., Wang,H.G., Sato,T., Krajewski,S., Aime-Sempe,C., Bodrug,S., Kitada,S., and Hanada,M. (1996). BCL-2 family proteins: regulators of cell death involved in the pathogenesis of cancer and resistance to therapy. J. Cell Biochem. *60*, 23-32.

Reutelingsperger,C.P., Hornstra,G., and Hemker,H.C. (1985). Isolation and partial purification of a novel anticoagulant from arteries of human umbilical cord. Eur. J. Biochem. *151*, 625-629.

Rowinsky,E.K. and Donehower,R.C. (1991). The clinical pharmacology and use of antimicrotubule agents in cancer chemotherapeutics. Pharmacol. Ther. *52*, 35-84.

Rudin,C.M. and Thompson,C.B. (1997). Apoptosis and disease: regulation and clinical relevance of programmed cell death. Annu. Rev. Med. *48*, 267-281.

Ruley,H.E. (1983). Adenovirus early region 1A enables viral and cellular transforming genes to transform primary cells in culture. Nature *304*, 602-606.

Salmon,S.E., Hamburger,A.W., Soehnlen,B., Durie,B.G., Alberts,D.S., and Moon,T.E. (1978). Quantitation of differential sensitivity of human-tumor stem cells to anticancer drugs. N. Engl. J. Med. *298*, 1321-1327.

Sambrook,J., Fritsch,E.F., and Maniatis,T. (1989). Molecular Cloning: A Laboratory Manual. (New York: Cold Spring Harbour Laboratory Press).

Sax,J.K. and El-Deiry,W.S. (2003). p53 downstream targets and chemosensitivity. Cell Death. Differ. *10*, 413-417.

Saxon,D.N., Mayer,L.D., and Bally,M.B. (1999). Liposomal anticancer drugs as agents to be used in combination with other anticancer agents: studies on a liposomal formulation with two encapsulated drugs. J. Liposome Res. *9*, 507-522.

Schlosser,P.M. and Bogdanffy,M.S. (1999). Determining modes of action for biologically based risk assessments. Regul. Toxicol. Pharmacol. *30*, 75-79.

Schneider,E., Hsiang,Y.H., and Liu,L.F. (1990). DNA topoisomerases as anticancer drug targets. Adv. Pharmacol. *21*, 149-183.

Schneider,J., Jimenez,E., Marenbach,K., Marx,D., and Meden,H. (1998). Co-expression of the MDR1 gene and HSP27 in human ovarian cancer. Anticancer Res. *18*, 2967-2971.

Scholze,M., Boedeker,W., Faust,M., Backhaus,T., Altenburger,R., and Grimme,L.H. (2001). A general best-fit method for concentration-response curves and the estimation of low-effect concentrations. Environ. Toxicol. Chem. *20*, 448-457.

Scudiero,D.A., Shoemaker,R.H., Paull,K.D., Monks,A., Tierney,S., Nofziger,T.H., Currens,M.J., Seniff,D., and Boyd,M.R. (1988). Evaluation of a soluble tetrazolium/formazan assay for cell growth and drug sensitivity in culture using human and other tumor cell lines. Cancer Res. *48*, 4827-4833.

Sengupta,S., Eavarone,D., Capila,I., Zhao,G., Watson,N., Kiziltepe,T., and Sasisekharan,R. (2005). Temporal targeting of tumour cells and neovasculature with a nanoscale delivery system. Nature *436*, 568-572.

Senior,J., Crawley,J.C., and Gregoriadis,G. (1985). Tissue distribution of liposomes exhibiting long half-lives in the circulation after intravenous injection. Biochim. Biophys. Acta *839*, 1-8.

Senior,J.H. (1987). Fate and behavior of liposomes in vivo: a review of controlling factors. Crit Rev. Ther. Drug Carrier Syst. *3*, 123-193.

Silva, E. Understanding the mechanisms underlying the joint action of xenoestrogens. 2003. School of Pharmacy, University of London. Thesis/Dissertation

Silva,E., Rajapakse,N., and Kortenkamp,A. (2002). Something from "nothing"--eight weak estrogenic chemicals combined at concentrations below NOECs produce significant mixture effects. Environ. Sci. Technol. *36*, 1751-1756.

Skeel,R.T. (1999). Handbook of Cancer Chemotherapy. (Philadelphia: Lippincott, Williams and Wilkins).

Skehan,P., Storeng,R., Scudiero,D., Monks,A., McMahon,J., Vistica,D., Warren,J.T., Bokesch,H., Kenney,S., and Boyd,M.R. (1990). New colorimetric cytotoxicity assay for anticancer-drug screening. J. Natl. Cancer Inst. *82*, 1107-1112.

Soule,H.D., Vazguez,J., Long,A., Albert,S., and Brennan,M. (1973). A human cell line from a pleural effusion derived from a breast carcinoma. J. Natl. Cancer Inst. *51*, 1409-1416.

Speth,P.A., van Hoesel,Q.G., and Haanen,C. (1988). Clinical pharmacokinetics of doxorubicin. Clin. Pharmacokinet. *15*, 15-31.

Steel,G.G. (1979). Terminology in the description of drug-radiation interactions. Int. J. Radiat. Oncol. Biol. Phys. *5*, 1145-1150.

Stone,K.R., Mickey,D.D., Wunderli,H., Mickey,G.H., and Paulson,D.F. (1978). Isolation of a human prostate carcinoma cell line (DU 145). Int. J. Cancer *21*, 274-281.

Strasser,A., O'Connor,L., and Dixit,V.M. (2000). Apoptosis signaling. Annu. Rev. Biochem. *69*, 217-245.

Tada,H., Shiho,O., Kuroshima,K., Koyama,M., and Tsukamoto,K. (1986). An improved colorimetric assay for interleukin 2. J. Immunol. Methods *93*, 157-165.

Tanikawa,C., Matsuda,K., Fukuda,S., Nakamura,Y., and Arakawa,H. (2003). p53RDL1 regulates p53-dependent apoptosis. Nat. Cell Biol. *5*, 216-223.

Tannock,I.F. and Lee,C. (2001). Evidence against apoptosis as a major mechanism for reproductive cell death following treatment of cell lines with anti-cancer drugs. Br. J. Cancer *84*, 100-105.

Tartaglia,L.A., Ayres,T.M., Wong,G.H., and Goeddel,D.V. (1993). A novel domain within the 55 kd TNF receptor signals cell death. Cell *74*, 845-853.

Thibodeau,P.A., Bissonnette,N., Bedard,S.K., Hunting,D., and Paquette,B. (1998). Induction by estrogens of methotrexate resistance in MCF-7 breast cancer cells. Carcinogenesis *19*, 1545-1552.

Thompson,C.B. (1995). Apoptosis in the pathogenesis and treatment of disease. Science *267*, 1456-1462.

Thornberry,N.A. and Lazebnik,Y. (1998). Caspases: enemies within. Science *281*, 1312-1316.

Tulpule,A., Yung,R.C., Wernz,J., Espina,B.M., Myers,A., Scadden,D.T., Cabriales,S., Ilaw,M., Boswell,W., and Gill,P.S. (1998). Phase II trial of liposomal daunorubicin in the treatment of AIDS-related pulmonary Kaposi's sarcoma. J. Clin. Oncol. *16*, 3369-3374.

U.S.EPA (2000). Draft Dioxin Reassessment, Part III. Integrated Summary and Risk Characterization for 2,3,7,8-Tetrachlorodibenzo-*p*-dioxin and Related Compounds. (Washington D.C.: U.S. Environmental Protection Agency).

U.S.EPA (2001). Draft Final Guidelines for Carcinogen Risk Assessment. (Washington D.C.: U.S. Environmental Protection Agency).

Unkelbach,H.D. (1992). What does the term "non-interactive" mean. Arch. Complex Environment. Studies *4*, 29-34.

Varfolomeev,E.E., Boldin,M.P., Goncharov,T.M., and Wallach,D. (1996). A potential mechanism of "cross-talk" between the p55 tumor necrosis factor receptor and Fas/APO1: proteins binding to the death domains of the two receptors also bind to each other. J. Exp. Med. *183*, 1271-1275.

Vayssade,M., Faridoni-Laurens,L., Benard,J., and Ahomadegbe,J.C. (2002). Expression of p53-family members and associated target molecules in breast cancer cell lines in response to vincristine treatment. Biochem. Pharmacol. *63*, 1609-1617.

Vogelstein,B. and Kinzler,K.W. (1993). The multistep nature of cancer. Trends Genet. *9*, 138-141.

Vousden,K.H. (2000). p53: death star. Cell *103*, 691-694.

Wampler,G.L., Carter,W.H., Jr., Campbell,E.D., and Goldman,I.D. (1987). Demonstration of a schedule-dependent therapeutic synergism utilizing the interacting drugs methotrexate and teniposide in L1210 leukemia. Cancer Treat. Rep. *71*, 581-591.

Wang,L., Klimpel,G.R., Planas,J.M., Li,H., and Cloyd,M.W. (1998). Apoptotic killing of CD4+ T lymphocytes in HIV-1-infected PHA-stimulated PBL cultures is mediated by CD8+ LAK cells. Virology *241*, 169-180.

Wang,S. and El-Deiry,W.S. (2003). TRAIL and apoptosis induction by TNF-family death receptors. Oncogene *22*, 8628-8633.

Ward,J.F. (1988). DNA damage produced by ionizing radiation in mammalian cells: identities, mechanisms of formation, and reparability. Prog. Nucleic Acid Res. Mol. Biol. *35*, 95-125.

Waring,M. (1970). Variation of the supercoils in closed circular DNA by binding of antibiotics and drugs: evidence for molecular models involving intercalation. J. Mol. Biol. *54*, 247-279.

Weinberg,R.A. (1983). Alteration of the genomes of tumor cells. Cancer *51*, 1971-1975.

Weisenthal,L.M. and Kern,D.H. (1991). Prediction of drug resistance in cancer chemotherapy: the Kern and DiSC assays. Oncology (Williston. Park) *5*, 93-103.

Weyermann,J., Lochmann,D., and Zimmer,A. (2005). A practical note on the use of cytotoxicity assays. Int. J. Pharm. *288*, 369-376.

Whitehouse,P.A., Knight,L.A., Di,N.F., Mercer,S.J., Sharma,S., and Cree,I.A. (2003). Heterogeneity of chemosensitivity of colorectal adenocarcinoma determined by a modified ex vivo ATP-tumor chemosensitivity assay (ATP-TCA). Anticancer Drugs *14*, 369-375.

Woo,M., Hakem,R., Soengas,M.S., Duncan,G.S., Shahinian,A., Kagi,D., Hakem,A., McCurrach,M., Khoo,W., Kaufman,S.A., Senaldi,G., Howard,T., Lowe,S.W., and Mak,T.W. (1998). Essential contribution of caspase 3/CPP32 to apoptosis and its associated nuclear changes. Genes Dev. *12*, 806-819.

Woodle,M.C., Newman,M.S., and Cohen,J.A. (1994). Sterically stabilized liposomes: physical and biological properties. J. Drug Target *2*, 397-403.

Yang,J., Liu,X., Bhalla,K., Kim,C.N., Ibrado,A.M., Cai,J., Peng,T.I., Jones,D.P., and Wang,X. (1997). Prevention of apoptosis by Bcl-2: release of cytochrome c from mitochondria blocked. Science *275*, 1129-1132.

Yang,X.H., Sladek,T.L., Liu,X., Butler,B.R., Froelich,C.J., and Thor,A.D. (2001). Reconstitution of caspase 3 sensitizes MCF-7 breast cancer cells to doxorubicin- and etoposide-induced apoptosis. Cancer Res. *61*, 348-354.

Yu,J., Zhang,L., Hwang,P.M., Kinzler,K.W., and Vogelstein,B. (2001). PUMA induces the rapid apoptosis of colorectal cancer cells. Mol. Cell *7*, 673-682.

Yuan,F., Dellian,M., Fukumura,D., Leunig,M., Berk,D.A., Torchilin,V.P., and Jain,R.K. (1995). Vascular permeability in a human tumor xenograft: molecular size dependence and cutoff size. Cancer Res. *55*, 3752-3756.

Zhang,Z., Li,M., Wang,H., Agrawal,S., and Zhang,R. (2003). Antisense therapy targeting MDM2 oncogene in prostate cancer: Effects on proliferation, apoptosis, multiple gene expression, and chemotherapy. Proc. Natl. Acad. Sci. U. S. A *100*, 11636-11641.

Zheng,T.S., Schlosser,S.F., Dao,T., Hingorani,R., Crispe,I.N., Boyer,J.L., and Flavell,R.A. (1998). Caspase-3 controls both cytoplasmic and nuclear events associated with Fas-mediated apoptosis in vivo. Proc. Natl. Acad. Sci. U. S. A *95*, 13618-13623.

Zhou,B.B. and Elledge,S.J. (2000). The DNA damage response: putting checkpoints in perspective. Nature *408*, 433-439.

Zoli,W., Ulivi,P., Tesei,A., Fabbri,F., Rosetti,M., Maltoni,R., Giunchi,D.C., Ricotti,L., Brigliadori,G., Vannini,I., and Amadori,D. (2005). Addition of 5-fluorouracil to doxorubicin-paclitaxel sequence increases caspase-dependent apoptosis in breast cancer cell lines. Breast Cancer Research *7*, 681-689.